Structural and functional studies of the cell cycle regulator RGC-32

by

Lina Chen

Submitted in total fulfilment of the requirements of the degree of

Doctor of Philosophy

Department of Chemistry and Biochemistry

School of Life Sciences

University of Sussex

October 2016

Declaration

I hereby declare that this thesis has not been and will not be, submitted in whole or in part to another University for the award of any other degree.

UNIVERSITY OF SUSSEX

Lina Chen

Doctor of philosophy

Structural and functional studies of the cell cycle regulator RGC-32

SUMMARY

Epstein-Barr virus (EBV) immortalises resting B-lymphocytes to lymphoblastoid cell lines (LCLs) and is associated with many cancers. The cell-cycle regulator response gene to complement 32 (RGC-32) is upregulated in EBV-infected cells, binds the mitotic kinases CDK1 and PLK1 and disrupted cell cycle checkpoints. RGC-32 may therefore play a role in EBV-mediated cell-cycle deregulation. RGC-32 has no homology with any other known proteins, so affinity-tagged forms of RGC-32 were expressed in E.coli for structure-function studies. Replacing a polyhistidine tag with a glutathione S-Transferase (GST) tag and optimising expression conditions improved RGC-32 solubility. Purified soluble RGC-32 was produced for structural studies, but no crystals were obtained. Using the GST-RGC-32 fusion protein I showed that RGC-32 interacts with CDK1, Plk1 and the kinetochore component Spc24 from B-cell lysates. Interestingly, RGC-32 did not interact with cyclin B1, suggesting that it may activate CDK1 in a cyclin-independent manner. Mapping the regions of interaction between RGC-32 and CDK1 and Plk1 revealed these kinases bind to different but adjacent regions of RGC-32. To investigate the role of RGC-32 in cell cycle disruption by EBV, I made a series of cell-lines stably expressing inducible RGC-32 constructs and RGC-32 disrupted G_2/M checkpoint in an additional B-cell line. Investigating the mechanism of RGC-32 transcription control in EBV-infected cells demonstrated that although EBV transcription factors bind to intronic regions of the RGC-32 gene, no regulation was detected in reporter assay. These data reveal a novel aspect of CDK1 activation by RGC-32, identify the sites of protein-protein interactions and provide new cell-lines for further investigation of RGC-32 function.

Acknowledgements

I would like to take this opportunity to give my tremendous appreciation to my supervisor Professor Michelle West for the academic guidance, significant support and valuable advice throughout the journey of my Ph.D. I also want to give my great thanks to Professor Alison Sinclair for her great understanding and advices for the research. Without the outstanding support from my supervisors, it would not allow me to complete the Ph.D study.

I have spent most of my laboratory time together with my lovely colleagues. They are the treasure of my Ph.D and for the rest of my life. I would like to thank everyone in lab for their endless support on my research work, especially those unforgettable help given during my thesis writing. I have a long list for this Andrea, David, French Michele, Hilda, Opy, Rajesh, Richard, Rob, Sarika, Sandra. I would also like to say thanks to everyone from Sinclair lab for their advice and friendship, Anja, Barak, Chris, Kay, Kirsty, Rajaei, Wei, Yaqi. I will not forget those helps from everyone in Mancini lab, Aaron, Jake, Leanne, Muzaffar. To all of the West and Sinclair's lab members, it was you taught me what team work is.

I would like to thank Dr. Chrisostomos Prodromou and Dr. Mohinder Pal for their great help on purification.

我要谢谢Sunny和刘婉。 谢谢老乔和花花。谢谢老爸老妈。你们是一切动力的来源！

Table of Contents

Abbreviations

ABHA	Azelaic bishydroxamine
AID	Activation-induced cytidine deaminase
ARL	AIDS-related lymphoma
ATM	Ataxia-telangiectasia mutated
ATP	Adenosine triphosphate
ATR	Ataxia-telangiectasia-mutated and Rad3-related
BARF1	BamHI-A rightward reading frame 1
BARTs	BamHI-A rightward transcripts
BHRF1	BamHI-H rightward reading frame 1
BIM	Bcl2-interacting mediator
BL	Burkitt's lymphoma
CAK	CDK-activating kinase
CAT	Chloramphenicol acetyltransferase
CCAN	Constitutive contromere associated network
CDK	Cyclin-dependent kinase
ChIP	Chromatin immunoprecipitation
Chk	Checkpoint kinase
Cp	C promoter
CsCl	Caesium chloride
CtBP	Carboxy-terminal binding protein
DMEM	Dulbecco modified eagles medium
DS	Dyad symmetry
EBER	Epstein-Barr virus encoded RNA
EBNA	Epstein-Barr nuclear antigen
EBNA LP	Epstein-Barr nuclear antigen leader protein
EBV	Epstein-Barr virus
FBS	Fetal bovine serum
GST	Glutathione-S-Transferase
H3K27me3	Histone 3 lysine 27 trimethylation
HIV	Human immunodeficiency virus
HL	Hodgkin's lymphoma
HLA	Human leukocyte antigen

IM	Infectious mononuleosis
IR	Internal repeat
KMN	Knl1-Mis12 complex-Ndc80 complex
LCL	Lymphoblastoid cell line
LMP	Latent membrane protein
MPF	M phase-promoting factor
NPC	Nasopharyngeal carcinoma
oriP	Origin of laent DNA replication
PBS	Dulbecco's phosphate buffered saline
PI	Propidium iodide
PIKK	Phosphoinositide 3-kinase-like kinase
Plk1	Polo-like kinase 1
PRC	Polycomb repressor complex
PSG	Penicillin/Streptomycin/Glutamine
PTLD	Post-transplantation lymphoproliferative disorder
Qp	Q promoter
RBP-Jκ	Recombination signal-binding protein 1 for Jκ
RINGO	Rapid inducer of G_2/M progression in oocytes
RGC-32	Response gene to complement 32
RUNX	Runt box
Spc	Spindle pole component
TBE	Tris/Borate/EDTA
TCL	Total cell lysate
Wp	W promoter
WT	Wild type

1 Introduction

1.1 Cell cycle

Cell division describes the process by which organisms precisely duplicate the DNA in the chromosomes and pass it on to two daughter cells. It is divided into four phases in eukaryotes G_1, S, M, G_2 and a resting phase, G_0 (Figure 1-1). In synthesis (S) phase, the DNA in the cell is replicated and chromosomes are duplicated from single chromatids to double (sister) chromatids. In mitosis (M) phase the cell is divided into two daughter cells followed by nuclear division. M phase is a complicated process which is composed of prophase, prometaphase, metaphase, anaphase and telophase. During prophase, chromatin condenses into chromosomes and in prometaphase the nuclear membrane breaks down. Chromosomes then line up along the equatorial plate in metaphase, separate at centromeres and sister chromatids then move to the cell poles in anaphase. During telophase a new nuclear membrane is formed and chromosomes decondense into chromatin. S and M phases are separated by two gap phases (G1 and G2) in which cells prepare for DNA replication or mitosis.

1.1.1 Cell cycle control system

Three main checkpoints in G1, G2 and mitosis make sure that appropriate processes in the cell cycle occur in the proper sequence, i.e. prevent progress into the next phase if the process is not completed. The key components of the cell cycle control system are cyclin-dependent kinases (CDKs) and cyclins

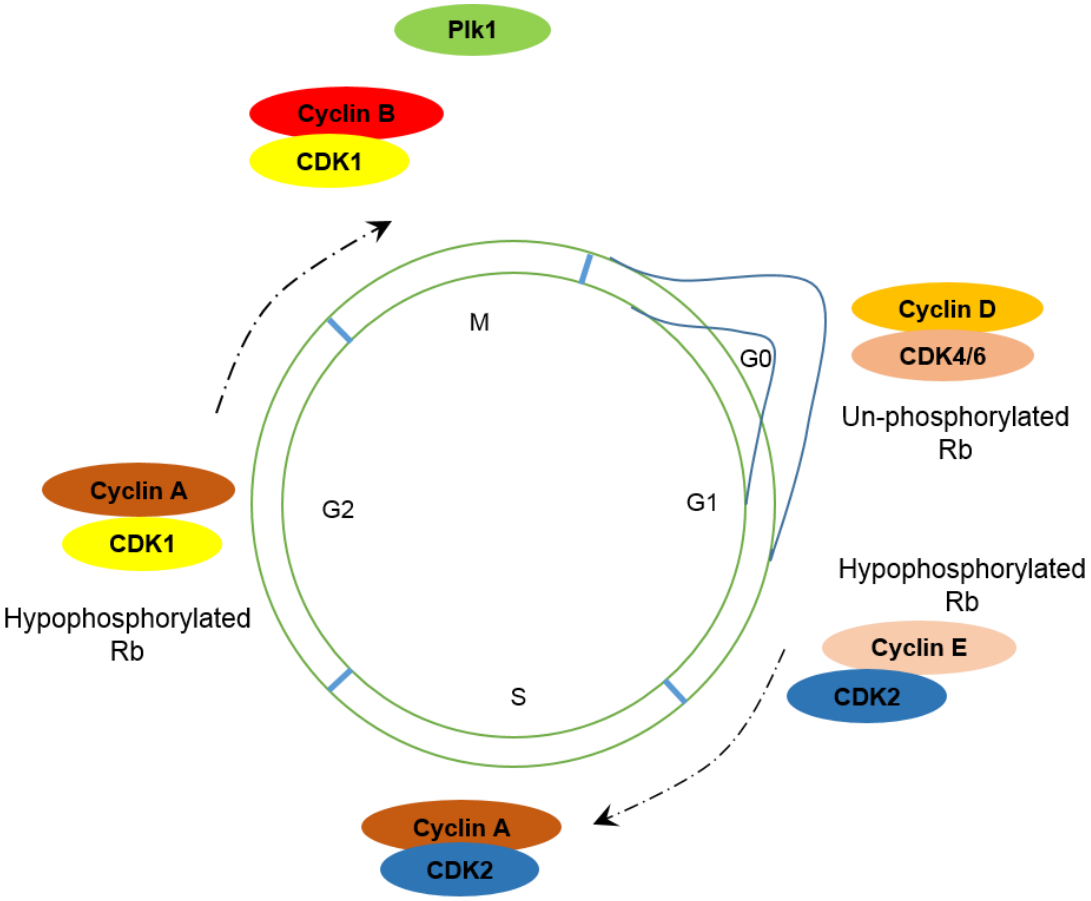

Figure 1-1 Cell cycle overview.

The cell cycle is divided into four phases (G1, S, G_2 and M) and a resting phase G_0. The CDK/Cyclin complexes, Plk1 and the status of Rb phosphorylation regulate progression of cells through the different phases of the cell cycle.

which are activated throughout the cell cycle and regulate the transition of each cell from one cell cycle state to the next (Pines 1995) (Figure 1-1).

1.1.2 CDK1 and Cyclin B1

Original investigations into genes which control cell size at cell division (Nurse 1990) and subsequent research on amphibian oocytes led to the identification of M phase-promoting factor (MPF) (Smith and Ecker 1971, Masui and Markert 1971). Later work with Xenopus oocytes revealed the components of MPF to be CDK1 (Gautier et al. 1988, Arion et al. 1988, Dunphy et al. 1988, Labbe et al. 1988) and cyclin B (Gautier et al. 1990, Labbe et al. 1989). The CDK1/cyclin B1 complex remains inactive until late G_2, although cyclin B1 is expressed in late S and G_2 phases (Pines and Hunter 1989, Nurse 1990, Maller 1991).

In normal cells, the assembly of CDK1 and cyclin B1 only produces a partly active complex and its full activity is reached through phosphorylation at Threonine 161 in CDK1 by CAK (cdk-activating kinase) (Solomon, Lee and Kirschner 1992), a complex of CDK7 and cyclin H. CAK activity is constant throughout the cell cycle (Tassan et al. 1994, Bartkova, Zemanova and Bartek 1996). CDK1 is however inactivated by phosphorylation on Threonine 14 and Tyrosine 15 by the kinases Wee1 and Myt1 (McGowan and Russell 1993, Mueller et al. 1995), even in the presence of CAK-catalyzed activating phosphorylation. The activities of both Wee1 and Myt1 are regulated by phosphorylation and localization (McGowan and Russell 1995, Watanabe, Broome and Hunter 1995, Wang et al. 2000, Liu et al. 1997). At the G2/M

transition, inhibitory phosphorylation on Threonine-14 and Tyrosine-15 of CDK1 is removed by the phosphatase CDC25 which allows cells to enter mitosis (Kumagai and Dunphy 1991) (Figure 1-2).

In addition, the activity of the CDK1/cyclin B1 complex is regulated by cellular localization (Hagting et al. 1998, Yang et al. 1998). In interphase, CDK1/cyclin B1 complexes localize to the cytoplasm (Pines and Hunter 1991, Ookata et al. 1993, Bailly et al. 1992) and during late prophase most CDK1/cyclin B1 complexes are translocated from cytoplasm to the nucleus (Hagting et al. 1999, Clute and Pines 1999). The phosphorylation of Threonine 161 by CAK is achieved in the nucleus where CAK is localized (Obaya and Sedivy 2002) and some evidence indicates that CDC25C is also localized in the cytoplasm during interphase and moves to the nucleus during prophase (Seki et al. 1992, Heald, McLoughlin and McKeon 1993, Kumagai and Dunphy 1991, Dalal et al. 1999, Graves et al. 2000).

If DNA is damaged, the G_2/M checkpoint is activated. Ataxia telangiectesia mutated (ATM) and ataxia telangiectasia and Rad3-related protein (ATR), two central components of the DNA damage response are activated (Elledge 1996). ATM is a 350 kDa protein and has homology to the phosphoinositide 3-kinases (Shiloh 1997, Perry and Kleckner 2003, Bakkenist and Kastan 2003, Savitsky et al. 1995). ATR is a 303 kDa protein with homology to other phosphoinositide 3-kinase-like kinase (PIKK) family members (Sancar et al. 2004). As downstream

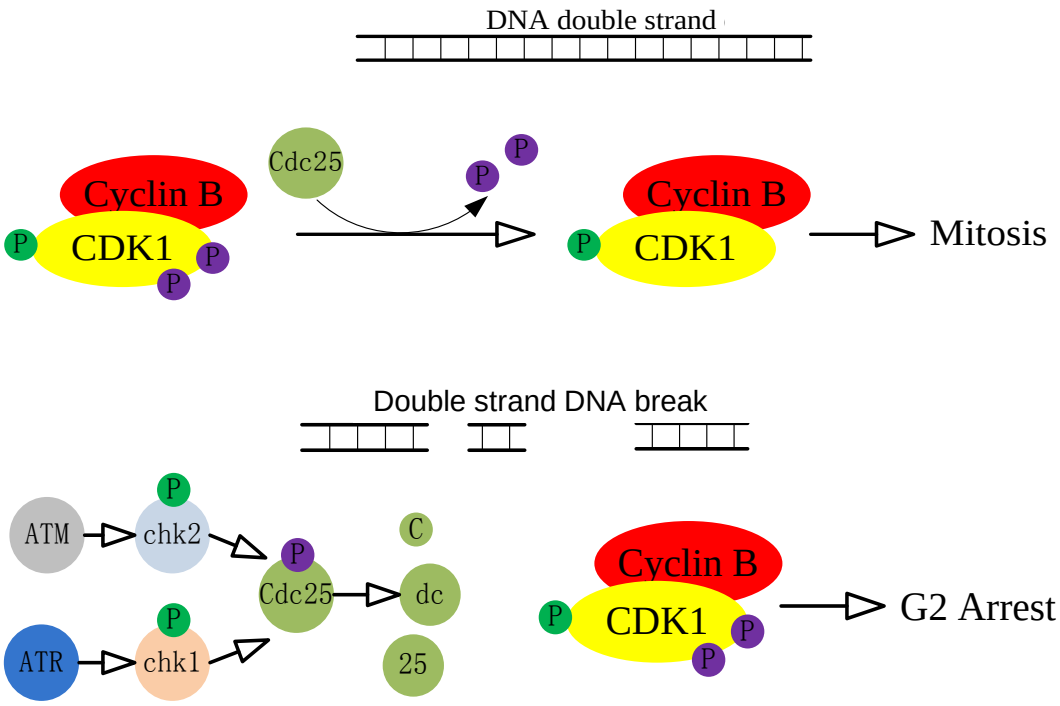

Figure 1-2. G2/M checkpoint.

In absence of cytotoxic stress, inhibitory phosphorylation on Threonine-14 and Tyrosine-15 of CDK1 is removed by the phosphatase CDC25 which allows cells to enter mitosis at the G2/M transition. In the presence of cytotoxic stress downstream activators of ATR and ATM, chk1 and chk2 can phosphorylate CDC25C on Serine-216 and this phosphorylation can result in CDC25 degradation, resulting in a failure to dephosphorylate CDK1 on Threonine-14 and Tyrosine-15. So CDC25 cannot remove those two inhibitory phosphates from CDK1 which leads to G2 arrest.

activators of ATR and ATM, chk1 and chk2 (Abraham 2001, Matsuoka, Huang and Elledge 1998)can phosphorylate CDC25C on Serine-216 and this phosphorylation can result in CDC25 degradation, resulting in a failure to dephosphorylate CDK1 on Threonine-14 and Tyrosine-15 (Matsuoka et al. 1998, Henle, Henle and Diehl 1968). The ATM-Chk2-CDC25 pathway responses to double-stranded DNA breaks caused by ionizing radiation and UV light exposure and the ATR-Chk1-CDC25 pathway responses to single-strand DNA breaks caused by replication errors and hydroxyurea. So once DNA is damaged, either the ATM-Chk2-CDC25 or the ATR-Chk1-CDC25 pathway is activated to arrest the cell cycle in G2 (Zhao and Piwnica-Worms 2001, Xu et al. 2002, Brown and Baltimore 2003).

1.1.3 Plk1

The polo gene was first discovered in *Drosophila* (Sunkel and Glover 1988) and five Plks (Plk1-5) have been identified in humans (Glover, Hagan and Tavares 1998, Andrysik et al. 2010). The human Plk1 was cloned in 1994 and is expressed highly at the mRNA level in tissues that contain dividing cells. Plk1 protein level changes in cell cycle, and are highest in mitosis (Golsteyn et al. 1994).

Aurora A can activate Plk1 by phosphorylating threonine 210 in the activation loop in the G2 phase, but only when Plk1 binds to Bora, an aurora A kinase activator in cell cycle (Macurek et al. 2008, Jang et al. 2002, Seki et al. 2008). The exact mechanism of how Bora and Plk1 interact is still not clear, but one

possibility is that the interaction is triggered through the phosphorylation of Bora by CDK1 (Chan et al. 2008). During the G_2/M transition, Plk1 phosphorylates CDK1/Cyclin B and Cdc25 leading to mitotic entry (Kumagai and Dunphy 1996). So there is controlling loop between CDK1 and Plk1.

When DNA is damaged, activation of the DNA damage pathway ATM/ATR-Chk2/1-p53 results in cell cycle arrest and Plk1 inactivation (Smits et al. 2000, Taylor and Stark 2001). The first Plk1 substrate that is involved in DNA damage recovery is Claspin which bridges ATR and Chk1 (Mamely et al. 2006, Peschiaroli et al. 2006). Claspin is phosphorylated by Plk1 and this phosphorylation causes degradation of claspin, which is necessary for the termination of the DNA replication checkpoint which allows cells to go into mitosis (Mailand et al. 2006, Mamely et al. 2006, Peschiaroli et al. 2006).

1.1.4 Spc24-25

Core components of the kinetochore are the constitutive centromere associated network (CCAN) and the Knl1-Mis12 complex-Ndc80 complex (KMN) which bind to centromeric DNA and microtubule respectively and both of them are conserved across eukaryotes (McAinsh and Meraldi 2011, Cheeseman et al. 2006). The KMN network (Figure 1-3) includes kinetochore null 1 (Knl1), the four-protein Mis segregation 12 (Mis12) complex and the four-protein nuclear division cycle 80 (Ndc80) complex (reviewed in (Foley and Kapoor 2013). The Ndc80 complex is a heterotetramer comprised of Ndc80 protein, nuclear filamentous 2 (Nuf2), spindle pole component 24 and 25 (Spc24-25) (reviewed

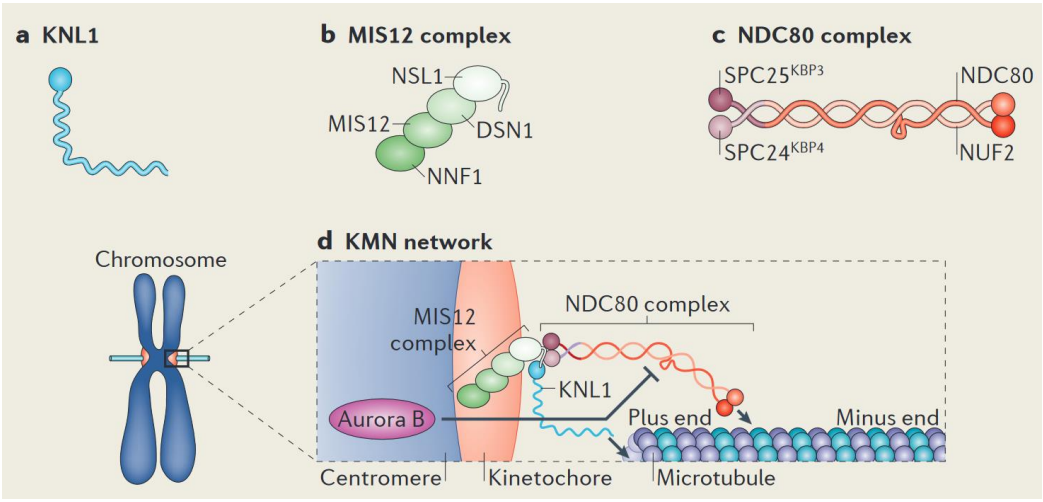

Figure 1-3. The KMN network.

The KMN network (Figure 1-3 d) is a kinetochore protein complexes. It is formed by kinetochore null 1 (Knl1, Figure 1-3 a), the mis-segregation 12 (Mis12) complex (Figure 1-3 b) and the nuclear division cycle 80 (Ndc80) Complex (Figure 1-3 c). This figure was taken from (Godek *et al*., 2015).

in (Foley and Kapoor 2013). CCAN localises to the inner kinetochore and KMN network localises to the outer kinetochore (Cheeseman and Desai 2008).

The four proteins in Ndc80 complex form a rod like structure and Ndc80 and Nuf2 form a complex which localises to the outer kinetochore and Spc24-25 form a complex which localises to the inner kinetochore (Cheeseman and Desai 2008). The Ndc80 complex is important for the attachment of kinetochore to microtubule and Spc24-25 interacts with yeast histone-fold protein Cnn1 (human homologue CENP-T) illustrating how this connection links microtubule to chromosome (Malvezzi et al. 2013). Cnn1 binds to the hydrophobic pocket located in the globular domain of Spc24-25 (Malvezzi et al. 2013).

1.2 EBV

Epstein-Barr virus (EBV) was originally discovered in 1964 in B lymphocytes cultured from an African Burkitt's lymphoma (BL) (Epstein, Achong and Barr 1964) and was the first herpes virus to have its genome completely cloned and sequenced. The virus causes a latent and persistent infection and is a gamma herpes virus known to be associated with several cancers such as Burkitt's lymphoma (BL), Hodgkin's lymphoma (HL), Nasopharyngeal carcinoma (NPC) and post-transplant lymphoproliferative disease (PTLD) (reviewed in Crawford 2001). *In vivo*, primary EBV infection usually occurs during childhood via saliva (Niederman et al. 1976) in about 90% of the world-wide population and is asymptomatic (De Matteo et al. 2003, Henle et al. 1969). However, infectious

mononucleosis (IM) can develop if primary infection occurs in adolescence (Niederman et al. 1968).

EBV is able to infect and transform B lymphocytes but can also infect epithelial cells and in some situations may infect T cells and natural killer cells (Kieff and Rickinson, 2007). EBV attaches to B cells due to a high-affinity interaction between major viral envelope glycoprotein gp350 and complement receptor CD21 (also known as CR2) on the B cell (Nemerow et al. 1985), then through the binding of a second glycoprotein gp42 to human leukocyte antigen (HLA) class II molecules as a co-receptor (Borza and Hutt-Fletcher 2002). After the virus attaches to the B cell surface, the virus fuses its envelope to the vesicle membrane through CD21 (Miller and Hutt-Fletcher 1992). The EBV DNA is found to occur after uncoating of the virion 12-16 hours after infection when coinciding with early latent viral gene expression (Adams and Lindahl 1975, Hurley and Thorley-Lawson 1988). Infection of epithelial cells takes place at the cell surface (Miller and Hutt-Fletcher 1992) and is thought to happen in a gp350-dependent or -independent manner (Fingeroth *et al*., 1999; Maruo *et al*., 2001). Recently it has been called transfer infection in which EBV infects epithelial cells by first binding to resting B cells which act as a transfer vehicle (Shannon-Lowe et al. 2006).

Two types of EBV has been described as EBV type 1 (EBV-1) and 2 (EBV-2) and the major difference between them is only 64% of the gene and 53% of the amino acids sequence of EBNA 2 is conserved between types (Adldinger et al.

1985). EBV-2 infection rarely happens in Western Europe and USA, but is common in Africa (Rowe et al. 1989, Young et al. 1987, Zimber et al. 1986).

1.2.1 EBV genome

The EBV genome is a linear 170 kb double-stranded DNA in the virion and becomes closed circular episome after infection (Hurley and Thorley-Lawson, 1988; Lindahl *et al*., 1976). *In vitro*, EBV can transform resting B cells to generate latently infected lymphoblastoid cell lines (LCLs) which express a limited set of viral genes, encoding six EBV nuclear antigens (EBNA1, 2 3A, 3B, 3C and -LP) and three latent membrane proteins (LMPs 1, 2A and 2B) (Figure 1-4) (Young and Rickinson 2004). EBV encoded RNAs (EBER1 and 2) which do not have a polyadenylated tail, so remain as untranslated RNA and are expressed in all forms of latency (Young and Rickinson 2004). EBV encodes multiple microRNAs (miRNA) from two independent transcripts, BamHIA rightward transcripts (BARTs) and BamHI rightward reading frame 1 (BHRF1) (Young and Rickinson 2004). This pattern of latent EBV gene expression which is activated only in B-cell infection is defined as latency III (reviewed in Young and Rickinson, 2004). EBV displays two other latency programmes in various EBV-related malignancies and in healthy infected hosts characterised by more restricted latent gene expression patterns (reviewed by (Shah and Young 2009): latency I and latency II. Latency I is associated with expression of EBNA 1 and Epstein-Barr virus Encoded RNAs (EBER 1 and EBER 2). Latency II is associated with expression of EBNA1, LMP 1, 2A, 2B and Epstein-Barr virus Encoded RNAs (EBER 1 and EBER 2) (summarised in Table 1-1).

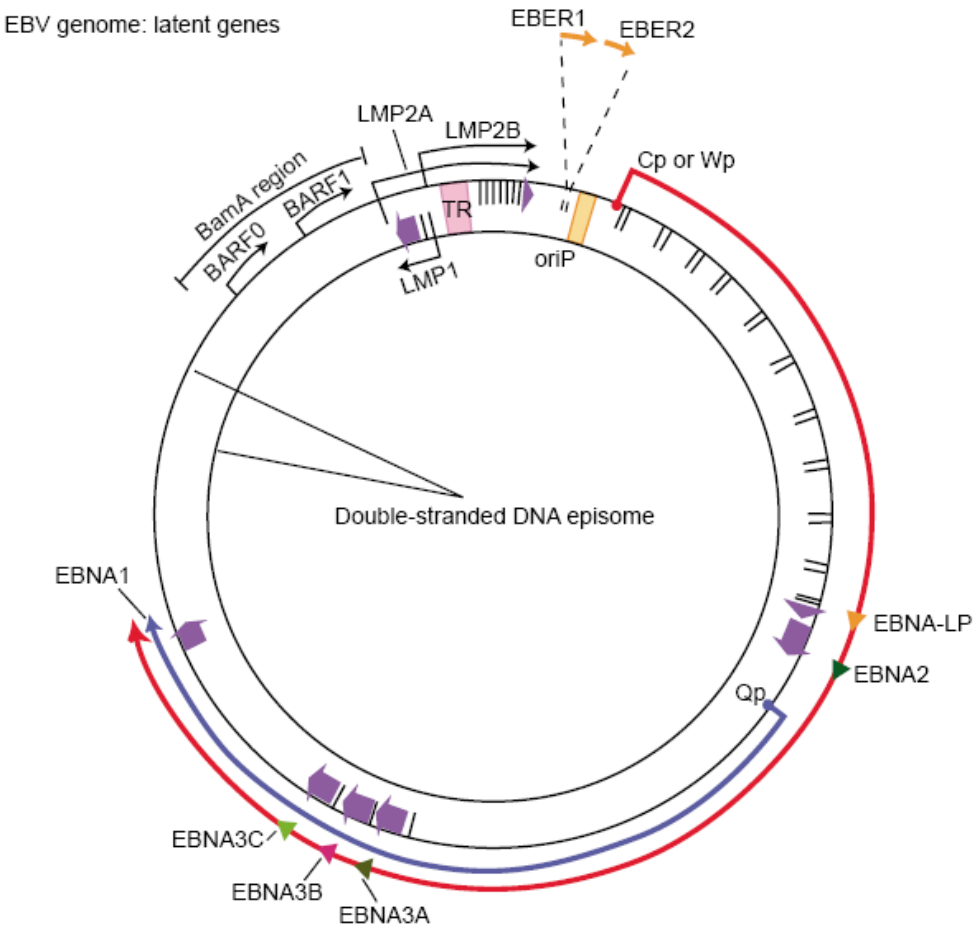

Figure 1-4. Location and transcription of the EBV latent genes on the double-stranded viral DNA episome.

The red circle line represents EBV transcription during latency III in which all the EBNAs are transcribed from promoter C or W. The blue circle line represents EBV transcription during latency I and II in which EBNA1 is transcribed from promoter Q during latency I and II. The yellow shows the origin of plasmid replication (*oriP*). The purple arrows represent exons encoding the latent proteins and the direction in which the genes are transcribed. The two yellow arrows on the top represent the non-polyadenylated RNAs EBER1 and 2 (Murray and Young 2001).

	Latency 0	Latency I	Latency II	Latency III
Gene expressed		EBNA 1 (Qp) EBER 1 EBER 2	EBNA 1 (Qp) LMP 1 LMP 2A LMP 2B EBER 1 EBER 2	EBNA 1 (Cp) EBNA 2 EBNA 3A EBNA 3B EBNA 3C EBNA LP LMP 1 LMP 2A LMP 2B EBER 1 EBER 2
Site *in vivo*	Periphery resting memory B cells	Periphery dividing memory B cells	Tonsil GC B cells	Tonsil naive B cells
Diseases		BL	HD, NC, T cell lymphomas	AIDS-associated lymphomas, PTLD

Table 1-1. EBV gene expression pattern during different states of infection and tumours (modified from (Thorley-Lawson 2015)).

In latency 0, no latent EBV protein is expressed. In latency I, EBNA 1, EBER 1 and 2 are expressed and this pattern of expression is found in Burkitt's lymphoma group I. In latency II, EBNA 1, LMP 1, 2A and 2B are expressed and this pattern of expression is found in Hodgkin's disease (HD), nasopharyngeal carcinoma (NC) and T cell lymphomas. In latency III, all latency EBV genes are expressed and this pattern of expression is found in AIDS-associated lymphomas and post-transplant lymphoproliferative disease (PTLD).

The EBV genome contains different promoters which contribute to the expression of the latent EBV proteins (reviewed in (Young and Rickinson 2004). The C promoter (Cp) and the W promoter (Wp) are both located within the EBV major internal repeat (IR-1). The Q promoter (Qp) only expresses EBNA 1 transcript. The activation of Wp by B cell transcription factors on initial infection causes the expression of EBNA2 and EBNA LP (Bell et al. 1998); Kirby *et al.*, 2000; (Walls and Perricaudet 1991, Kirby, Rickinson and Bell 2000). Within 36 hours after infection, Cp activation by EBNA 2 switches promoter usage from Wp to Cp which leads to the expression of all EBNA proteins ((Puglielli, Woisetschlaeger and Speck 1996); (Woisetschlaeger et al. 1990). Qp drives the expression of EBNA 1 in the absence of Cp activation and EBNA 2 expression ((Nonkwelo et al. 1996); (Schaefer, Strominger and Speck 1995). In EBV-infected B-cells, Cp and promoters of the vial LMP1, 2A and 2B genes is activated by EBNA 2 (Abbot et al. 1990, Fahraeus et al. 1990, Ghosh and Kieff 1990, Jin and Speck 1992, Sung et al. 1991, Wang et al. 1990). In absence of EBNA 2 in latency II, the expression of LMP1 is maintained by cytokine-induced activity of signal transducers and activators of transcription (STAT) and also transcription factors of the CCAAT enhancer-binding protein (C/EBP) family (Chen et al. 2001, Chen et al. 2003, Kis et al. 2006, Kis et al. 2010, Kis et al. 2011, Noda et al. 2011). The EBNA 3 genes (EBNA 3A, 3B and 3C) are arranged in tandem sequence in the EBV genome and transcribed as alternatively spliced tanscripts from the very long mRNA initiated by the Cp (White et al. 2010) which is active in EBV transformed lymphoblastoid cell lines (LCLs) but blocked in some EBV-associated cancers through hypermethylation (reviewed in (Allday, Bazot and White 2015).

More than 90% of the human population are infected by EBV (Henle et al. 1969) carrying the virus as a life-long persistent latent infection in B lymphocytes (Babcock et al. 1998, Thorley-Lawson, Miyashita and Khan 1996) with virus production into the saliva (Niederman et al. 1976, Yao, Rickinson and Epstein 1985).

1.2.2 EBV infection in vivo

1.2.2.1 EBV infection in healthy hosts

How EBV infects and persists in the host is not fully understood, but a proposed model has been described as a dynamic equilibrium between the immune system response and the different states of infection (Figure 1-5) (Young and Rickinson 2004). In primary infection, EBV infects naive B cells and transforms them to B blasts expressing all latent EBV proteins (latency III) (Babcock et al. 1999). The B blasts differentiate to germinal centre cells which display EBNA 1, LMP1 and 2A (latency II) probably because the expression of EBNA 2 blocks the differentiation of B cells to memory cells and therefore it is silenced (Polack et al. 1996). The germinal centre cells then differentiate to resting viral-genome-positive memory B cells in which all latent gene expression is turned off (latency 0) (Babcock et al. 1999). In the rarely dividing memory B cells, expression of EBNA 1 from the Q promoter is observed (latency I) to make sure the episome is not lost during cell division in hosts (Davenport and Pagano 1999, Hochberg et al. 2004).

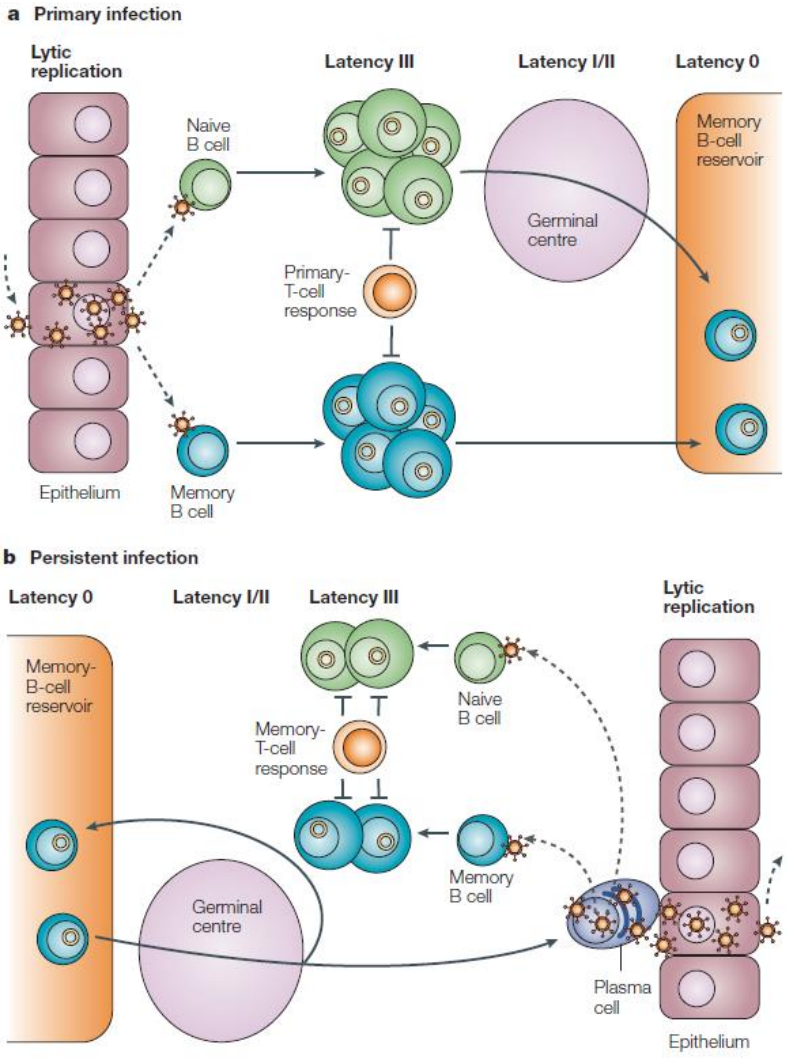

Figure 1-5. *In vivo* model of interactions between EBV and host cells (Young and Rickinson 2004).

a. Primary infection. Virus establishes lytic replication in the oropharynx then spreads to the lymphoid tissues as a latent (latency III) growth-transforming infection of B cells. Many proliferating cells are removed by the latent-antigen-specific primary T-cell response, but some escape by downregulating antigen expression and establishing a reservoir of resting viral-genome-positive memory B cells (latency 0) in which viral antigen expression is mostly suppressed. **b. Persistent infection.** The reservoir of EBV-infected memory B cells migrate and differentiate under physiological control. These EBV-infected cells might be recruited into germinal centre, after which either re-enter the reservoir as memory cells or move to mucosal sites in the oropharynx and activate the viral lytic cycle (reviewed in (Young and Rickinson 2004).

1.2.2.2 Latent EBV gene expression in diseases

Unlike other herpes viruses, EBV has the unique ability to transform resting B cells to immortal latently infected lymphoblastoid cell lines (LCLs) *in vitro* indicating its tumourigenic ability (Pope, Horne and Scott 1968). Different patterns of latent EBV gene expression are observed in EBV-related diseases (summarised in Table 1-1). In latency I, only EBNA 1 and two EBERs are expressed and this pattern is observed in many Burkitt's lymphoma tumour cells (Rowe et al. 1987, Brooks et al. 1993). In Wp-restricted Burktt's lymphoma, EBNA 1, 3A, 3B, 3C and -LP are expressed in the absence of ENBA 2 and the LMPs (Kelly et al. 2006). In latency II, EBNA 1, all three LMPs and the two EBERs are expressed and this pattern is detected in Hodgkin's disease, nasopharyngeal carcinoma and T cell lymphomas (Brooks et al. 1992, Deacon et al. 1993, Chen et al. 1993). In latency III, all latency EBV genes including EBNA 1, 2, 3A, 3B, 3C, LP, all three LMPs and the two EBERs are expressed and this pattern is found in AIDS-associated lymphomas and post-transplant lymphoproliferative disease (Young et al. 1989, Gratama et al. 1991).

1.2.3 EBV latent proteins

1.2.3.1 EBNA 1

Epstein-Barr nuclear antigen 1 (EBNA1) is expressed in all patterns of EBV latency and it was the first latency protein identified by anti-complement immunofluorescence in EBV-immortalized cells (Reedman and Klein 1973). It is necessary for B lymphocyte transformation (Lee, Diamond and Yates 1999). EBNA 1 is 641 amino acids in length from the prototype EBV type 1 strain B95-

8 (see section 1.2 EBV) and has a molecular weight of approximately 76 kD on SDS-PAGE gels.

EBNA 1 plays a key role in replication and mitotic segregation of EBV episome to ensure vial persistence in latent infection and also activates transcription of other EBV latency genes (reviewed in (Frappier 2015). EBNA 1 is the only viral protein required for the replication of the origin of latent DNA replication (*oriP*) (Figure 1-4) (Yates, Warren and Sugden 1985). EBV episomes replicate only once in each cell cycle alongside host DNA (Yates and Guan 1991) and the dyad symmetry (DS) element, one of two functional elemens in *oriP* (Reisman, Yates and Sugden 1985), is essential and sufficient for plasmid replication in the presence of EBNA 1 (Wysokenski and Yates 1989, Harrison, Fisenne and Hearing 1994, Yates, Camiolo and Bashaw 2000). The central Gly-Arg repeat region of EBNA 1 (325-376) binding to its recognition sites in the family of repeats (FR), the other functional elements in *oriP*, is necessary for its segregation function (Shire et al. 1999). EBNA 1 plays a role in inducing the expression of latency genes in latent infection by activating expression from the viral Cp and LMP promoters (Sugden and Warren 1989, Gahn and Sugden 1995). The 65-83 N-terminal sequence (Wu, Kapoor and Frappier 2002, Kennedy and Sugden 2003) and the central Gly-Arg repeat region are required for transcriptional activation (Ceccarelli and Frappier 2000, Wang et al. 1997, Van Scoy et al. 2000).

Importantly EBNA 1 can auto-downregulate its own expression by binding to two sites located downstream of the Q promoter (Sample, Henson and Sample 1992). This autoregulation mechanism functions to reduce EBNA 1 expression when its level is high, since it will only bind to the two Qp sites when its expression is high enough to saturate the DS and FR elements first, due to the high affinity for these elements than the two Qp sites (Jones, Hayward and Rawlins 1989, Ambinder et al. 1990).

EBNA 1 has been shown to play a role in regulating cellular protein function. The cellular ubiquitin-specific protease USP7, also known as HAUSP, is one of several cellular proteins identified to be bound by EBNA 1 (Holowaty et al. 2003, Malik-Soni and Frappier 2012). The expression of EBNA 1, but not a USP7-binding mutant of EBNA 1 in U2OS cells has been reported to reduce the accumulation of p53 in response to DNA damage and apoptosis (Saridakis et al. 2005). Similar results have been shown that EBNA 1 expression in CNE2 NPC cells decreased the accumulation of p53 in response to DNA damage (Sivachandran, Sarkari and Frappier 2008). These findings suggest that EBNA 1 might modulate p53 to promote cell survival in EBV-infected epithelial cells. EBNA 1 has been reported to affect several signalling pathways. First it increases the expression of STAT1 in three different carcinoma cell lines (Wood et al. 2007, Kim and Lee 2007). Second, its expression decreases the expression of TGF-β-responsive genes implying that EBNA 1 is involved in TGF-β signalling (Wood et al. 2007, Kim and Lee 2007). Third, EBNA 1 inhibits NF-κB activity and DNA binding in carcinoma cell lines (Valentine et al. 2010).

1.2.3.2 EBNA 2

EBNA 2 is a 487 amino acid protein in the prototype EBV type 1 strain B95-8 (see section 1.2 EBV) (Baer et al. 1984, Skare et al. 1982) which has a molecular weight of about 84 kDa on SDS-PAGE gels. Transcription of EBNA 2 initiates first from Wp following primary infection of B cells, then generally switches to Cp, which is upstream of Wp, activated during later stages of infection or in LCLs (Alfieri, Birkenbach and Kieff 1991, Bodescot, Perricaudet and Farrell 1987, Woisetschlaeger et al. 1990, Woisetschlaeger et al. 1991).

EBNA 2 is essential for B cell transformation. EBV strain P3HR-1 which has a deletion of EBNA2 has no B cell immortalizing capacity (Miller et al. 1974) and it is able to transform primary B cells when the cloning fragment containing the EBNA 2 gene is reconstituted into the EBV genome (Cohen et al. 1989, Hammerschmidt and Sugden 1989). EBV-1 and EBV-2, two main types of EBV, differ in their ability to immortalise primary B cells (Adldinger et al. 1985, Dambaugh et al. 1984) due to mainly difference of sequence in the C terminus of them (Tzellos et al. 2014, Tzellos and Farrell 2012) and they due to the difference of sequence in the EBNA 2. EBNA 2 is not expressed in latently infected memory B cells of healthy hosts or EBV-associated malignancies of immunocompetent patients, such as Burkitt’s lymphoma or Hodgkin’s disease (reviewed in (Bornkamm and Hammerschmidt 2001, Macsween and Crawford 2003).

Instead binding to DNA directly, EBNA 2 utilises RBP-Jκ, the cellular Notch-pathway adapter protein CBF1, to bind upstream of and activate the latent Cp (Sung et al. 1991, Jin and Speck 1992), LMP1, 2A and 2B (Fahraeus et al. 1990, Ghosh and Kieff 1990, Wang et al. 1990). EBNA 2 minimal binding domain with RBP-Jκ is mapped at aa 318-327 on EBNA 2 (Ling and Hayward 1995). In addition to viral gene, EBNA 2 is found to regulate many cellular genes by microarrays analysis using EBNA 2 conditional LCLs or EBV negative BL cells expressing only EBNA 2 (Cahir-McFarland et al. 2004, Thompson et al. 1999, Maier et al. 2006). The cellular EBNA 2 targets include CD21 (Cordier et al. 1990), the B cell activation marker CD23 (Wang et al. 1987), the proto-oncogene *Myc* (Kaiser et al. 1999), the B cell transcription factor RUNX 3 (Spender et al. 2002) and the G1 Cyclin D2 (Sinclair et al. 1994).

1.2.3.3 EBNA-LP

Transcription of EBNA leader protein (-LP) is required for B cell immortalisation (Allan et al. 1992, Mannick et al. 1991). EBNA-LP co-activate EBNA 2 during infection as Chloramphenicol acetyltransferase (CAT) reporter assays containing upstream Cp or LMP1p are enhanced by co-expression of EBNA 2 and -LP by 10-30 fold compared to expression of EBNA 2 alone, but EBNA-LP repressed the transcription from LMP1p and Cp in the absence of EBNA 2 (Harada and Kieff 1997). In addition to viral genes, EBNA-LP has been shown to co-stimulate EBNA 2-dependent transcription of the Cyclin D2 gene (Sinclair et al. 1994) and the transcription factor HES1 (Portal et al. 2011).

EBNA-LP is a phosphoprotein (Petti, Sample and Kieff 1990). Phosphorylation of EBNA-LP, occurs predominately on serine residues and is detected throughout the cell cycle. EBNA-LP is hypophosphorylated during G1/S and hyperphosphorylated during G2/M (Kitay and Rowe 1996). Serine 35 in EBNA-LP is a predicted CDK1 site and phosphorylation of it is crucial for EBNA-LP mediated transcriptional function (Peng et al. 2000a, Peng, Tan and Ling 2000b, McCann et al. 2001, Yokoyama et al. 2001).

1.2.3.4 EBNA3 family

The EBNA3 family of proteins was first detected as an extra 142 kD band along with other previously identified latent proteins EBNA1, 2, and LMP1 by Western blotting using human sera from rheumatoid arthritis patients and normal EBV-infected people (Hennessy, Fennewald and Kieff 1985, Rickinson and Moss 1997b). It has been shown that EBNA3A and EBNA3C are necessary for B-cell immortalization (Tomkinson, Robertson and Kieff 1993), but EBNA3B is not (Tomkinson and Kieff 1992). However EBNA3B is one of the main targets in immortalized cells to be recognized by cytotoxic T cells (Rickinson and Moss 1997a) and has been reported as a virus-encoded tumour suppressor because its inactivation promotes immune evasion and virus-driven lymphomagenesis (White et al. 2012)

1.2.3.4.1 Transcriptional regulation by the EBNA 3s

EBNA3 proteins function as transcriptional regulators by interacting with many cellular DNA binding proteins or other transcription factors instead of directly

binding to DNA (reviewed in (Bhattacharjee et al. 2016). All three EBNA3 proteins are proved to interact with the RBP-Jκ and the interacting domains overlap with the most highly conserved domain amino acids 90-320 (Robertson et al. 1995, Robertson, Lin and Kieff 1996, Waltzer et al. 1996). Interestingly all three EBNA 3 proteins can bind RBP-Jκ and repress EBNA 2-activated transcription by destablilising the binding of RBP-Jκ to DNA (Johannsen et al. 1996, Waltzer et al. 1996). EBNA 2 can activate Cp via RBP-Jκ and mutation in the RBP-Jκ binding site lead to the loss of the transforming ability of EBV (Fuentes-Panana et al. 2000, Sung et al. 1991, Yalamanchili et al. 1994). So EBNA 3 proteins form a negative feedback loop which may lead to the abrogation of EBNA 2 upregulation of EBNA 3 transcription. The interaction region of each EBNA 2 with RBP-Jκ is located in the middle of the homology domain between 170-221 aa for EBNA 3A, 176-227 aa for EBNA 3B and 180-231 aa for EBNA 3C (Bourillot et al. 1998, Calderwood et al. 2011, Dalbies-Tran et al. 2001, Lee et al. 2009, Maruo et al. 2005, Maruo et al. 2009, Robertson et al. 1996). Also all EBNA3 proteins are reported to repress the activation of LMP1 and LMP2 by EBNA 2 (Le Roux et al. 1994, Waltzer et al. 1996). Inactivation of EBNA 3A and 3C does not increase the activation of some target promoters containing RBP-Jκ binding sites by EBNA 2 in infected cells (Maruo et al. 2005, Maruo et al. 2009).

EBNA 3A and 3C, but not EBNA 3B, interact with the co-repressor carboxy-terminal binding protein (CtBP) (Hickabottom et al. 2002, Touitou et al. 2001) which is identified as one of a highly conserved family of co-repressors of transcription (Chinnadurai 2007). There are two transcription factors: CtBP1 and

CtBP2 which share substantial sequence homology (Chinnadurai 2002, Chinnadurai 2009). EBNA 3A contains two non-consensus CtBP binding motifs, located at the C-terminal region, ALDLS (aa 857-861) and VLDLS (aa 886-890) (Hickabottom et al. 2002). The PLDLS (aa 728-732) motif in the C-terminal of EBNA 3C is essential and sufficient for EBNA 3C to interact with CtBP1 (Touitou et al. 2001). Although the requirement for CtBP binding is not yet understood, it has been shown that C terminus of EBNA 3C, specifically the PLDLS CtBP-binding site, is essential to rescue proliferation in EBNA 3C-conditional LCLs culture without the activator (Lee et al. 2009).

The finding that expression of both EBNA 3A and 3C is necessary to repress the transcription of *BCL2L11* (BIM) shows the first evidence that EBNA 3A and 3C can cooperate to regulate host cell genes using EBNA 3 knockout recombinant B95.8-derived EBVs to infect EBV-negative BL31 BL-derived cells (Anderton et al. 2008). Bcl2-interacting mediator (BIM) is a pro-apoptotic member of the BH (BCL2 homology) 3-only family and is encoded by the *BCL2L11* gene (O'Connor et al. 1998). BIM expression reduction has been found very soon after EBV infection in cultured B cells (Anderton et al. 2008, Skalska et al. 2013). Also EBNA 3C is necessary to repress the expression of the CDK inhibitor $p16^{INK4a}$ shown by using a recombinant Akata EBV encoding a conditional EBNA 3C fused to a modified oestrogen receptor (Maruo et al. 2006). $p16^{INK4a}$ (cyclin-dependent kinase inhibitor 2A) is a tumour suppressor protein encoded by the *CDKN2A* gene (Stone et al. 1995). EBNA 3A also plays a role in repression of *CDKN2A* in LCLs established with EBNA 3A knockout and conditional viruses (Maruo et al. 2011, Skalska et al. 2010). The reduction

of BIM and $p16^{INK4a}$ does not involve CpG methylation, but correlated with loss of histone acetylation, deposition of histone H3 lysine 27 trimethylation (H3K27me3) and the recruitment of polycomb repressor complex 1 and 2 (PRC1, 2) (Paschos et al. 2009, Paschos et al. 2012, McClellan et al. 2012, McClellan et al. 2013, Skalska et al. 2010).

1.2.3.4.2 Cell cycle regulation

The role of the EBNA 3 proteins in cell cycle regulation has been shown in Raji cells. An EBV positive Burkitt's lymphoma derived cell line in which EBNA 3C is deleted, could be arrested in the G1 phase in the cell cycle and the cell cycle activity was restored by EBNA 3C expression (Allday and Farrell 1994). It has been shown that EBNA 3C can physically interact with many important proteins involved in cell cycle regulation at both G1/S and G2/M checkpoints, for example tumour suppressor proteins pRb and p53, oncoproteins cyclin D1 and *Myc* and DNA damage responder Chk2 and H2AX (Jha et al. 2013, Jha et al. 2014, Saha and Robertson 2013). All these data suggest its ability to disrupt cell cycle control.

It has been shown that NIH3T3 cells expressing EBNA 3C rescue the growth arrest at G1 phase caused by serum starvation and continue through G2/M while EBNA 3C negative cells arrest in G1 (Parker, Touitou and Allday 2000). The initial clue for a possible mechanism of EBNA 3C overriding G1/S checkpoint is the expression of EBNA 3C rescue Raji cells arrested in G1 phase through increasing the phosphorylation of Rb (Allday and Farrell 1994). Later

EBNA 3C is found to form a complex with Rb (Knight, Sharma and Robertson 2005, Kashuba et al. 2008) and the interaction between them is stabilised in the presence of proteasomal inhibitor which indicates that EBNA 3C might also play a role in Rb degradation apart from regulating its phosphorylation (Knight *et al.*, 2005). But EBNA 3C maintains a hyperphosphorylation status of Rb but is not involved in its degradation in the studies using LCLs with conditionally active EBNC 3C (Maruo et al. 2006, Zhao et al. 2011). All these data and the earlier findings that EBNA 3C can increase the kinase activity of CDK6/Cyclin D1 (G1 phase) and CDK2/Cyclin A (S phase) suggest that it disrupts G1/S checkpoint by regulating the phosphorylation of Rb (Knight et al. 2004, Saha et al. 2011).

EBNA 3A, 3B and 3C expressing LCLs disrupt the G2/M checkpoint response induced by treatment with the histone deacetylase inhibitor azelaic bishydroxamine (ABHA) (Krauer et al. 2004). These three proteins can reduce the accumulation of inactive CDK1 which is inhibited by phosphorylation at threonine 14 and tyrosine 15 during G2/M arrest (Krauer et al. 2004). Further research shows that EBNA 3A and 3C can bind and inactivate Chk2 which is a downstream target kinase of ATM-dependent DNA damage signal pathway (Krauer et al. 2004, Choudhuri et al. 2007). The interaction between EBNA 3C and Chk2 can phosphorylate CDC25 on Serine-216 to cause its sequestration and degradation (Krauer et al. 2004, Choudhuri et al. 2007), so it cannot remove the inhibitory phosphates on CDK1 which results in G_2 arrest (Matsuoka et al. 1998). Recent research shows that inhibition of ATM and Chk2 increases transformation efficiency of primary B cells and EBNA 3C is required to attenuate the DNA damage response induced by EBV (Nikitin et al. 2010, Li

and Hayward 2011). All these findings suggest a possible mechanism by which EBNA 3C disrupts the G2/M checkpoint to maintain the continuous proliferation of EBV-transformed B cells.

1.2.4 EBV-associated diseases

1.2.4.1 Infectious Mononuleosis

During primary infection, adolescents and young adults are more likely to experience infectious mononucleosis (IM) than children (Krabbe, Hesse and Uldall 1981). IM was identified as an EBV-related disease in 1968 (Henle *et al.*, 1968) and symptoms can range from mild transient fever to several weeks of pharyngitis, lymphadenopathy (Niederman et al. 1968). It also increases the risk of Hodgkin's disease but the association between the occurrence of IM and the risk of Hodgkin's disease still remains uncertain (Hjalgrim et al. 2000).

1.2.4.2 Lymphomas in immunocompromised patients

Post-transplant lymphoproliferative disorders (PTLDs) is a complication in transplant patients who are using immunosuppressive drugs (Penn 2000) and 70 to 100% of these disorders is associated with EBV (Juvonen et al. 2003). A latency III type EBV gene expression pattern was found in early PTLDs (Knowles 1999, Young et al. 1989, Gratama et al. 1991). The lower amount of EBV-specific cytotoxic T cells are not able to fight the infection and allow the B cells to proliferate because the immune system is suppressed in the patients by using immunosuppressive drugs (Holmes and Sokol 2002). Rituximab

monotherapy, a monoclonal antibody directed against CD20, is a highly effective treatment for EBV-positive PTLD (Taylor, Marcus and Bradley 2005). AIDS-related lymphomas (ARLs) are mostly of B cell origin and unlike PTLDs, only 30 to 40% of AIDS-related BL is associated with EBV (Neri et al. 1991, Shibata et al. 1993).

1.2.4.3 Lymphomas in immunocompetent patients

1.2.4.3.1 Burkitt's lymphoma (BL)

Burkitt's lymphoma (BL) was originally described in equatorial Africa where it is the commonest childhood cancer (Burkitt and O'Conor 1961). EBV is present in about 95% of endemic BLs in Africa but only 10%-20% in Europe and the USA and this difference is caused by the early age of EBV infection in Africa compared with industrial countries (Magrath, Jain and Bhatia 1992). In the endemic tumours among which Wp-restricted latency BLs are comparatively common, only EBNA 1 is expressed (latency I) (Rowe et al. 1986). BL is characterised by *Myc* translocation from chromosome 8 to the Ig heavy chain on chromosome 14 leading to the overexpression of c-myc (Zech et al. 1976). After translocation *Myc* is active and promotes cell cycle progression (Bhatia et al. 1993, Cesarman et al. 1987, Magrath 1990). EBV infection in latency I program promotes BL cell growth by inhibiting apoptosis induced by *Myc* through the upregulation of Bcl-2 and downregulation in *Myc* expression (Ruf et al. 2001).

In 1969 malaria was found to play a role in the generation of BL (Burkitt 1969). The role of malaria in BL and the mechanisms of how malaria induces the pathogenesis of BL are still not clear. The possible mechanisms include expansion of the EBV-infected B cells, suppression of EBV-specific T cell immunity, reactivation of EBV induced and activation-induced cytidine deaminase (AID)-dependent genomic translocation by malaria (reviewed by van Tong *et al*., 2017). B cell activation in malaria has been shown both experimentally and clinically and the risk of expansion and transition of EBV-infected B cells enhanced by increasing proliferation of polyclonal B cells could lead to the emergence of a malignant B cell clone (Rochford *et al*., 2005). In malaria patients, the failure of EBV-specific T cells to control EBV-infected cells causes the expansion and abnormal proliferation of EBV-infected B cells (Whittle *et al*., 1984). The finding that *Plasmodium falciparum* infection causes more mature B cell lymphomas by stimulating prolonged AID expression in germinal centre B cells uncovers that AID is a key player for the controlling of chronic malaria and the lymphomagenesis induced by malaria (Robbiani *et al*., 2015).

1.2.4.3.2 Hodgkin's disease (HD)

Hodgkin's disease is characterised by the presence of malignant Hodgkin/Reed-Sternberg cells (HRS) cells (Kuppers 2009) which are large, often multinucleated with a peculiar morphology and an unusual immunophenotype that is not similar to any normal cell in the body (Kuppers and Hansmann 2005) and some studies showed that in many cases of HD HRS

cells are derived from germinal centre B cells (Marafioti et al. 1997). The relationship of EBV and HD was established in 1989 due to the detection of monoclonal EBV in the HRS cells from HD (Weiss et al. 1989). EBNA 1, LMPs, the non-coding EBERs and miRNAs are expressed in EBV-infected HRS cells (Deacon et al. 1993, Niedobitek et al. 1997, Murray et al. 1992, Grasser et al. 1994).

1.2.4.4 Epithelial and other malignancies

1.2.4.4.1 Nasopharyngeal carcinoma (NPC)

NPC is a common malignancy in southern China (Yu and Ho et al., 1981) and the reports suggest that environmental factors inherent in southern Chinese are responsible for the high incidence of NPC in the region (Warnakulasuriya et al., 1999; McCredie et al., 1999; Buell, 1974). Ingestion of salted fish which is a traditional southern Chinese food favoured by the Cantonese was suggested as a cause of the high incidence of NPC (Ho et al., 1978). Several nitrosamines have been reported in Chinese salted fish (Tannenbaum et al., 1985; Zou et al., 1992; Zou et al., 1994). Other preserved foods, e.g. salted vegetables and preserved meat, were found to be related to an increase risk of NPC and like salted fish, these foods contain carcinogenic nitrosamines and other genotoxic substances (Ward et al., 2000).

The EBV genome was detected in malignant epithelial cells of patients with NPC in 1975 (Wolf, Werner and zur Hausen 1975, Davenport and Pagano 1999) (Pagano et al. 1975). Compared with EBV infection in B cells, epithelial cells are

more difficult to infect (see section 1.2 EBV) and the EBV genome is frequently missing in stable cell lines established in tumours (Dittmer et al. 2008, Cheung et al. 1999, Lin et al. 1990). It is characterised by the abundant transcription of BARF1 (Brink et al. 1998, Decaussin et al. 2000, Chen et al. 1992), which is located in the BamHI-A fragment of EBV genome and has activity as an oncogene in epithelial cells (Sbih-Lammali et al. 1996, Decaussin et al. 2000, Wei et al. 1994).

1.2.4.4.2 Gastric carcinoma

EBV was first detected in gastric adenocarcinomas in USA in 16% of the cases (Shibata and Weiss 1992) and about 10% of human gastric carcinomas are EBV-positive (Iizasa et al. 2012). The EBV genome in EBV-associated gastric carcinomas is monoclonal (Imai et al. 1994) and LMP2A is expressed in about half of EBV-associated gastric carcinomas (Sugiura et al. 1996, Luo et al. 2005). The BARF1 gene is expressed in nearly 100% of EBV-associated gastric carcinomas so it is thought that BARF1 may play as the alternative viral transforming factor (zur Hausen et al. 2000). Expression of BARF1 in gastric carcinoma cells induces significant alterations in host gene expression, particularly genes related to proliferation and apoptosis and cells expressing BARF1 show chemoresistance and increased Bcl-2 and Bax ratio (Wang et al. 2006).

1.3 RGC-32

Response gene to complement-32 (RGC-32) was first identified using mRNA differential display PCR in primary rat oligodendrocytes (OLG) in a screen to find novel genes whose expression changed as a result of sub-lytic complement treatment with C5b-9 to mimic complement activation of the cells (Badea et al. 1998). 32 cDNA species were identified in the screen and the cDNAs were designated as RGC-1 to 32 according to the order of identification (Badea et al. 1998).

The rat RGC-32 gene encodes a protein of 137 amino acids and the human RGC-32 gene encodes a protein of 117 amino acids (Badea et al. 1998). Human RGC-32 has 92% sequence similarity with rat and mouse RGC-32 (Badea et al. 1998). RGC-32 is located at 13q14.11 and this chromosomal area is involved in loss of heterozygosity (LOH) or loss of copy number in glioma cells (Nishizaki et al. 1998, Kunwar et al. 2001). Human RGC-32 has two transcript variants, a shorter and a longer form (Figure 1-6). The shorter form lacks the end of exon 1 and the start of exon 2 (Badea et al. 2002) and the longer form encodes a protein with 20 more amino acids at the N terminus (NM_014059). Data from the West laboratory confirmed the expression of the shorter form in B cell lines (Schlick et al. 2011) and the longer form has not been detected in any cells to date.

RGC-32 mRNA in rat was detected in brain, heart, kidney, lung, skin, spleen and thymus , but not in testis or liver (Badea et al. 1998). Human RGC-32 mRNA expression was found in many tissues like artery, bladder, brain, breast,

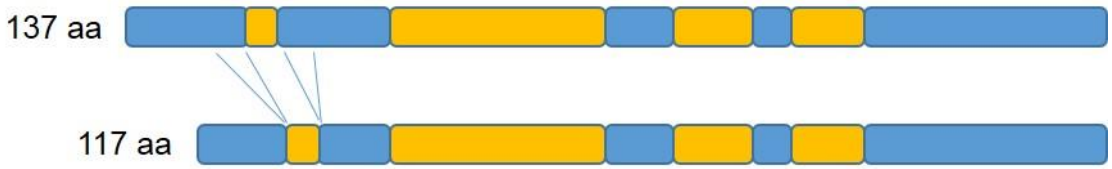

Figure 1-6. Two RGC-32 transcript variants (modified from Schlick *et al*., 2011).

Blue boxes show exons and yellow boxes show introns. Blue lines show that the end of exon 1 and the start of exon 2 of longer RGC-32 (C13ORF15) transcript (nm_014059) are spliced in shorter RGC-32 transcript (AF036549). The longer form encodes a protein with an additional 20 amino acids close to the N terminus.

cervix, colon, heart, kidney, liver, lung, muscle, nerve, ovary, pancreas, skin, stomach, testis, thyroid (NCBI GTEx). Genotype-Tissue Expression (GTEx) project is a database of gene expression on RNA level in human tissues. RGC-32 protein in human was detected in brain, heart and liver (Badea et al. 2002). RGC-32 mRNA expression was up-regulated in breast cancer (Kang et al. 2003, Fosbrink et al. 2005), colon cancer (Fosbrink et al. 2005), lung cancer (Fosbrink et al. 2005), ovarian cancer (Donninger et al. 2004), stomach cancer (Fosbrink et al. 2005), but down-regulated in multiple myeloma (Zhan et al. 2006), drug-resistant glioblastoma (Bredel et al. 2006, Saigusa et al. 2007) and high-grade astrocytomas (Saigusa et al. 2007). Overexpression of RGC-32 protein level has been reported in several human tumours including bladder, breast, lung and prostate (Fosbrink et al. 2005). All these data suggest a dual role for RGC-32 in cancer development or progression perhaps depending on the tissue type.

RGC-32 (protein sequence see Figure 4-7.) has no homology with any other known protein and contains no motif that could suggest its biochemical function (Badea et al. 1998). Human RGC-32 is localised in the cytoplasm then translocated to the nucleus when smooth muscle cells are exposed to activated complement (Badea et al. 2002). Saigusa et al. have shown that RGC-32 located in the cytoplasm of tumour cells during interphase and concentrates in centrosomes and spindle poles during prometaphase and metaphase (Saigusa et al. 2007).

Some evidence have been shown that RGC-32 plays a role on tumour promotion. Overexpression of RGC-32 in the OLG-C6 glioma cell line leads to an increase in DNA synthesis in response to serum growth factors (Badea et al. 1998). Sublytic C5b-9 induces cell cycle activation and an increase in kinase activity of CDK1, 2 and 4 (Niculescu, Badea and Rus 1999, Rus, Niculescu and Shin 1996). It has been shown that RGC-32 directly binds to CDK1 and increases its activity by glutathione S-transferase pull-down assay *in vitro* and immunoprecipitation *in vivo* and western blot (Badea et al. 2002). RGC-32 was phosphorylated by CDK1-cyclinB1 *in vitro* and mutation on Thr-91 of RGC-32 prevented the phosphorylation mediated by CDK1 (Badea et al. 2002). Overexpression of RGC-32 protein leads to S-phase and G_2/M entry in smooth muscle cells (Badea et al. 2002). RGC-32 has also been suggested to influence muscle cell differentiation as its expression is increased to 50-fold after 24 hours treatment in a microarray analysis of transforming growth factor (TGF)-β-treated neural crest cells to identify downstream targets of TGF-β-induced smooth muscle cell differentiation (Li et al. 2007). Our group supported the role of RGC-32 in proliferation of EBV-infected cells by showing stable overexpression of it alone is enough to disrupt the G2/M checkpoint in B cell lines (Schlick et al. 2011). All these findings show that RGC-32 plays a role in the promotion of cell proliferation and cell differentiation.

Other studies also suggest the role of RGC-32 as a tumour suppressor. RGC-32 expression is frequently silenced in glioma cell lines compared with normal brain and restoration of RGC-32 causes the suppression of glioma cell growth (Saigusa et al. 2007). Overexpression of RGC-32 protein delayed mitotic

progression in HeLa cells (Saigusa et al. 2007). It is associated with centrosome/spindle poles in mitosis by immunocytochemical analysis (Saigusa et al. 2007) and Plk1 is also located to the central spindle in mitosis (Barr, Sillje and Nigg 2004). Further experiments demonstrate that RGC-32 forms a complex with polo-like kinase 1 (Plk1) during mitosis and is phosphorylated by Plk1 (Saigusa et al. 2007). This suggests that RGC-32 might negatively regulate the cell cycle.

RGC-32 has been shown as a transcriptional target of p53 (Saigusa et al. 2007). It has also been identified as one of the potential downstream targets of RUNX1 as silencing of RUNX1 mRNA expression mediated by siRNA reduced the level of RGC-32 markedly (Jo and Curry 2006). We found that RGC-32 protein is differentially upregulated in EBV-positive cell lines and RGC-32 mRNA expression in human B-cells is controlled by RUNX1c (Schlick et al. 2011). We also reported that EBNA 2 activated RUNX1 expression by binding to RUNX1 upstream super-enhancer (Gunnell et al. 2016). RUNX1 super-enhancer binding by EBNA 3B and 3C attenuated the activation of RUNX1 by EBNA2 in BL cells (Gunnell et al. 2016). All these data show that the expression of RGC-32 levels depend on the balance of many transcriptional factors, e.g. EBNAs, p53 and RUNX1.

Interestingly, we found that the RGC-32 protein expression is not consistent with its mRNA expression in EBV-positive cell lines latency I and latency III due to the blocking of its translation at a post-initiation stage in latency I cells

(Schlick et al. 2011). It is still unclear how the changes of RGC-32 mRNA level by EBNAs influence the expression of its protein level.

1.4 Speedy/Ringo

RGC-32 has no homology to other human proteins, but as a CDK1 activator it may work similarly to Speedy/Ringo another class of CDK1 activator proteins.

Speedy (xSpy) was first identified to induce rapid maturation of *Xenopus* oocytes resulting in activation of M-phase promoting factor (MPF) (Lenormand et al. 1999) and *Xenopus* Rapid INducer of G_2/M progression in oocytes (xRINGO) was identified in an expression-cloning screen for genes involved in G_2/M progression in *Xenopus* oocytes (Ferby et al. 1999). The first human homologue identified has 40% homology to xSpy/xRINGO and was named Spy1 and it was proposed to be a new cell cycle regulator which can promote cell proliferation by activating CDK2 at G_1/S transition (Porter, Kong-Beltran and Donoghue 2003).

xSpy/xRINGO can directly activate CDK1 and CDK2 (Karaiskou et al. 2001) and mammalian Speedy/RINGO family members can bind to and activate CDK1 and CDK2 with different efficiencies, but cannot activate CDK4 and CDK6 (Cheng et al. 2005a, Dinarina et al. 2005). Interestingly, the activation of CDK1 and CDK2 by Speedy/RINGO proteins does not require phosphorylation in the activation loop of the kinase domain by CAK (Karaiskou et al. 2001,

Cheng et al. 2005a, Cheng et al. 2005b), which is necessary for full activation of CDKs by cyclins. Another important difference from CDK/cyclin complexes is that CDK1 and CDK2 activated by xRINGO are less sensitive to inhibition by Myt1 which negatively regulates CDK1 activity through phosphorylation on residues Threonine 14 and Tyrosine 15 (Karaiskou et al. 2001).

1.5 Aim of the project

RGC-32 is upregulated in EBV-infected cells, binds CDK1 and Plk1 and plays a role in cell cycle regulation. RGC-32 has no homology with any other known proteins. This project set out to express and purify soluble milligram quantities of RGC-32 for functional and structural studies, investigate the interaction between RGC-32 and CDK1, Cyclin B1 and Plk1, examine the effect of RGC-32 on cell cycle regulation and investigate the potential role of EBV latency III gene products in the regulation of RGC-32 mRNA expression.

2 Materials and Methods

2.1 Reagents

Phosphate buffer:

Buffer	0.1M PO_4 buffer pH7.5
1M Na_2HPO_4	15ml
1M NaH_2PO_4	5ml
MilliQ H2O	180ml
Total vol	**200ml**

Blotting buffer: 1 litre Methanol (Fisher), 75 g Glycine (Fisher), 15 g Tris (hydroxymethyl)-methylamine (Fisher) and 4 litre dH_2O.

Buffers for His-RGC-32 purification:

Buffer A: 40 mM PO_4 buffer pH7.5, 300 mM NaCl, 2 mM Benzamidine, 2 mM Imidazole and 3.55 mM B-ME.

Buffer B: 40 mM PO_4 buffer pH7.5, 300 mM NaCl, 2 mM Benzamidine, 2 mM Imidazole, 3.55 mM B-ME and 10% NP40.

Buffer C: 40 mM PO_4 buffer pH7.5, 1 M NaCl, 2 mM Benzamidine, 2 mM Imidazole, 3.55 mM B-ME and 10% NP40.

Buffer D: 40 mM PO_4 buffer pH7.5, 300 mM NaCl, 2 mM Benzamidine, 2 mM Imidazole, 3.55 mM B-ME.

Buffer E: 40 mM PO_4 buffer, 300 mM NaCl and 100 mM EDTA.

Buffer F: 20 mM PO_4 buffer and 200 mM NaCl.

Buffer (volume/final concentration)	X	Y
1M HEPES (KOH) pH7.5	2.5ml / 50mM	1.25ml / 50mM
100% Glycerol	5ml / 10%	2.5ml / 10%
200mM Benzamidine (add just before use)	500ul / 2mM	250ul / 2mM
GuHCL (powder)	4.7765g / 1M	14.3295ul / 6M
MilliQ H_2O	42ml	21ml
Total vol (final pH7.5)	50mls	25mls

Buffers for GST-RGC-32 purification:

Lysis buffer: 20 mM HEPES Ph7.5, 500 mM NaCl and 5 mM EDTA.

Elution buffer (pH 7.5): 20 mM HEPES Ph7.5, 500 mM NaCl and 20 mM L-Glutathione

PreScission buffer: 20 mM HEPES Ph7.5, 500 mM NaCl,

CsCl plasmid purification buffers:

CsCl prep solution I: 50 mM Glucose, 25 mM Tris-HCl pH 8.0, 10 mM EDTA (Sigma).

CsCl prep solution II: 200 mM NaOH, 1% SDS.

CsCl prep solution III: 300 ml 5 M KAC, 57.5 ML Glacial Acetic Acid, 142.5 ml H_2O.

CsCl-saturated butanol: 100 g Caesium Chloride (Invitrogen) in 200 ml H_2O and 200 ml butanol.

The destaining buffer (kinase assay): 10% Ethanol, 5% Acetic Acid and 85% H_2O.ECL solution: Solution I: 2.5 mM Luminol, 396 µM Coomaric Acid and 100 mM Tris pH 8.5 in 2ml H_2O. Solution II: 0.0192% Hydrogen Peroxide (H_2O_2) and 100 mM Tris pH 8.5 in 2 ml H_2O. Mix solution I and II before use.

Fixing and staining buffer (kinase assay): 40% Methanol, 7% Acetic Acid and 1.14 mg/ml Brilliant Blue R (Sigma-Aldrich) and 53% H_2O.

GSB (gel sample buffer): 50 mM Tris, 4% SDS, 5% 2-Mercaptoethanol (Sigma), 10% glycerol, 1 mM EDTA and 0.01% Bromophenol Blue.

Lysis buffer (Niculescu et al. 1997): 50 mM Tris-HCl pH 7.5, 150 mM NaCl, 20 mM MgCl2, 10 mM EDTA, 1% Nonidet P-40 (Sigma) and 0.5% (w/v) Sodium Deoxycholate.

PBS-T: 100 PBS tablets (Fisher) and 10 ml Tween 20 (Fisher) in 10 litre dH_2O.

2.2 Cell lines

Akata

Akata cell line was derived from a Japanese patient with Burkitt's lymphoma and t(8;14) translocation (Takada et al., 1991).

BJAB

BJAB cell line was isolated from human Burkett's lymphoma which is EBV negative, but does not have a c-myc translocation characteristic of Burkitt's lymphoma cell lines.

DG75

DG75 cell line was a gift from M. Rowe and was established from a 10-year-old boy with EBV-negative Burkitt's lymphoma in 1975 (Ben-Bassat *et al*., 1977).

Mutu I

The Mutu I cell line clone 179 was a gift from Martin Rowe (University of Birmingham). Mutu I cells only express EBNA1 and EBERs (Gregory, Rowe and Rickinson 1990) and are cultured in RPMI supplemented with 10% FBS and 1% PSG. Mutu I cells are passaged 1 in 5 twice per week.

Mutu III

The Mutu III cell line clone 48 was a gift from Martin Rowe. Mutu III cells arose spontaneously from Mutu I cells and express all EBV genes: EBNA1, 2, 3A, 3B and 3C and LMP1, 2A and 2B and EBERs (Sinclair et al. 1995).

Adherent cell lines

HEK293

HEK293 cell line was generated by transformation of human embryonic kidney (HEK) cells with sheared fragments of human adenovirus type 5 (Ad5) DNA (Davies et al., 1977).

HeLa

HeLa cell line was derived from a human cervical carcinoma from a 31 years old woman in 1951, which is epithelial cell line and were transformed by human papillomavirus 8 (Scherer et al., 1953). HeLa cells were cultured in DMEM supplemented 10% FBS and 1% PSG at 37°C with 5% CO2 and were passaged by trypsinization 1 in 10 twice weekly.

2.3 Molecular Biology

2.3.1 Agarose gel electrophoresis

1 g agarose powder (Helena BioSciences) was added to 100 ml 1×Tris/Borate/EDTA (TBE) buffer, dissolved by heating in a microwave and then cooled. 0.5 µl Gel Red (Biotium) was added and the agarose mixture was then poured into a BioRad Mini-Sub Cell GT tank (BIO-RAD) with a comb to set. The

comb was removed once the gel was set and the gel was submerged in 1×TBE then run at 90 V 400 mA for about 1 hour.

2.3.2 Transformation of bacterial cells

Around 100 ng of plasmid DNA was mixed with 100 µl of competent *E.coli* DH5α cells and incubated on ice for 45 minutes. The cells were then heat-shocked at 42°C for 45 seconds and left on ice for 2 minutes. Transformed cells were spread on agar plates with appropriate antibiotics using a sterile glass spreader then colonies grown at 37°C overnight.

2.3.3 Small-scale purification of DNA (Miniprep)

A colony was picked using a pipette tip and grown in 2 ml LB containing appropriate antibiotics. The transformed bacteria were incubated at 37°C overnight with shaking. The overnight culture was pelleted by centrifugation at 13,000 rpm (16,060 x g) for 1 minute using accuSpin Micro R Benchtop Centrifuge (Fisher). Plasmid DNA was extracted using a QIAprep Spin Miniprep Kit (250) (Qiagen) according to manufacturer's instructions.

2.3.4 Large-scale Caesium chloride (CsCl) DNA purification

5 ml LB with proper antibiotics was inoculated with a single colony and grown at 37°C during the day with shaking.The culture was transferred into 400 ml LB with appropriate antibodies and cultured at 37°C overnight. Cells were pelleted by centrifugation at 6,000 rpm (10,598 x g) for 10 minutes at 4°C using a JA-10

rotor in Beckman Coulter Avanti J-20 XP centrifuge. The cell pellet was resuspended in 14 ml solution I and then 28 ml of solution II to lyse the cells. 22 ml solution III was then added and cell debris was pelleted by centrifugation at 7,000 rpm (10,644 x g) for 10 minutes at 4°C using Heraeus Megafuge 8R centrifuge (Thermo Scientific). The supernatant was filtered through Kim wipes. 0.6 volume of isopropanol was added and the sample was left 5-10 minutes at room temperature to precipitate DNA. The samples were spin down at 4,000 rpm (6,082 x g) for 15 minutes at 4°C using Heraeus Megafuge 8R centrifuge (Thermo Scientific) and then the pellets were dissolved in 6 ml MilliQ H_2O and 5 M NH4 acetate was added to precipitate the RNA.

After 1 hour incubation on ice, the samples were spin down at 4,000 rpm (6082 x g) for 10 minutes at 4°C using Heraeus Megafuge 8R centrifuge (Thermo Scientific) and 2 volume of 100% ethanol was added to the supernatant to precipitate DNA. After 10 minutes incubation at room temperature the samples were centrifuged at 4,000 rpm (6,082 x g) for 10 minutes at 4°C using Heraeus Megafuge 8R centrifuge (Thermo Scientific). Resuspended the pellets in 4 ml MilliQ H_2O and 4.3 g CsCl and 1 mg Ethidium Bromide was added. The samples were removed to optiseal centrifuge tube (Beckman) and placed in Vti 65.2 rotor. The centrifugation at 50,000 rpm (376,250 x g) overnight was used to separate plasmid DNA and chromosomal DNA in Beckman Optima LE-80K centrifuge.

Used a 19G needle to extract the plasmid DNA and Ethidium bromide was washed by adding an equal volume of CsCl saturated butanol several times. Dilute the DNA with 3 volume MilliQ H_2O and 2 volume of ethanol. After 1 hour incubation at -20°C, spin down at 4,000 rpm (6,082 x g) for 20 minutes at 4°C using Heraeus Megafuge 8R centrifuge (Thermo Scientific) and resuspended in 250 µl nuclease free H_2O. The concentration of plasmid DNA was determined by spectrophotometry.

2.3.5 Spectrophotometric determination of DNA concentration

2 µl of DNA were diluted in 98 µl H_2O in a UV-cuvette micro (Plastibrand) and measured in Eppendorf BioPhotometer at 260nm.

2.3.6 Coomassie staining

After SDS-PAGE, the gel was washed with MilliQ H_2O twice for 5 minutes and then submerged in Bio-Safe Coomassie stain (BIO-RAD) for 1 hour on a shaker. The gel was washed with MilliQ H_2O three times for 5 minutes and left in MilliQ H_2O overnight at room temperature on a shaker. The gel was placed on filter paper and then dried using a vacuum gel dryer for 45 minutes at 80ºC.

2.3.7 Immunoprecipitation

2×10^7 cells were lysed in 1 ml lysis buffer (Niculescu et al. 1997) with 1 mM PMSF, protease inhibitor cocktail and phosphatase inhibitor cocktail and left on ice for 30 minutes. Samples were then sonicated at 30% amplitude for 5 × 10

seconds with 10 seconds intervals. The debris was removed by centrifugation for 5 minutes at 13,000 rpm (16,060 x g) at 4ºC using accuSpin Micro R Benchtop Centrifuge (Fisher). The lysates were pre-cleared with 40 µl 1:1 Protein A-Sepharose beads slurry (Sigma-Aldrich) by incubating for 30 minutes at 4ºC with rotating. Then lysates were spun briefly and 2 µg of normal mouse IgG, anti-cyclin B1 antibody (GNS1, Santa Cruz) or anti-CDK1 antibody (cdc2 p34, Santa Cruz) were added and the samples incubated on ice for 30 minutes. The immune complex was captured by adding 40 µl 1:1 Protein A-Sepharose beads (Sigma-Aldrich) slurry and incubated at 4ºC with rotation overnight. The following day, the beads were washed with 3 × 0.5 ml lysis buffer and 2 × 0.5 ml kinase buffer. After washing, the samples were divided into two for kinase assay and western blotting.

2.3.8 Kinase Assay (in vivo)

After immunoprecipitation, beads were spun down and resuspended in 5.2 µl mastermix including 3 µl kinase buffer, 2 µl 1 mg/ml Histone H1 and 0.2 µl 5 µCi/µl ^{32}P-γATP. After incubation at 37ºC for 10 minutes, samples were placed on ice and 20 µl 2 × GSB then added followed by western blotting.

2.3.9 Kinase Assay (in vitro)

cdk1/cdc2 Kinase Assay Kit (upstate) method:

2 units of recombinant CDK1/cyclin B1 (NEB) in a 1:10 dilution of Assay Dilution Buffer I (ADBI) (cdk1/cdc2 Kinase Assay Kit upstate) were mixed with 0.7 µM, 1.4 µM and 2.8 µM of RGC-32 protein in elution buffer.

After 10 minutes incubation at 30 ºC, 12.5 µl of 5×GSB was added and the samples were heated at 95ºC for 10 minutes for SDS-PAGE. After SDS-PAGE, the gel was fixed and stained by rocking 1 hour in fixing and staining buffer and then destained by rocking in destaining buffer and changing the buffer several times during destaining. Finally, the gel was dried onto filter paper (Whatman) for 45 minutes at 80 ºC. The dried gel was then exposed to a phosphor screen for various times depending on the intensity of the radioactivity. The phosphor screen was scanned by a Storm 860 scanner and analysed using ImageQuant 5.1 software (Amersham Biosciences).

In house kinase assay method:

2 units of recombinant CDK1/cyclin B1 (NEB) in kinase buffer, 8 µg Histone H1 (MERCK) was mixed with 0.7 µM, 1.4 µM and 2.8 µM of RGC-32 protein in elution buffer.

2.3.10 Histidine-tagged RGC-32 preparation

The *E. coli* strain BL21 pLysS was transformed with pET-16b-RGC-32 (Schlick et al., 2011). The bacteria were streaked out on a plate with 100 µg/ml ampicillin and 42 µg/ml chloramphenicol and grown overnight at 37ºC. The following day

50 ml LB with appropriate antibiotics was inoculated with a single colony and grown overnight at 37ºC. The next day 4 ml of the culture was added to each of 5×flasks with 400 ml LB and grow at 37ºC until the OD 600 nm reached 0.5. 1 mM IPTG was added and cells grown at 37ºC for 4 hours. The cells were then pelleted at 8,000 rpm (14,131 x g) at 4ºC for 15 minutes using a JA-10 rotor in Beckman Coulter Avanti J-20 XP centrifuge and the pellets were resuspended in total 80 ml cold Buffer A. To lyse the cells, the bacteria were frozen and thawed 3 times and then left at room temperature for 15 minutes after adding 10 µg/ml DNase I. The cell lysates were sonicated 6×10 seconds with 10 seconds gaps at 25% amplitude using Vibra-Cell sonicator (SONICS) and then centrifuged at 9,800 rpm (22,666 x g) at 4ºC for 20 minutes using JA-20 rotor (Beckman) in a Beckman Coulter Avanti J-20 XP centrifuge and resuspended in 20 ml Buffer X. This step was repeated and afterwards centrifuged at same condition but repsuspended in 20 ml Buffer Y.

1:1 slurry of HIS-Select Nickel Affinity Gel (Sigma-Aldrich) was added into the supernatant and rotated for 90 minutes at 4ºC. To refold the protein, beads were then washed twice with 25 ml Buffer A, Buffer B, Buffer C and Buffer A. To elute the protein, 1 ml Buffer E was added and the beads were rotated for 20 minutes at 4ºC. This step was repeated 5 times and the first 3 elutions pooled together. 40 µl of each sample of elution 1~3, 4, 5 and 6 was added 10 µl 5 × GSB.

2.3.11 Dialysis

RGC-32 protein elutions 1~3 was dialysed following the instructions by Slide-A-Lyzer Dialysis Cassettes (Thermo SCIENTIFIC) for 2 hours at 4ºC against 600 ml Buffer F. The buffer was then changed and samples dialyzed for another 2 hours. Following another change of buffer, samples were dialyzed overnight at 4ºC.

2.3.12 GST-tagged RGC-32 preparation

RGC-32 was cut out of pFLAG-RGC-32 (created by Helen Webb) as a BamHI/NotI fragment and cloned into pGEX-6P3 digested with BamHI/NotI (Figure 2-1). The pGEX-6P3-RGC-32 was transformed into competent cells (Rosetta or Arctic cells). One colony was used to inoculate 100 ml of LB media containing 150 µg/ml ampicillin, which was placed in a 37°C shaker overnight. The next day 100 ml out of this overnight culture was used to inoculate 10 L of LB media (10 ml overnight culture used per 1 L) containing 150 µg/ml ampicillin and 30 µg/ml chloramphenicol. When the OD 600 nm reached 0.8 the flasks were put on ice for 45 minutes and then the cells were induced by 0.8 mM IPTG overnight at 18°C. The next day the cells were harvested by centrifugation at 4,000 rpm (7,066 x g) for 20 minutes using a JA-10 rotor in Beckman Coulter Avanti J-20 XP centrifuge. The cell pellet was either stored at -20°C until required or used directly for purification. The clarified cell extract was incubated with 5ml of Glutathione Sepharose 4B beads (GE Healthcare), pre-washed with lysis buffer three times, with rotation for 4 hours at 4ºC. The beads were then washed twice with 35ml wash buffer (20 mM HEPES pH7.5 and 500 mM NaCl). The protein was eluted with 3ml of elution buffer re-adjusted pH to 7.5 (20 mM

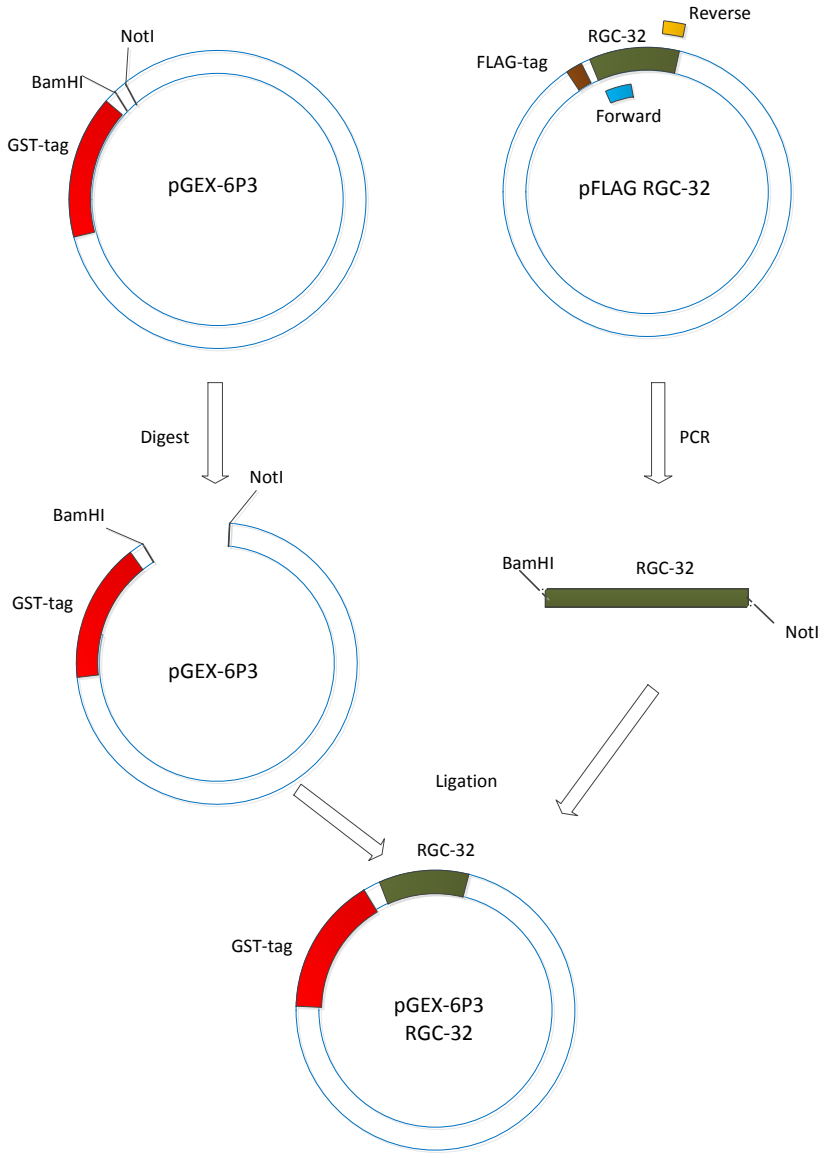

Figure 2-1. Schematic graph of cloning process.

RGC-32 was cut out of the pFLAG-RGC-32 plasmid (created by Helen Webb) as a BamHI/NotI fragment and cloned into pGEX-6P3 vector.

HEPES pH7.5, 500 mM NaCl and 20 mM L-Glutathione) then incubated at room temperature for 10minutes. The eluted protein was incubated with PreScission buffer (200µl 2mg/ml PreScission in 20 mM HEPES pH7.5, 500 mM NaCl and 1 mM DTT) with rotation at 4°C overnight. The protein was then injected onto a desalting column pre-equilibrated in 20 mM HEPES pH7.5, 500 mM NaCl and 1 mm DTT. The eluted protein was then passed through a 5ml GSTrapTM pre-equilibrated with 20 mM HEPES pH7.5, 500 mM NaCl and 0.5 mM tris (2-carboxyethyl) phosphine (TCEP) to remove cleaved GST. The sample was further purified using a gel filtration column S75 16/600 pre-equilibrated in 20 mM HEPES pH7.5, 500 mM NaCl and 0.5 mM TCEP.

2.3.13 Bradford Assay

10 µl diluted or undiluted protein samples were added to 200 µl 1:5 dye reagent (BIO-RAD) and absorbance at 600 nm was measured using GloMax-Multi Detection System (Promega).

2.3.14 SDS-PAGE

Cell lysates in gel sample buffer (GSB) were heated at 95ºC for 10 minutes and vortexed. 5 µl of SeeBlue Plus2 Pre-Stained Standard marker (Invitrogen) and 15 µl of each sample were loaded onto NuPAGE Bis-Tris gels (Invitrogen) and the gels were run in 1×MES or 1×MOPS NuPAGE SDS running buffer (Invitrogen) according to the size of proteins. Gels were electrophoresed at 200V for 35 minutes for MES or 50 minutes for MOPS.

2.3.15 Western Blotting

After SDS-PAGE, proteins were transferred to Protran Nitrocellulose Transfer Membrane (Whatman) in blotting buffer at 85 V for 90 minutes using a Trans-Blot Cell (BIO-RAD). The membrane was stained in Ponceau S stain for 1 minute, rinsed in PBS-T and then blocked with shaking in 5% milk in PBS-T for 1 hour to prevent non-specific binding. The appropriate primary antibody diluted in 10 ml 5% milk in PBS-T was added to the membrane and incubated on a rocker overnight at 4ºC. The following day the membrane was washed with PBS-T three times for 10 minutes and then incubated in secondary antibody conjugated to horseradish peroxidise diluted in 10 ml 5% milk in PBS-T for 1 hour on a rocker. The membrane was then washed again with PBS-T three times for 10 minutes. The membrane was incubated with 4 ml enhanced chemiluminescence (ECL) solution and then exposed to Fuji medical X-ray film (Fisher) for different times. The films were developed using a Konica SRX-101A processor.

2.3.16 Pull down assay

The pGEX-6P3, pGEX-6P3-RGC-32 and pGEX-6P3-RGC-32 T91A were transformed into competent cells (Rosetta cells). One colony was used to inoculate 100 ml of LB media containing 150 µg/ml ampicillin and 30 µg/ml chloramphenicol. pGEX vector has ampicillin resistance and Rosetta has pLysS which is a designation given to hosts carrying a chloramphenicol-resistant plasmid. When the OD 600 nm reached 0.8 the flasks were put on ice for 45 minutes and then the cells were induced by 0.8 mM IPTG overnight at 18°C.

The next day the cells were harvested by centrifugation at 4,000 rpm (6,082 x g) for 20 minutes at 4°C using Heraeus Megafuge 8R centrifuge (Thermo Scientific). Cell pellets were dissolved in 1 ml lysis buffer (20 mM HEPES pH7.5, 500 mM NaCl, 5 mM EDTA and 1 tablet per 50 ml proteinase inhibitor cocktail EDTA-free (Roche)) and sonicated at 40% amplitude 10 minutes with 10 seconds on and 20 seconds off. The cell debris was pelleted at 13,000 rpm (16,060 x g) for 1 hour at 4°C using accuSpin Micro R Benchtop Centrifuge (Fisher) and the supernatant was incubated with 50 µl glutathione beads, pre-washed with purification buffer three times, with rotation at 4°C overnight.

2×10^7 BJAB or Mutu I cells were lysed in 1 ml lysis buffer (Niculescu et al. 1997) with 1 mM PMSF, protease inhibitor cocktail and phosphatase inhibitor cocktail and left on ice for 30 minutes. Samples were then sonicated at 30% amplitude for 5 × 10 seconds with 10 seconds intervals. The debris was removed by centrifugation for 5 minutes at 13,000 rpm (16,060 x g) at 4ºC using accuSpin Micro R Benchtop Centrifuge (Fisher). The lysates were added into the glutathione beads and left at room temperature for 30 minutes. The beads were washed with 2 × 0.5 ml lysis buffer. After washing, the samples were used for Western blot.

2.3.17 Transient transfection (Electroporation)

Cells were split 1 in 3 one day before electroporation . The next day cells were pelleted at 1,300 rpm (1,606 x g) for 10 minutes at 4ºC using accuSpin Micro R Benchtop Centrifuge (Fisher) and the supernatant was kept as conditioned

media. DNA in total maximum volume of 50 µl was incubated on ice for 10 minutes in electroporation cuvettes (Bio-Rad). The cells were resuspended in serum free media to count, then pelleted and resuspended at 2 x 10^7 cells/ml in cold serum free media. 1 x 10^7 cells were added to each cuvette and mixed, then incubated on ice for 10 minutes. The samples were electroporated at 230 V and 950 µF using a BioRad Gene Pulser II. Cells were incubated at 37 ºC for 30 minutes then transferred to flasks containing 9 ml conditioned media. The samples were incubated at 37ºC for 48 hours. Cells were pelleted and resuspended in 10 ml PBS, then counted. Then cells were pelleted and resuspended in 1 ml PBS to transfer into a 1.5 ml tube. The cells were pelleted at 6,000 rpm (7,412 x g) for 5 minutes using accuSpin Micro R Benchtop Centrifuge (Fisher) and the supernatant was removed. The cell pellets were snap frozen on dry ice and stored at -80ºC until required.

2.3.18 Transient transfection (Effectene Transfection Reagent from QIAGEN)

Day before transfection, 7x10^5 cells were seeded in 60 mm dish in 5 ml appropriate growth medium containing serum and antibiotics. On the day of transfection (40-80% confluent), dilute 3 µg of DNA (empty & fusion) with a minimum concentration of 0.1µg/µl with the DNA condensation buffer EC to a final volume of 450 µl. After 24 µl of Enhancer was added, samples were mixed by vortexing for 1 second and incubated at room temperature for 2-5 minutes then span down for a few seconds. 75 µl Effectene Transfection reagent was added to the DNA-Enhancer mixture. Samples were mixed by pipetting up and

down 5 times, or by vortexing for 10 seconds. The samples were incubated for 5-10 minutes at room temperature to allow transfection-complex formation. The growth medium was gently aspirated from the plate and cells were washed once with 4 ml of PBS. 4 ml fresh growth medium (complete) was added to the cells and 1 ml growth medium to the transfection complex. It was mixed by pipetting twice and added immediately drop-wise onto the cells in the dish. The dish was gently swirled to ensure uniform distribution of the transfection complexes. The cells were incubated with the transfection complexes for 18 hours then washed with PBS and 5 ml of fresh growth medium (complete) was added to cells. The cells were harvested and check for protein expression by western blotting.

2.3.19 Stable transfection

RGC-32 was cut of pUC19 RGC-32 as an SfiI/SfiI fragment and cloned into pRTS-1 (gift from Georg W. Bornkamm Figure 2-2) digested by SfiI. 10 µg pRTS-1α RGC-32 was transfected into DG75 cells using electroporation and cells were incubated for 48 hours at 37ºC and 5% CO_2. Cells were then counted and plated into 96-well plates in 100 µl at a density of 5, 50 and 500 viable cells per well and the spare cells were bulk cultured in flasks. Cells were cultivated in growth medium supplemented with 100 µM α-thioglycerol and 3 mM sodium pyruvate. After 5-6 days, 100 µl supplemented growth medium was added containing 200 µg/ml hygromycin B. After that, replace 50 µl of the cell supernatant with supplemented selection medium weekly.

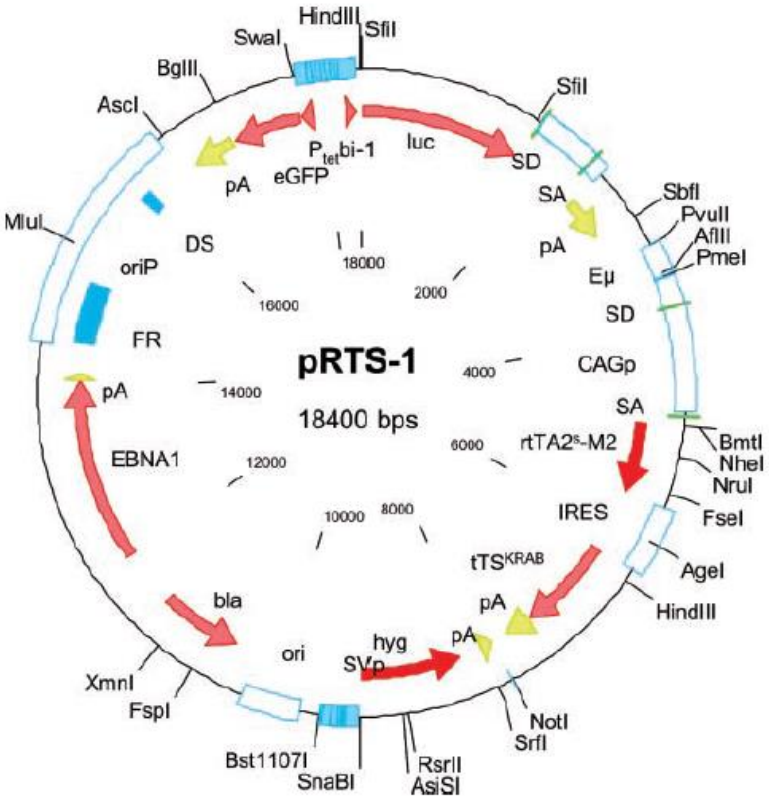

Figure 2-2. pRTS-1 vector map.

It has a bidirectional promoter driving expression of two genes (firefly luciferase and eGFP) and ampicillin-resistance gene, hygromycin B resistance gene, the EBV episomal origin of replication (*oriP*) and the EBNA 1 gene. (Bornkamm et al., 2005). Ptetbi-1 is the bidirectional tetracycline-regulated promoter. *oriP* is the EBV episomal origin of replication carrying the family of repeats (FR) and the dyad symmetry elements (DS). RGC-32 was cut of pUC19 RGC-32 as an SfiI/SfiI fragment and cloned into pRTS-1 digested by SfiI.

2.3.20 Doxycycline treatment of stable expression of RGC-32 DG75 cells

1 µg/ml doxycycline was added to stable expression of RGC-32 DG75 cells and after 48 hours, the expression of RGC-32 was verified by Western blot.

2.3.21 Luciferase assay

48 hours after transfection cells were pelleted at 1,300 rpm (1,606 x g) for 10 minutes at 4ºC using accuSpin Micro R Benchtop Centrifuge (Fisher) and resuspended in 10 ml PBS and 1 ml was used as samples for Western blot analysis. The remaining 9 ml cells were pelleted and the cell pellet lysed in 90 µl passive lysis buffer (Promega) at room temperature for 30 minutes followed by another 30 minutes on ice. Cell debris were pelleted at 13,000 rpm (16,060 x g) for 5 minutes using accuSpin Micro R Benchtop Centrifuge (Fisher) and the supernatant was transferred to a new eppendorf. 2 x 10 µl of each lysate was added to a 96-well plate. 50 µl of Luciferase Assay Reagent II (LAR II) reagent followed by 50 µl of Stop and Glo reagent (Promega luciferase dual assay kit) were added to the lysates, then the signals were measured using injector Dual-luciferase protocol of Promega.

2.3.22 Etoposide treatment

Different concentrations (depend on the cell type) of etoposide were added to cells and incubate at 37ºC with 5% CO_2 for 8, 24 or 48 hours. The cells were harvested and washed. After counting in PBS, half of the cells was fixed in 1 ml

of 70% ethanol per 10^6 cells at 4ºC for at least 30 minutes then stained with prodidium iodide. The other half was used for protein analysis.

2.3.23 Propidium Iodide staining

After cells were washed in PBS and counted, 1 x 10^6 cells were transferred to a FACS tube and pelleted at 1,000 rpm (1,235 x g) for 5 minutes at 4ºC using accuSpin Micro R Benchtop Centrifuge (Fisher). Celle were fixed by suspending in ethanol at 1 x 10^6 cells/ml then washed twice in PBS. The pellet was resuspended in 500 µl PI stain containing 12 µl Rnase (2 mg/ml) and samples were incubated at room temperature for at least 30 minutes. The cell cycle distribution was analysed with the BD FACSCanto Flow Cytometer (BD Biosciences).

2.3.24 Real-time Polymerase Chain Reaction

Quantitative PCR (qPCR) was performed in duplicate using an Applied Biosystems 7500 real-time PCR machine. For ChIP-qPCR analysis, 3 µl DNA was added to a SYBR master mix containing 7.5 µl 2×GoTaq qPCR Master Mix (Promega), 150 µM forward and reverse primers and sterile Millipore water to a final volume of 15 µl. Input controls were diluted 4 fold to generate a standard curve for each primer set. The following conditions was used: initial denaturation step at 95ºC for 10 minutes, 40 cycles amplification step at 95ºC for 15 seconds and 60ºC for 1 minute. A dissociation curve was used by one cycle at 95ºC for 15 seconds, at 60ºC for 1 minute and 95ºC for 15 seconds.

3 Purification of RGC-32 for functional and structural studies

3.1 Introduction

RGC-32 was first identified in rat and encodes a protein of 137 amino acids. The human RGC-32 gene encodes a protein of 117 amino acids as a result of differential splice site usage and runs with a molecular weight of 15 kD on SDS-PAGE (Badea et al. 1998, Badea et al. 2002). Human and mouse RGC-32 share 92% homology with rat RGC-32, but human RGC-32 has no homology with other human proteins (Badea et al. 1998, Badea et al. 2002). Secondary structure prediction using JPRED (http://www.compbio.dundee.ac.uk/jpred/) identifies three possible α-helical regions in RGC-32 (Figure 3-1). The aim of this chapter was to express and purify soluble milligram quantities of RGC-32 for functional and structural studies.

3.2 Can RGC-32 increase CDK1 activity without cyclin B1?

RGC-32 was shown to bind to the CDK1/cyclin B complex *in vitro* and increase its activity (Badea et al. 2002). This activation was dependent on phosphorylation of threonine 91 of RGC-32 by CDK1 (Badea et al. 2002). RGC-32 has no homology with other proteins and there is no motif that could imply its function (Badea et al. 1998). However, the action of a protein (RINGO) described as rapid inducer of G_2/M progression in *Xenopus* oocytes could indicate a possible mechanism for CDK1 activation by RGC-32. RINGO has no

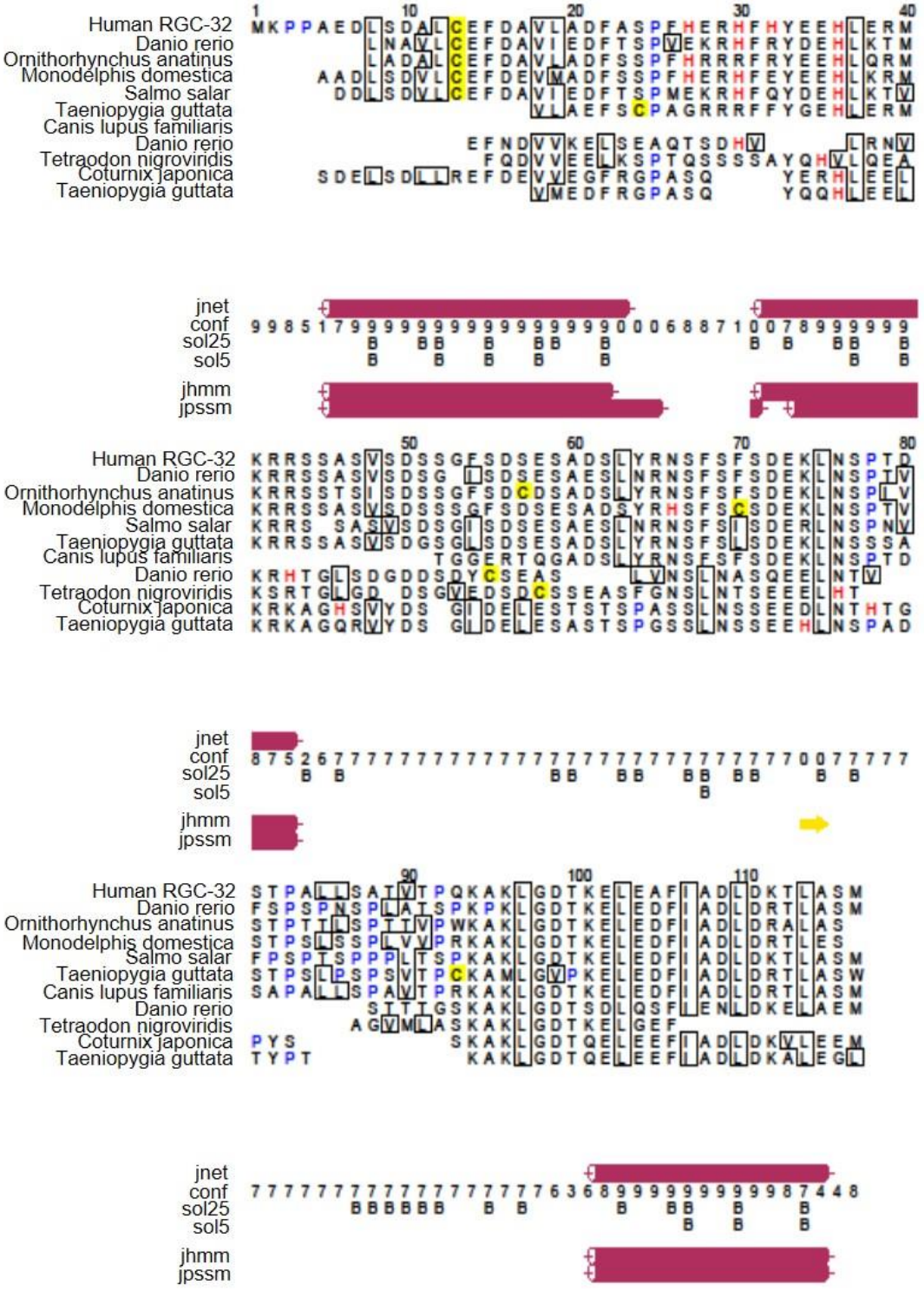

Figure 3-1. RGC-32 secondary structure prediction using JPRED.

RGC-32 amino acid sequence was aligned in UniRef database which combines identical sequences from any organism. The accession numbers link to the corresponding UniProtKB and UniParc records. Cysteine is highlighted as yellow, proline as blue and histidine as red. Aliphatic residues (Isoleucine, leucine and valine) are boxed. The three predicted α-helices in RGC-32 are shown as red cylinders under the sequences.

homology with RGC-32, but may be a functional homologue as it also binds and activates the kinase activity of CDK1 (Badea et al. 2002, Ferby et al. 1999). Interestingly, RINGO associates with CDK1 in the absence of cyclin B1 (Ferby et al. 1999).

Experiments were therefore designed to test whether RGC-32 can increase CDK1 activity in the absence of cyclin B1. Previously purified recombinant His-RGC-32 prepared via denaturation from inclusion bodies and renaturation would be incubated with extracts from Sf9 insect cells infected with a recombinant baculovirus expressing untagged human CDK1 (gift from D. Morgan) and the kinase activity would be determined using Histone H1 kinase assays based on previous protocol (Badea et al. 2002) (see figure 3-2). CAK, a complex of CDK7 and cyclin H, phosphorylates CDK1 and cyclin B1 complex at Threonine 161 in CDK1 to make it reach the full activity (Solomon et al. 1992). The CDK1 in extract used in this experiment was activated by insect CAK. Recombinant His-tagged cyclin B1 (165-433) (plasmid provided by E. Petri) purified from *E. coli* cells will be used.

RGC-32 cloned in pET-16b vector was expressed in E.coli strain BL21 *pLysS* as a tagged protein with an N-terminal His tag. His-RGC-32 expression was induced by IPTG and purified using denaturation and renaturation techniques. The purity of His-RGC-32 after Nickel affinity purification was checked by SDS-PAGE followed by Coomassie staining. The His-tagged RGC-32 protein has a molecular weight of 14 kD and around 3 ml His-RGC-32 (0.4 mg/ml) was

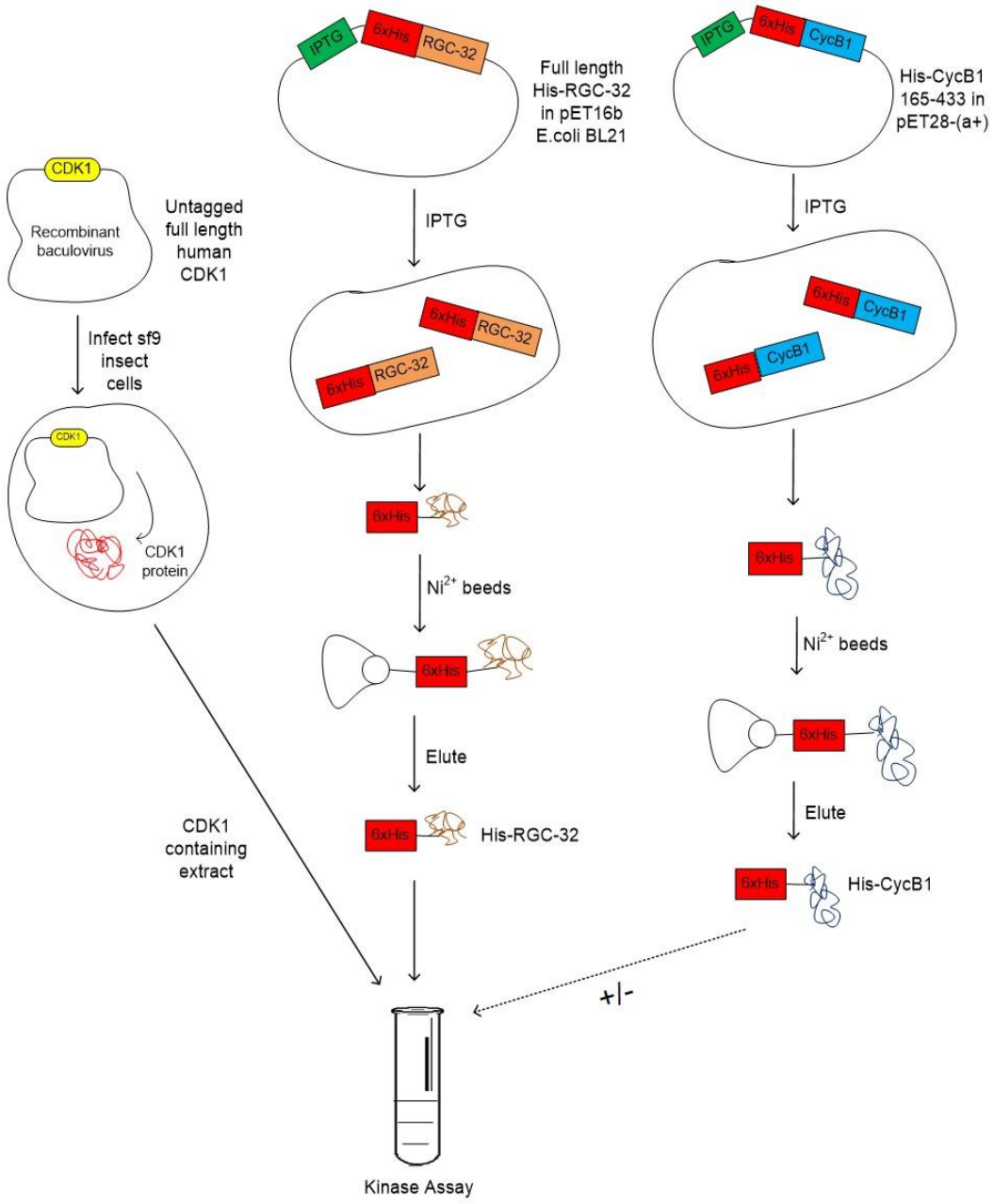

Figure 3-2. The strategy to study if RGC-32 can activate CDK1 activity in the absence of Cyclin B1.

Recombinant RGC-32 is incubated with extract from insect cells infected with a CDK1-expressing recombinant baculovirs (gift from D. Morgan) and histone H1 kinase assays is carried out. Control experiments use soluble, active, bacterially expressed truncated Cyclin B (plasmid provided by E. Petri) to activate CDK1.

obtained from 2 L culture. His-RGC-32 was yielded with a high degree of purity from the pooled elutions 1~3 (0.25 mg/ml) and the concentration decreased in following elutions (Figure 3-3).

Recombinant baculovirus carrying untagged full length CDK1 was used to infect Sf9 insect cells and an extract was made. Western blotting analysis confirmed expression of CDK1 in infected Sf9 cells. The full length CDK1 protein has a molecular weight of 34 kD and strongest expression was when the cells were infected at 0.5% and 1% (Figure 3-4).

Expression of pET-28(a+) cyclin B1 (residues 165-433) was carried out in *E. coli* strain BL21 *plysS*. N-terminal 165 residues of Cyclin B1, which is removed from Cyclin B1 to improve solubility has been demonstrated natively unfolded (Cox et al. 2002). Cyclin B1 (165-433) containing a PEST sequence on C-terminal and Cyclin box required for CDK1 activity and binding has been purified in previous experiments successfully (Petri et al. 2007). Cyclin B1 (residues 165-433) protein has a molecular weight of around 30 kD and was induced as expected on incubation in the presence of IPTG (Figure 3-4). Different induction temperatures were used (15ºC and 37ºC) and Cyclin B1 protein was then purified using His-select Nickel affinity beads. Compared with 37ºC, more soluble Cyclin B1 was obtained when the induction was carried out at 15ºC (Figure 3-5). However, expression levels were low and not enough soluble protein was obtained after affinity purification (Figure 3-6).

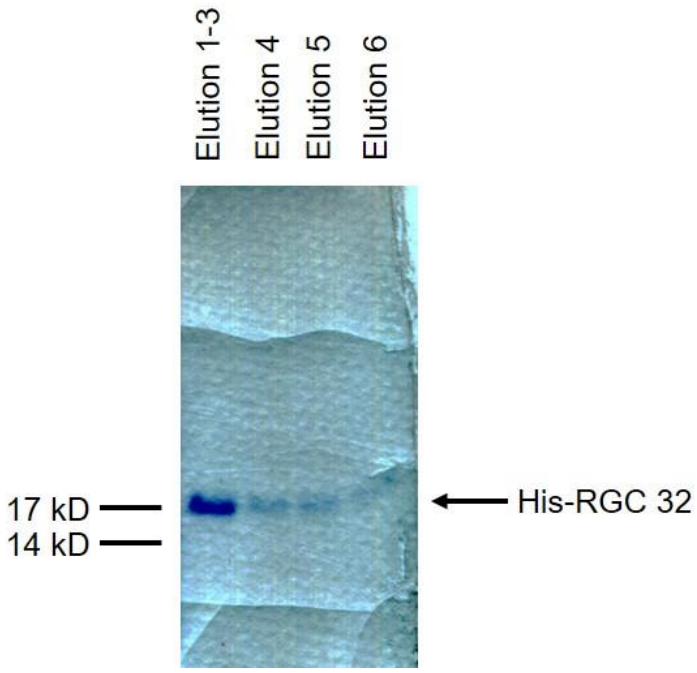

Figure 3-3. SDS-PAGE gel analysis of purified His-RGC-32.

1/375 of elution 1-3, 1/12.5 of elution 4, 5 and 6 from 2 L culture (pooled 1-3, 4, 5 and 6) of purified His-RGC-32 protein from His-select nickel affinity resin were loaded in a SDS-PAGE gel and the gel stained with Coomassie stain.

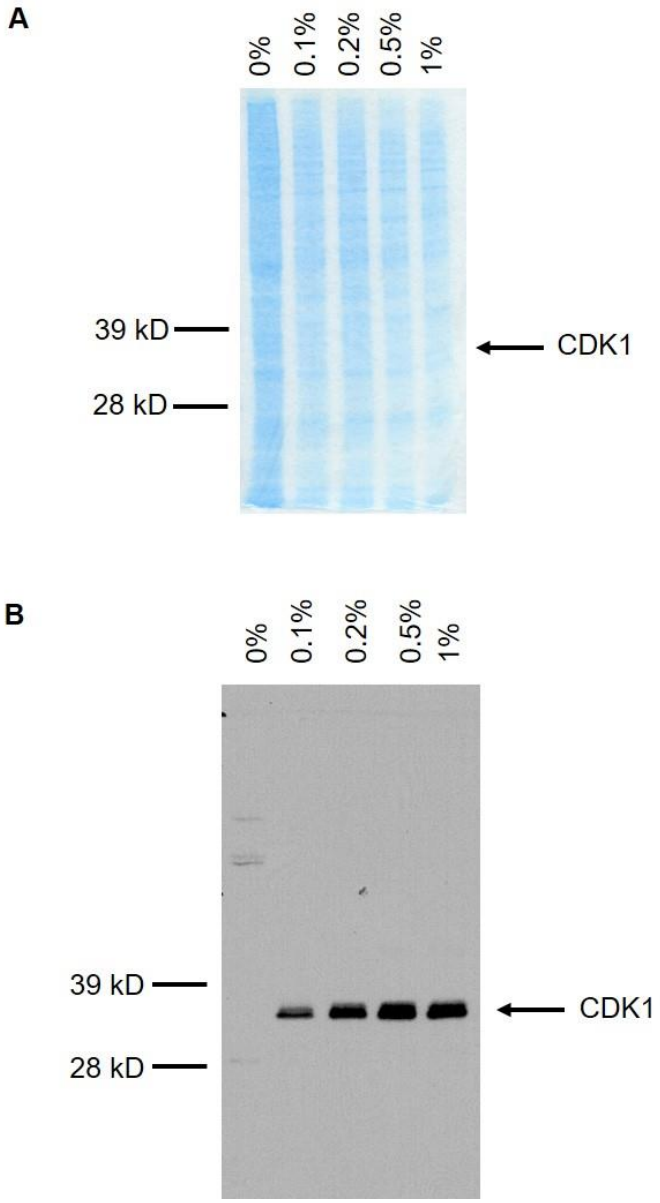

Figure 3-4. Coomassie staining and western blot analysis of CDK1 expressionin insect cells.

Sf9 insect cells were infected with different concentrations (0%, 0.1%, 0.2%, 0.5% and 1%) of baculovirus. Total cell lysate was separated on a Novex Bis-Tris gel (Invitrogen). **A.** Gel stained with Coomassie staining (Bio-Rad). **B.** Nitrocellulose membranes containing the transferred proteins were probed with CDK1 antibody. Bands were visualised with ECL.

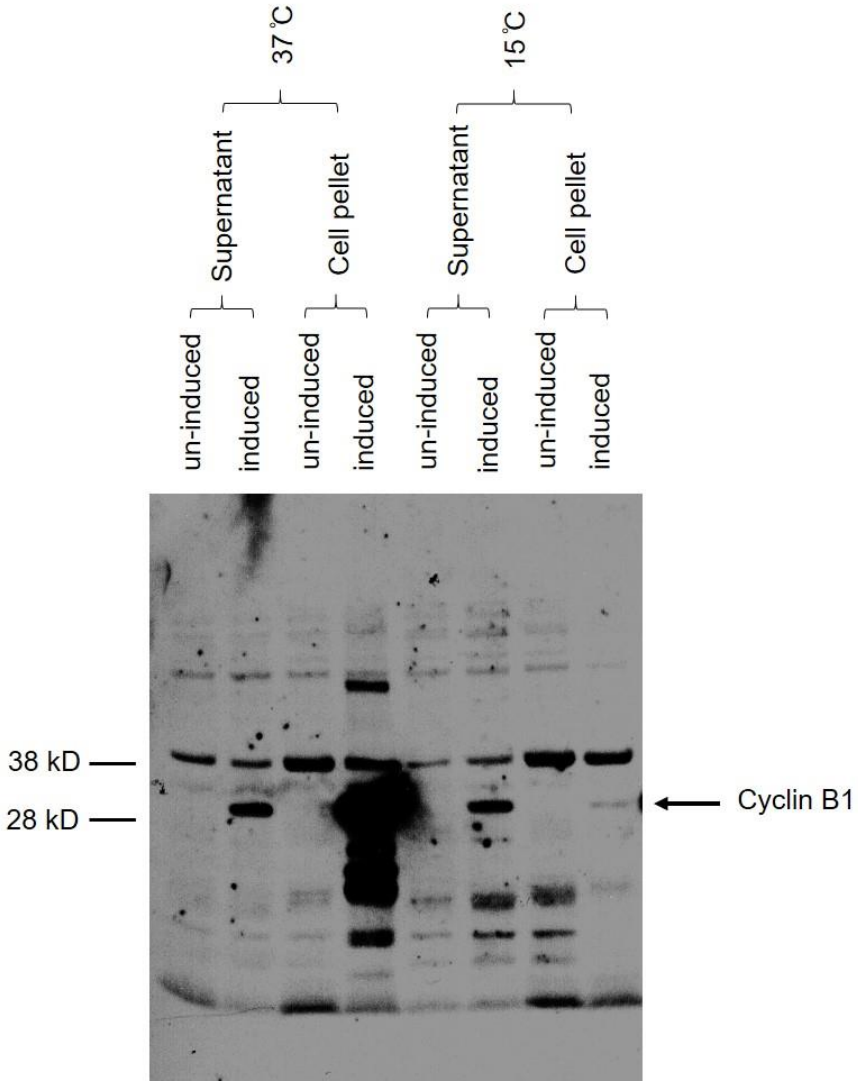

Figure 3-5. Western blotting analysis of cyclin B1 expression and solubilisation.

Temperature of 15°C and 37°C expression from 50 ml culture was carried out at prior to extraction in buffer contained 20mM Ph8.3 Tris, 0.8M NaCl and 10% glycerol. 1/400 of pellet and 1/400 of supernatant were separated using an SDA-PAGE gel.

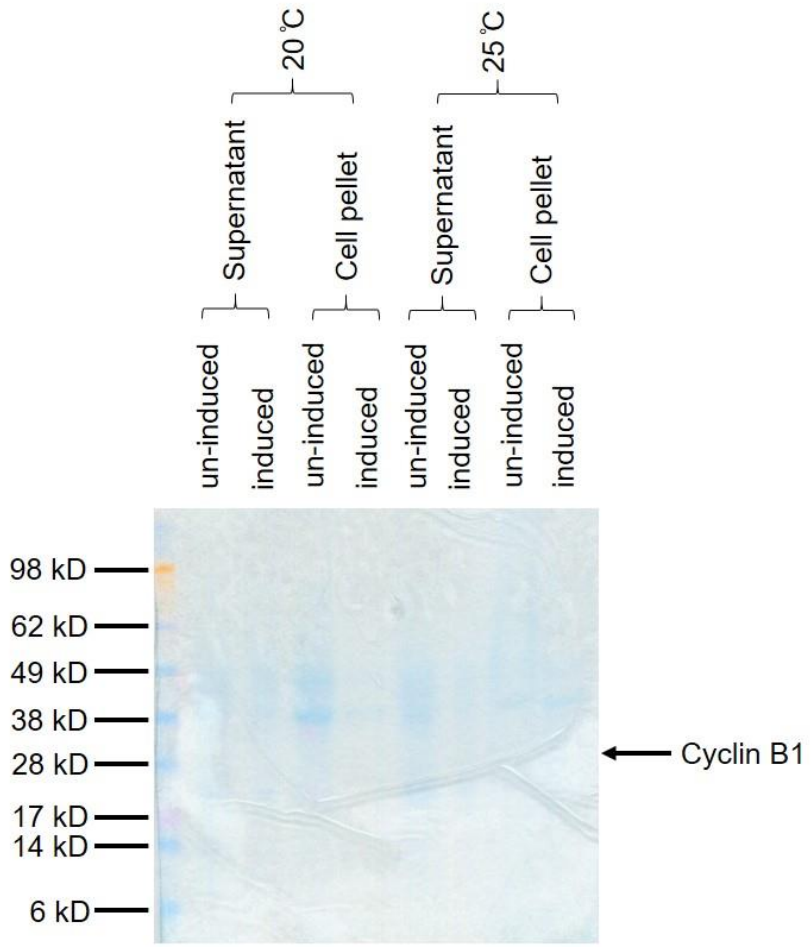

Figure 3-6. Coomassie staining analysis of cyclin B1 purification.

Temperature of 20°C and 25°C expression from 1 L culture was carried out at prior to extraction in buffer contained 20mM pH 8.3 Tris, 0.8M NaCl and 10% glycerol. 1/25000 of pellet and 1/25000 of supernatant were separated using an SDA-PAGE gel. The gel stained with Coomassie stain.

3.3 The effect of RGC-32 on CDK1 kinase activity

RGC-32 was shown to pull down the CDK1/Cyclin B1 complex *in vitro* and immunoprecipitate CDK1 *in vitro* and increase the activity of CDK1 in a manner dependent on the phosphorylation of threonine 91 on RGC-32 by CDK1 (Badea et al. 2002). Other evidence showed that transiently overexpressed Flag- or Myc-RGC-32 did not co-precipitate with exogenously expressed Cyclin B1 in HEK 293-T cells (Saigusa et al. 2007). Previously in the West lab, purified recombinant His-RGC-32 was observed to increase the activity of CDK1 *in vitro* by Histone H1 kinase assay measuring the phosphorylation of Histone H1 by CDK1 using ^{32}P-labelled ATP (Schlick et al. 2011). Purity of RGC-32 purified was assessed as good enough to test whether His-RGC-32 was functional using kinase assays. To check if the purified His-RGC-32 generated was active, *in vitro* kinase assays were carried out. CDK1 activity increased more than 4-fold at the highest His-RGC-32 protein concentration (1.4 µM) (Figure 3-7) indicating that the purified His-RGC-32 was active.

To investigate the mechanism of the activation of CDK1 by RGC-32, we collaborated with Jane Endicott and Nick Brown (initially University of Oxford, now University of Newcastle). To determine whether the activation of CDK1 by RGC-32 was dependent on CAK phosphorylation of CDK1 and whether RGC-32 can activate other CDKs such as CDK2, *in vitro* kinase assays were carried out. Purified recombinant dialysed and undialysed His-RGC-32 protein was used. Purified CDK1 and CDK complexes in activated (pCDK1/Cyclin B and pCDK2/Cyclin A) and unactivated (CDK1/Cyclin B) forms provided as part of

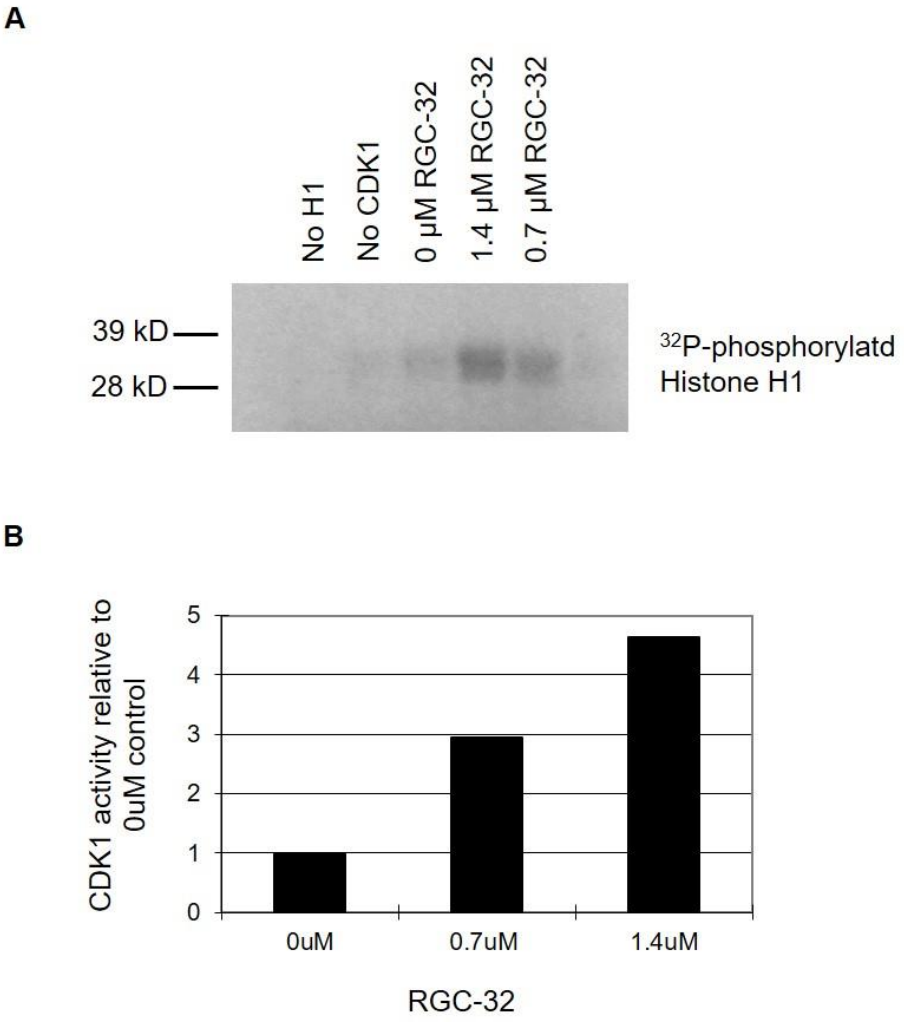

Figure 3-7. The effect of His-RGC-32 on CDK1 kinase activity.

Recombinant CDK1/cyclin B1 (NEB) was mixed with His-RGC-32 to a final concentration of 0.7 and 1.4 µM in the presence of γ-^{32}P ATP and histone H1 as substrate. **A.** Samples were separated using a 10% NuPAGE Novex Bis-Tris gel (Invitrogen). **B.** Radioactively phosphorylated histone H1 was measured using a phosphorimager. CDK1 activity was quantified and expressed relative to the control (no RGC-32) (n=1).

collaboration with University of Oxford (Figure 3-8). Initially, whether RGC-32 can activate pCDK1/Cyclin B, pCDK2/Cyclin A or CDK1/Cyclin B was examined. Whether RGC-32 can activate CDK1 without CAK (CDK7/Cyclin H) phosphorylation was also examined.

Two-thirds of the purified His-RGC-32 from 2 L culture was dialysed in dialysis buffer (20 mM PO_4 buffer and 200 mM NaCl) and undialysed protein was retained in elution buffer (40 mM PO_4 buffer, 300 mM NaCl and 100 mM EDTA). Unfortunately, the experiments carried out by Nick Brown in University of Oxford failed to show RGC-32 activation of any of the kinases (pCDK1/Cyclin B, pCDK2/cyclin A and CDK1/Cyclin B) (Figure 3-8). Kinase activity was measured by quantifying the phosphorylation of Histone H1 by kinases using ^{32}P-labelled ATP and there was no increase in the levels of phospho-Histone H1 compared in the presence of RGC-32. Undialysed RGC-32 inhibited the activity of any kinases as no radioactive activity was detected in experiments containing undialysed RGC-32 (lane 3, 6, 9, 12 and 15). This was because the undialysed His-RGC-32 used was eluted in 40 mM PO_4, 300 mM NaCl and 100 mM EDTA. Mg^{2+} is required for kinase activity was therefore likely to be chelated by EDTA. Although some dialysed His-RGC-32 in 20 mM PO_4 buffer pH 7.5 was also used, it was too dilute (RGC-32:CDK1 14 ng: 1 ng) in the experiment done in University of Oxford compared to our experiment (RGC-32:CDK1 500 ng: 1 ng), in which CDK1 activity increased more than 4-fold at the highest His-RGC-32 protein concentration (Figure 3-7). The dialysed RGC-32 produced for these experiments was therefore at too low concentration.

A

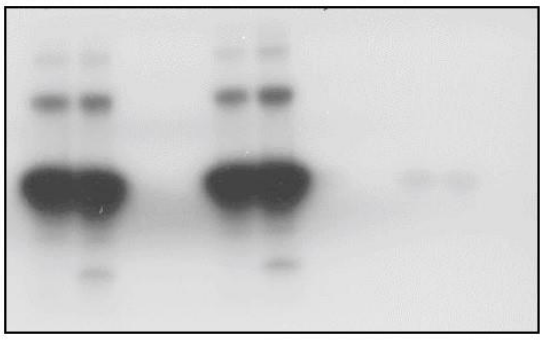

	1	2	3		4	5	6		7	8	9
pCDK1/Cyclin B	+	+	+		–	–	–		–	–	–
pCDK2/Cyclin A	–	–	–		+	+	+		–	–	–
CDK1/Cyclin B	–	–	–		–	–	–		+	+	+
RGC-32 dialysed	–	+	–		–	+	–		–	+	–
RGC-32 un-dialysed	–	–	+		–	–	+		–	–	+
Histone H1	+	+	+		+	+	+		+	+	+

B

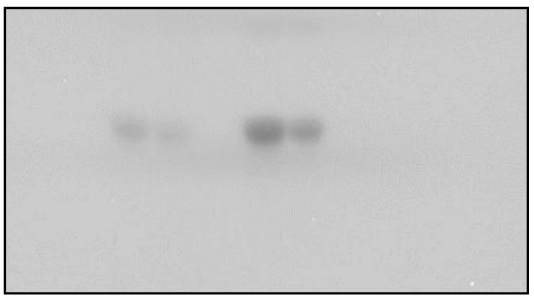

	10	11	12	13	14	15	16	17	18
CDK1	+	+	+	+	+	+	–	–	–
pCDK7/Cyclin H	–	–	–	+	+	+	–	–	–
RGC-32 dialysed	–	+	–	–	+	–	–	+	–
RGC-32 un-dialysed	–	–	+	–	–	+	–	–	+
Histone H1	+	+	+	+	+	+	+	+	+

Figure 3-8. The effect of His-RGC-32 on different CDK/cyclin complexes.

Recombinant kinases or kinase complexes were mixed with dialysed and un-dialysed His-RGC-32 in the presence of γ-^{32}P ATP and histone H1 and samples were separated in a 12.5% SDS-PAGE gel. Experiment carried out by Nick Brown (initially University of Oxford, now University of Newcastle). **A.** Analysis of the CDK1 and CDK2 complexes. **B.** Analysis of the CDK7/Cyclin H complex.

To determine whether adding an excess of magnesium cations could improve the kinase assay results with the undialysed protein, Mg^{2+} was added to the reaction to a final concentration of 35 mM. 35 mM Mg^{2+} was higher than the concentration of EDTA (10 mM) in the purified His-RGC-32 protein preparation. The results showed that the activity of CDK1/Cylin B was increased by 2-fold using 1 ng Oxford-purifed CDK1 (Figure 3-9C), and 2.5-fold using 2 ng Oxford-purified CDK1 (Figure 3-10 C) with the highest His-RGC-32 protein concentration used (2.8 µM). This is lower than previously demonstrated in our lab which showed that CDK1 activity was enhanced by up to 12-fold with 5 µM RGC-32 protein (Schlick *et al*., 2011). We therefore examined the quality of the RGC-32 protein.

3.4 Examination of His-RGC-32 aggregation

Dynamic Light Scattering (DLS), a technique to measure the size and distribution of proteins, was carried out to investigate whether there was any protein aggregation in the His-RGC-32 we purified (Figure 3-11). It showed that all His-RGC-32 preparations were homogenous but both the undialysed and dialysed samples contained a lot of aggregation (Figure 3-11). The dialysed sample (Figure 3-11B) was centrifuged to pellet aggregates and the remaining soluble RGC-32 (Figure 3-11C) had a smaller volume in DLS, consistent with the lack of aggregates.

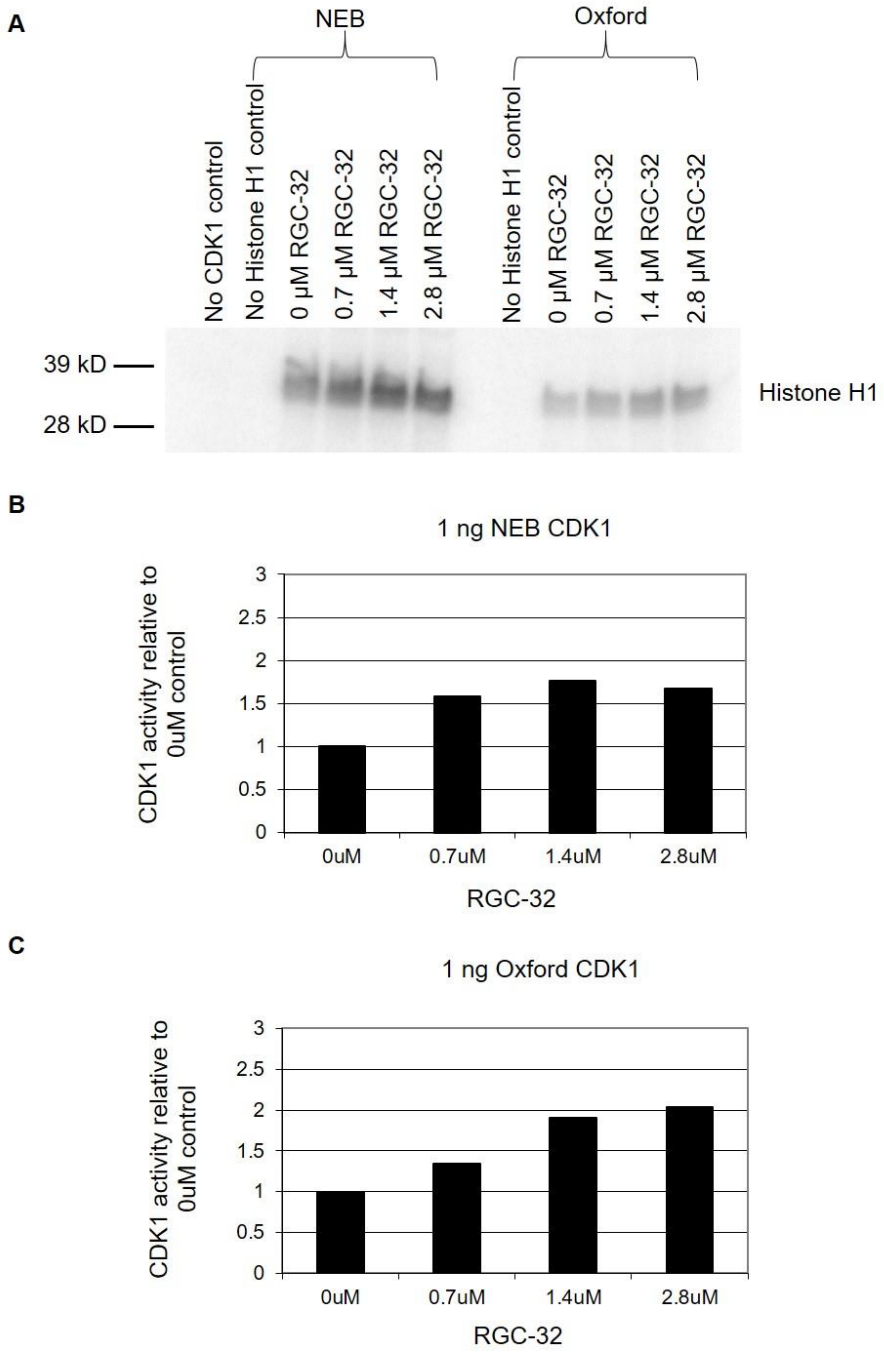

Figure 3-9. The effect of His-RGC-32 CDK1 kinase activity in CDK1/cyclin B1 preparations.

1ng recombinant CDK1/Cyclin B1 (NEB) or pCDK1/cyclin B1 (Oxford) was mixed with His-RGC-32 to a final concentration of 0.7, 1.4 and 2.8 μM in the presence of γ-^{32}P ATP and histone H1. The concentration of Mg^{2+} was 35 mM (n=1). **A.** SDS-PAGE analysis of histone H1 phosphorylatioin using 1 ng recombinant CDK1/cyclin B1 (NEB) or pCDK1/cyclin B1 (Oxford). **B & C.** CDK1 activity in **A** was quantified.

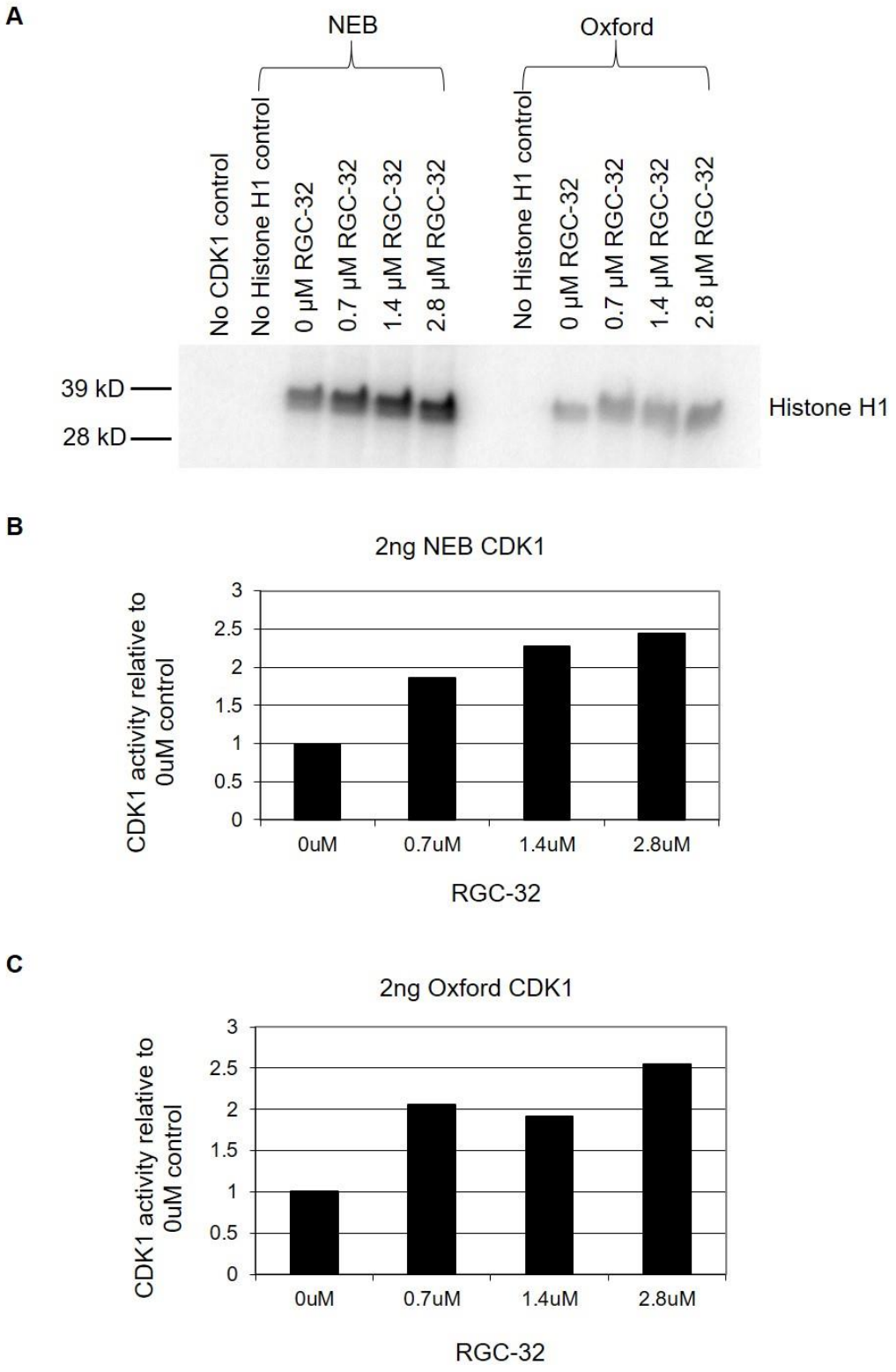

Figure 3-10. The effect of His-RGC-32 CDK1 kinase activity in CDK1/cyclin B1 preparations.

Recombinant CDK1/Cyclin B1 (NEB) or pCDK1/cyclin B1 (Oxford) was mixed with His-RGC-32 to a final concentration of 0.7, 1.4 and 2.8 μM in the presence of γ-^{32}P ATP and histone H1. The concentration of Mg^{2+} was 35 mM (n=1). **A.** SDS-PAGE analysis of histone H1 phosphorylatioin using 2 ng recombinant CDK1/cyclin B1 (NEB) or pCDK1/cyclin B1 (Oxford). **B & C.** CDK1 activity in **A** was quantified.

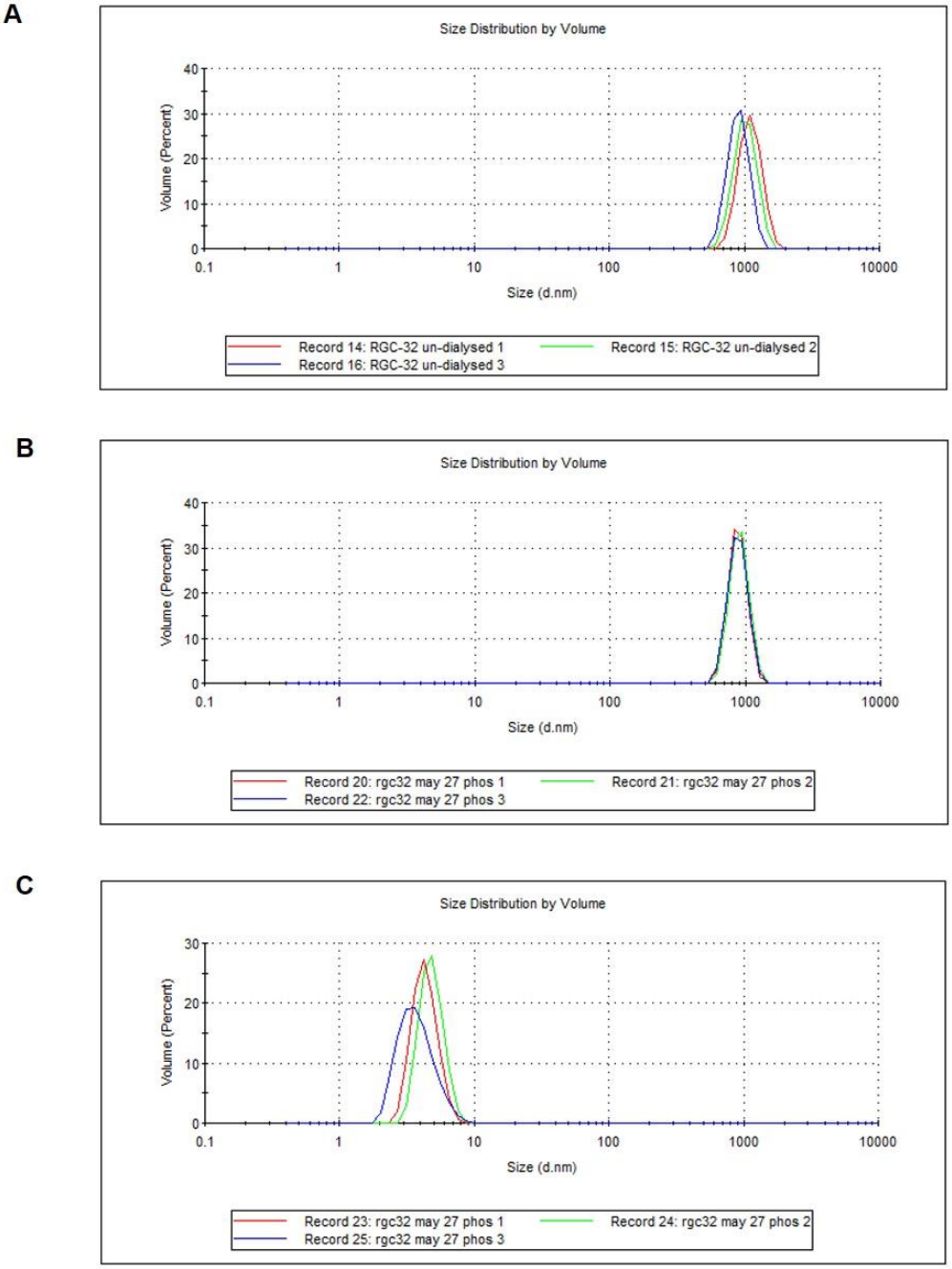

Figure 3-11. Analysis of His-tagged RGC-32 using Dynamic Light Scattering.

Three measurements are shown as different colors. **A.** Un-dialysed His-tagged RGC-32. **B.** Dialysed His-tagged RGC-32. **C.** Supernatant from **B** after centrifugation. Larger volume indicates aggregates.

3.5 Expression of GST-RGC-32

To improve solubility, RGC-32 was re-cloned as a Glutathione-S-Transferase (GST) fusion protein using the pGEX-6P3 vector, since GST often improves the solubility of proteins. Expression and solubilisation of GST-RGC-32 was compared to His-RGC-32 using Rosetta™ 2(DE3) pLysS Singles™ competent cells (Novagen) and Arctic Express (DE3) competent cells (Agilent Technologies) and different extraction buffers. Rosetta 2 cells are BL21 derivatives designed to enhance the expression of eukaryotic proteins that contain codons rarely used in *E. coli* (Novagen). Arctic cells are derived from BL21 competent cells and co-express chaperonins Cpn10 and 60 from the psychrophilic bacterium, *Oleispira Antarctica* (Agilent Technologies) which show high protein refolding activities at temperatures of 4 to 12ºC (Ferrer et al. 2003).

RGC-32 fusion protein expression was induced by addition of 0.8 mM IPTG at 12°C and 18°C respectively for Arctic and Rosetta cells. Cell pellets were resuspended in different buffers in the presence of protease inhibitors and 5 mM EDTA. Buffer A contained 20 mM HEPES pH7.5 and 500 mM NaCl. Buffer B contained 20 mM HEPES pH7.5 and 200 mM NaCl. Buffer C contained 20 mM HEPES pH7.5, 200 mM NaCl and 10% glycerol. Buffer D contained 20 mM HEPES pH7.5, 200 mM NaCl and 1% Tween 20. The supernatant and pellet after lysis of Arctic (Figure 3-12) or Rosetta (Figure 3-13) cells were loaded on a gel.

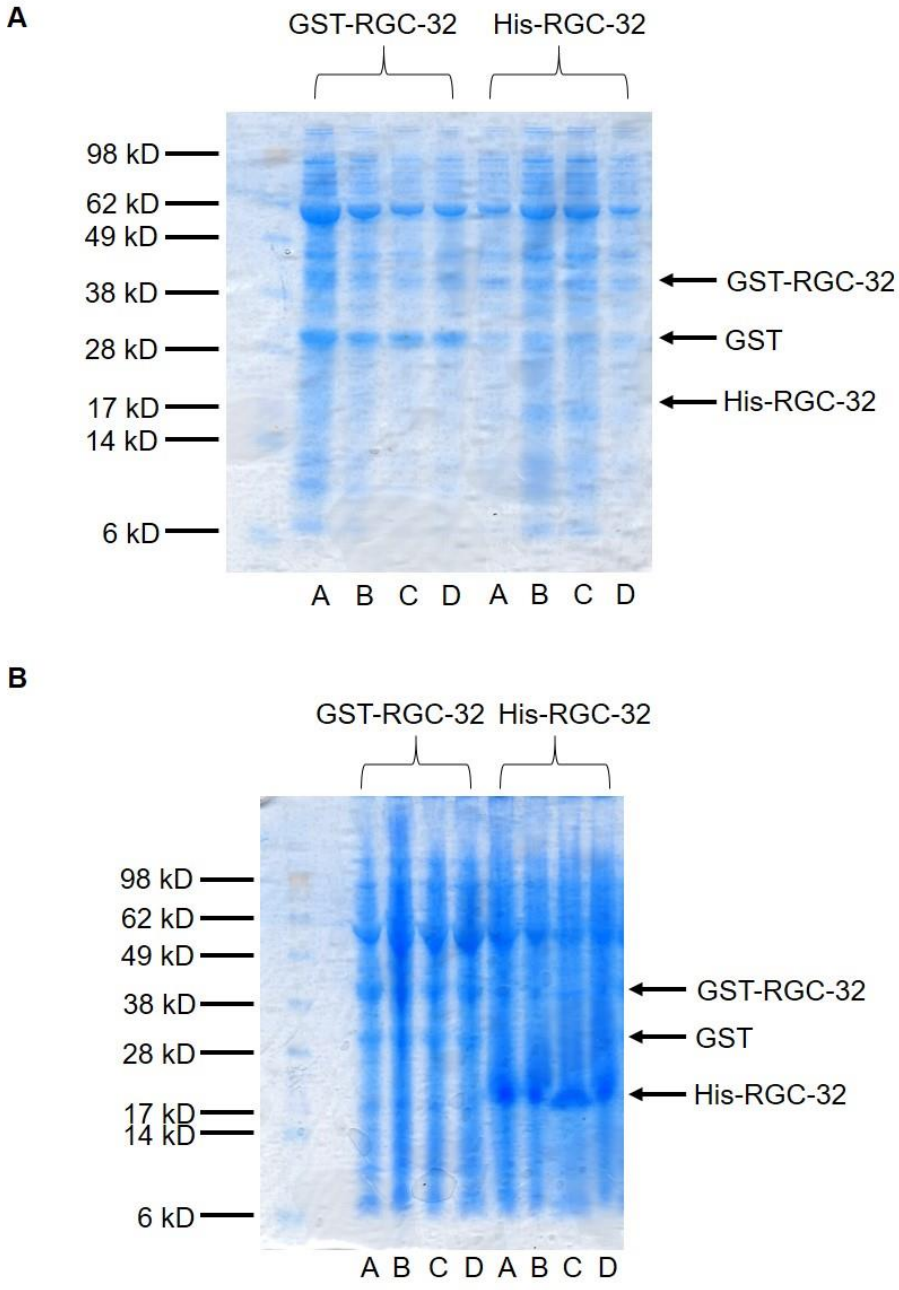

Figure 3-12. His-tagged RGC-32 and GST-tagged RGC-32 purification test in Arctic cells.

A. Stained SDS-PAGE gel of supernatant from lysates of Arctic cells induced to express His-RGC-32 or GST-RGC-32. Cells were lysed in different buffers (A-D) and 1/60 of soluble supernatant as analysed. **B.** Stained SDS-PAGE gel 1/60 cell pellets from lysates of Arctic cells. The His-RGC-32 protein has a molecular weight of 17 kD and GST-RGC-32 protein has a molecular weight of 40 kD.

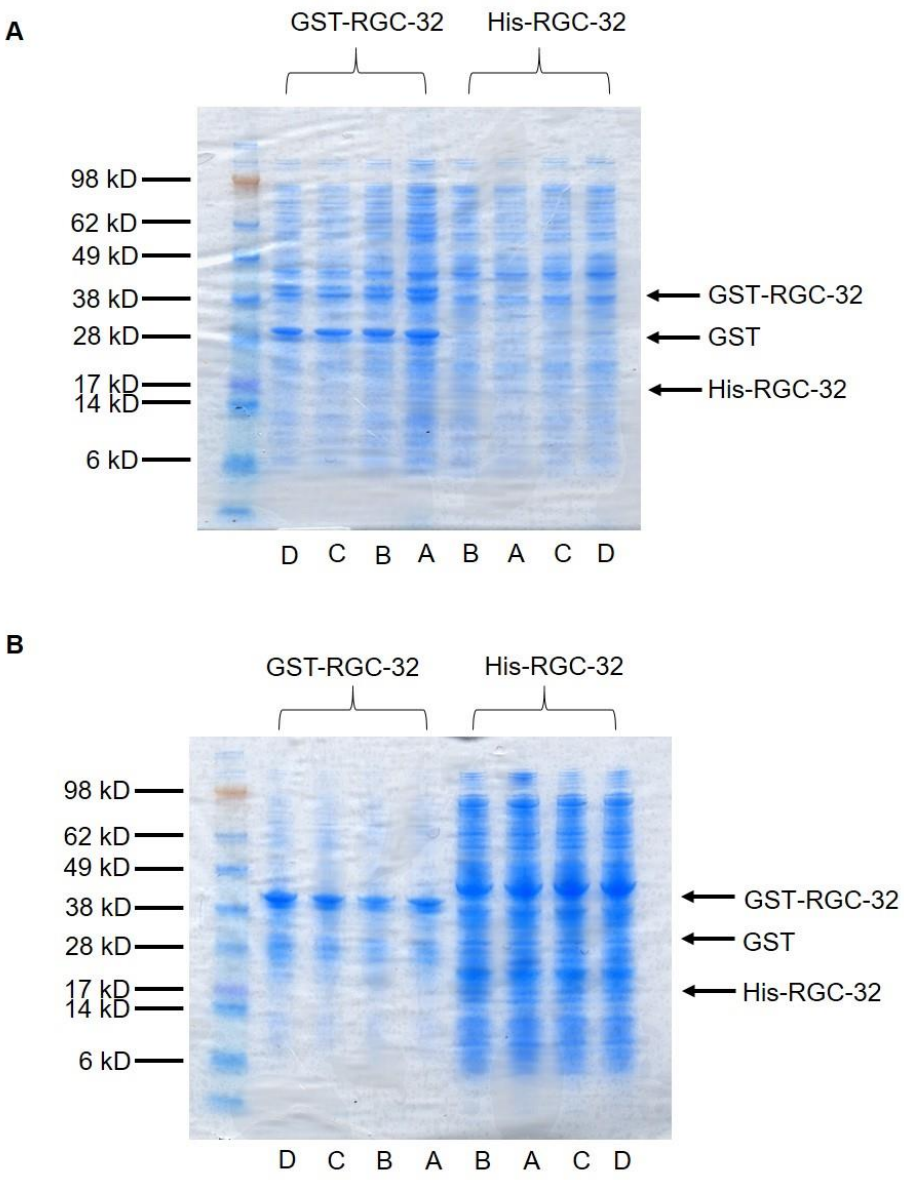

Figure 3-13. His-tagged and GST-tagged RGC-32 purification test in Rosetta cells.

A. Stained SDS-PAGE gel of supernatant from lysates of Rosetta cells induced to express His-RGC-32 or GST-RGC-32. Cells were lysed in different buffers (A-D) and 1/60 of soluble supernatant were analysed. **B.** Glutathione or His beads were added to the supernatant and protein purified on beads was loaded on a gel.

For Arctic cells, more soluble GST-RGC-32 was detected when using lysis buffer A and for His-RGC-32 buffer B and C are better than buffer A and D for solubility (Figure 3-12A). GST was self-cleaved in each buffer (Figure 3-12A). Also insoluble GST-RGC-32 and His-RGC-32 were detected in pellet when using all lysis buffers (Figure 3-12B).

For Rosetta cells, less soluble His-RGC-32 protein was obtained compared with GST-RGC-32 protein in the supernatant (Figure 3-13A). More GST-RGC-32 could be detected when lysed in buffer A than other buffers and GST was again self-cleaved in each buffer (Figure 3-13A). Glutathione or His beads was added to the supernatant and protein purified on beads were loaded on the gel. GST-RGC32 protein was purified effectively (Figure 3-13B).

To summarise, in the purification test of GST-RGC-32 in Rosetta or Arctic cells, more soluble RGC-32 was obtained using Rosetta cells rather than Arctic cells and more RGC-32 protein was obtained when using buffer A. For further experiments GST-RGC-32 was expressed using Rosetta cells and buffer A. GST-RGC-32 was more soluble so used this from now on. Further experiments with GST-RGC-32 are described in Chapter 4. Since we had optimised GST-RGC-32 purification we attempted to obtain sufficient purified soluble RGC-32 for structural studies.

3.6 Large scale GST-RGC-32 purification using Rosetta cells

3L of Rosetta cells expressing pGEX-6P3 RGC-32 were induced by IPTG to express GST-RGC-32 protein and lysates prepared using buffer A. The RGC-32 on beads was eluted with elution buffer contained 20 mM HEPES pH 7.5, 500 mM NaCl and 20 mM L-Glutathione. Then the eluted protein was incubated with the PreScission protease (200 µl 2 mg/ml PreScission in 20 mM HEPES pH7.5, 500 mM NaCl and 1 mM DTT) to cleave the GST tag. Samples of elution and GST tag cleaved off were loaded on a gel (Figure 3-14A). The GST protein is visible as a 26 kD protein and RGC-32 as a 14 kD protein. The GST tag was successfully cleaved from GST-RGC-32 protein. To verify that the cleaved product was RGC-32, samples were analysed using an anti-RGC-32 antibody by Western blotting (Figure 3-14B). Different sizes of proteins (61, 44, 32, 15 and 12 kD) were detected. The detected proteins were RGC-32 plus additional larger proteins that could be dimers or trimers. There were also some smaller species that may be cleavage products. Purified RGC-32 was concentrated to 0.9 mg/ml in a total volume of 100 µl.

This experiment demonstrated that we were able to purify soluble RGC-32 for crystal trials to offer more structural information of RGC-32, so we next scaled-up the preparation to obtain milligram quantities. Also, we needed to examine the interaction between RGC-32 and CDK1 using GST-RGC-32 we made to carry on the collaboration with Professor Jane Endicott and Dr. Nick Brown (University of Newcastle) (see Chapter 4).

To obtain mg amounts of RGC-32 for crystalisation, GST-RGC-32 was purified

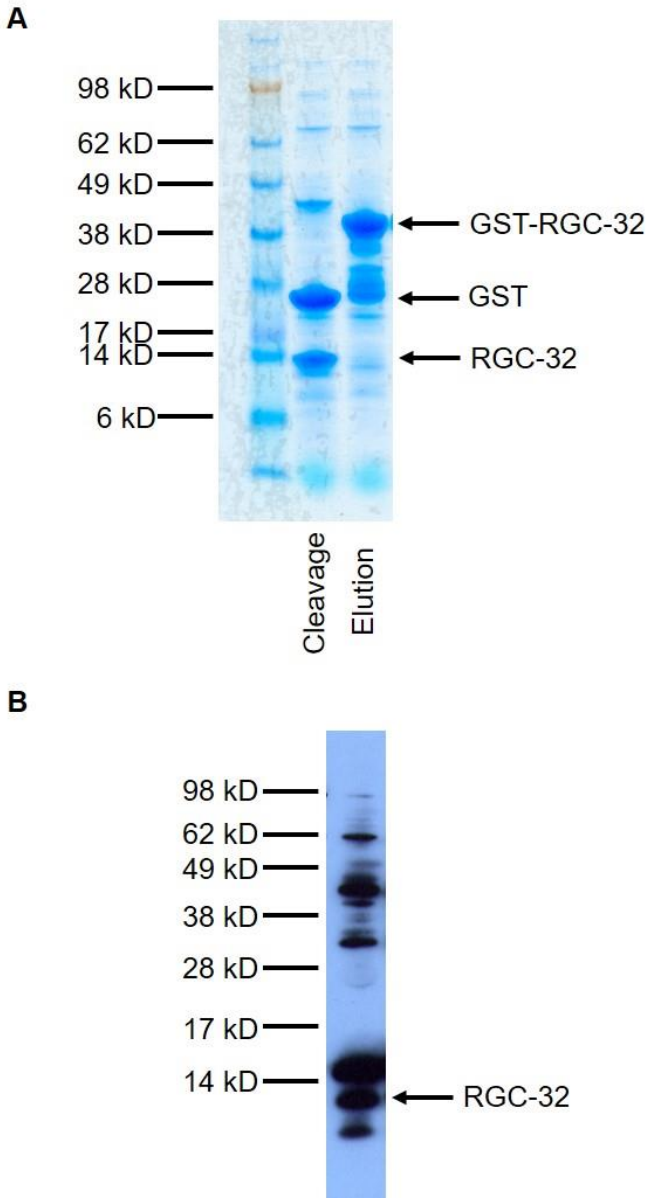

Figure 3-14. GST-RGC-32 purification from 3L Rosetta culture.

A. GST-RGC-32 elution before and after precission treatment. **B.** Purified cleaved RGC-32 analysed by western blotting using polyclonal anti-RGC-32 antibody

from 10 L of Rosetta cells. GST-RGC-32 was eluted and the GST tag cleaved off using the PreScission protease (Figure 3-15). A HiTrap desalting column (GE Healthcare Life Sciences) was then used to remove free glutathione and a GSTrap 4B column (GE Healthcare Life Sciences) was used to remove GST from cleaved RGC-32. GST was completely removed after running through a GSTrap column (Figure 3-16).

RGC-32 protein was concentrated and applied to a gel filtration column S75 16/60 to further purify the sample. Fraction C10 to D1 was confirmed as containing RGC-32 protein (Figure 3-17A) by SDS-PAGE analysis (Figure 3-17B). It has a very low absorbance because of no tryptophan residues in RGC-32. The high molecular weight contaminants (first peak from gel filtration in Figure 3-17A) were successfully removed after gel filtration (Figure 3-17B). The purified RGC-32 was concentrated to 1.5 mg/ml in a total volume of 170 µl.

3.7 Crystallisation trials

Crystallization screening was performed with RGC-32 at a concentration of 1.5 mg/ml using Crystal Phoenix (Art Robbins Instruments) employing the sitting drop vapour diffusion method. Commercial screening kits used were Structure Screen 1+2 (Molecular Dimensions), PEG/Ion HT (Hampton Research), Natrix HT (Hampton Research), Index HT (Hampton Research), SaltRx HT (Hampton Research) and JCSG-*plus* (Molecular Dimensions).

Structure Screen 1 & 2 is a 96 reagent, sparse-matrix screen for Structure

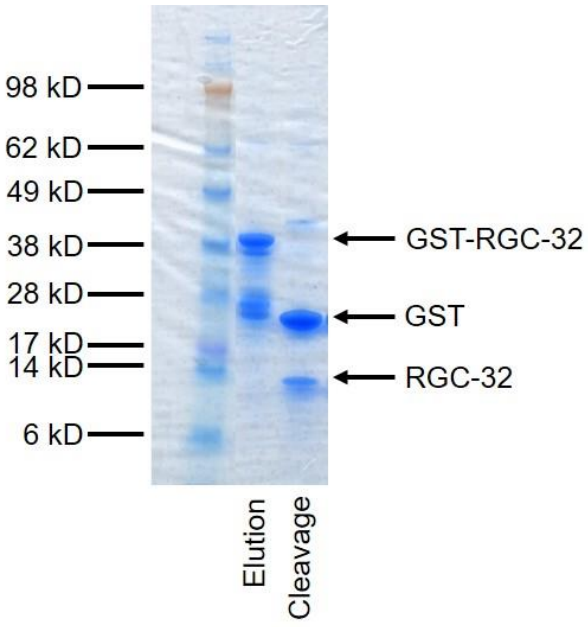

Figure 3-15. GST-RGC-32 purification from 10L Rosetta culture.

GST-RGC-32 elution before and after precission treatment.

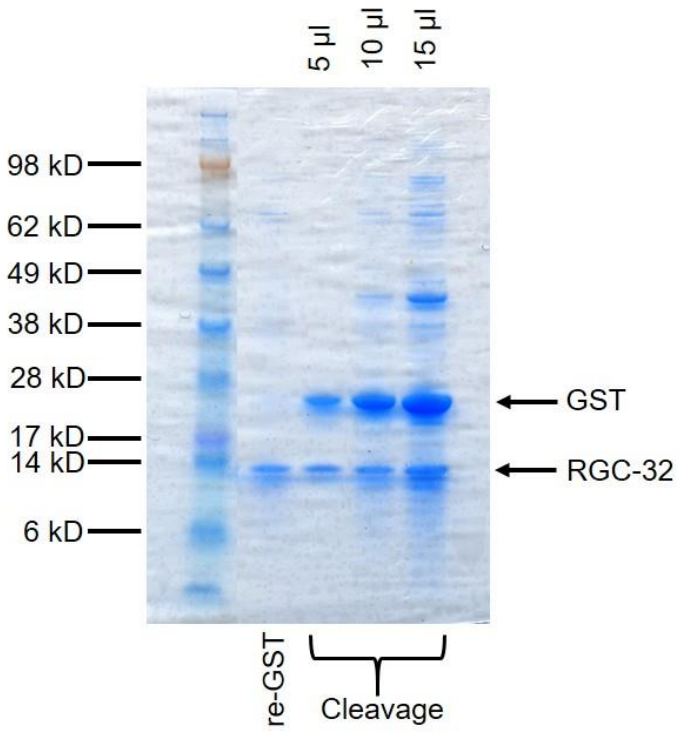

Figure 3-16. GST-RGC-32 purification from 10L Rosetta culture.

RGC-32 after precission treatment (5, 10 and 15 µl) and after passing through a Glutathione column to remove GST protein from sample.

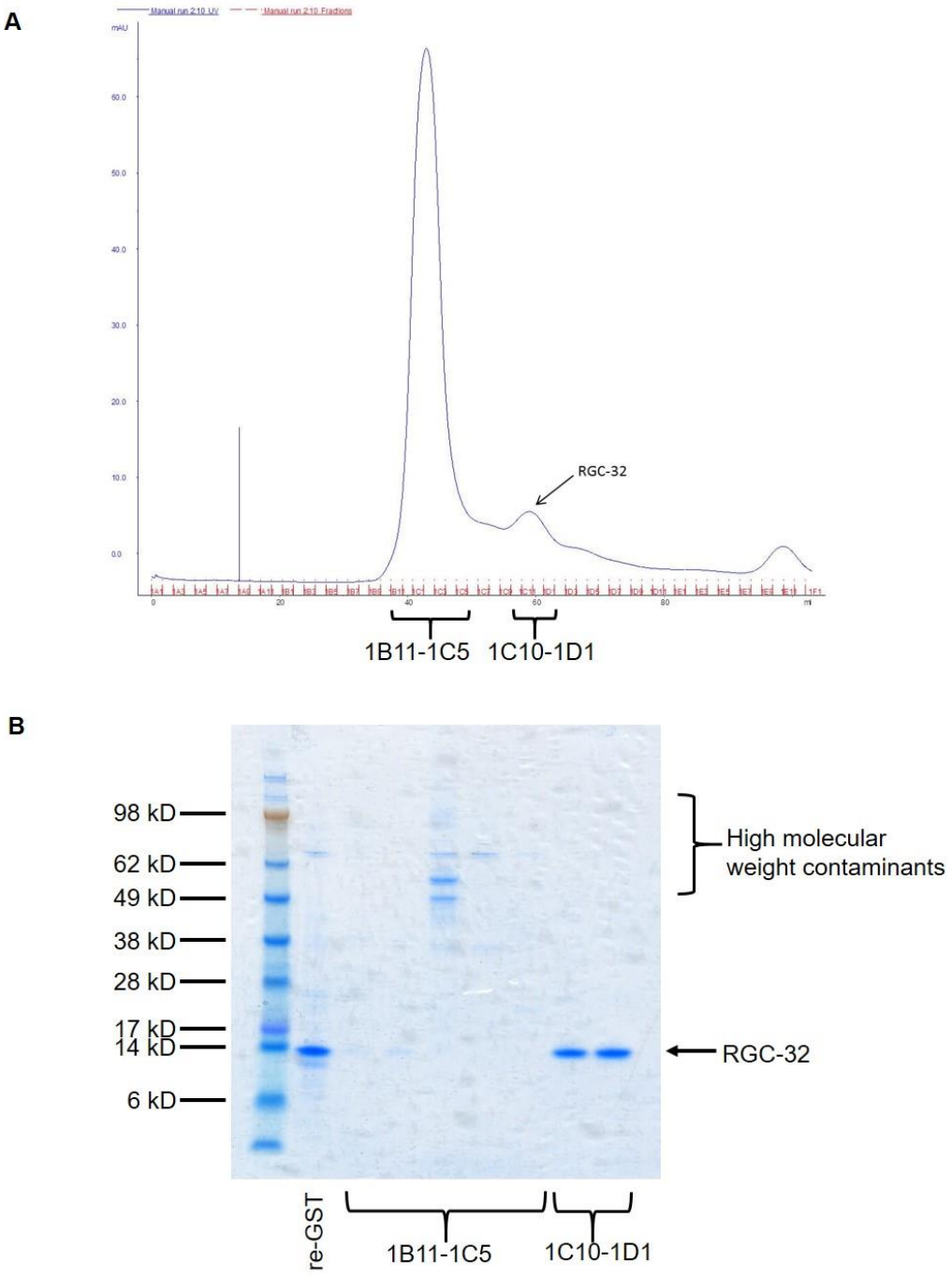

Figure 3-17. **Gel filtration purification of RGC-32.**

(A) RGC-32 was concentrated and applied to an S75 16/60 gel filtration column pre-equilibrated in 10 mM HEPES pH7.5, 500 mM NaCl and 0.5 mM TCEP. 1.7 ml fractions were collected. **(B)** Samples (fraction 1B11 to 1C5 from first peak and fraction C10 to D1 from second peak) after gel filtration were analysed by SDS-PAGE and gel staining.

Screen 1 and the classic extension to this screen Structure Screen 2 (Jancarik and Kim, 1991). PEG/Ion HT combines PEG/Ion and PEG/Ion 2 in a single 96 deep well block. PEG/Ion is a sparse matrix profile of anions and cations in the presence of monodisperse polyethylene glycol (PEG) 3,350 over pH 4.5 – 9.2 and PEG/Ion 2 is a profile of titrated organic acids in the presence of monodisperse PEG 3,350 over pH levels 3.7 – 8.8 (http://hamptonresearch.com/product_detail.aspx?sid=30&pid=11). Natrix HT contains 1 ml of each reagent from Natrix and Natrix 2 (https://hamptonresearch.com/product_detail.aspx?cid=1&sid=27&pid=8). Natrix contains 48 unique reagents, 10 ml each and is based on the sparse matrix formulation (Scott et al., 1995). As an extension of Natrix, Natrix 2 contains 48 unique reagents, 10 ml each and based on extracting patterns from crystallization data as well as reagent formulations (Berger et al., 1996). Index HT contains 10 ml 96 unique reagents in a single deep well block format (http://hamptonresearch.com/product_detail.aspx?sid=24&pid=5). SaltRx HT contains the 96 reagents from SaltRx 1 and SaltRx 2 in a single deep well block format. SaltRx 1 and SaltRx 2 contain 10 ml unique reagents 1-48 and 49-96 of the original SaltRx 96 reagent kit (http://hamptonresearch.com/product_detail.aspx?sid=32&pid=12). JCSG-*plus* contains 10 ml each of 96 sterile filtered reagents incorporating PEG, salts, neutralised organic acids or organic precipitants across a pH range from 4.0 to 10.5, and including a range of salt additives (Newman et al., 2005).

Plates were kept at 20°C to allow the crystals grow. Unfortunately no crystal hits were obtained. To increase the concentration of RGC-32 obtained from

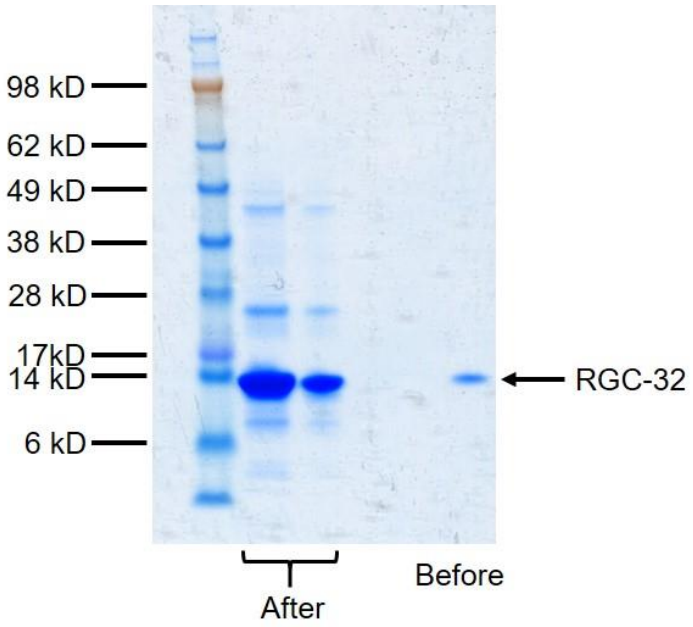

Figure 3-18. Purified RGC-32 from 20 L cell culture.

Samples of RGC-32 after concentration (10 µl and 3 µl) and before concentration were analysed by SDS-PAGE and gel staining.

purification, 20 L Rosetta cells expressing pGEX-6P3 RGC-32 were cultured and protein purified to higher concentration up to 4.5 mg/ml for 200 µl (Figure 3-18). Again the sitting drop vapour diffusion technique was employed with the commercial screening kits Structure Screen 1+2 (Molecular Dimensions), Natrix HT (Hampton Research), Index HT (Hampton Research), SaltRx HT (Hampton Research) and JCSG-*plus* (Molecular Dimensions) at 4 and 20°C. No crystal hits were obtained at either temperature.

3.8 Discussion

RGC-32 can bind to CDK1/Cyclin B1 complex *in vitro* (Badea et al. 2002), but other evidence shows that transiently overexpressed Flag- or Myc-RGC-32 did not co-precipitate with exogenously expressed Cyclin B1 in HEK 293-T cells (Saigusa et al. 2007). It implies a possibility of RGC-32 competing with Cyclin B1 for CDK1. RGC-32 has been shown to increase CDK1 activity in a manner dependent on the phosphorylation of threonine 91 in RGC-32 by CDK1 (Badea et al. 2002). Kinase assays using recombinant RGC-32 protein confirmed this increase of CDK1 activity. Like RGC-32, xRINGO/Speedy has been shown to activate CDK1 but does not associate with CDK1/Cyclin B complexes (Gastwirt, McAndrew and Donoghue 2007). Further evidence confirms that xRINGO can bind CDK1 and Cyclin B individually but not the CDK1/Cyclin B complex (Ferby et al. 1999). More interestingly Speedy/RINGO could even bypass the requirement for phosphorylation in the activation loop of CDKs (Karaiskou et al. 2001). Like the ability of RGC-32 disrupting the cell cycle, overexpression of Speedy/RINGO was shown to reduce the percentage of cells in G_1 phase of the cell cycle, promoted late S phase progression and disrupted the G_2/M

checkpoint (Porter et al. 2002, Cheng and Solomon 2008). It would be interesting to see if RGC-32 works at similar way to Speedy/RINGO. Previously experiments were designed to test whether RGC-32 can increase CDK1 activity in the absence of cyclin B1 (Figure 3-2). The initial experiments designed to determine whether RGC-32 can increase CDK1 activity without Cyclin B1 were not conclusive because we could not purify enough soluble Cyclin B1. So we changed the strategy of the experiments to use the CDK1 and Cyclin B1 provided as part of collaboration with Professor Jane Endicott and Dr. Nick Brown (initially University of Oxford, now University of Newcastle).

Previously in the West lab, RGC-32 was purified as a His-tagged protein from inclusion bodies using denaturation and renaturation. To improve the solubility of RGC-32 protein, we successfully cloned RGC-32 DNA into pGEX-6P3 vector and expressed it in Rosetta and Arctic cells. In the purification test, the results showed that the solubility of RGC-32 is better with a GST tag than His tag and in Rosetta cells than Arctic cells. Therefore RGC-32 was purified using a glutathione column and gel filtration and 4.5 mg/ml for 200 µl (900 µg in total) was achieved from 20 L cells. Unfortunately no crystal has been yielded to date. Further crystallisation trials could be made with higher concentration of RGC-32 or the temperature for setting up the crystal trials. Another attempt is to co-crystallise RGC-32 with one of its interaction partner to yield diffraction quality crystals, e.g. CDK1 becausae the complex formed could be more soluble and stable compared with single protein.

Next, it is important to determine whether there is an interaction between RGC-32 and CDK1, or Cyclin B1, or Plk1 in B cells. It can be achieved by pull-down assays using GST-RGC-32 (see Chapter 4). The interaction of RGC-32 and CDK1 or Cyclin B1 *in vitro* could also be tested using surface plasmon resonance (SPR) which is an optical technique used for detecting two different molecules in which one is mobile (analyte) and one is fixed on a thin film (ligand) (Schuck 1997). Binding of the analyte to ligand changes the refractive index of the film and the angle of extinction of light reflected after polarised light impinges on the film is changed and measured in reflected intensity (Drescher, Ramakrishnan and Drescher 2009). Firstly, RGC-32 will be immobilised by an amine-coupling reaction on a senor chip (Biacore) which is inserted into the flow chamber. Then CDK1 or CDK1/Cyclin B1 complex will flow through the chip fixed with RGC-32 to produce a small change in refractive index at the gold surface which can be quantified, so binding affinities can be yielded from the ratio of rate constants to obtain a characterisation of RGC-32 and CDK1 or CDK1/Cyclin B1 interaction.

4 Mechanism of RGC-32 disrupting cell cycle

4.1 Introduction

RGC-32 has been shown to bind CDK1/Cyclin B1 complex *in vitro* and *in vivo* (Badea et al. 2002). This interaction appears to be specific since RGC-32 does not bind CDK2 or CDK4 (Badea et al. 2002). RGC-32 activates CDK1 kinase activity and both binding and the enhancement of CDK1 activity appear to depend on the phosphorylation of RGC-32 by CDK1 at Threonine 91 (Badea et al. 2002). Our lab confirmed that RGC-32 activates CDK1/Cyclin B1 *in vitro* (Schlick et al. 2011), but the mechanism of CDK1 activation by RGC-32 remains unclear. Others have reported that RGC-32 can associate with the centrosome-associated polo-like kinase 1 (Plk1) in human embryonic kidney (HEK) 293-T cells and can be phosphorylated by Plk1 *in vitro* (Saigusa et al. 2007). These authors also stated that they were unable to co-precipitate Cyclin B1 with RGC-32 (Saigusa et al. 2007). Initial attempts to address whether RGC-32 activates CDK1 in the absence of Cyclin B1 in Chapter 3 were not conclusive so we next investigated the interaction between RGC-32 and CDK1 and Cyclin B1 and Plk1 using pull-down assays.

The role for RGC-32 in the promotion of cell proliferation was demonstrated in oligodendrocytes (OLG) (Badea et al. 1998) and G1 arrested smooth muscle cells (Badea et al. 2002). Our group showed that overexpression of RGC-32 alone can disrupt the G2/M checkpoint (Schlick et al. 2011). Interestingly, other studies have revealed the role of RGC-32 as a tumour suppressor as it was found to be absent in glioma cell lines and restoration of it caused suppression

of cell growth (Saigusa et al. 2007). In this chapter, we set out to further examine the effect of RGC-32 on cell cycle regulation by generating stable cell-lines containing inducible RGC-32 expression constructs.

4.2 RGC-32 can interact with CDK1 and Plk1 but not Cyclin B

To verify the association of RGC-32 with CDK1 and Plk1, GST pull-down assays were carried out using GST-tagged RGC-32 incubated with lysates from the EBV negative B cell lymphoma cell line BJAB. We found that GST-tagged RGC-32 was able to pull down CDK1 and Plk1. This interaction was specific because beads alone or GST alone did not pull down RGC-32 (Figure 4-1). It has been shown that the Threonine 91 is the phosphorylation site of RGC-32 by CDK1 and important for RGC-32 increasing CDK1 kinase activity (Badea et al. 2002). So we also tested if RGC-32 with a threonine 91 to alanine substitution (T91A) could influence the interaction of RGC-32 and CDK1 or Plk1. Our results showed that GST-tagged RGC-32 mutant T91A could also pull down CDK1 and Plk1 (Figure 4-1). The interaction of RGC-32 with CDK1 appears to be specific because we showed that GST-tagged RGC-32 failed to pull down CDK2 (Figure 4-1) which is consistent with previous reports (Badea et al. 2002). Saigusa *et al*. stated that they could not demonstrate a physical interaction between RGC-32 and Cyclin B1 (Saigusa et al. 2007). Our results showed that GST-tagged RGC-32 did not pull down Cyclin B1 (Figure 4-1) which strengthen the evidence that Cyclin B1 is not in the complex of CDK1 and RGC-32. The pull-down assays in another Burkitt's lymphoma cell line Mutu I showed similar results that GST-tagged RGC-32 could pull down CDK1, but not CDK2 and Cyclin B1 and that

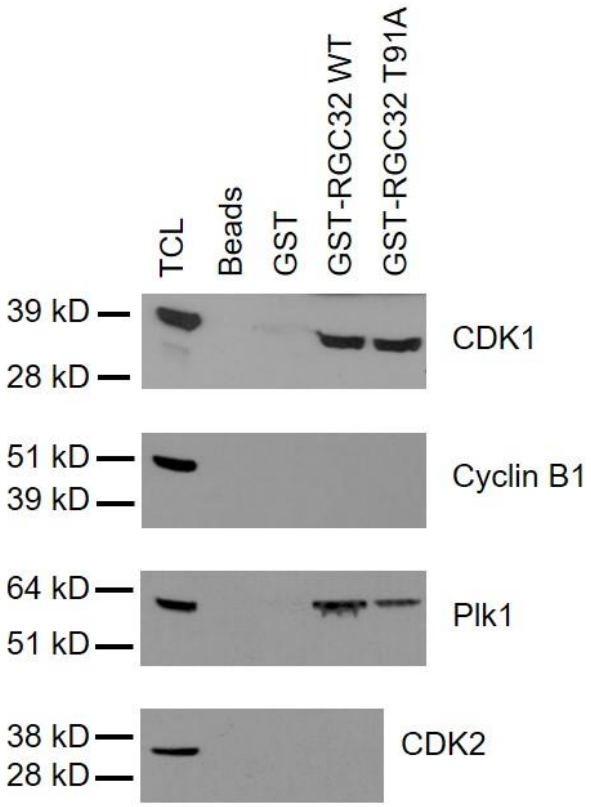

Figure 4-1. Western blot analysis of *in vitro* interaction of RGC-32 in BJAB cells.

Glutathione agarose beads or beads bound to GST, GST-RGC-32 (WT) or GST-RGC32 mutant (T91A) were mixed with BJAB total cell lysates. CDK2 was used as a negative control.

this interaction of RGC-32 with CDK1 is not dependent on Threonine 91 of RGC-32 (Figure 4-2).

4.3 Mapping the regions of interaction between RGC-32 and CDK1 or Plk1

To identify the regions of RGC-32 required for the interaction with CDK1 and Plk1 we generated deletion mutants of RGC-32. To help in the design of mutants we used JPred to predict RGC-32 secondary structure (Figure 3-1). The protein sequence was searched against UniRef 90 to identify regions of α-helix, β-strand and coil. Three predicted α-helices (5-23 aa, 31-43 aa and 101-115 aa) predicted were identified (Figure 3-1). Next, to localize the region of RGC-32 that directly interacts with CDK1 or Plk1, we generated four GST-tagged truncation mutants designed to delete each of the predicted helices sequentially (Figure 4-3). Truncation 1-25, spanning amino acid residues 1-25, contains one potential α-helices; truncation 1-50, spanning amino acid residues 1-50, contains two potential α-helices; truncation 1-75 or 1-100, spanning amino acid residues 1-75 or 1-100, contains two potential α-helices and following 25 or 50 residues. Mutants were expressed and purified on Glutathione beads and used in GST pull-down assays to identify regions required for the interaction of RGC-32 with CDK1 or Plk1.

In two independent experiments (Figure 4-4), truncation 1-75 and 1-100 pulled down CDK1, but truncations 1-25 and 1-50 did not. This indicates that 50-75 residues of RGC-32 are crucial for CDK1 binding (Figure 4-6).

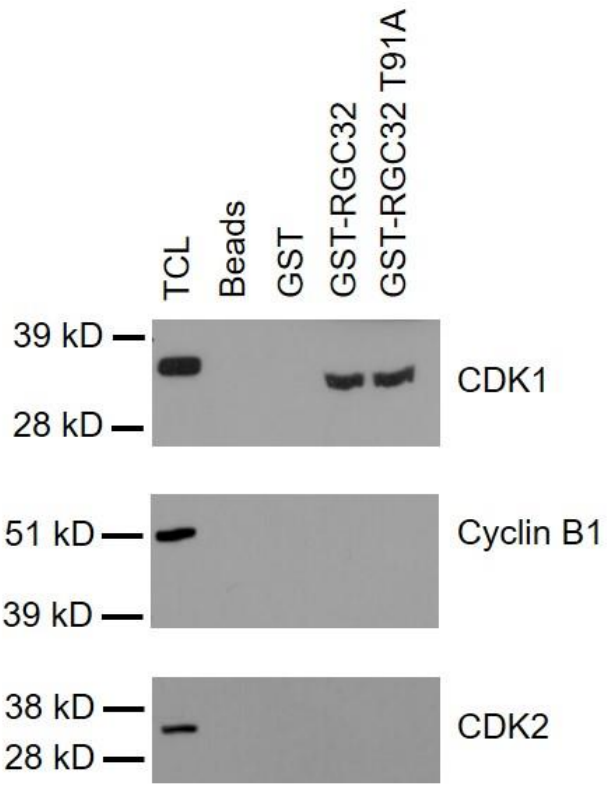

Figure 4-2. Western blot analysis of *in vitro* interaction of RGC-32 in Mutu I cells.

Glutathione agarose beads or beads bound to GST, GST-RGC-32 (WT) or GST-RGC32 mutant (T91A) were mixed with Mutu I total cell lysates. CDK2 was used as a negative control

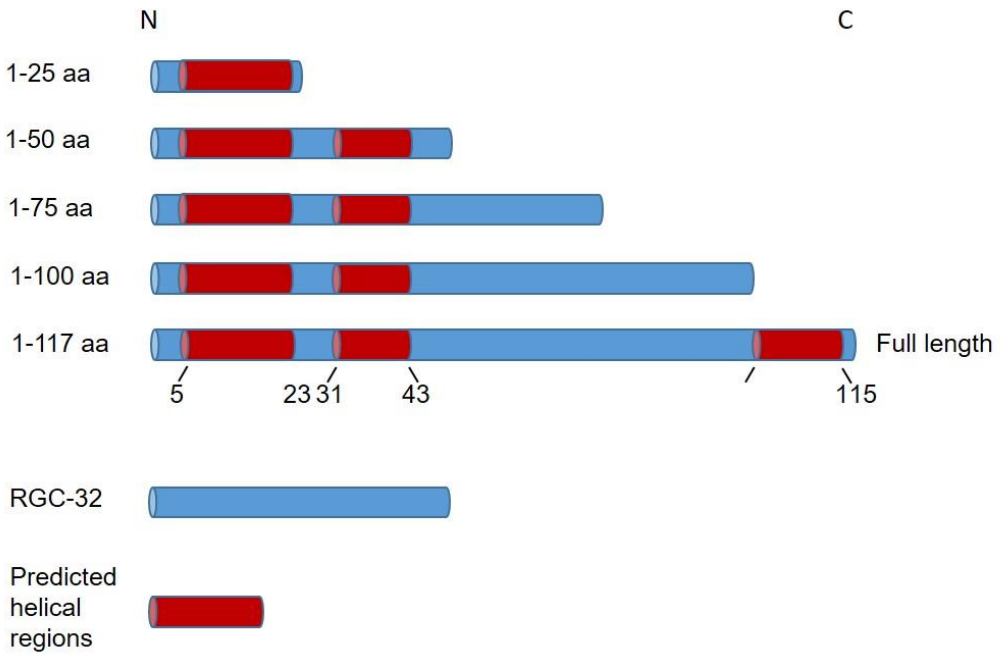

Figure 4-3. Schematic diagram of RGC-32 truncations.

RGC-32 was shown as blue bars and three predicted helical regions in RGC-32 were shown as red bars.

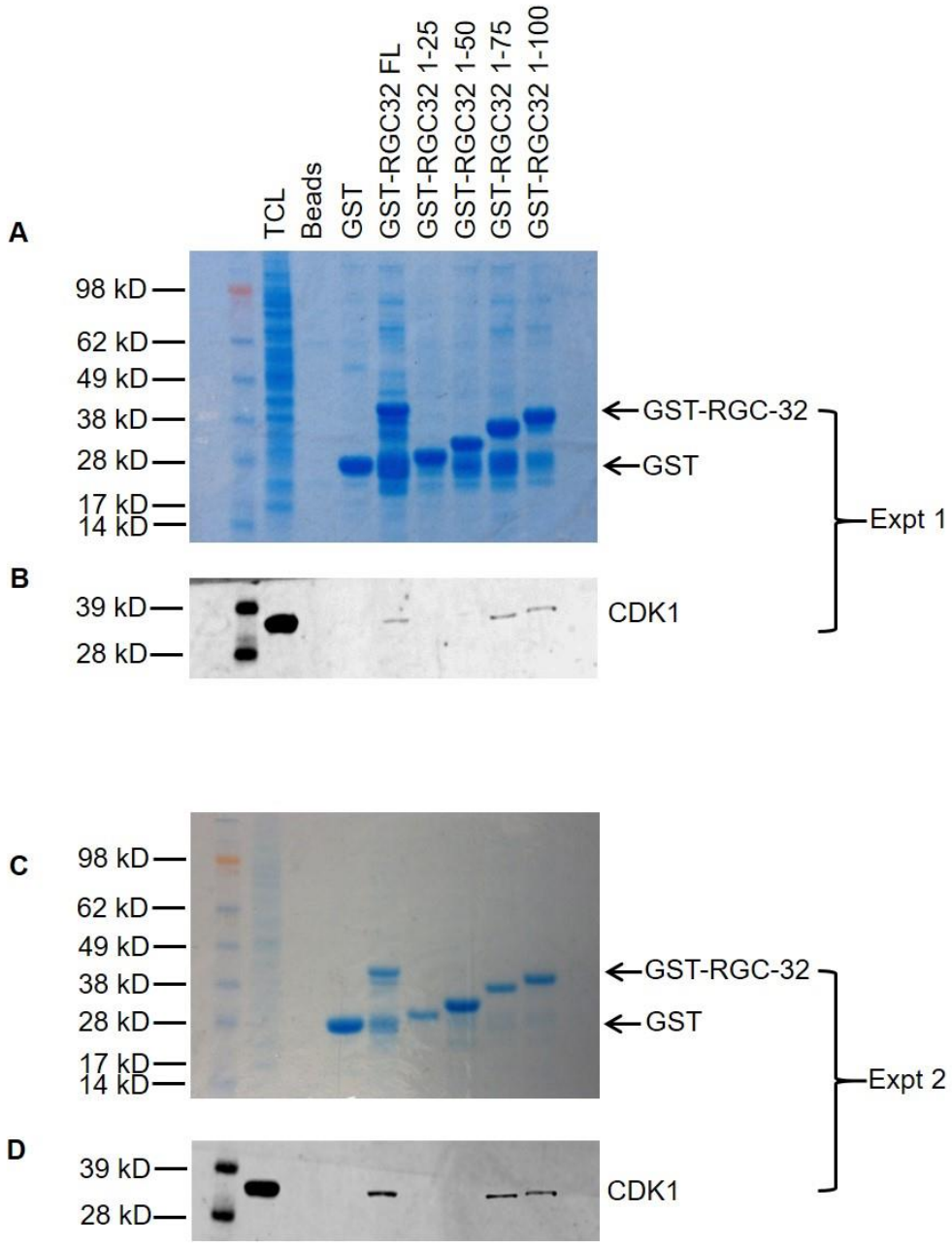

Figure 4-4. *In vitro* interaction of RGC-32 truncations with CDK1.

Glutathione agarose beads or beads bound to GST, GST-RGC-32 FL or truncations were mixed with BJAB total cell lysates. **A and C.** SDS-PAGE gel analysis of GST, GST-RGC-32 FL and truncations used in pull-down assay. **B and D.** Western blot analysis of interaction of RGC-32 truncations with CDK1.

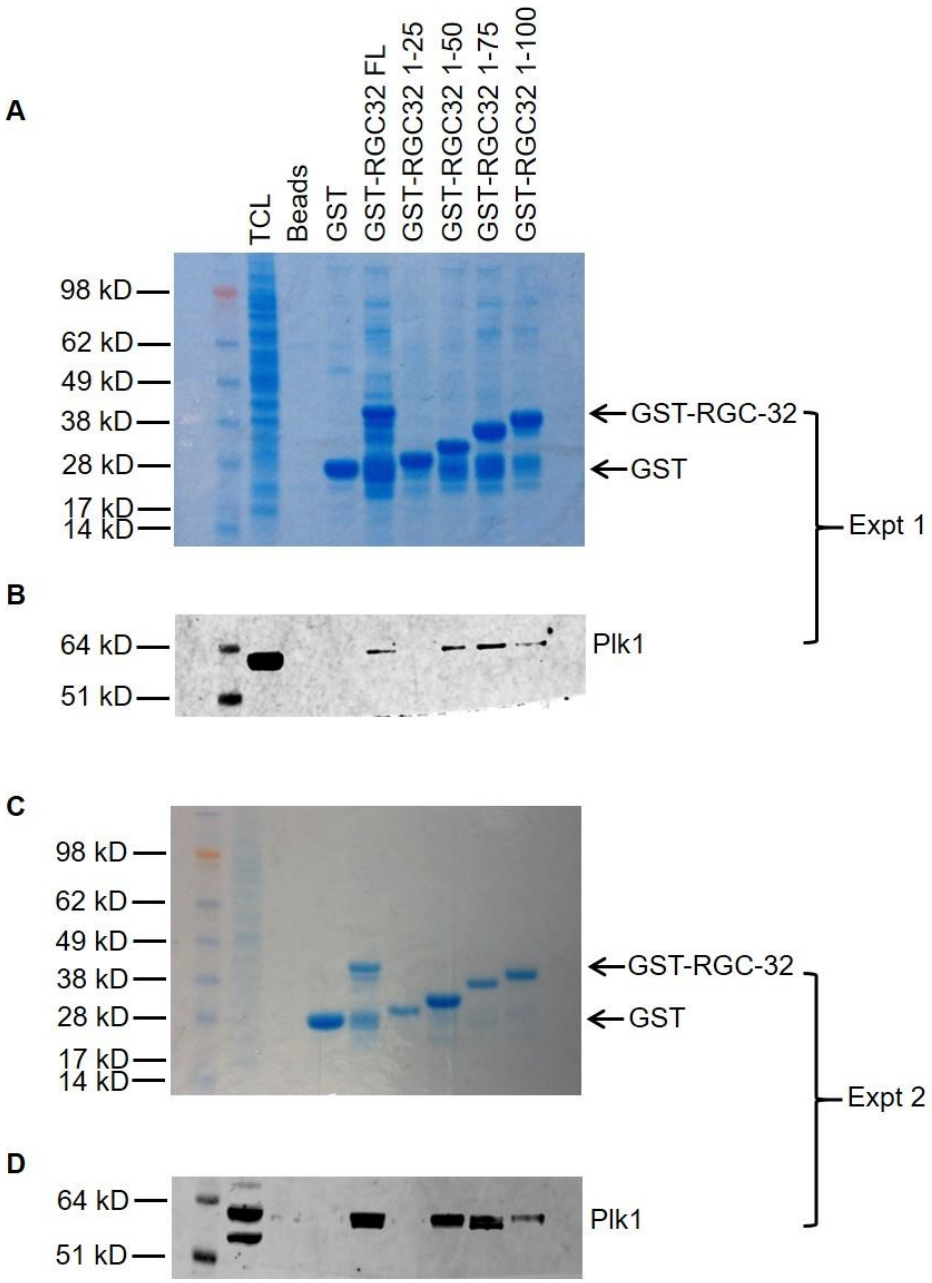

Figure 4-5. *In vitro* interaction of RGC-32 truncations with Plk1.

Glutathione agarose beads or beads bound to GST, GST-RGC-32 FL or truncations were mixed with BJAB total cell lysates. **A** and **C.** SDS-PAGE gel analysis of GST, GST-RGC-32 FL and truncations used in pull-down assay. **B** and **D.** Western blot analysis of interaction of RGC-32 truncations with Plk1.

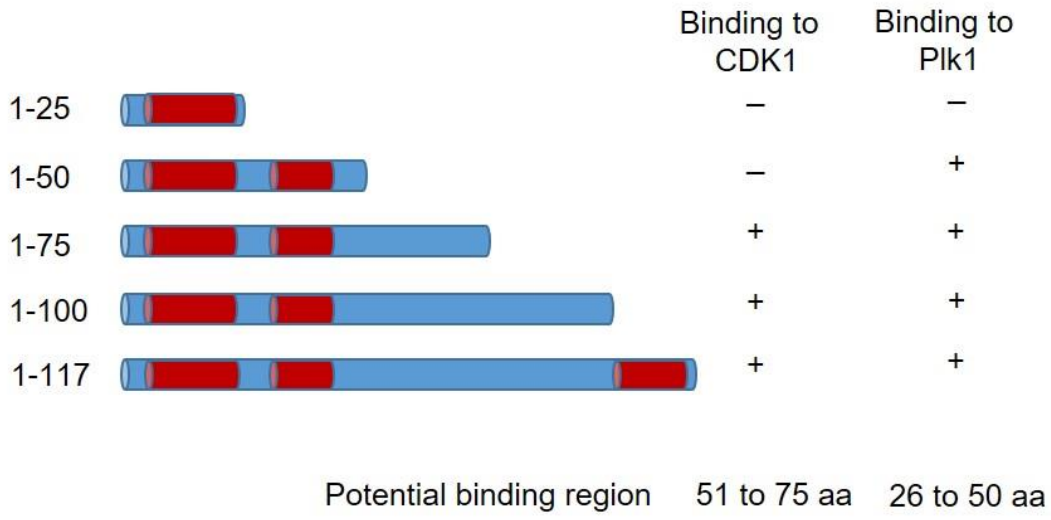

Figure 4-6. Summary of potential RGC32 binding domains with CDK1 and Plk1.

RGC-32 was shown as blue bars and three predicted helical regions in RGC-32 were shown as red bars. – means there is no binding between RGC-32 truncations and CDK1 or Plk1 and + means there is binding.

For Plk1 binding (Figure 4-5), only truncation 1-25 failed to pull down Plk1. All other truncations (1-50, 1-75 and 1-100) and full length RGC-32 pulled down Plk1 successfully. Hence amino acid residues between 25 and 50 in the RGC-32 are required for Plk1 binding (Figure 4-6).

4.4 Mutation analysis of RGC-32 binding to CDK1 or Plk1

To further identify the functional binding sites of RGC-32, we aligned RGC-32 in difference species to identify amino acids within the regions identified as important for CDK1 or Plk1 binding that are conserved (NCBI) (Figure 4-7). We then identified conserved amino acids that may play a role in protein-protein interactions to mutate (amino acid framed in black boxes in Figure 4-8). To study CDK1 binding, we mutated the hydrophobic amino acids phenylalanine 68 and 70 to alanine (Figure 4-8). To study PLK1 binding, we mutated the hydrophobic amino acids tyrosine 33 to A and positively-charged cluster lysine 41, arginine 42 and 43 to negatively charged glutamic acid (Figure 4-8).

The results of two independent experiments showed that substituting both phenylalanine to alanine in RGC-32 increased the binding activity for CDK1 to 1.8-fold compared to RGC-32 wildtype (Figure 4-9E). But this change was not significant using statistical analysis so it indicated the interaction of RGC-32 and CDK1 was not dependent on F68 and 70 on RGC-32.

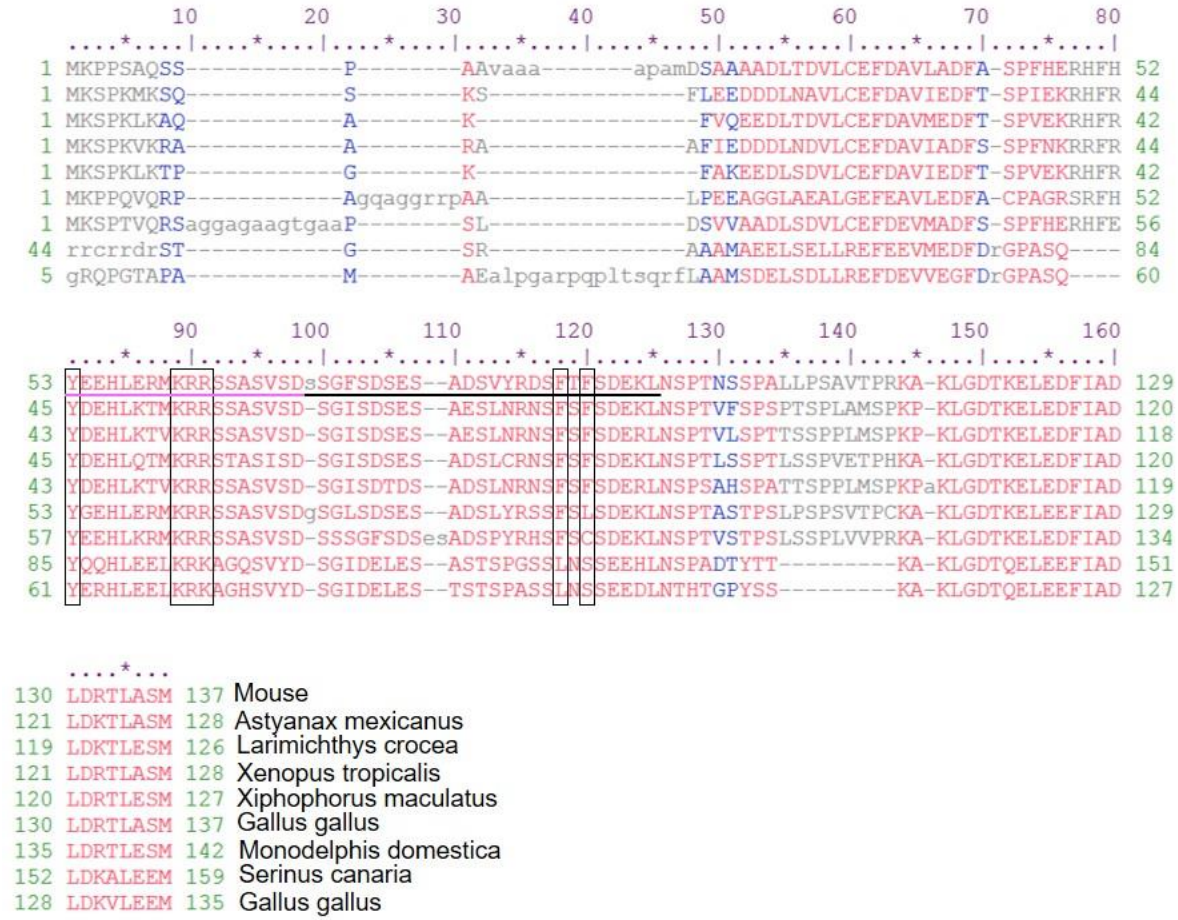

Figure 4-7. Conserved domains alignment of RGC-32 in different species.

The alignment was done using Conserved Domains (NCBI). Upper case amino acids are aligned and lower case grey amino acids are unaligned. The red to blue color scale shows the degree of conservation with red representing highly conserved. Gi number represents the different species. Potential interaction domains of RGC-32 and CDK1 or Plk1 are underlined as pink and black. Amino acids framed are the mutated residues for CDK1 and Plk1 binding (also see Figure 4-7).

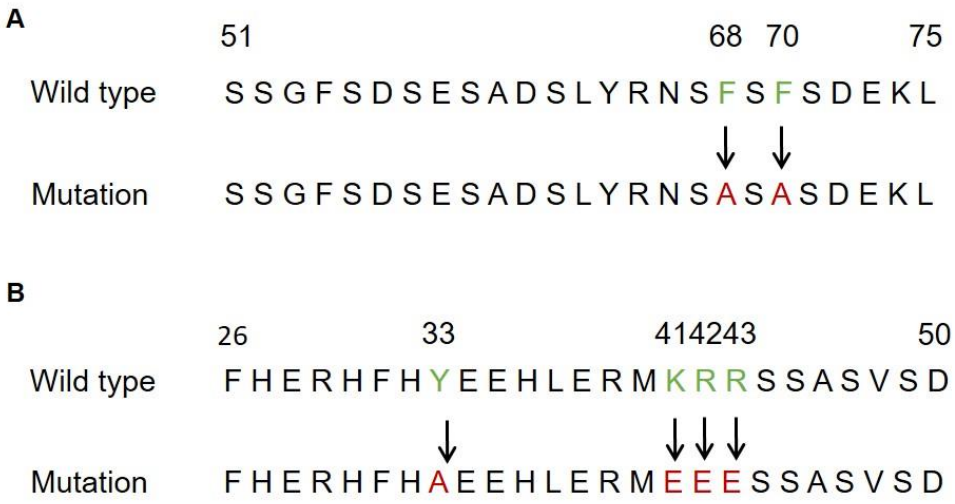

Figure 4-8. Mutated residues in RGC-32 for CDK1 or Plk1 binding (also see Figure 4-10).

A. Mutation of RGC-32 (F68A, F70A) for CDK1 binding. **B.** Mutation of RGC-32 (Y33A,K41E, R42E, R43E) for Plk1 binding.

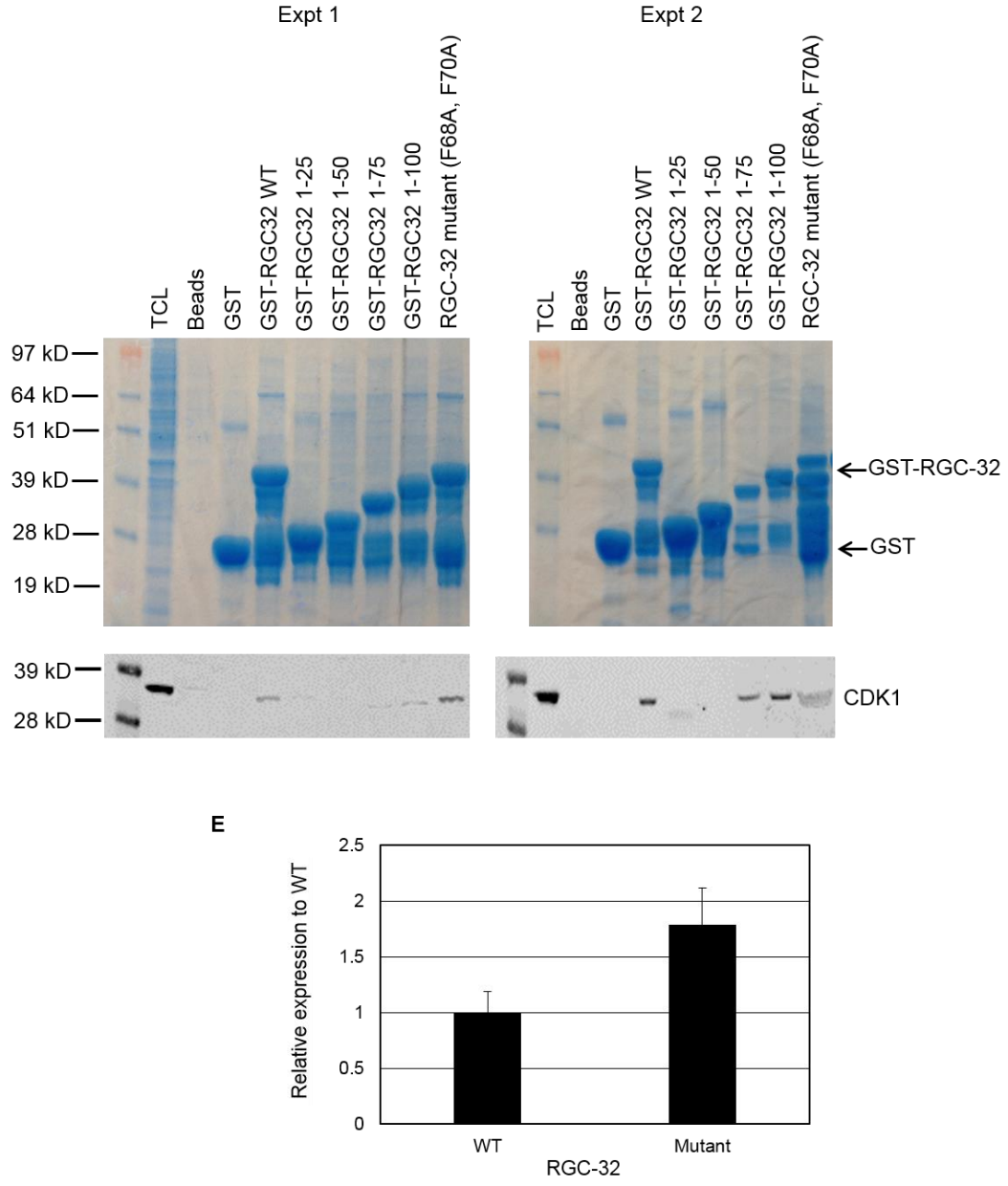

Figure 4-9. *In vitro* interaction of RGC-32 mutant with CDK1.

Glutathione agarose beads or beads bound to GST, GST-RGC-32 WT, truncations or mutant were mixed with BJAB total cell lysates. **A** and **C.** SDS-PAGE gel analysis of GST, GST-RGC-32 WT, truncations and mutant used in GST pull-down assay. **B** and **D.** Western blot analysis of interaction of RGC-32 mutant with CDK1. **E.** The intensity of bands was quantified using Licor and relative to the WT. This figure shows the mean of 2 independent experiments.

For Plk1 binding, Y33 K41 R42 R43 mutating to A33 E41, 42 and 43, which were present in the predicted helix, decreased the binding activity for PLK1 to around 40% compared to RGC-32 wildtype (Figure 4-10C). Since this was the result of one experiment, this would need to be repeated to confirm this observation and due to time constraints this was not possible.

4.5 RGC-32 can interact with Spc24

During the course of this study, we identified the third α-helix (Figure 3-1) has a homology to the N terminus of histone-fold protein Cnn1 using HHpred (Figure 4-11). It has been shown that Cnn1 is bound as an α-helix in a hydrophobic cleft at the interface between Spc24 and Spc25 (Malvezzi et al., 2013). Spindle pole component 24 and 25 (Spc24-25) are Ndc kinetochore complex component and play a role in the attachment of kinetochore to microtubule (Malvezzi et al. 2013) (see section 1.1.4). Next, we tested if there was an interaction of RGC-32 and Spc24. We found that GST-tagged RGC-32 was able to pull down Spc24 (Figure 4-12). RGC-32 truncation mutants were used to identify the domains required for binding to Spc24. Only truncation 1-25 failed to pull down Spc24. All other truncations (1-50, 1-75 and 1-100) and full length RGC-32 pulled down Spc24 successfully (Figure 4-12). Hence amino acid residues between 25 and 50 in the RGC-32 are the required for Spc24 binding (Figure 4-13). RGC-32 has been reported to concentrate in centrosomes and spindle poles during prometaphose and metaphase (Saigusa et al. 2007). Our results suggest that RGC-32 might play a role in the attachment of kinetochore to microtubule by interacting with Spc24.

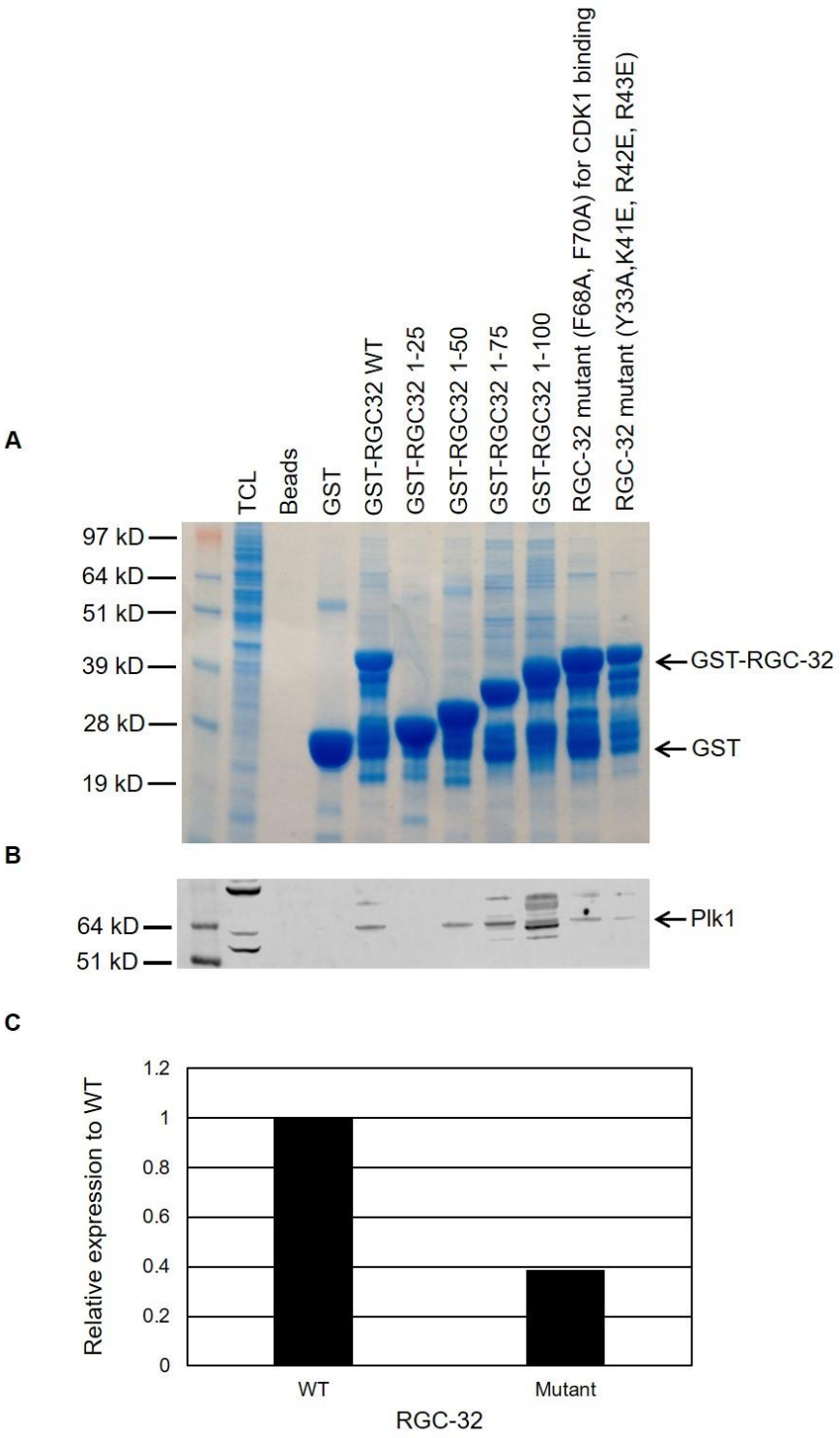

Figure 4-10. *In vitro* interaction of RGC-32 mutant with Plk1.

Glutathione agarose beads or beads bound to GST, GST-RGC-32 WT, truncations or mutant were mixed with BJAB total cell lysates. **A.** SDS-PAGE gel analysis of GST, GST-RGC-32 WT, truncations and mutant used in GST pull-down assay. **B.** Western blot analysis of interaction of RGC-32 mutant with Plk1. **C.** The intensity of bands was quantified using Licor and relative to the WT. This figure shows data of one experiment.

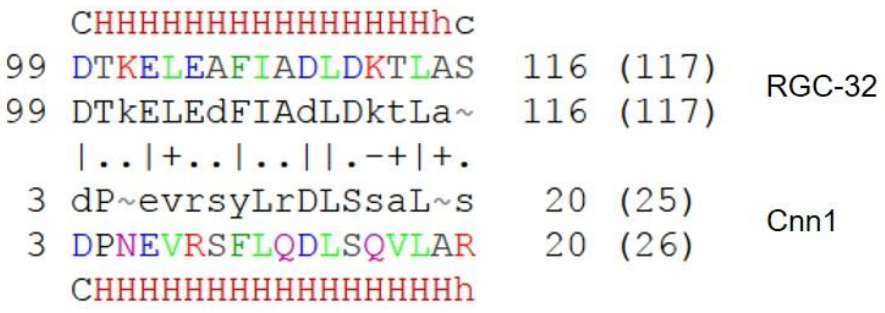

Figure 4-11. Sequence alignment of RGC-32 and Cnn1 using HHpred.

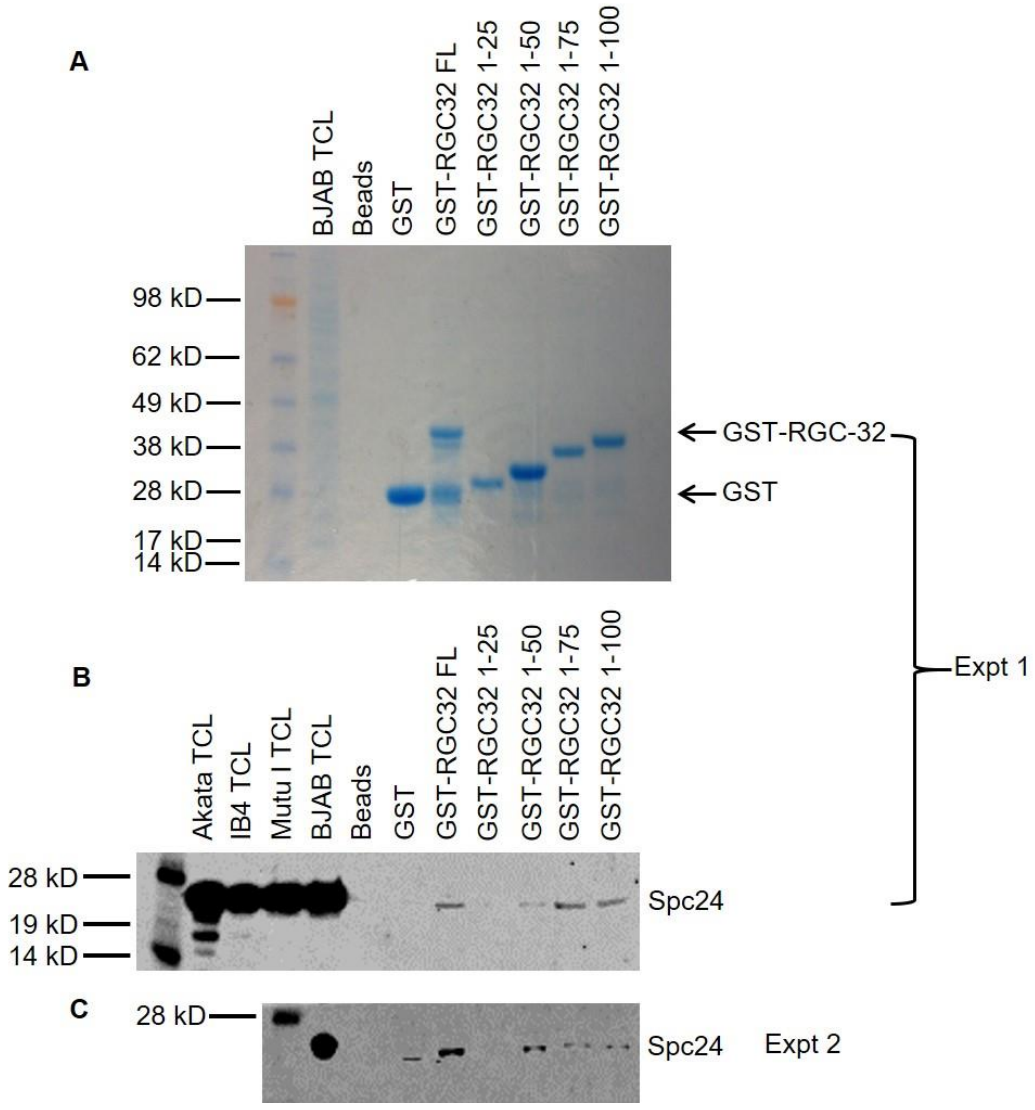

Figure 4-12. *In vitro* interaction of RGC-32 truncations with Spc24.

Glutathione agarose beads or beads bound to GST, GST-RGC-32 FL or truncations were mixed with BJAB total cell lysates. **A.** SDS-PAGE gel analysis of GST, GST-RGC-32 FL and truncations used in pull-down assay. **B** and **C.** Western blot analysis of interaction of RGC-32 truncations with Spc24.

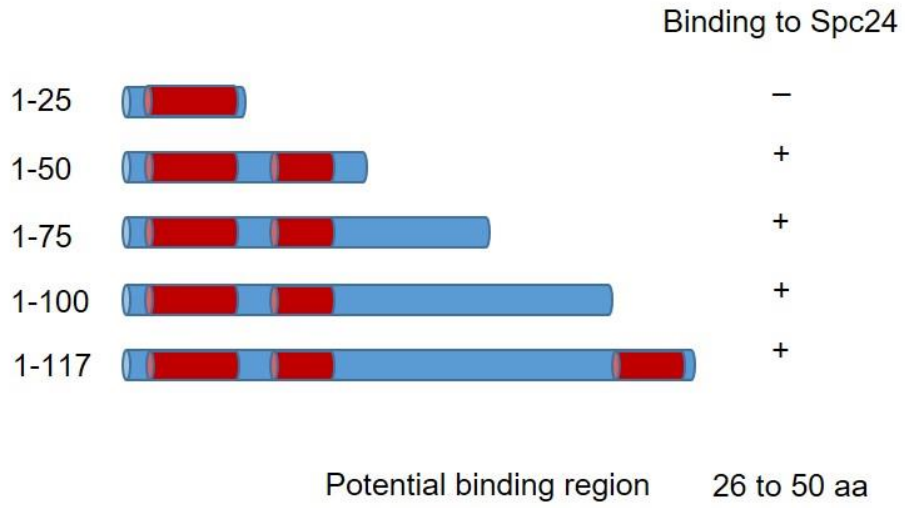

Figure 4-13. Summary of potential RGC32 binding domains with Spc24.

RGC-32 was shown as blue bars and three predicted helical regions in RGC-32 were shown as red bars. – means there is no binding between RGC-32 truncations and Spc24 and + means there is binding

4.6 Characterisation of stable RGC-32 expressing cell lines

Expression of RGC-32 has been shown to promote S and M phase entry of smooth muscle cells following G1 arrest (Badea et al. 2002). Our group demonstrated that stable overexpression of RGC-32 alone is sufficient to disrupt the G2/M checkpoint (Schlick et al. 2011). Unfortunately, continued culture of the stable cell lines overexpressing RGC-32 that were generated for this work led to the loss of their cell-cycle disruption phenotype.

We therefore set out to generate stable cell lines expressing inducible RGC-32 to avoid the accumulation of compensatory mutations. RGC-32 was cloned into pRTS-1 vector (Figure 2-2) between *SfiI* restriction sites to replace the luciferase gene. This Doxycycline-dependent expression system has a bidirectional promoter which allows the expression of two genes, eGFP and the gene of interest. The expression of the gene of interest is switched on or off by adding doxycycline or not. This vector carries the EBV plasmid origin of replication (*ori*P) and EBNA1 which binds to *ori*P and maintains episomal replication of the episome to daughter cells (Bornkamm et al. 2005).

4.6.1 DNA test using HEK293T cells

Initially, RGC-32 was cloned into this vector and transfected into the EBV negative BL cell line DG75. Stable cell lines were selected by limited dilution in the presence of 200 µg/ml hygromycin. The expressions of EBNA 1 and RGC-32 were not detected in total cell lysates by western blotting (data not shown). Therefore we tested the DNA for transfection using HEK293T cells which have higher transfection efficiency than DG75.

HEK293T cells were transiently transfected with pRTS1 empty vector or pRTS1-RGC-32 (old and new) and Doxycline (DOX) was add 24 hours post-transfection to induce the expression of eGFP and luciferase or RGC-32. Luciferase assay showed that addition of Doxycline induced the expression of eGFP (Figure 4-14). Then we tested using old DNA which had been stored at -20°C after being made and new DNA which were used without storage -20°C to see if the way storing DNA made difference for transfection. Flow cytometry experiments showed that transfection efficiency is higher using new DNA than old DNA (Figure 4-15) and Western blot analysis confirmed the expression of EBNA1 and RGC-32 using both DNAs (Figure 4-16).

4.6.2 Stable Akata cell line expressing RGC-32

4.6.2.1 Optimisation of DOX induction

Akata cells were transfected with pRTS1 empty vector or pRTS1-RGC-32 and then cultivated in growth medium. The hygromycin concentration in medium was increased gradually to 100 µg/ml by replacing the medium with hygromycin containing medium weekly. Within the next 2-4 weeks, hygromycin resistant cells grew out.

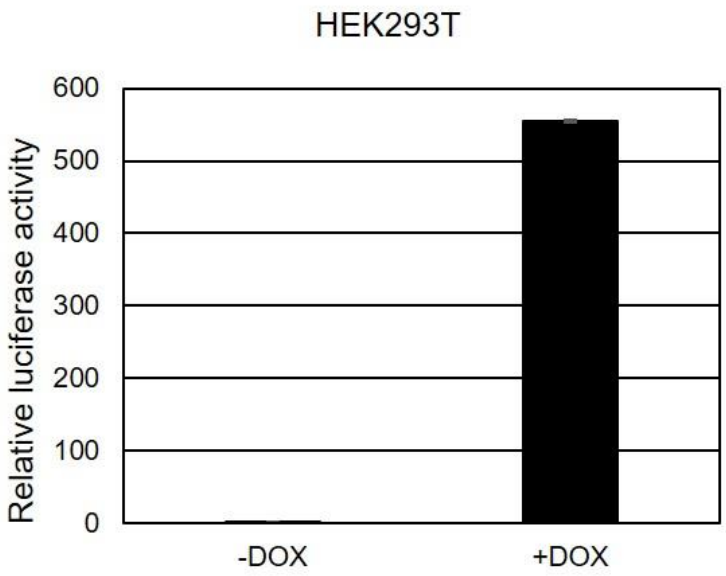

Figure 4-14. Verification of DNA used in making stable cell lines using HEK293T cells.

Luciferase assay of with/without DOX induction in HEK293T cells transfected with pRTS-1 vector. This figure shows the mean of 2 independent experiments.

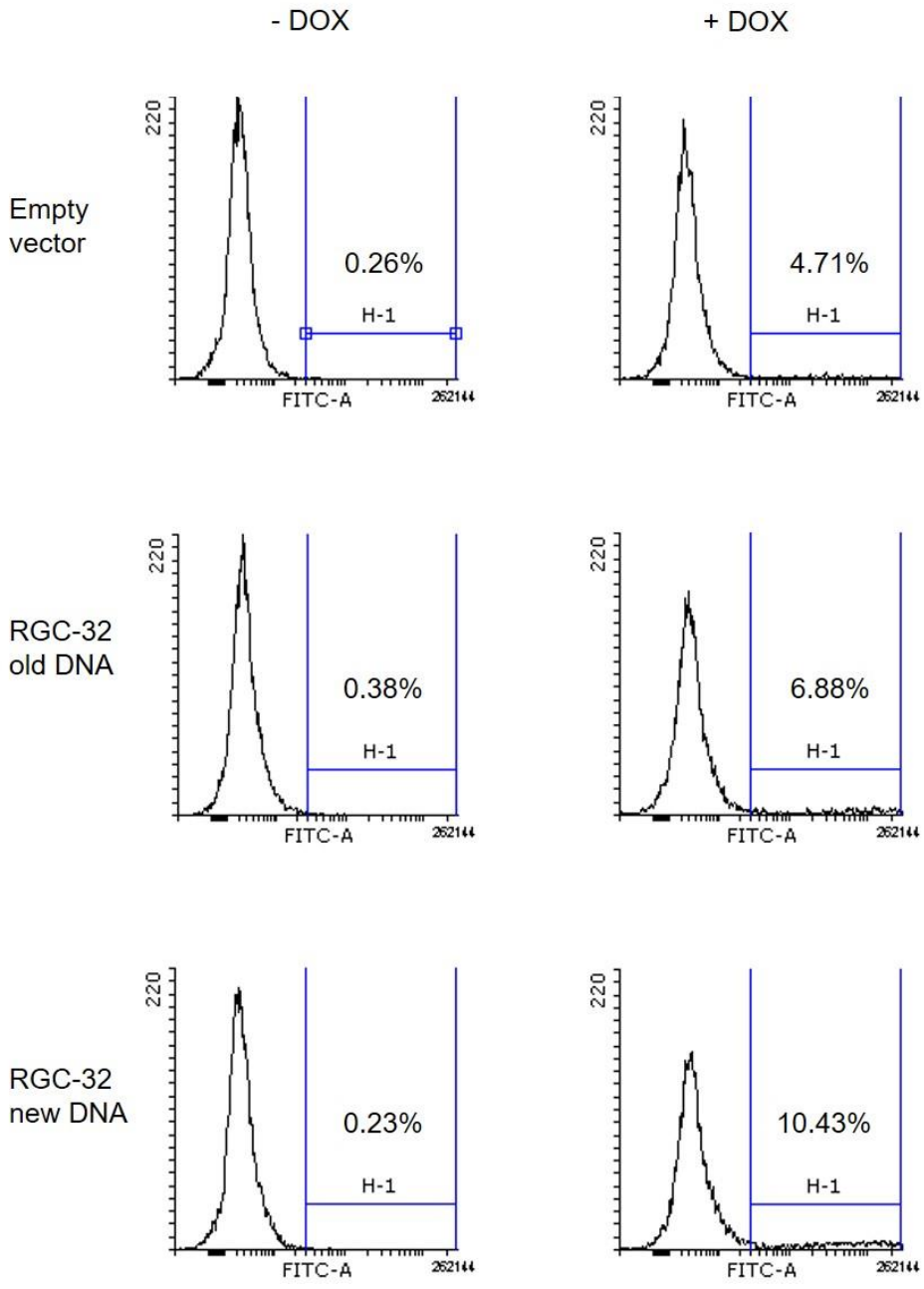

Figure 4-15. FACS analysis of transiently transfected HEK293T cells.

HEK293T cells were transiently transfected with old pRTS-1-RGC-32 (DNA had been stored at -20 °C before transfection) and new pRTS-1-RGC-32 (DNA was used in transfection after made). 3 µg DNA was transfected using Effectene Transfection Reagent (QIAGEN). Cells were harvested 48 hours and the percentage eGFP-positive cells determined by flow cytometry.

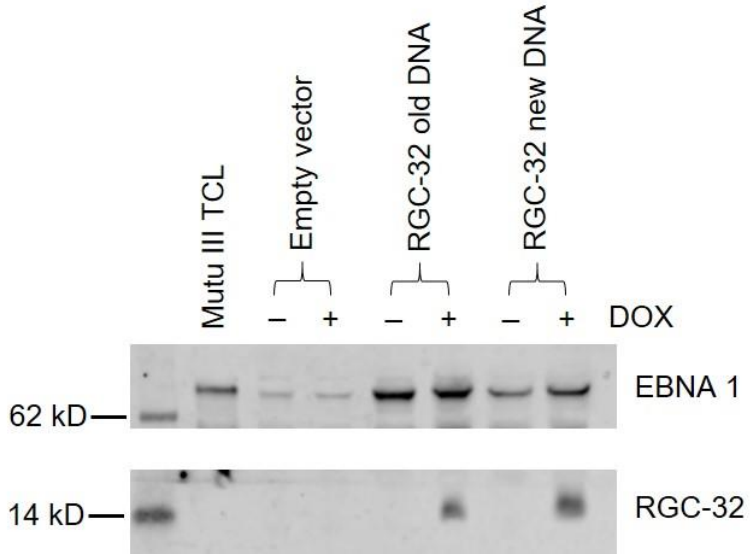

Figure 4-16. Western blot analysis of EBNA 1 and RGC-32 expression in HEK293T.

HEK293T cells were transiently transfected with old DNA (DNA had been stored at -20 °C before transfection) and new DNA (DNA was used in transfection after made). Cells were harvested and total cell lysates of -/+ DOX induction were separated on a gel. The Mutu III cell line total cell lysate was used as a positive control for EBNA 1 and RGC-32 expression.

To optimise the expression of RGC-32 in Akata cells, 1 or 2 µg/ml Doxycycline and 24 or 48 hours induction time were tested. Western blotting analysis showed that the expression of both EBNA 1 and RGC-32 were higher at 48 hours than 24 hours (Figure 4-17). More RGC-32 was expressed using 1 µg/ml Doxycycline induction compared to 2 µg/ml at 48 hours (Figure 4-17). 1 µg/ml Doxycycline and 48 hours induction time were used for further experiments.

4.6.2.2 The effects of stable RGC-32 overexpression

To investigate the effect of RGC-32 overexpression on the G_2/M checkpoint, etoposide, a topoisomerase II inhibitor, was used to induce double stranded DNA breaks and arrest cells in G_2. DOX was added to induce RGC-32 and then etoposide was added 48 hours post DOX induction. Cells without DOX induction are used as control. Western blotting analysis confirmed the expression of EBNA 1 and RGC-32 in cells before and after etoposide treatment (Figure 4-18). The proportion of cells in each cell cycle phase was analysed after 8, 24 and 48 hours etoposide treatment. DOX induction increased apoptosis, such as a sub-G_1 population by 8% without etoposide (Figure 4-19). The results showed that compared to Akata cells not overexpressing RGC-32, Akata cells overexpressing RGC-32 cells displayed an increased proportion of cells in G_0/G_1 and a decreased proportion of cells in G2/M (Figure 4-19). RGC-32 overexpressing Akata cells showed 2%, 5% and 13% increase in the G_0/G_1 phase after 8, 24 and 48 hours etoposide treatment respectively, compared with control cells (Figure 4-20). The G_2/M population of Akata cells expressing RGC-32 decreased 6%, 25% and 14% after 8, 24 and

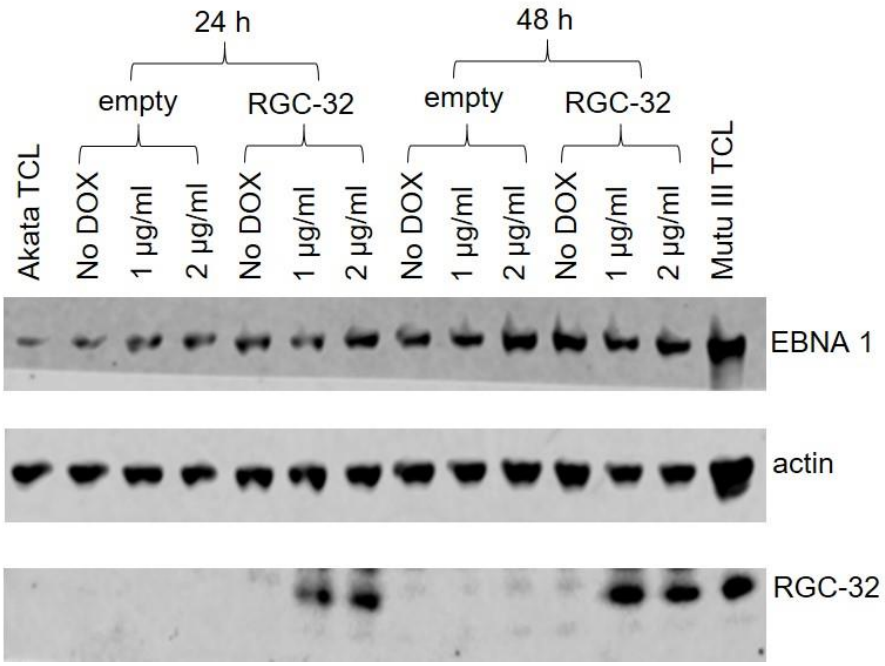

Figure 4-17. Western blotting analysis of stable Akata cell lines after DOX induction.

Akata cells were stable transfected with pRTS-1α empty vector or pRTS-1α RGC-32 then harvested 24 or 48 hours post doxycycline treatment (1 or 2 µg/ml) and whole cell lysates of -/+ DOX induction were separated on a gel. The Mutu III cell line is a positive control for EBNA 1 and RGC-32 expression. Actin is a loading control.

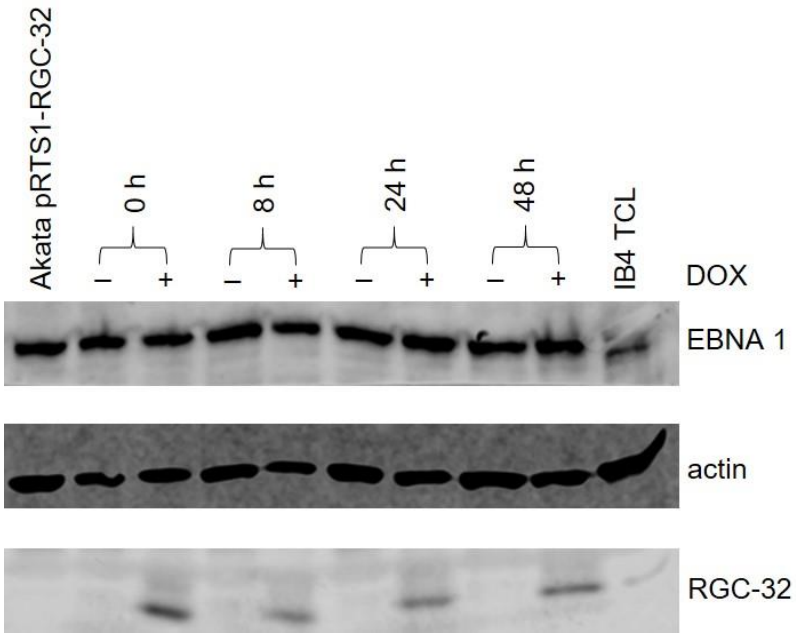

Figure 4-18. Western blotting analysis of stable Akata cells after etoposide treatment.

Akata cell lines stably expressing RGC-32 were exposed to 400 nM etoposide for 8, 24 and 48 hours after 48 hours of DOX induction. Whole cell lysates were separated on a gel. The IB4 cell line is a positive control for EBNA 1 and RGC-32 expression. Actin is a loading control.

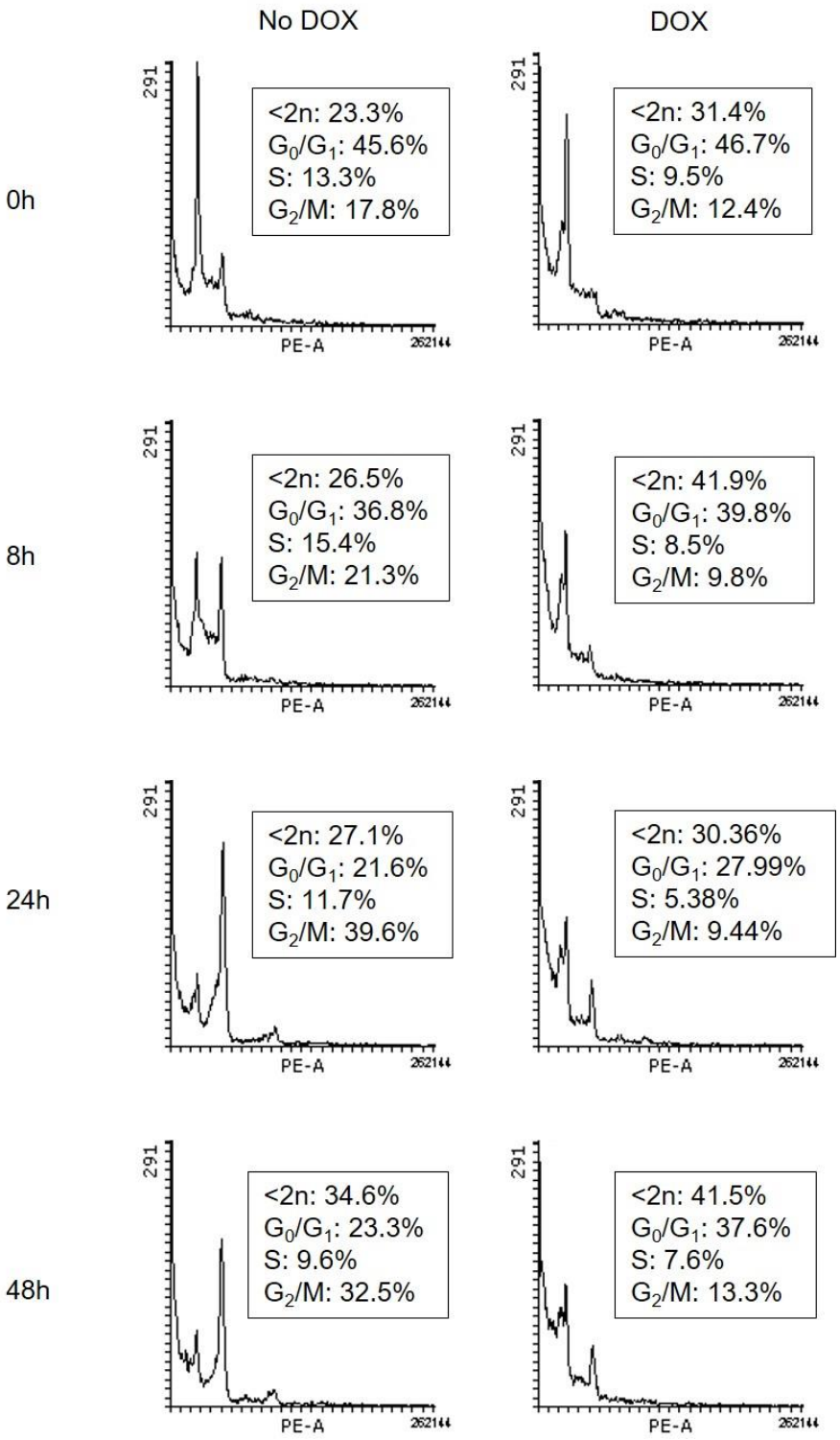

Figure 4-19. FACS analysis of stably transfected Akata cells after etoposide treatment.

Akata cell lines stably expressing RGC-32 were exposed to 400 nM etoposide for 0, 8, 24 and 48 hours (n=1). Cells were stained with propidium iodide to visualise cell cycle distribution.

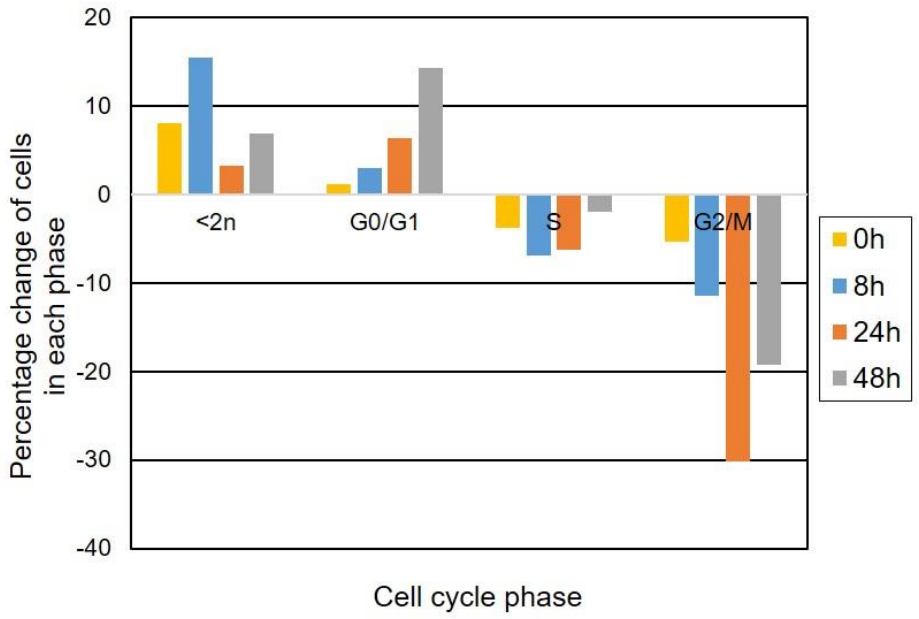

Figure 4-20. Percentage change of Akata cells -/+ etoposide in each phase.

Akata cell lines stably expressing RGC-32 were exposed to 400 nM etoposide for 8, 24 and 48 hours. The percentage change of cells -/+ etoposide in each phase was relative to control cells.

48 hours etoposide treatment respectively, compared with control cells (Figure 4-20). It indicated RGC-32 disrupted G_2/M checkpoint in Akata cell line which was consistent with our previously published data in BJAB and DG75 cell lines (Schlick et al. 2011). It is possible that RGC-32 expression activates CDK1 activity which results that the cells override etoposide-induced G_2 arrest.

4.6.3 Stable HEK293 cell line expressing RGC-32

4.6.3.1 Optimisation of DOX induction

HEK293 cells were transfected with pRTS1 empty vector or pRTS1-RGC-32 and then cultivated in growth medium. The hygromycin concentration in medium was increased gradually to 50 µg/ml by replacing the medium with hygromycin containing medium weekly. Within the next 2-4 weeks, hygromycin resistant cells grew out.

To optimise the expression of RGC-32 in the HEK293 cell line, 0.5, 1 or 2 µg/ml Doxycycline and 8, 24 or 48 hours induction time were tested. Western blot showed that the expression of both EBNA 1 and RGC-32 was higher at 48 hours than 8 and 24 hours (Figure 4-21). More RGC-32 was expressed using 1 µg/ml Doxycycline induction compared to 0.5 and 2 µg/ml at 48 hours (Figure 4-21). 1 µg/ml Doxycycline and 48 hours induction time were used for further experiments.

4.6.3.2 The effects of stable RGC-32 overexpression

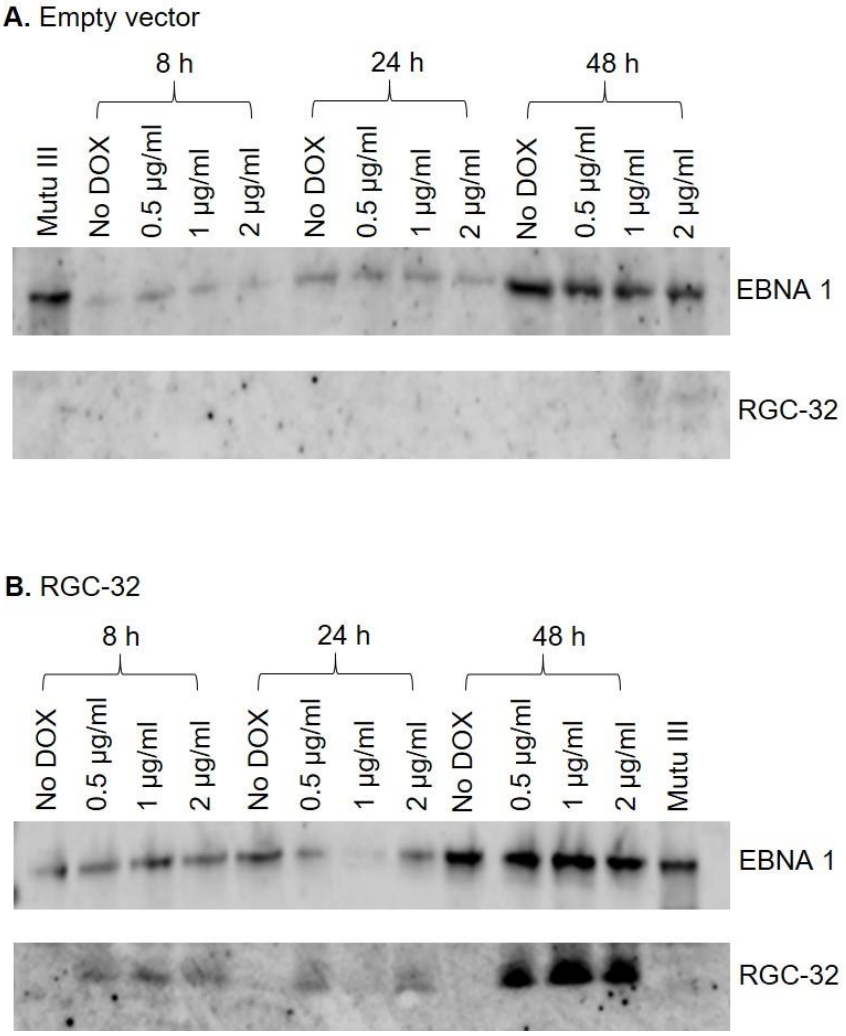

Figure 4-21. Western blotting analysis of stable HEK293 cell lines after DOX induction.

HEK293 cells were stable transfected with **A.** pRTS-1α empty vector or **B.** pRTS-1α RGC-32 then harvested 8, 24 or 48 hours post doxycycline treatment (0.5, 1 or 2 µg/ml) and whole cell lysates of -/+ DOX induction were separated on a gel. The Mutu III cell line is a positive control for EBNA 1 and RGC-32 expression. There is some problem with sample at 24 hours with 1 µg/ml DOX as no expression of both EBNA 1 and RGC-32 had been shown.

Western blotting analysis confirmed the expression of EBNA 1 at 8, 24 and 48 hours and RGC-32 at 8 and 48 hours before and after etoposide treatment (Figure 4-22). There was very little RGC-32 expression at 24 hours. The proportion of cells in each cell cycle phase was analysed after 8, 24 and 48 hours of etoposide treatment (Figure 4-23). The results showed that HEK293 cells did not arrest at G_2/M after 8, 24 or 48 hours etoposide treatment (Figure 4-24). It is possible the concentration of etoposide was not high enough to arrest the cells, but due to time constraints I was not able to perform any further titrations.

4.6.4 Stable HeLa cell line expressing RGC-32

4.6.4.1 Optimisation of DOX induction

HeLa cells were transfected with pRTS1 empty vector or pRTS1-RGC-32 and then cultivated in growth medium. The hygromycin concentration in medium was increased gradually to 100 µg/ml by replacing the medium with hygromycin containing medium weekly. Within the next 2-4 weeks, hygromycin resistant cells grew out.

To optimise the expression of RGC-32 in HeLa cells, 1 or 2 µg/ml Doxycycline with 24 or 48 hours induction time were tested. Western blotting analysis showed that the expression of both EBNA 1 and RGC-32 were similar at 24 and 48 hours, but less actin was expressed when induction time was 48 hours compared to 24 hours (Figure 4-25). More RGC-32 was expressed using 1 µg/ml Doxycycline induction compared to 2 µg/ml at 24 or 48 hours (Figure 4-

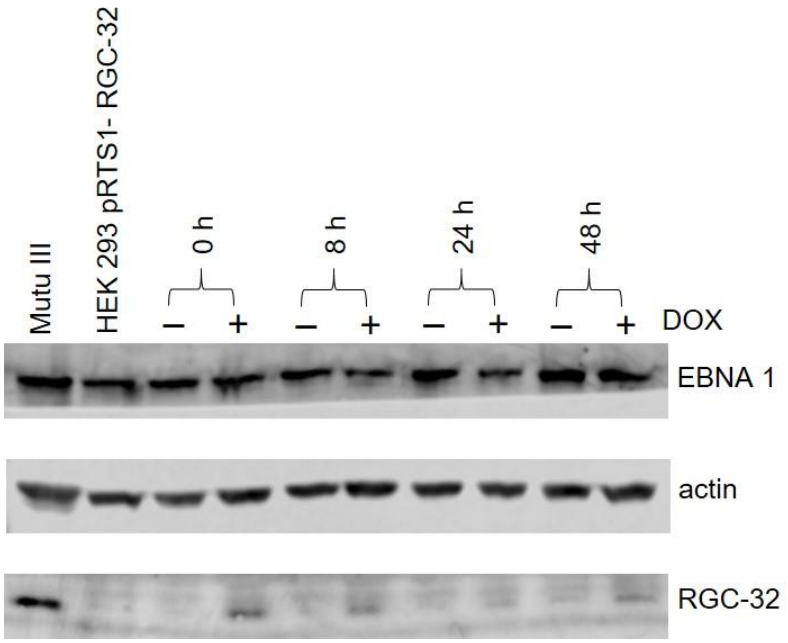

Figure 4-22. Western blotting analysis of stable HEK293 cells after etoposide treatment.

HEK293 cell lines stably expressing RGC-32 were exposed to 1 µM etoposide for 8, 24 and 48 hours after 48 hours of DOX induction. Whole cell lysates were separated on a gel. The Mutu III cell line is a positive control for EBNA 1 and RGC-32 expression. Actin is a loading control.

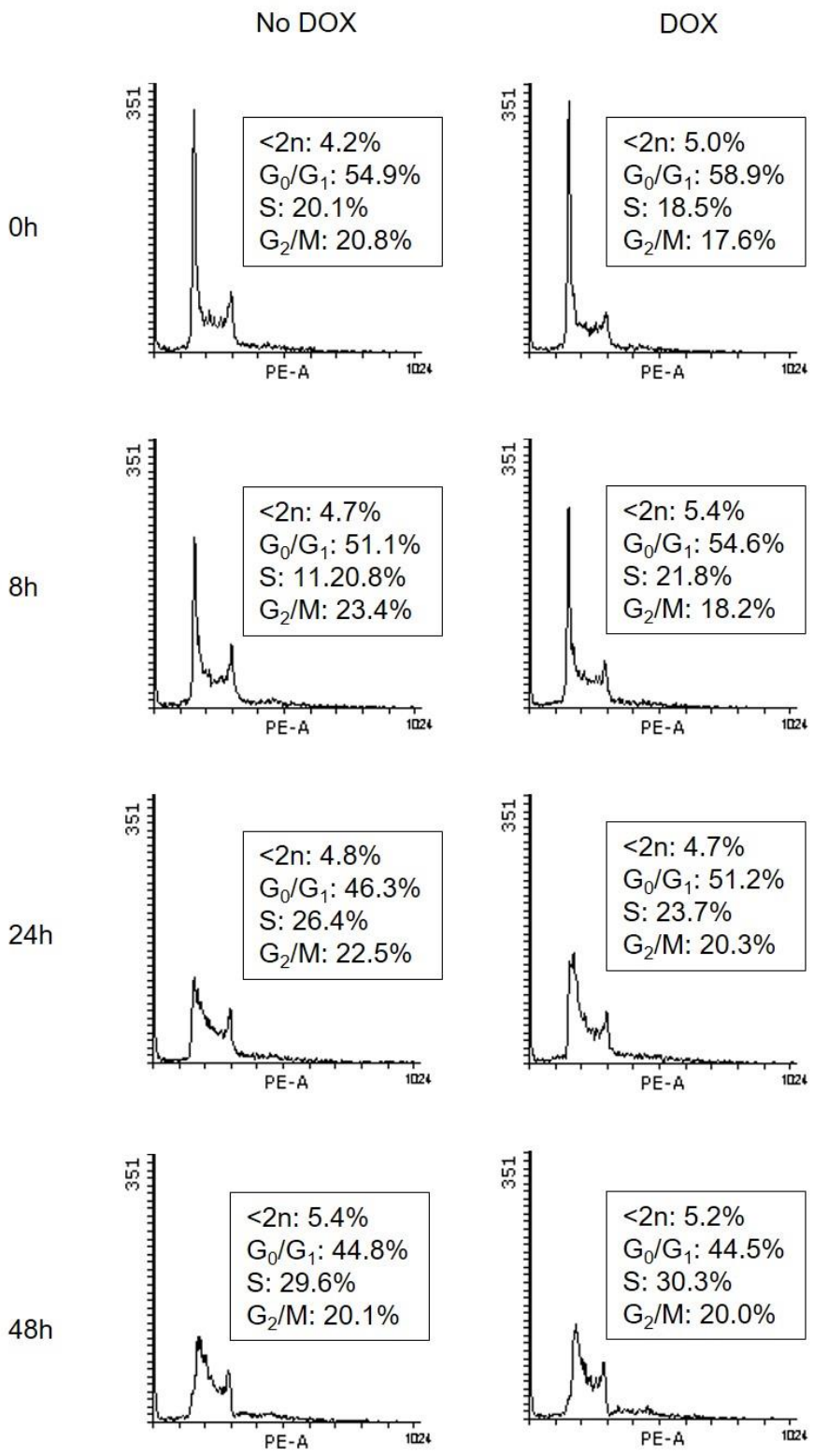

Figure 4-23. FACS analysis of stably transfected HEK293 cells after etoposide treatment.

HEK293 cell lines stably expressing RGC-32 were exposed to 1 μM etoposide for 0, 8, 24 and 48 hours. Cells were stained with propidium iodide to visualise cell cycle distribution.

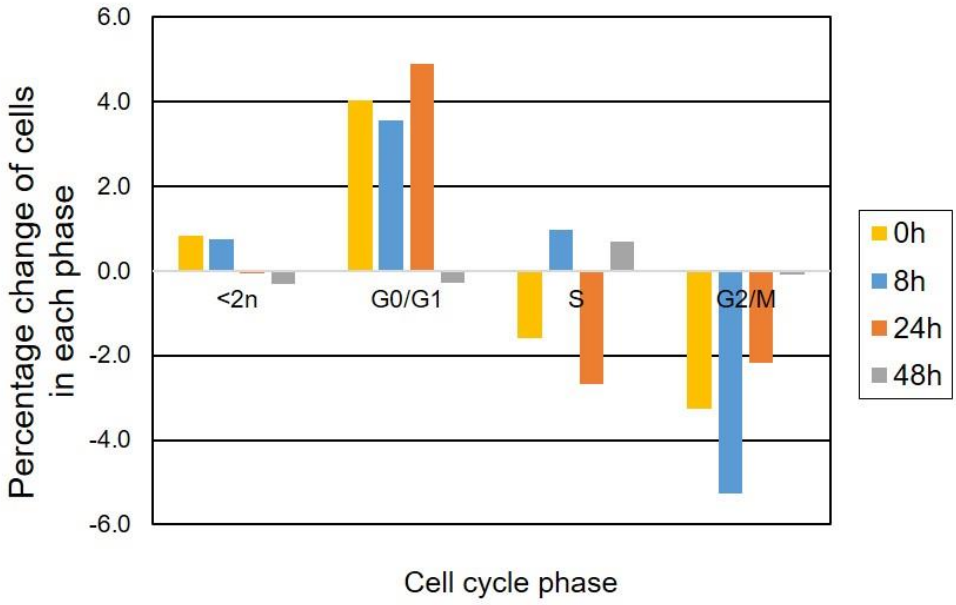

Figure 4-24. Percentage change of HEK293 cells -/+ etoposide in each phase.

HEK293 cell lines stably expressing RGC-32 were exposed to 1 µM etoposide for 8, 24 and 48 hours. The percentage change of cells -/+ etoposide in each phase was relative to control cells.

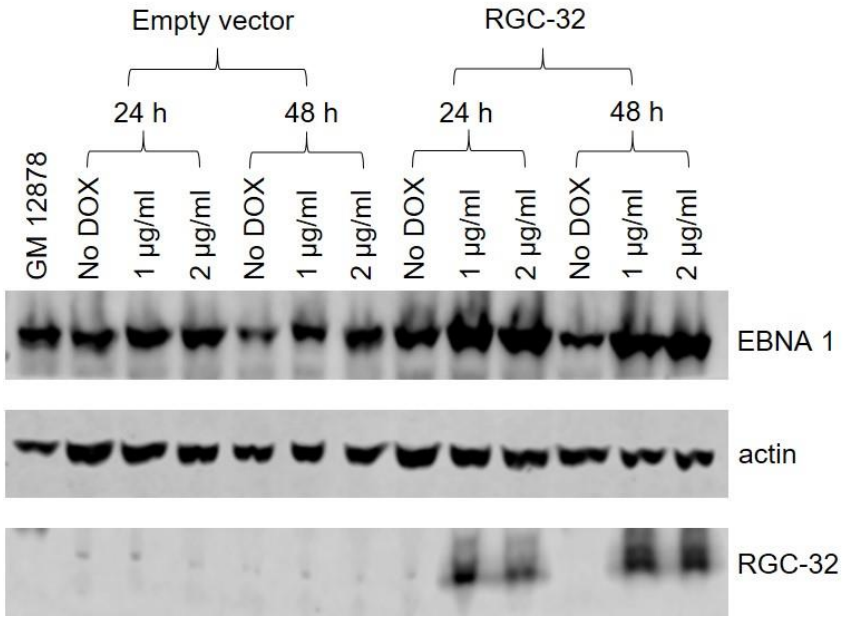

Figure 4-25. Western blotting analysis of stable HeLa cell lines after DOX induction.

HeLa cells were stable transfected with pRTS-1α empty vector or pRTS-1α RGC-32 then harvested 24 or 48 hours post doxycycline treatment (1 or 2 µg/ml) and whole cell lysates of -/+ DOX induction were separated on a gel. The GM12878 cell line is a positive control for EBNA 1 and RGC-32 expression. Actin is a loading control.

25). 1 µg/ml Doxycycline and 48 hours induction time were used for further experiments.

4.6.4.2 The effects of stable RGC-32 overexpression

Western blot confirmed the expression of EBNA 1 and RGC-32 before and after etoposide treatment (Figure 4-26). The proportion of cells in each cell cycle phase was analysed after 8, 24 and 48 hours of etoposide treatment (Figure 4-27). The HeLa cells expressing RGC-32 were arrested at G_2 phase only at 48 hours, but the expression of RGC-32 did not change the proportion of cells in each phase (Figure 4-28). Interestingly, Saigusa *et al*. has shown the similar results of HeLa cells overexpressing RGC-32 protein display simultaneous transition into G_2/M phase from G_1, but delayed transition into G1 phase from G2/M phase compared with control cells (Saigusa et al. 2007). Due to time constraints, I was not able to perform any further titrations of etoposide concentration.

4.7 Discussion

In this chapter, which regions are involved in the CDK1 and Plk1 interaction and the mechanism of RGC-32 disrupting cell cycle were investigated. Previously RGC-32 was found to associate with the recombinant CDK1/Cyclin B1 complex *in vitro* (Badea et al. 2002). Our results provided the first evidence that RGC-32 interacted with CDK1 in B-cells but interestingly not with Cyclin B1. It is possible that activation by RGC-32 is Cyclin-independent or RGC-32 competing with

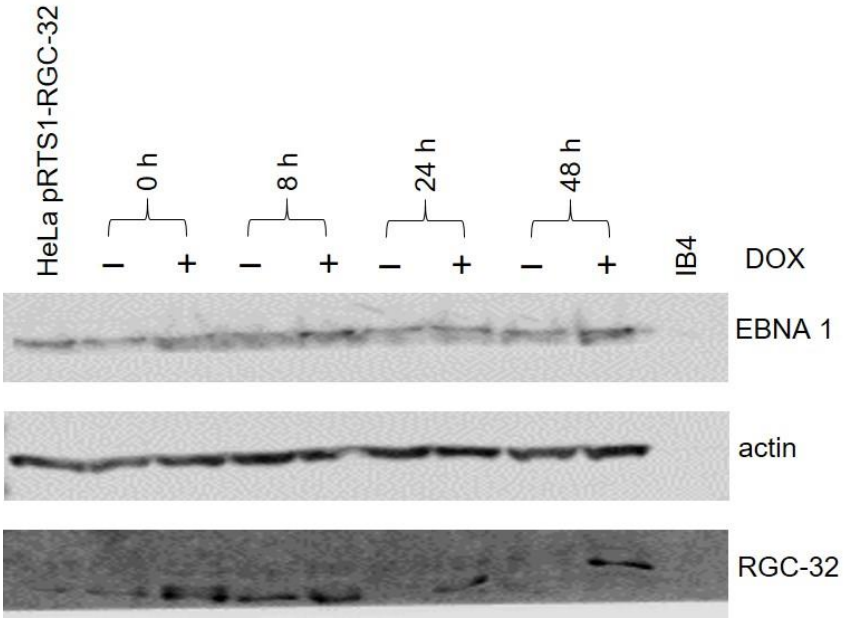

Figure 4-26. Western blotting analysis of HeLa stable cells after etoposide treatment.

HeLa cell lines stably expressing RGC-32 were exposed to 1 μM etoposide for 8, 24 and 48 hours after 48 hours of DOX induction. Whole cell lysates were separated on a gel. The IB4 cell line is a positive control for EBNA 1 and RGC-32 expression. Actin is a loading control.

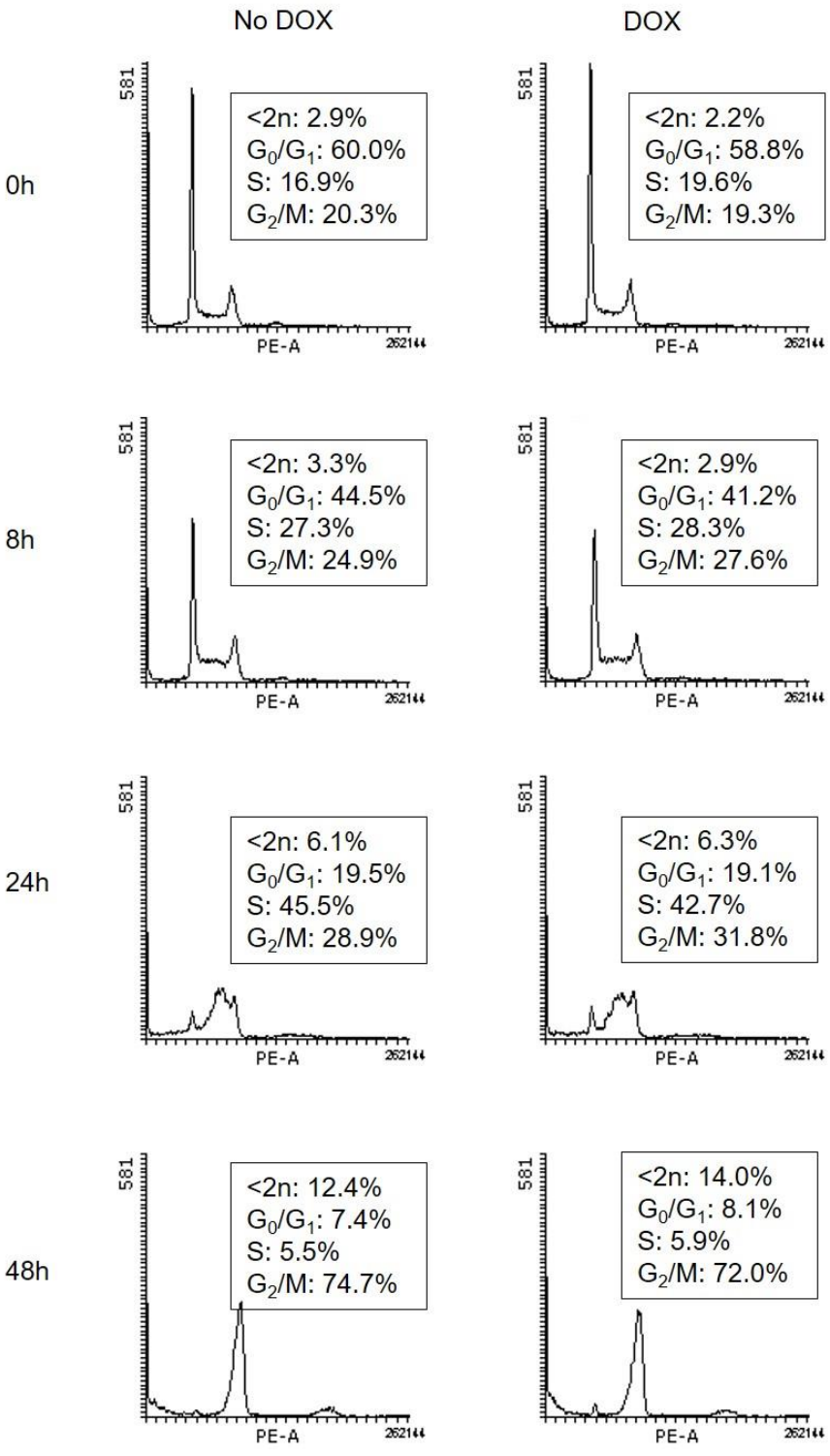

Figure 4-27. FACS analysis of stably transfected HeLa cells after etoposide treatment.

HeLa cell lines stably expressing RGC-32 were exposed to 1 µM etoposide for 0, 8, 24 and 48 hours. Cells were stained with propidium iodide to visualise cell cycle distribution.

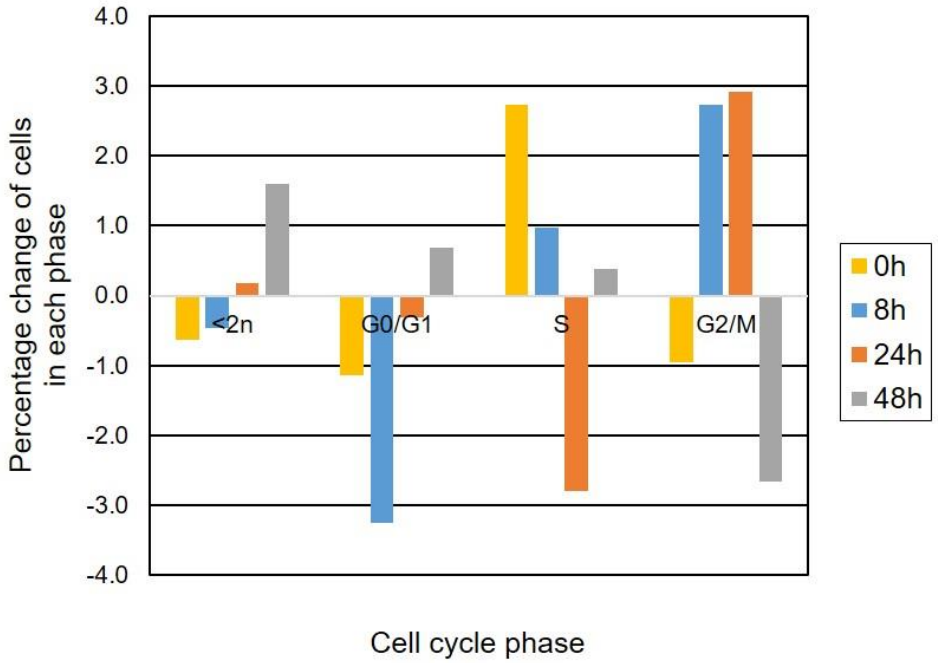

Figure 4-28. Percentage change of HeLa cells -/+ etoposide in each phase.

HeLa cell lines stably expressing RGC-32 were exposed to 1 μM etoposide for 8, 24 and 48 hours. The percentage change of cells -/+ etoposide in each phase was relative to control cells.

Cyclin B1 for CDK1. It indicated that the interaction of RGC-32 and CDK1 was specific. RGC-32 was shown to activate CDK1 in a manner of dependent on its Thr 91 phosphorylated by CDK1 (Badea et al. 2002). Mutation of RGC-32 protein at threonine 91 did not show any change compared to the ability of RGC-32 wildtype to bind CDK1 in our pull-down assays. So it might suggest that phosphorylation of Thr 91 in RGC-32 is important for its activity but not its binding with CDK1.

To further identify the potential regions of RGC-32 binding to CDK1, RGC-32 truncations were constructed based on secondary prediction derived using JPred. Pull-down results showed 50-75 aa was the potential domain involved in CDK1 binding which didn't include any predicted α-helix. Next we could do kinase assays using these truncations to map the domain which is crucial for increasing CDK1 activity.

RGC-32 was shown to interact with Plk1 upon phosphorylation by it *in vitro* but not with CDK1, indicating another possible way in which RGC-32 level mediates cell cycle control (Saigusa et al. 2007). During the G_2/M transition, Plk1 phosphorylates CDK1/Cyclin B and Cdc25 leading to mitotic entry (Kumagai and Dunphy 1996). We showed that RGC-32 bound to both CDK1 and Plk1. In our pull-down results, GST-tagged RGC-32 interacted with Plk1 in B-cells and the potential binding region identified as 25-50 aa which included one predicted α-helix. To test if RGC-32 binds to CDK1 and Plk1 at the same time, we could purified them separately then do gel filtration chromatography which is a

technique to separate proteins based on molecular size: the larger molecules will elute before the smaller ones.

In the West lab, overexpression of RGC-32 in two different B-cell backgrounds previously shown to disrupt the G2/M checkpoint (Schlick et al. 2011) which indicated a role of it in EBV-mediated cell cycle deregulation. It has been shown that overexpression of RGC-32 alone can disrupt the G2/M checkpoint in B-cell lines (Schlick et al. 2011). But the cell cycle disruption phenotype was reduced in the following experiments. The attempt of making stable DG75 overexpressing RGC-32 did not work due to the low transfection efficiency. So stable cell line overexpressing RGC-32 was make in Akata, an EBV positive BL cell line. It was confirmed that RGC-32 alone can disrupt the G2/M checkpoint. Combined with the pull-down experiments which showed that RGC-32 can interact with CDK1 and Plk1 which are important in G2/M checkpoint, it implied the possible way RGC-32 interrupting G2/M checkpoint is through CDK1 or Plk1. This stably expressing RGC-32 Akata cell line can be used to test more drugs to see their effect on cell cycle. Also the concentration of drugs using to arrest HEK293 and HeLa cells need to be titrated for further investigation of RGC-32 expression on cell cycle disruption.

5 Mechanism of RGC-32 expression on transcriptional level

5.1 Introduction

RGC-32 is expressed at the RNA level in many different human tissues including artery, bladder, brain, breast, cervix, colon, heart, kidney, lung, liver, lung and pancreas. RGC-32 is overexpressed at the RNA level in multiple human tumours including bladder, breast, colon, lung, prostate and ovaries (Kang et al. 2003, Donninger et al. 2004, Fosbrink et al. 2005). Interestingly West's lab has shown that RGC-32 protein is not expressed in EBV-negative and EBV-positive latency I B cell lines, however highly expressed in EBV-positive latency III B cell lines (Figure 5-1A). The RGC-32 mRNA expression has shown the opposite since it is higher in some EBV-negative and EBV-positive latency I B cell lines than in EBV-positive latency III B cell lines (Figure 5-1B). Although RGC-32 mRNA expression is low in latency III cell lines, EBNAs may keep it high enough so RGC-32 protein can be made. It suggests that EBNAs might play a role in regulation of RGC-32 expression in EBV-infected cells. Therefore, this chapter aims to investigate the potential role of EBV latency III gene products in the regulation of RGC-32 mRNA expression.

Figure 5-2 summarised how RGC-32 mRNA expression is regulated by EBV transcription factors in different cell line backgrounds. RGC-32 mRNA expression is negatively regulated by EBNA 2 in EBV-negative B cell line (Maier et al. 2006). Two EBV-negative B cell lines were used to perform a screen for

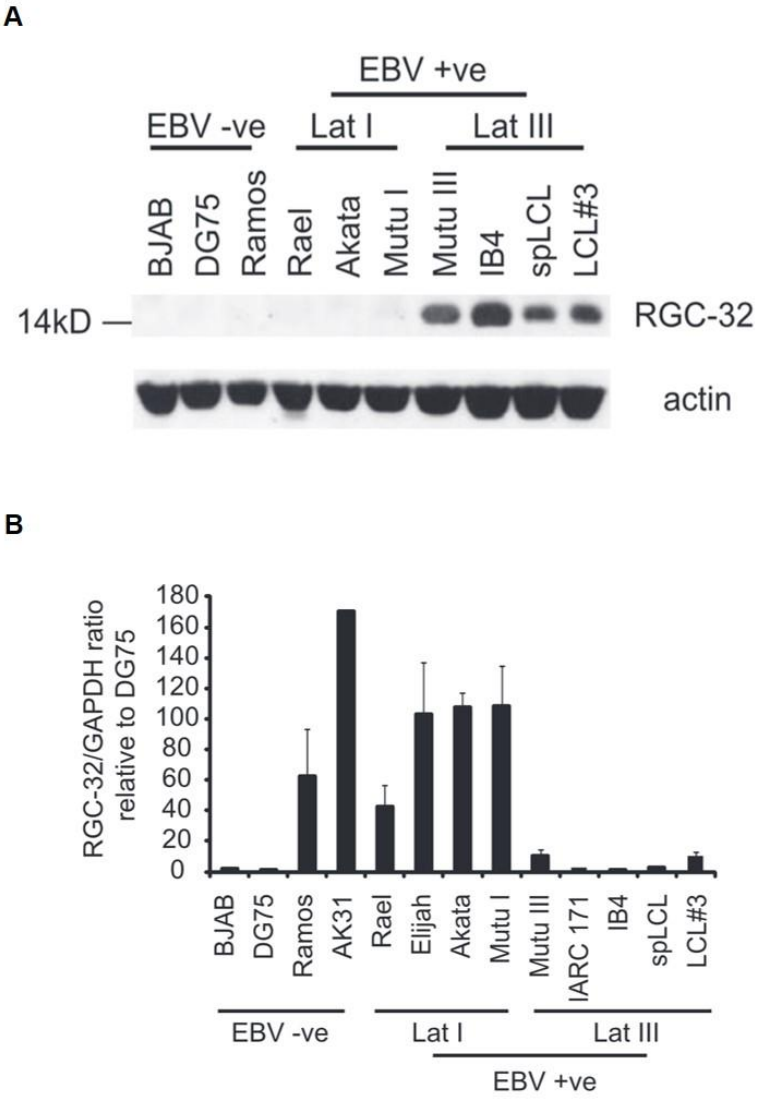

Figure 5-1. RGC-32 expression on protein and mRNA levels in different types of EBV latency (Schlick et al. 2011).

A. Western blotting analysis of RGC-32 protein expression in EBV negative and positive B cell lines. Actin is used as a loading control. **B.** q-PCR analysis of RGC-32 mRNA expression in EBV negative and positive B cell lines. Results show the mean of 3 independent experiments +/- standard deviation. This figure was taken from (Schlick et al. 2011).

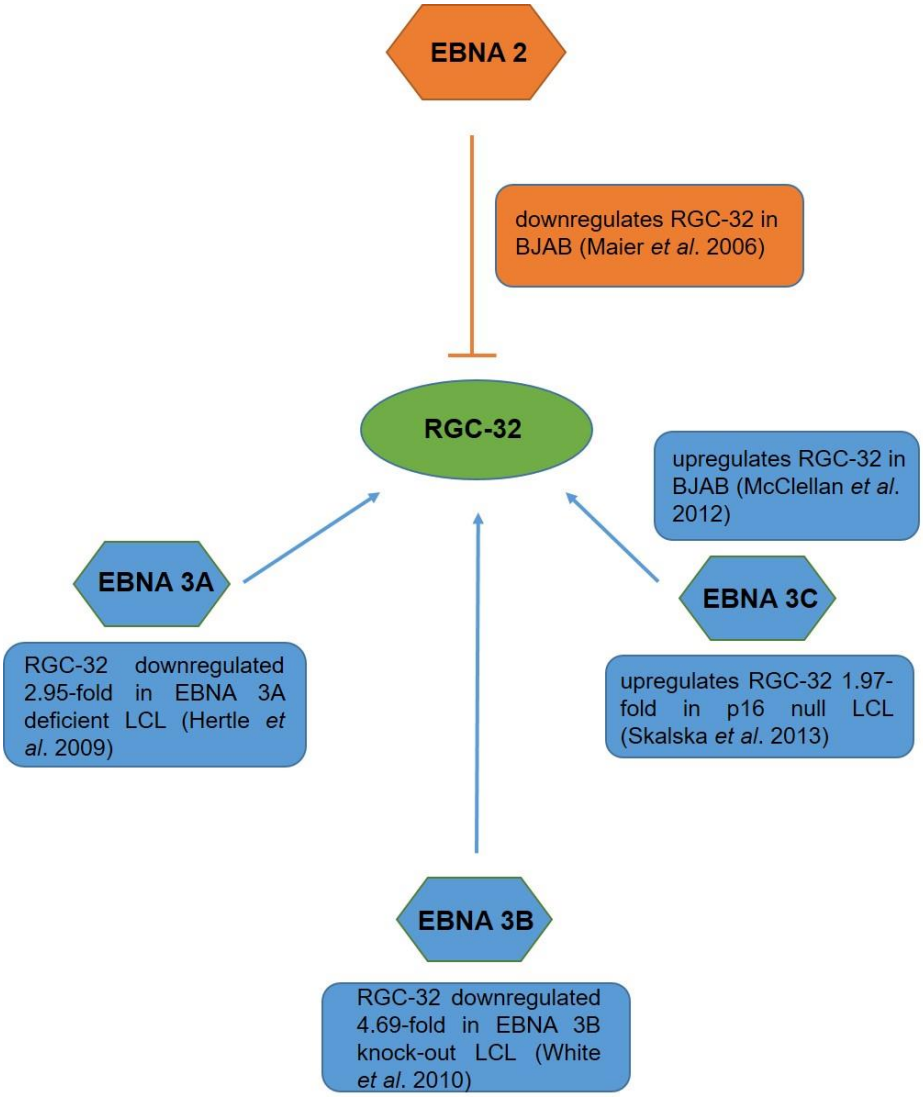

Figure 5-2. Summary of how RGC-32 is regulated by EBNA 2 or EBNA 3A, 3B or 3C in different cell background.

Orange indicates that the EBV gene product has a negative effect on the expression of RGC-32 and blue indicates that the EBV product has a positive effect on the expression of RGC-32. The 2.95-fold change of RGC-32 downregulation in EBNA 3A deficient LCL is the average of 2 EBNA 3A mutants from all 3 donors.

EBNA 2 targets and both of them expressed a chimeric EBNA 2 protein fused to estrogen receptor EBNA 2 (ER/EBNA 2). The expression of EBNA 2 can be switched on and off by estrogen. It has shown that RGC-32 expression is decreased after EBNA 2 activation (Maier et al. 2006).

RGC-32 is positively regulated by EBNA 3A, 3B and 3C in LCLs (Hertle et al. 2009, Skalska et al. 2013, White et al. 2010) (see Figure 5-3). The West's lab has shown that RGC-32 is positively regulated in EBV-negative B cell line (McClellan et al. 2012). We carried out a microarray analysis of the effects of EBNA 3C on cellular gene expression in BJAB cell line which expresses higher levels of EBNA 3C than are present in latently infected cells. RGC-32 expression is upregulated with higher EBNA 3C expression.

Figure 5-3 showed the dotplots analysis of RGC-32 expression regulation of by EBNA 3A (Figure 5-3A), 3B (Figure 5-3B) and 3C (Figure 5-3C) proteins in LCLs. This dotplots analysis is done by Professor Martin Allday's group (http://www.epstein-barrvirus.org.uk/).

Two different EBNA 3A mutant viruses were used in genome wide analysis of cellular genes differentially expressed by EBNA 3A positive and negative LCLs (Hertle et al. 2009) (Figure 5-3A). Mutant A (MutA) carried a deletion of the second exon of EBNA 3A and mutant B (MutB) has the entire EBNA 3A coding sequence deleted. It has shown that RGC-32 downregulated 2.95-fold in EBNA

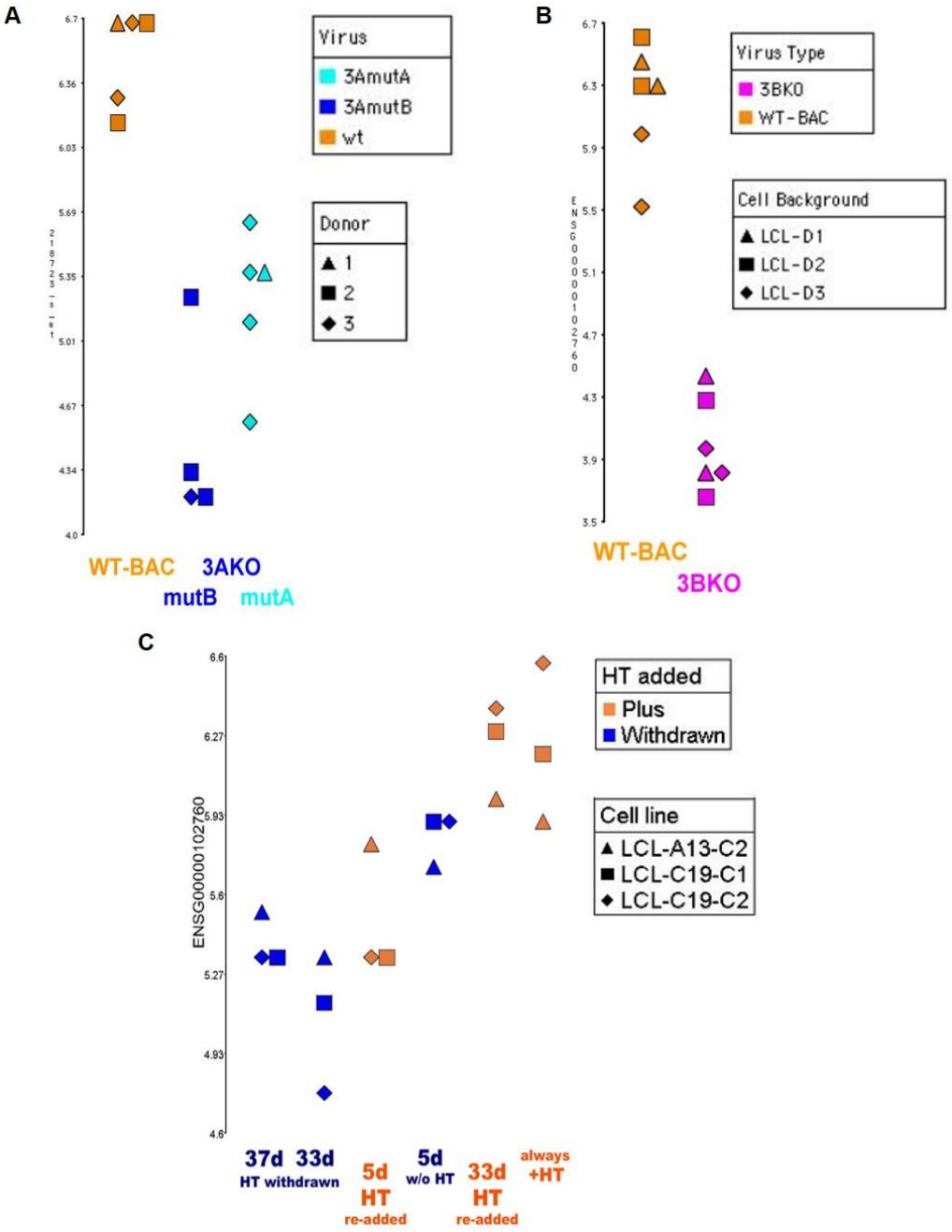

Figure 5-3. Dotplots analysis of RGC-32 mRNA regulation by EBNA 3A, 3B and 3C in LCLs by Professor Martin Allday group (http://www.epstein-barrvirus.org.uk/).

Shapes of dots in the plot represent different donors. WT-BAC is wild type B95.8 bacterial artificial chromosome (BAC) EBV. **A.** RGC-32 expression when EBNA 3A WT is expressed (orange) or EBNA 3A is mutated (dark and light blue) (Hertle *et al*. 2009). MutA carries a deletion of the second exon of EBNA 3A and mutB is lack of the whole EBNA 3A coding sequence. **B.** RGC-32 expression when EBNA 3B is expressed (orange) or EBNA 3B is knock-out (pink) (White *et al*. 2010). 3BKO is EBNA 3B knockout-infected LCLs. **C.** RGC-32 expression when EBNA 3C is expressed (orange) or EBNA 3C is withdrawn (blue) (Skalska *et al*. 2013). HT plus represents there is EBNA 3C expression and withdrawn represents there is no EBNA 3C expression.

3A deficient LCLs. This fold in raw data is the average of two EBNA 3A mutants for all three donors (Hertle et al. 2009). Data reanalysed by Allday group are 3A deficient LCLs. This fold in raw data is the average of two EBNA 3A mutants for all three donors (Hertle et al. 2009). Data reanalysed by Allday group are shown with wild type EBV-BAC LCLs compared to the mutants as two independent groups (http://www.epstein-barrvirus.org.uk/arrays2.php). So EBNA 3A has a positive effect of RGC-32 mRNA expression.

White *et al*. have shown RGC-32 expression is downregulated in EBNA 3B knock-out LCLs (White et al. 2010) (Figure 5-3B). Wild type EBV LCLs and EBNA 3B knockout (3BKO) were generated by infecting primary B cells with the B95-8 strain BAC (WT-BAC) and EBNA 3B exon2 deleted viruses from three donors (http://www.epstein-barrvirus.org.uk/arrays2.php).

3CHT virus, which is an EBV containing an EBNA 3C fused at its C terminus to a modified estrogen receptor which controls EBNA 3C expression dependent on the presence of 4-hydroxy tamoxifen (HT), were used in a microarray (Skalska et al. 2013) (Figure 5-3C). Figure 5-4 showed the microarray strategy. 4HT was washed out of cell lines that had been established in the presence of 4HT (day 0). These cells were cultured in the absence of 4HT and same cell line in the presence of 4HT. After 32 days, cell with 4HT were split into two and one culture washed out of 4HT. Those cells grown in the absence of 4HT were also split into two. 4HT was re-added to one culture. At day 37, RNA was harvested for microarray analysis. RGC-32 expression is upregulated when EBNA 3C

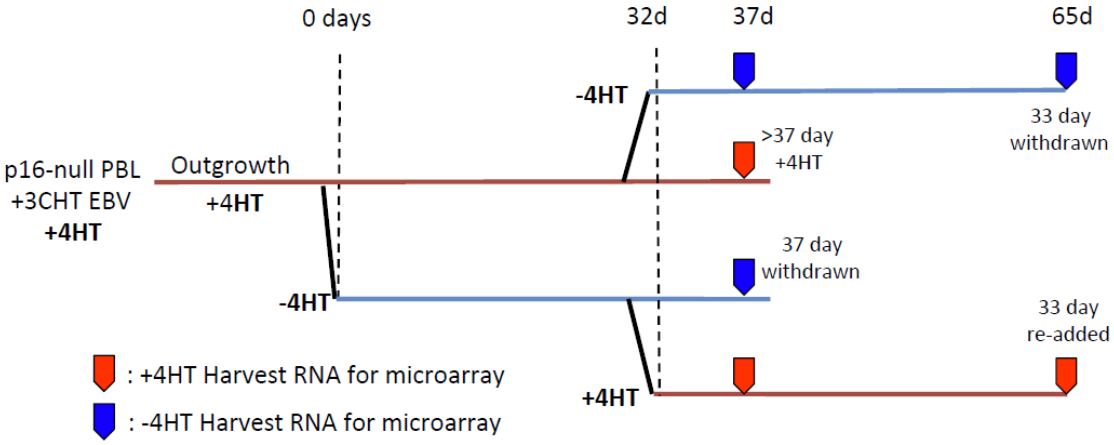

Figure 5-4. Schematic representation of microarray results in Figure 5-3C.

Horizontal lines indicate the growth either in the absence (blue lines) or presence (red lines) of 4HT. Block arrows represent the time points at which RNA was harvested for Microarray analysis. This figure was taken from (Skalska *et al*., 2013).

expression is restored by adding 4HT (http://www.epstein-barrvirus.org.uk/arrays2.php).

Microarray analysis indicates EBV-encoded EBNAs play a role in regulation of RGC-32 mRNA expression. To study how RGC-32 is regulated by EBNAs and whether this regulation is direct or indirect, we examined ChIP-sequencing data we obtained for EBNA 2, 3A, 3B and 3C to detect binding sites on RGC-32 locus in Mutu III cell line (McClellan et al. 2013) (Figure 5-5). Mutu III is a Burkitt's lymphoma cell line expressing the full panel of EBV latent genes.

5.2 EBNA 2 binds to the second intron of RGC-32 in Mutu III cell line

ChIP-seq data analysis detected four binding sites for EBNA 2 (E2, E4, E6 and E8) at the second intron of RGC-32 gene (Figure 5-5). To verify that EBNA 2 is able to associate with these binding sites, ChIP-qPCR was carried out to confirm the binding by using primer sets located at the binding sites. EBNA 2 binding at the transcription start site of PPIA (peptidylprolyl isomerase 1) and the previously characterized CTBP2 binding site were used as negative and positive binding controls (McClellan et al. 2013). Our group has shown that EBNA 3A, 3B and 3C bind the C-terminal binding protein 2 (CTBP2) enhancer (McClellan et al. 2013). EBNA 2 binding at all four sites was confirmed by ChIP-qPCR (Figure 5-6). These data indicate that EBNA 2 may repress RGC-32 transcription directly by binding to intronic regulatory sites. To examine the potential role for the second intron of RGC-32 as a regulatory region, we

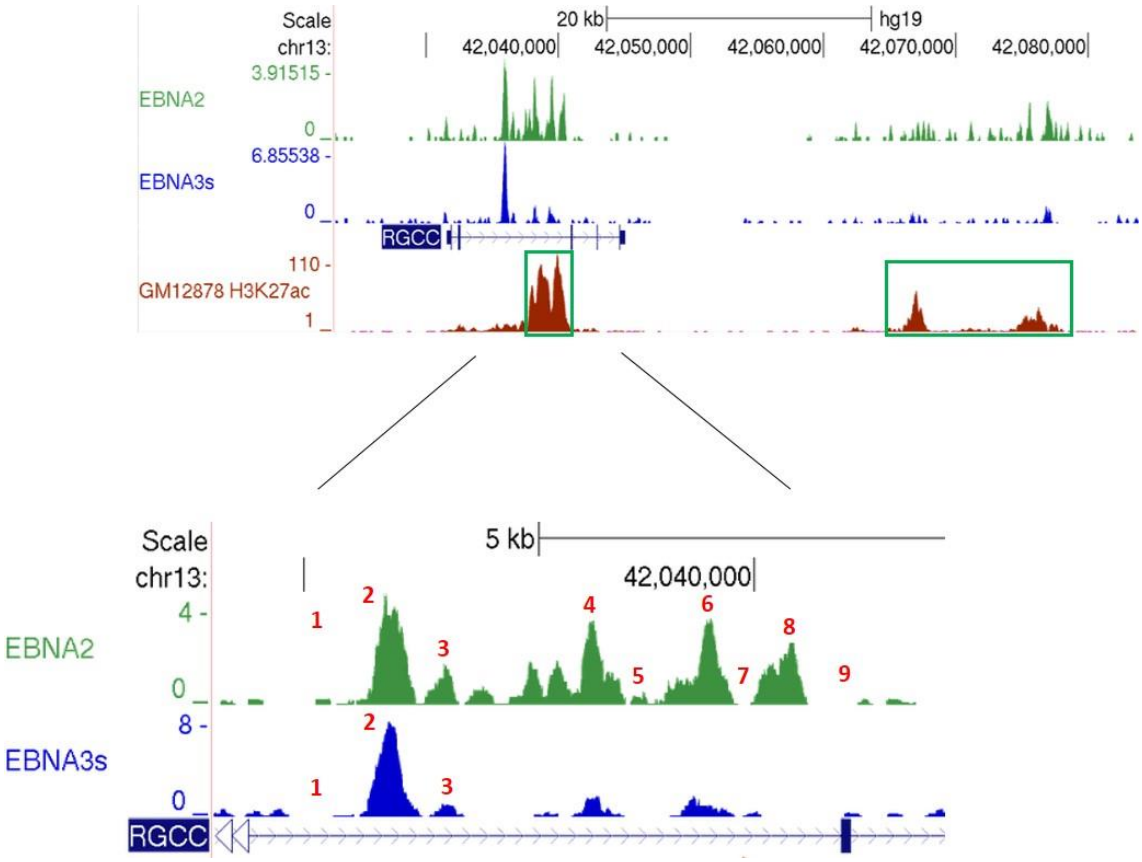

Figure 5-5. EBNA 3s and EBNA 2 binding at the RGC-32 locus.

EBNA 2 and EBNA 3 proteins ChIP-seq reads in Mutu III cells and H3K27Ac signals in GM12878 from ENCODE. RGC-32 runs left to right in the human genome. Numbering indicates the potential binding sites in Mutu III cells (McClellan et al. 2013)

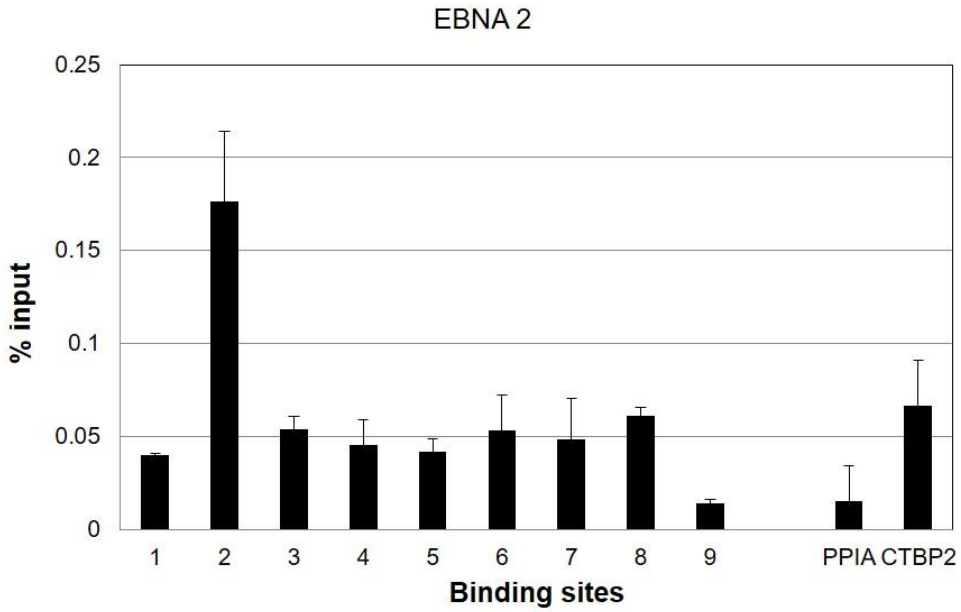

Figure 5-6. ChIP qPCR analysis of EBNA 2 binding in Mutu III cells.

Precipitated DNA was analysed using to primer sets designed at the binding sites (2, 3, 4, 6 and 8) or trough regions (1, 5, 7 and 9). 3 µl DNA was added to a SYBR master mix containing GoTaq qPCR Master Mix (Promega), forward and reverse primers and sterile water to a final volume of 15 µl. EBNA 2 binding at the transcription start site of PPIA and CTBP2 were used as negative and positive control respectively. The mean percentage input signals of two independent ChIP experiments are shown after subtraction of no antibody controls (n=2).

examined publicly available histone modification data. ChIP-seq analysis of the active chromatin mark, histone H3 lysine 27 acetylation was high in the GM12878 LCL in the region bound by enhancer 2 (green box in figure 5-5).

5.3 EBNA 2 has no effect on the RGC-32 promoter reporters that contain enhancer peaks

To examine whether EBNA 2 regulates RGC-32 mRNA expression via these binding sites, each of the four binding sites were cloned into luciferase reporter constructs containing the RGC-32 promoter -1150 to +62. DG75 cells were transiently transfected using differenct amounts of EBNA 2 expressing plasmid pSG5-EBNA 2 (0, 10 20 µg). Positive control experiments were carried out with C promoter-reporter constructs. EBNA 2 has been shown to stimulate the expression of C promoter, the major latency promoter (Woisetschlaeger et al. 1991). Negative control experiments were carried out with pGL3 Basic which has no promoter and pGL3 RGC-32 which has the RGC-32 promoter only. The luciferase assays did not show any significant effect of EBNA 2 on transcription form the RGC-32 promoter (Figure 5-7).

5.4 EBNA 3C binds to RGC-32 in Mutu III cell line

We identified a single binding site (E2) for EBNA 3 proteins in the second intron of RGC-32 (Figure 5-3). To confirm the ChIP-sequencing data, ChIP-qPCR was carried out to see which EBNA binds. As our ChIP-seq analysis was carried out using an antibody that precipitated all three EBNA 3 proteins, ChIP-qPCR in

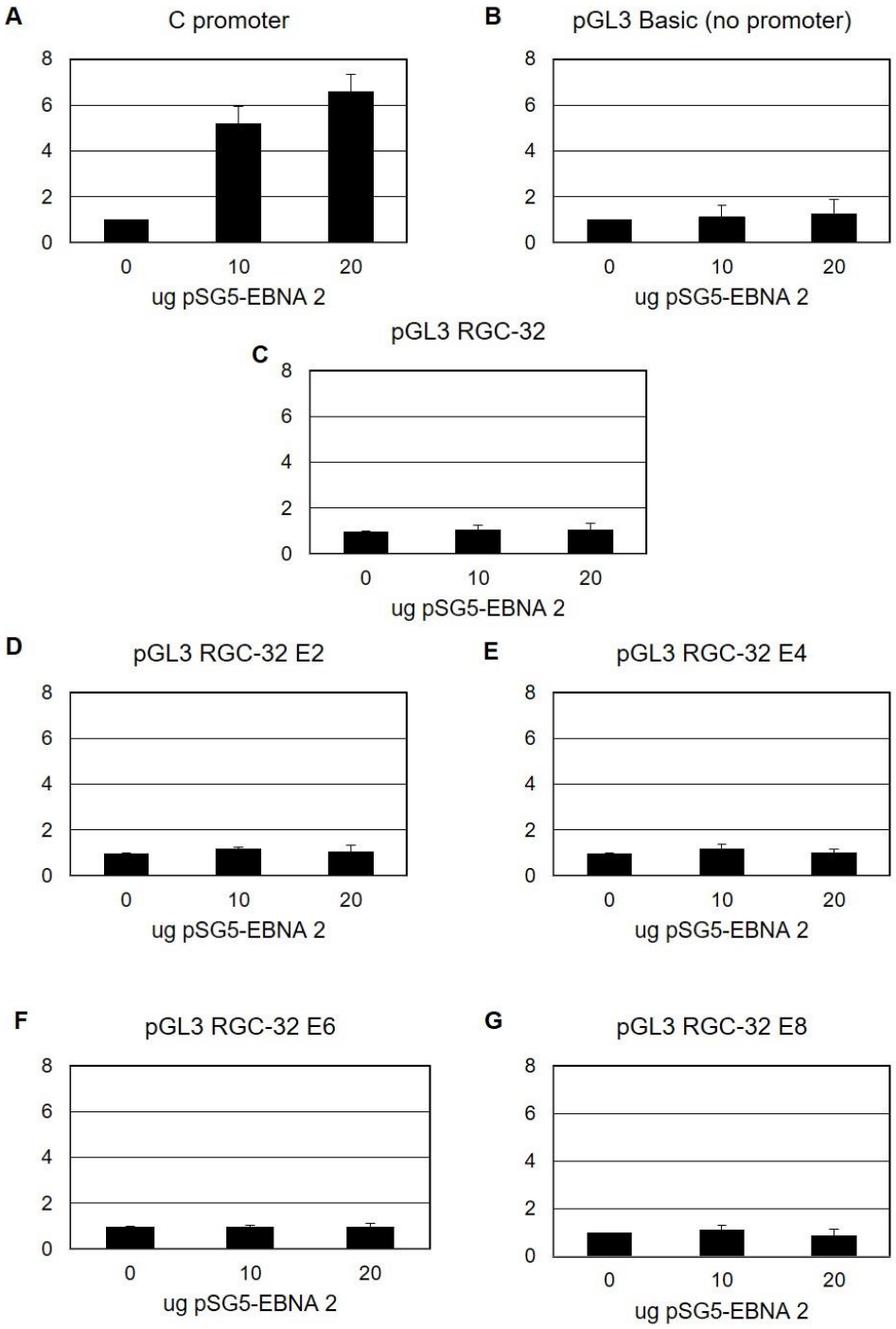

Figure 5-7. Luciferase analysis of RGC-32 enhancer elements.

DG75 cells (EBV negative cell lines) were transiently transfected with different amounts of firefly luciferase reporter plasmid containing **A.** the C promoter (positive control), **B.** pGL3 basic (no promoter), **C.** the RGC-32 promoter alone, D-G. the RGC-32 promoter in the presence of each enhancer cloned upstream E2, E4, E6 and E8. Results shows 3 independent experiments +/- standard deviation in which RGC-32 promoter activation was measured and are displayed relative to the 0 µg EBNA 2 negative control (n=3).

Mutu III cells was carried out to examine the binding of EBNA 3A, 3B and 3C proteins individually using anti-EBNA 3A, anti-EBNA 3B and anti-ENBA 3C antibodies. We found that only EBNA 3C bound to RGC-32 intron at enhancer 2 (Figure 5-8). It is possible that EBNA 3C might activate RGC-32 transcription by binding to enhancer 2.

5.5 Discussion

Our results showed that EBNA 2 binds to the second intron of RGC-32 in the Latency III BL cell line Mutu III, but no regulation was detected using reporter assays. The possible reason is those binding sites do not control the expression of RGC-32 mRNA individually, therefore we could investigate whether this whole region respond to EBNA 2. On further examination of the data we identified a cluster of EBNA 2 binding sites at 20 kb downstream from RGC-32 gene (blue box in figure 5-9). EBNA 2 and 3 proteins have been shown to regulate cellular genes through their associations with long distance regulatory elements (McClellan et al. 2012, McClellan et al. 2013). Next, the distal binding sites need to be confirmed by ChIP-qPCR. It would be interesting to investigate whether these binding sites control the expression of RGC-32 mRNA using reporter assays.

To investigate whether EBNA 2 expression alters expression of other genes, microarray analysis could be performed using EBNA 2 knockout LCLs. RGC-32 mRNA expression is negatively regulated by EBNA 2 in EBV-negative B cell line (Maier et al. 2006). It is possible to repress RGC-32 expression by knocking

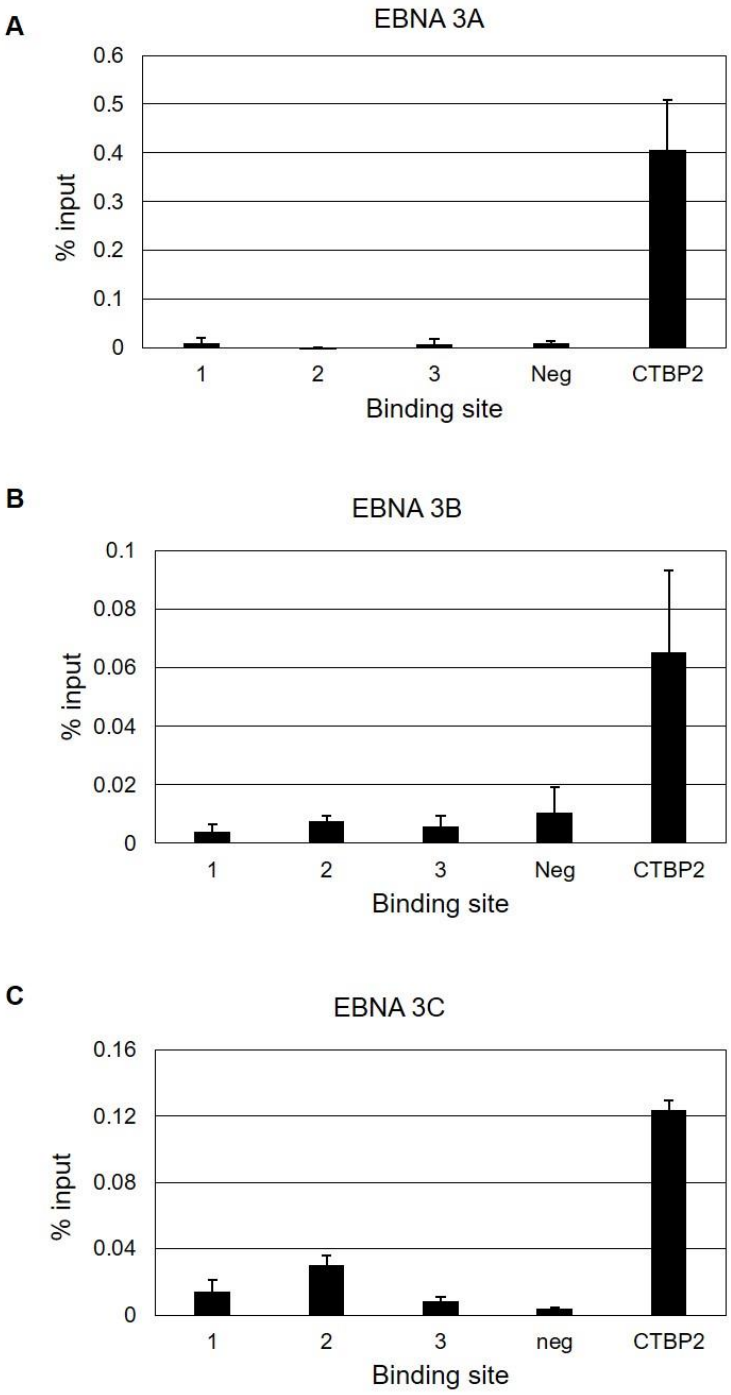

Figure 5-8. ChIP qPCR analysis of EBNA 3A (A.), EBNA 3B (B.) and EBNA 3C (C.) binding at RGC-32 in Mutu III cells.

ChIPed DNA was used according to primer sets designed at the binding sites (2 and 3) or trough regions (1). EBNA 3s binding sites at the preciously characterized T6 which is a trough region adjacent to the binding sites and shows very low signal (Gunnell et al. 2016) were used as negative control. Binding sites CTBP2 were used as positive control. The mean percentage input signals of two independent ChIP experiments are shown -/+ standard deviation after subtraction of no antibody controls.

	E2	E4	E6	E8
Transcription factors (signal intensity)	SPI1 (1000)	MTA3 (308)	ZEB1 (127)	POLR2A (1000)
	RUNX3 (302)	MAZ (179)	CEBPB (283)	BCL3 (216)
		NFATC1 (517)	EP300 (272)	
		NFIC (269)	RUNX3 (1000)	
		RAD21 (185)	SPI1 (344)	
		MEF2A (181)	TAF1 (336)	
		RUNX3 (871)	BCLAF1 (208)	
		PAX5 (685)	ELF1 (695)	
		EGR1 (237)	NFIC (722)	
		SP1 (160)	MTA3 (443)	
		EBF1 (275)	YY1 (237)	
		TCF12 (463)	IRF4 (459)	
			BHLHE40 (255)	
			PAX5 (522)	
			FOXM1 (590)	
			POU2F2 (270)	
			EBF1 (259)	
			EGR1 (156)	
			MEF2A (280)	
			ATF2 (577)	
			ETS1 (143)	
			TCF3 (803)	
			NFATC1 (450)	
			SRF (273)	
			BATF (1000)	
			PBX3 (218)	
			RAD21 (190)	
			TCF12 (869)	
			BCL3 (430)	
			SP1 (427)	
			BCL11A (441)	

Table 5-1. Transcription factors binding at E2, E4, E6 or E8 (Genome browser).

Transcription factors ChIP-seq reads in GM12878 cells (McClellan et al., 2013). The signal intensity is showed in brackets and the green highlight represents the highest scoring site of a Factorbook-identified canonical motif for the corresponding factor.

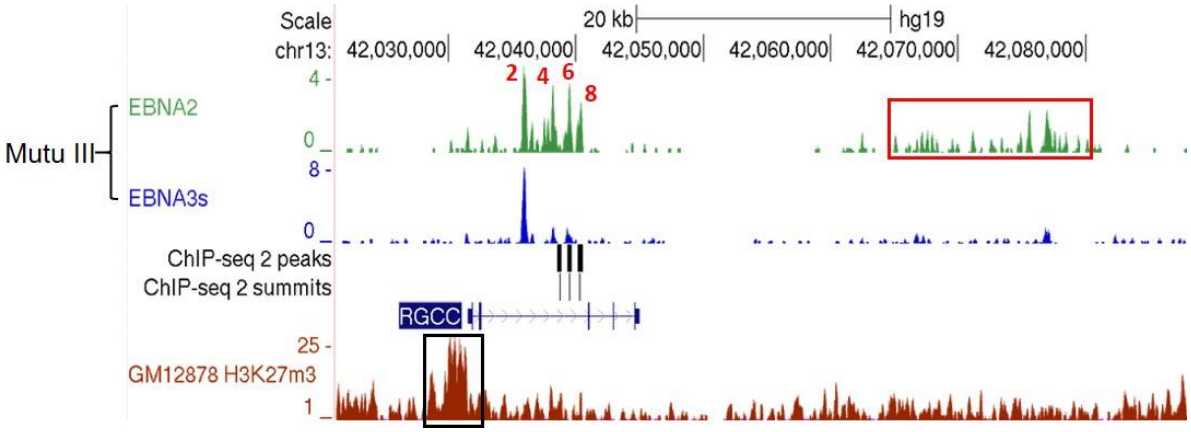

Figure 5-9. EBNA2, 3A, 3B, 3C and RBP-Jκ binding at the RGC-32 locus.

EBNA 2, 3A, 3B and 3C ChIP-sequencing reads in Mutu III (McClellan et al. 2013), H3K27me3 signals in the EBV-immortalised LCL, GM12878 from ENCODE and RBP-Jκ ChIP-sequencing reads in the EBV-immortalised LCL, IB4 detected by MACS (Zhao *et al*., 2011). RGC-32 runs left to right in the human genome. The black bars indicate the wholly enriched region from start to end. Summits indicate the highest pile up point within the peak region.

off a better activator. I examined the ChIP-seq data to identify other genes binding at the second intron of RGC-32 gene and summarised in table 5-1. The genes binding at E2, E4, E6 and E6 are present and the binding intensity is shown in brackets. The maximum of signal intensity is 1000 which represents the strongest binding and the genes highlighted in green are the highest scoring site of identified motif for the corresponding factor. RUNX3 binds to enhancer 2, 4 and with high scoring of binding. Our previous data show that RUNX3 represses the expression of RUNX 1 and RUNX1 activates expression of RGC-32 mRNA (Gunnell et al. 2016). It would be interesting to investigate whether expression of RUNX3 regulates RGC-32 expression. Also we examined publicly available histone modification data, we identified some signal of Histone 3 lysine 27 trimethylation (H3K27m3) from ENCODE (black box in figure 5-9) which is associated with lower of transcription and there defined as repression mark. Our previous date show that RGC-32 mRNA level is low in latency III cell lines (Schlick et al. 2011), so it is possible that mRNA expression of RGC-32 is repressed through histone modification in this region.

EBNA 3C binds to RGC-32 in Mutu III at enhancer 2. It has been shown that EBNA 3C bound strongly to the p14ARF promoter through SPI1/IRF4/BATF/RUNX3, establishing RBPJ-κ, Sin3A-, and REST-mediated repression (Jiang et al. 2014). Interestingly SPI1 (PU.1), IRF4, BATF and RUNX3 all bind at the second intron of RGC-32 gene which suggests it is possible that EBNA 3C might form a complex with them to control RGC-32 transcription. But the low expression of IRF4 in DG75 cell line, used for

luciferase assays, might abolish the association between EBNA 3C and RGC-32 gene.

6 Discussion and future work

6.1 What is the mechanism of CDK1 activation by RGC-32?

RINGO/Speedy has been shown to function like RGC-32 in cell cycle progression (Gastwirt et al. 2007). RINGO/Speedy was initially described as a protein which induces the G_2/M transition during oocyte maturation (Lenormand et al. 1999, Ferby et al. 1999). It was later shown to be able to activate CDK1 and CDK2, although these proteins have no amino acid homology to Cyclins (reviewed in (Gastwirt et al. 2007). RINGO binds to CDK1 and Cyclin B1 separately but not the CDK1/Cyclin B1 complex and it can activate CDK1 in the absence of Cyclin B1 (Ferby et al. 1999). RGC-32 also binds and activates CDK1 activity *in vitro* (Badea et al. 2002). Interestingly, RGC-32 did not interact with the CDK1/Cyclin B1 complex in immunoprecipitation experiments carried out in HEK293T cells (Saigusa et al. 2007) raising the possibility that RGC-32 competes with Cyclin B1 for CDK1 as found for RINGO/Speedy proteins (reviewed in (Gastwirt et al. 2007). Our *in vitro* pull-down assays showed that RGC-32 only interacts with CDK1, but not Cyclin B1 in B cells (Badea et al. 2002) suggesting it may activate CDK1 in a cyclin-independent manner like RINGO/Speedy protein. To further confirm our conclusion, surface plasmon resonance (SPR) is being carried out in University of Newcastle is being done as part of a collaboration with Professor Jane Endicott and Dr. Nick Brown. SPR provides a way to observe protein-protein interactions in real time. Initial experiments have indicated that RGC-32 binds to CDK1 at much higher affinity than the CDK1-Cyclin B complex. These experiments also confirmed that RGC-

32, unlike RINGO, seems to have specificity for CDK1 as no binding to CDK2 was detected.

In vivo and *in vitro* RINGO was found to activate CDK1 independent of the phosphorylation of threonine 161 in the activation loop on CDK1 (Ferby et al. 1999, Karaiskou et al. 2001). Further experiments showed RINGO could bind and activate CDK2 in the absence of cyclin and independent of threonine 160 phosphorylation (Karaiskou et al. 2001, Porter et al. 2002). So it would be interesting to test if RGC-32 activates CDK1 through a mechanism alleviating the requirement for activation by CDK-activating kinase (CAK).

CDK1 has also been shown to bind other proteins to control critical cell cycle events, e.g. Cyclin-dependent kinase subunit (Cks). Cks protein was identified in a screen for genes that can suppress the termperature-sensitive phenotype of CDK1 alleles(Hayles et al. 1986). Cks proteins bind to CDKs and Cyclins (Zhang et al. 2004). Cks proteins enhance the phosphorylation of selected CDK1 substrates in mitosis (Patra et al. 1999). Structural studies have determined the structures of Cks with CDK1 alone and CDK1/Cyclin B complex (Brown et al. 2015). It is possible that RGC-32 could bind to CDK1 alone and CDK1/Cyclin B1 like Cks.

6.2 What is the role of cellular localisation of RGC-32 in recruitment of CDK1, Plk1 or Spc24?

In U-87 MG cells, ectopically expressed RGC-32 protein is located in the cytoplasm during interphase with the strongest signal around the nuclear membrane (Saigusa et al. 2007). In prophase, RGC-32 protein levels increase at the centrosome and in prometaphase and metaphase they reach maximal levels at the centrosome and spindle poles. During telophase and cytokinesis RGC-32 protein levels remain low in centrosome (Saigusa et al. 2007). These data is consistent with a role of RGC-32 in mitotic progression.

RGC-32 interacts with the centrosome-associated polo-like kinase (Plk1) and is phosphorylated by Plk1 in vitro (Saigusa et al. 2007). Our *in vitro* pull-down assays showed that GST-RGC-32 interacted with Plk1 in B cells and further we mapped the potential domain on RGC-32 which is crucial for the interaction. Plk1 is a key regulator in mitosis (Barr et al. 2004) and expression and kinase activity of it has been shown to elevate in many kinds of cancers (Dietzmann et al. 2001, Takai et al. 2005). It is possible that RGC-32 may regulate the cell cycle through the interaction with Plk1. Cytoplasmic linker protein (CLIP) 170 promotes the localisation of Plk1 at kinetochore in early mitosis through a Polo-Box domain (Amin et al. 2014) and Plk1 localises at kinetochores in prometaphase to stabilise the kinetochore and microtubule attachment (Liu, Davydenko and Lampson 2012). During cell division, chromosome segregation is dependent on the kinetochore-microtubule attachment on the mitotic spindle, which progresses chromosome alignment (Tanaka, Stark and Tanaka 2005, Tanaka 2012, Tanaka 2013). It would be interesting to test whether RGC-32 localises to kinetochore and investigate the role of RGC-32 in the recruitment of Plk1 to kinetochore. We mapped the regions of interaction between RGC-32

and Plk1 by *in vitro* pull-down assays. RGC-32 deletion which lacks the interaction regions with Plk1 could be fused to a fluorescent marker then transfected into cells to visualise its expression and localisation using fluorescent microscope.

During the course of this study, we identified the third predicted α-helix of RGC-32 as having homology to a receptor motif in the N terminus of the histone-fold protein Cnn1 from *Saccharomyces cerevisiae* using HHpred. This receptor motif is required for the association of Cnn1 with Spc24-25 heterodimer (Schleiffer et al. 2012). We showed that RGC-32 interacts with Spc24 in pull-down assays suggesting RGC-32 might play a role in kinetochore assembly or in recruiting kinases there. Three conserved hydrophobic residues phenylalanine 69, lysine 70 and 73 in Cnn1 are required for its interaction with Spc24-25 as these residues face the hydrophobic pocket of Spc24-25 globular domain (Malvezzi et al. 2013). Interestingly these three residues were present in the third α-helix of RGC-32. The structure of the budding yeast Spc24-25 and Cnn1 interaction has been deposited in the Protein Data Bank with accession code 4GEQ (Malvezzi et al. 2013). We substituted those three conserved residues (phenylalanine 69, lysine 70 and 73) in Cnn1 by corresponding amino acids in RGC-32 to model RGC-32 in the structure with Spc24-25 (Figure 6-1). The substitution of RGC-32 could still fit in the hydrophobic pocket of Spc24-25 globular domain. Next, we could mutate RGC-32 on these three residues and determine whether they are required for the interaction of RGC-32 and Spc24 using *in vitro* pull-down assays.

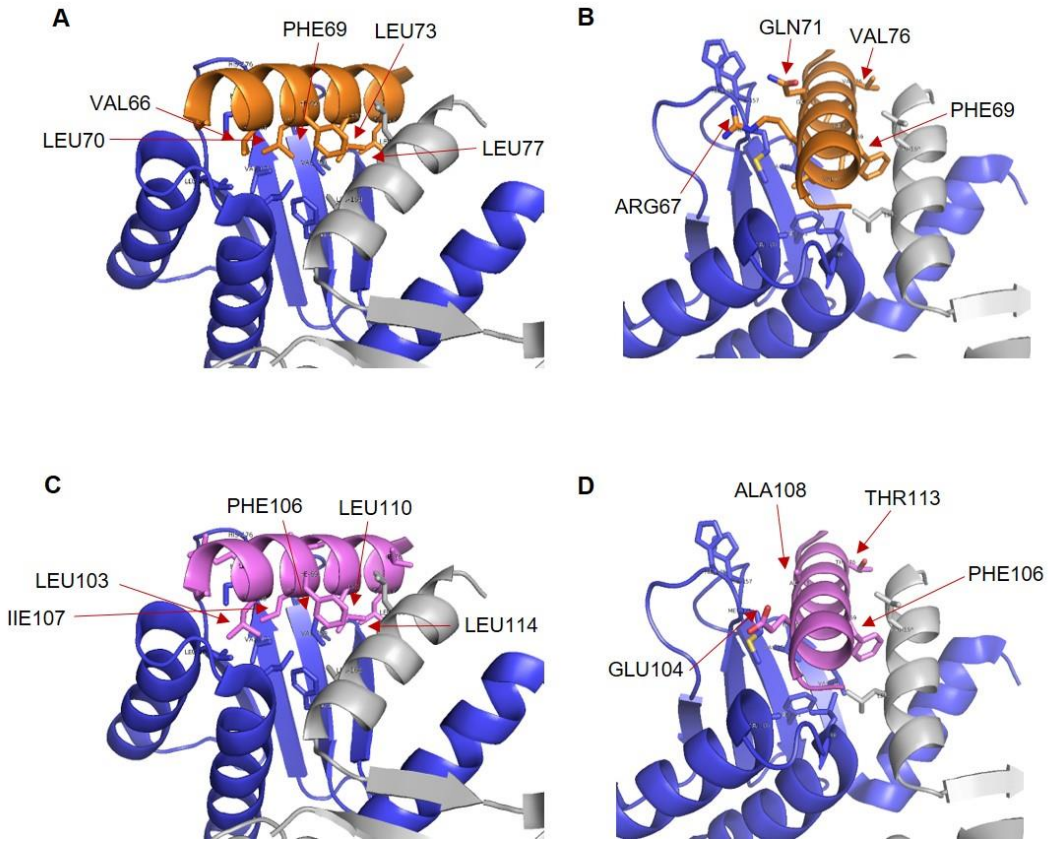

Figure 6-1. Structural analysis by substituting amino acids on Cnn1 with corresponding amino acids on RGC-32.

A. and **B.** Close-up view of the Cnn1 and Spc24-25 interaction network (Accession number 4GEQ) (Malvezzi *et al*., 2013). The secondary structure of Cnn1, Spc24 and Spc25 is shown as orange, blue and grey respectively. **C.** and **D.** Amino acids on Cnn1 were substituted by corresponding amino acids on RGC-32. These amino acids are present in the third α-helical of RGC-32 which is identified to be homologous to the N-terminus of Cnn1.

CDK1 phosphorylation of the N terminus of CENP-T has been shown to play a role in kinetochore assembly in human cells (Gascoigne et al. 2011). Malvezzi *et al*. have shown that CDK1 phosphorylation of the Cnn1 N terminus is not required for the interaction between Spc24-25 and Cnn1 (Malvezzi et al. 2013). So it would be interesting to investigate if CDK1 could phosphorylate the N terminus of RGC-32 which is the homologue with Cnn1. It has been shown that RGC-32 mutation at threonine 91 abolishes the CDK1-mediated phosphorylation and leads to loss of CDK1 kinase enhancing activity (Badea et al. 2002). Interestingly, threonine 91 on RGC-32 is near the potential interaction helix of RGC-32 and Spc24-25. Next, we would investigate whether mutation of RGC-32 at threonine 91 is required for the interaction of RGC-32 and Spc24-25 using pull-down assays. It is possible that phosphor status of RGC-32 could ensure that it interact stably with the kinetochore and spindle only at the correct time during mitosis.

6.3 Is RGC-32 an oncogene or tumour suppressor?

Overexpression of RGC-32 in the OLG-C6 glioma cell line leads to an increase in DNA synthesis in response to serum growth factors (Badea et al. 1998) and leads to S-phase and G_2/M entry in smooth muscle cells (Badea et al. 2002). RGC-32 mRNA expression was up-regulated in breast cancer (Kang et al. 2003, Fosbrink et al. 2005), colon cancer (Fosbrink et al. 2005), lung cancer (Fosbrink et al. 2005), ovarian cancer (Donninger et al. 2004), stomach cancer (Fosbrink et al. 2005). This evidence indicates that RGC-32 is an oncogene. Other studies however, point to a role for RGC-32 as a tumour suppressor. RGC-32 gene was

absent in glioma cell lines and restoration of it caused the suppression of cell growth and overexpression of its protein delayed mitotic progression in HeLa cells (Saigusa et al. 2007).

Our previous data showed that stable overexpression of RGC-32 alone is sufficient to disrupt the G_2/M checkpoint in the EBV-negative B cell line DG75 and BJAB (Schlick et al. 2011). I generated new cell lines expressing inducible RGC-32 for further investigation of RGC-32 function. It has been shown that RGC-32 directly binds to CDK1 and increases its activity by pull-down assay *in vitro* and immunoprecipitation *in vivo* (Badea et al. 2002). It is interesting to investigate whether cells overexpressing RGC-32 still can overcome G_2/M checkpoint when the CDK1 activity is inhibited by CDK1 inhibitor e.g. 1NM-PP1. 1NM-PP1 is a cell-permeable inhibitor of kinases that have been mutated by a single base substitution to become analogue sensitive compared to wild type kinases (Cayman chemical CAS 221244-14-0). It can inhibit the kinase activity of CDK1.

6.4 What is the role of RGC-32 in EBV transformation?

RGC-32 expressed at the RNA level in many different human tissues including artery, bladder, brain, breast, cervix, colon, heart, kidney, lung, liver, lung and pancreas. RGC-32 overexpressed at the RNA level in multiple human tumours including bladder, breast, colon, lung, prostate and ovaries (Kang et al. 2003, Donninger et al. 2004, Fosbrink et al. 2005). Our previously data has shown that RGC-32 mRNA expression is significantly higher in Latency I BL cell lines

and in some EBV-negative cell lines compared to latency III cell lines (Schlick et al. 2011). It is possible that EBV latency III gene products play a role in the regulation of RGC-32.

Further evidence indicates RUNX genes also play a role in regulation of RGC-32 expression. Therefore we summarised the regulation of RGC-32 mRNA expression by EBNAs and RUNX (Figure 6-2). EBNA 2 downregulates RGC-32 expression in EBV-negative B cell line (Maier et al. 2006). EBNA 3A, 3B and 3C activate RGC-32 expression in LCLs (Hertle et al. 2009, Skalska et al. 2013, White et al. 2010). Our previous data shows that RGC-32 mRNA expression in human B cells is activated by RUNX1c (Schlick et al. 2011). Also our previous data has revealed RUNX gene regulation is controlled by the EBNAs in EBV-infected cells (Gunnell et al. 2016). EBNA 2, 3B and 3C activate RUNX3 expression (Gunnell et al. 2016). EBNA 2 activates, however EBNA 3B and 3C repress the expression of RUNX1 (Gunnell et al. 2016). RUNX 3 represses RUNX1 expression (Gunnell et al. 2016). EBNA 3A activates the expression of RUNX1 in LCLs (White et al. 2010) and EBNA 3B activates the expression of RUNX1 in LCLs (Hertle et al. 2009). It suggests that the expression of RGC-32 is a consequence of collaborative working of EBV encoded EBNAs and RUNX.

Although a number of microarray analyses have been done on RGC-32 mRNA expression, these studies do not show whether RGC-32 mRNA expression changes leads to a change in protein expression. Surprisingly our previous data has shown that RGC-32 protein expression is not consistent with its mRNA

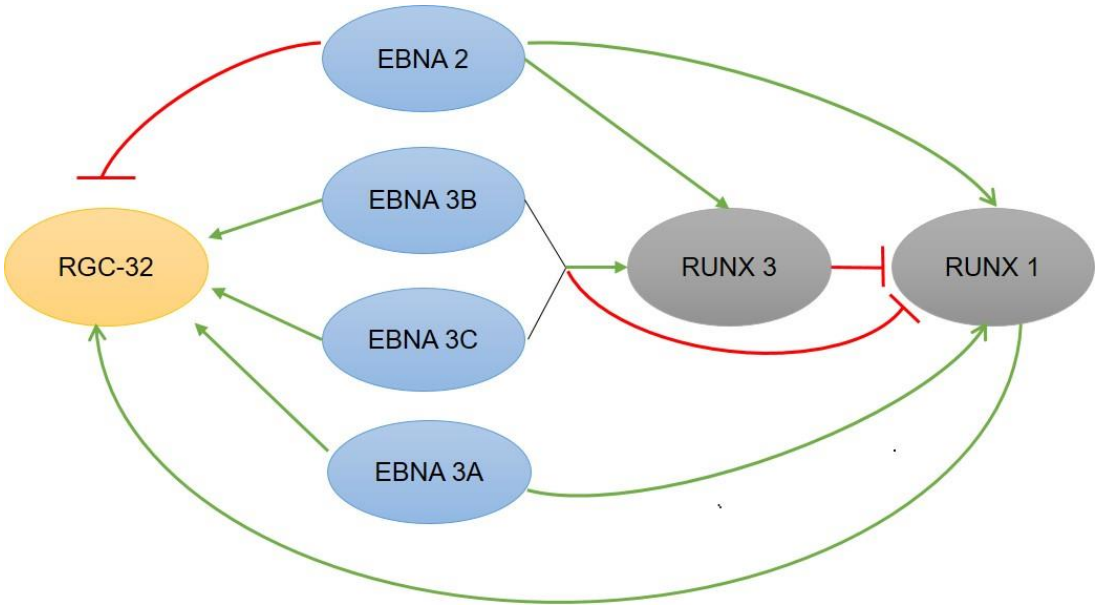

Figure 6-2. RGC-32 gene regulation by the EBNAs and RUNX (modified from Gunnell et al., 2016).

EBNA 2 downregulates RGC-32 expression and EBNA 3A, 3B and 3C upregulate RGC-32 expression. RUNX1 upregulates RGC-32 expression. EBNA 2, 3B and 3C activate RUNX3 expression by binding to a distal upstream super-enhancer. Then RUNX3 represses RUNX1 transcription by binding to the RUNX1 P1 promoter. The activation of RUNX1 transcription by EBNA 2 is through an upstream super-enhancer and cell type specific. The repression of RUNX1 transcription is also cell type specific. Total RUNX1 expression depends on the balance between the expression of RUNX1 which drives RUNX1 repression, EBNA 2 activation and EBNA 3B and 3C repression which are controlled by super-enhancer binding.

expression in EBV-positive cell lines latency I and latency III due to the blocking of its translation at a post-initiation stage in latency I cells (Schlick et al. 2011). It is still unclear how RGC-32 protein expression is regulated in EBV-transformed cells. Although the microarray data have suggested RGC-32 expression promotes tumour development, it would be still too early to draw any conclusion in the investigation of the role of RGC-32 in EBV transformation.

7 Appendices

7.1 Antibodies

Antibody	Host	Dilution	Informaiton	Company/Cat. No.
Anti RGC32	Rabbit	1:500	Polyclonal	Eurogentec
Anti CDK1	Mouse	1:500	Monoclonal	Invitrogen/33-1800
Anti CDK1	Mouse	1:1000	Monoclonal	Santa Cruz/sc-54
Anti Cyclin B1 (GNS1)	Mouse	1:1000	Monoclonal	Santa Cruz/sc-245
Anti CDK2 (D-12)	Mouse	1:3000	Monoclonal	Santa Cruz/sc-6248
Anti Plk1	Mouse	1:1000	Monoclonal	abcam/ab14210
Anti Spc24	Rabbit	1:500	Polyclonal	abcam/ab157184
Anti EBNA 1 (M. Stacey serum)	Human	1:200	Polyclonal	Gift from M. Rowe.
Anti actin	Rabbit	1:5000	Polyclonal	Sigma

7.2 Plasmids

Plasmid	Information	Reference/ Company
pET16 RGC-32	RGC-32 was cut of pFLAG RGC-32 as an SalI/BamHI fragment and cloned into pET16b (Sigma) digested with XhoI/BamHI.	Sigma and created by Helen Webb
pET28 Cyclin B1	Cyclin B1 (residues 165-433) was amplified by PCR and cloned into pET28a (Novagen).	Gift from E. Petri (Petri *et al*., 2007)
pGEX RGC-32	RGC-32 was amplified from pFLAG RGC-32 and cloned into pGEX-6P3 as a BamHI/NotI fragment.	Created by Lina Chen
pGEX RGC-32 T91A	RGC-32 was amplified from pFLAG RGC-32 T91A and cloned into pGEX-6P3 as a BamHI/ NotI fragment.	Created by Lina Chen
pFLAG RGC-32	RGC-32 was amplified from BJAB E3C-4 (Wang *et al*., 1990) cDNA and cloned into pFLAG-CMV-2 as an XbaI/BamHI fragment.	Created by Helen Webb
pGEX RGC-32 1-25	RGC-32 (residues 1-25) was amplified from pFLAG RGC-32 and cloned into pGEX-6P3 as a BamHI/XhoI fragment.	Created by Lina Chen
pGEX RGC-32 1-50	RGC-32 (residues 1-50) was amplified from pFLAG RGC-32 and cloned into pGEX-6P3 as a BamHI/XhoI fragment.	Created by Lina Chen
pGEX RGC-32 1-75	RGC-32 (residues 1-75) was amplified from pFLAG RGC-32 and cloned into pGEX-6P3 as a BamHI/XhoI fragment.	Created by Lina Chen
pGEX RGC-32 1-100	RGC-32 (residues 1-100) was amplified from pFLAG RGC-32 and cloned into pGEX-6P3 as a BamHI/XhoI fragment.	Created by Lina Chen
pMA RGC32 mutant for CDK1 binding	RGC-32 mutant (F68A, F70A) was inserted into pMA as a KpnI/SacI fragment.	Life technologies
pMA RGC32 mutant for Plk1 binding	RGC-32 mutant (Y33A, K41E, R42E, R43E) was inserted into pMA as an SfiI/SfiI fragment.	Life technologies
pGEX RGC-32 mutant for CDK1 binding	RGC-32 mutant (F68A, F70A) was cut of pMA RGC-32 mutant for CDK1 binding and cloned into pGEX-6P3 as a BamHI/NotI fragment.	Created by Lina Chen
pGEX RGC-32 mutant for Plk1 binding	RGC-32 mutant (Y33A, K41E, R42E, R43E) was cut of pMA RGC-32 mutant for Plk1 binding and cloned into pGEX-6P3 as a BamHI/NotI fragment.	Created by Lina Chen

pRTS-1 RGC-32	RGC-32 was cut of pUC19 RGC-32 as an SfiI/SfiI fragment and cloned into pRTS-1 (Georg W. Bornkamm) digested by SfiI.	Created by Lina Chen
pSG5 EBNA 2	The EBNA 2 open reading frame of EBV strain W91 under the control of the SV40 early promoter in pSG5 vector	Gift from M. Rowe
pGL2 RGC-32	1.2 kb fragment (approximately from -1150 to +62 relative to predicted transcription start site) of the RGC-32 promoter was amplified from genomic DNA and cloned into pGL2 Basic cut with HindIII/KpnI.	Created by Helen Webb
pGL3 RGC-32	The RGC-32 promoter fragment was but with HindIII/KpnI out of pGL2 RGC-32 and cloned into a pGL3 Basic vector.	Created by Sandra Schlick
pGL3 RGC-32 E2	The RGC-32 enhancer element 2 (approximately 600 bp) was amplified from genomic DNA and cloned into pGL3 RGC-32 cut with KpnI.	Created by Lina Chen
pGL3 RGC-32 E4	The RGC-32 enhancer element 4 (approximately 700 bp) was amplified from genomic DNA and cloned into pGL3 RGC-32 cut with KpnI.	Created by Lina Chen
pGL3 RGC-32 E6	The RGC-32 enhancer element 6 (approximately 800 bp) was amplified from genomic DNA and cloned into pGL3 RGC-32 cut with KpnI.	Created by Lina Chen
pGL3 RGC-32 E8	The RGC-32 enhancer element 8 (approximately 700 bp) was amplified from genomic DNA and cloned into pGL3 RGC-32 cut with KpnI.	Created by Lina Chen

7.3 PCR primers

Gene	Sequence
RGC-32 primers for making pGEX RGC-32 or pGEX RGC-32 T91A	
MW 594 (forward primer)	GCG GAT CCT CTA GAA TGA AGC CGC CC
MW 525 (reverse primer)	CGG CGG CCG CTC ACA TAC TTG CTA AAG T
RGC-32 primers for making pGEX RGC-32 1-25	
MW 594 (forward primer)	GCG GAT CCT CTA GAA TGA AGC CGC CC
MW 730 (reverse primer)	GCT CGA GTC AGG GCG ACG CGA AGT CGG CCA G
RGC-32 primers for making pGEX RGC-32 1-50	
MW 594 (forward primer)	GCG GAT CCT CTA GAA TGA AGC CGC CC
MW 731 (reverse primer)	GCT CGA GTC AGT CGC TGA CAC TGG CGC TGC T
RGC-32 primers for making pGEX RGC-32 1-75	
MW 594 (forward primer)	GCG GAT CCT CTA GAA TGA AGC CGC CC
MW 732 (reverse primer)	GCT CGA GTC ACA GTT TTT CAT CAC TGA AGC T
RGC-32 primers for making pGEX RGC-32 1-100	
MW 594 (forward primer)	GCG GAT CCT CTA GAA TGA AGC CGC CC
MW 733 (reverse primer)	GCT CGA GTC ATG TGT CTC CTA ATT TAG CTT T

7.4 qPCR primers

Gene	Sequence
RGC-32 ChIP qPCR E1	
MW 629 (forward primer)	GCC AGT GTC TCG CAT GAA
MW 630 (reverse primer)	GTT GGT GCA CCT TCA GAC AG
RGC-32 ChIP qPCR E2	
MW 631 (forward primer)	CCA GCA TGA CAG ATG GCT TA
MW 632 (reverse primer)	AGG CTC CTC ATT GGC CTT A
RGC-32 ChIP qPCR E3	
MW 633 (forward primer)	GTG ATC AGC CAG CAA CAC AT
MW 634 (reverse primer)	AGC CGG ACA TCC TGT TCT T
RGC-32 ChIP qPCR E4	
MW 635 (forward primer)	GAT AGA GAG CGG AGG TGT GG
MW 636 (reverse primer)	CCG TGG CTA TGA AGG ATA CC
RGC-32 ChIP qPCR E5	
MW 637 (forward primer)	GGC CAG CTT CCT GTG TGT A
MW 638 (reverse primer)	CTC CGT GGA ACC TTA CTT GG
RGC-32 ChIP qPCR E6	
MW 639 (forward primer)	GAG CCA TGA TGT CAC TCC AA
MW 640 (reverse primer)	CTT CAG ATA AGC CAG AAG GTC AA
RGC-32 ChIP qPCR E7	
MW 641 (forward primer)	GTG ATC TTG GCT CAC TGC AA
MW 642 (reverse primer)	TAG CCA GGC ATA GTG GTG TG
RGC-32 ChIP qPCR E8	
MW 774 (forward primer)	ACA CCT GAA GAG CCA CTT CTC T
MW 775 (reverse primer)	CTG GCT GAG CAG CAC TGA
RGC-32 ChIP qPCR E9	
MW 776 (forward primer)	AGA GGG CAG AAG GGA CAT ATT
MW 777 (reverse primer)	TGT GTC AAA TCA AGT ATA CCA AAG G

8 References

Abbot, S. D., M. Rowe, K. Cadwallader, A. Ricksten, J. Gordon, F. Wang, L. Rymo & A. B. Rickinson (1990) Epstein-Barr virus nuclear antigen 2 induces expression of the virus-encoded latent membrane protein. *J Virol,* 64**,** 2126-34.

Abraham, R. T. (2001) Cell cycle checkpoint signaling through the ATM and ATR kinases. *Genes Dev,* 15**,** 2177-96.

Adams, A. & T. Lindahl (1975) Epstein-Barr virus genomes with properties of circular DNA molecules in carrier cells. *Proc Natl Acad Sci U S A,* 72**,** 1477-81.

Adldinger, H. K., H. Delius, U. K. Freese, J. Clarke & G. W. Bornkamm (1985) A putative transforming gene of Jijoye virus differs from that of Epstein-Barr virus prototypes. *Virology,* 141**,** 221-34.

Alfieri, C., M. Birkenbach & E. Kieff (1991) Early events in Epstein-Barr virus infection of human B lymphocytes. *Virology,* 181**,** 595-608.

Allan, G. J., G. J. Inman, B. D. Parker, D. T. Rowe & P. J. Farrell (1992) Cell growth effects of Epstein-Barr virus leader protein. *J Gen Virol,* 73 (Pt 6)**,** 1547-51.

Allday, M. J., Q. Bazot & R. E. White (2015) The EBNA3 Family: Two Oncoproteins and a Tumour Suppressor that Are Central to the Biology of EBV in B Cells. *Curr Top Microbiol Immunol,* 391**,** 61-117.

Allday, M. J. & P. J. Farrell (1994) Epstein-Barr virus nuclear antigen EBNA3C/6 expression maintains the level of latent membrane protein 1 in G1-arrested cells. *J Virol,* 68**,** 3491-8.

Ambinder, R. F., W. A. Shah, D. R. Rawlins, G. S. Hayward & S. D. Hayward (1990) Definition of the sequence requirements for binding of the EBNA-1 protein to its palindromic target sites in Epstein-Barr virus DNA. *J Virol,* 64**,** 2369-79.

Amin, M. A., G. Itoh, K. Iemura, M. Ikeda & K. Tanaka (2014) CLIP-170 recruits PLK1 to kinetochores during early mitosis for chromosome alignment. *J Cell Sci,* 127**,** 2818-24.

Anderton, E., J. Yee, P. Smith, T. Crook, R. E. White & M. J. Allday (2008) Two Epstein-Barr virus (EBV) oncoproteins cooperate to repress expression of the proapoptotic tumour-suppressor Bim: clues to the pathogenesis of Burkitt's lymphoma. *Oncogene,* 27**,** 421-33.

Andrysik, Z., W. Z. Bernstein, L. Deng, D. L. Myer, Y. Q. Li, J. A. Tischfield, P. J. Stambrook & M. Bahassi el (2010) The novel mouse Polo-like kinase 5 responds to DNA damage and localizes in the nucleolus. *Nucleic Acids Res,* 38**,** 2931-43.

Arion, D., L. Meijer, L. Brizuela & D. Beach (1988) cdc2 is a component of the M phase-specific histone H1 kinase: evidence for identity with MPF. *Cell,* 55**,** 371-8.

Babcock, G. J., L. L. Decker, R. B. Freeman & D. A. Thorley-Lawson (1999) Epstein-barr virus-infected resting memory B cells, not proliferating lymphoblasts, accumulate in the peripheral blood of immunosuppressed patients. *J Exp Med,* 190**,** 567-76.

Babcock, G. J., L. L. Decker, M. Volk & D. A. Thorley-Lawson (1998) EBV persistence in memory B cells in vivo. *Immunity,* 9**,** 395-404.

Badea, T., F. Niculescu, L. Soane, M. Fosbrink, H. Sorana, V. Rus, M. L. Shin & H. Rus (2002) RGC-32 increases p34CDC2 kinase activity and entry of aortic smooth muscle cells into S-phase. *J Biol Chem,* 277**,** 502-8.

Badea, T. C., F. I. Niculescu, L. Soane, M. L. Shin & H. Rus (1998) Molecular cloning and characterization of RGC-32, a novel gene induced by complement activation in oligodendrocytes. *J Biol Chem,* 273**,** 26977-81.

Baer, R., A. T. Bankier, M. D. Biggin, P. L. Deininger, P. J. Farrell, T. J. Gibson, G. Hatfull, G. S. Hudson, S. C. Satchwell, C. Seguin & et al. (1984) DNA sequence and expression of the B95-8 Epstein-Barr virus genome. *Nature,* 310**,** 207-11.

Bailly, E., J. Pines, T. Hunter & M. Bornens (1992) Cytoplasmic accumulation of cyclin B1 in human cells: association with a detergent-resistant compartment and with the centrosome. *J Cell Sci,* 101 (Pt 3)**,** 529-45.

Bakkenist, C. J. & M. B. Kastan (2003) DNA damage activates ATM through intermolecular autophosphorylation and dimer dissociation. *Nature,* 421**,** 499-506.

Barr, F. A., H. H. Sillje & E. A. Nigg (2004) Polo-like kinases and the orchestration of cell division. *Nat Rev Mol Cell Biol,* 5**,** 429-40.

Bartkova, J., M. Zemanova & J. Bartek (1996) Expression of CDK7/CAK in normal and tumor cells of diverse histogenesis, cell-cycle position and differentiation. *Int J Cancer,* 66**,** 732-7.

Bell, A., J. Skinner, H. Kirby & A. Rickinson (1998) Characterisation of regulatory sequences at the Epstein-Barr virus BamHI W promoter. *Virology,* 252**,** 149-61.

Bhatia, K., K. Huppi, G. Spangler, D. Siwarski, R. Iyer & I. Magrath (1993) Point mutations in the c-Myc transactivation domain are common in Burkitt's lymphoma and mouse plasmacytomas. *Nat Genet,* 5**,** 56-61.

Bhattacharjee, S., S. Ghosh Roy, P. Bose & A. Saha (2016) Role of EBNA-3 Family Proteins in EBV Associated B-cell Lymphomagenesis. *Front Microbiol,* 7**,** 457.

Bodescot, M., M. Perricaudet & P. J. Farrell (1987) A promoter for the highly spliced EBNA family of RNAs of Epstein-Barr virus. *J Virol,* 61**,** 3424-30.

Bornkamm, G. W., C. Berens, C. Kuklik-Roos, J. M. Bechet, G. Laux, J. Bachl, M. Korndoerfer, M. Schlee, M. Holzel, A. Malamoussi, R. D. Chapman, F. Nimmerjahn, J. Mautner, W. Hillen, H. Bujard & J. Feuillard (2005) Stringent doxycycline-dependent control of gene activities using an episomal one-vector system. *Nucleic Acids Res,* 33**,** e137.

Bornkamm, G. W. & W. Hammerschmidt (2001) Molecular virology of Epstein-Barr virus. *Philos Trans R Soc Lond B Biol Sci,* 356**,** 437-59.

Borza, C. M. & L. M. Hutt-Fletcher (2002) Alternate replication in B cells and epithelial cells switches tropism of Epstein-Barr virus. *Nat Med,* 8**,** 594-9.

Bourillot, P. Y., L. Waltzer, A. Sergeant & E. Manet (1998) Transcriptional repression by the Epstein-Barr virus EBNA3A protein tethered to DNA does not require RBP-Jkappa. *J Gen Virol,* 79 (Pt 2)**,** 363-70.

Bredel, M., C. Bredel, D. Juric, G. E. Duran, R. X. Yu, G. R. Harsh, H. Vogel, L. D. Recht, A. C. Scheck & B. I. Sikic (2006) Tumor necrosis factor-alpha-induced protein 3 as a putative regulator of nuclear factor-kappaB-mediated resistance to O6-alkylating agents in human glioblastomas. *J Clin Oncol,* 24**,** 274-87.

Brink, A. A., M. B. Vervoort, J. M. Middeldorp, C. J. Meijer & A. J. van den Brule (1998) Nucleic acid sequence-based amplification, a new method for analysis of spliced and unspliced Epstein-Barr virus latent transcripts, and its comparison with reverse transcriptase PCR. *J Clin Microbiol,* 36**,** 3164-9.

Brooks, L., Q. Y. Yao, A. B. Rickinson & L. S. Young (1992) Epstein-Barr virus latent gene transcription in nasopharyngeal carcinoma cells: coexpression of EBNA1, LMP1, and LMP2 transcripts. *J Virol,* 66**,** 2689-97.

Brooks, L. A., A. L. Lear, L. S. Young & A. B. Rickinson (1993) Transcripts from the Epstein-Barr virus BamHI A fragment are detectable in all three forms of virus latency. *J Virol,* 67**,** 3182-90.

Brown, E. J. & D. Baltimore (2003) Essential and dispensable roles of ATR in cell cycle arrest and genome maintenance. *Genes Dev,* 17**,** 615-28.

Brown, N. R., S. Korolchuk, M. P. Martin, W. A. Stanley, R. Moukhametzianov, M. E. Noble & J. A. Endicott (2015) CDK1 structures reveal conserved and unique features of the essential cell cycle CDK. *Nat Commun,* 6**,** 6769.

Burkitt, D. & G. T. O'Conor (1961) Malignant lymphoma in African children. I. A clinical syndrome. *Cancer,* 14**,** 258-69.

Burkitt, D. P. (1969) Etiology of Burkitt's lymphoma--an alternative hypothesis to a vectored virus. *J Natl Cancer Inst,* 42**,** 19-28.

Cahir-McFarland, E. D., K. Carter, A. Rosenwald, J. M. Giltnane, S. E. Henrickson, L. M. Staudt & E. Kieff (2004) Role of NF-kappa B in cell survival and transcription of latent membrane protein 1-expressing or Epstein-Barr virus latency III-infected cells. *J Virol,* 78**,** 4108-19.

Calderwood, M. A., S. Lee, A. M. Holthaus, S. C. Blacklow, E. Kieff & E. Johannsen (2011) Epstein-Barr virus nuclear protein 3C binds to the N-terminal (NTD) and beta trefoil domains (BTD) of RBP/CSL; only the NTD interaction is essential for lymphoblastoid cell growth. *Virology,* 414**,** 19-25.

Ceccarelli, D. F. & L. Frappier (2000) Functional analyses of the EBNA1 origin DNA binding protein of Epstein-Barr virus. *J Virol,* 74**,** 4939-48.

Cesarman, E., R. Dalla-Favera, D. Bentley & M. Groudine (1987) Mutations in the first exon are associated with altered transcription of c-myc in Burkitt lymphoma. *Science,* 238**,** 1272-5.

Chan, E. H., A. Santamaria, H. H. Sillje & E. A. Nigg (2008) Plk1 regulates mitotic Aurora A function through betaTrCP-dependent degradation of hBora. *Chromosoma,* 117**,** 457-69.

Cheeseman, I. M., J. S. Chappie, E. M. Wilson-Kubalek & A. Desai (2006) The conserved KMN network constitutes the core microtubule-binding site of the kinetochore. *Cell,* 127**,** 983-97.

Cheeseman, I. M. & A. Desai (2008) Molecular architecture of the kinetochore-microtubule interface. *Nat Rev Mol Cell Biol,* 9**,** 33-46.

Chen, C. L., R. H. Sadler, D. M. Walling, I. J. Su, H. C. Hsieh & N. Raab-Traub (1993) Epstein-Barr virus (EBV) gene expression in EBV-positive peripheral T-cell lymphomas. *J Virol,* 67**,** 6303-8.

Chen, H., L. Hutt-Fletcher, L. Cao & S. D. Hayward (2003) A positive autoregulatory loop of LMP1 expression and STAT activation in epithelial cells latently infected with Epstein-Barr virus. *J Virol,* 77**,** 4139-48.

Chen, H., J. M. Lee, Y. Zong, M. Borowitz, M. H. Ng, R. F. Ambinder & S. D. Hayward (2001) Linkage between STAT regulation and Epstein-Barr virus gene expression in tumors. *J Virol,* 75**,** 2929-37.

Chen, H. L., M. M. Lung, J. S. Sham, D. T. Choy, B. E. Griffin & M. H. Ng (1992) Transcription of BamHI-A region of the EBV genome in NPC tissues and B cells. *Virology,* 191**,** 193-201.

Cheng, A., S. Gerry, P. Kaldis & M. J. Solomon (2005a) Biochemical characterization of Cdk2-Speedy/Ringo A2. *BMC Biochem,* 6**,** 19.

Cheng, A. & M. J. Solomon (2008) Speedy/Ringo C regulates S and G2 phase progression in human cells. *Cell Cycle,* 7**,** 3037-47.

Cheng, A., W. Xiong, J. E. Ferrell, Jr. & M. J. Solomon (2005b) Identification and comparative analysis of multiple mammalian Speedy/Ringo proteins. *Cell Cycle,* 4**,** 155-65.

Cheung, S. T., D. P. Huang, A. B. Hui, K. W. Lo, C. W. Ko, Y. S. Tsang, N. Wong, B. M. Whitney & J. C. Lee (1999) Nasopharyngeal carcinoma cell line (C666-1) consistently harbouring Epstein-Barr virus. *Int J Cancer,* 83**,** 121-6.

Chinnadurai, G. (2002) CtBP, an unconventional transcriptional corepressor in development and oncogenesis. *Mol Cell,* 9**,** 213-24.

--- (2007) Transcriptional regulation by C-terminal binding proteins. *Int J Biochem Cell Biol,* 39**,** 1593-607.

--- (2009) The transcriptional corepressor CtBP: a foe of multiple tumor suppressors. *Cancer Res,* 69**,** 731-4.

Choudhuri, T., S. C. Verma, K. Lan, M. Murakami & E. S. Robertson (2007) The ATM/ATR signaling effector Chk2 is targeted by Epstein-Barr virus nuclear antigen 3C to release the G2/M cell cycle block. *J Virol,* 81**,** 6718-30.

Clute, P. & J. Pines (1999) Temporal and spatial control of cyclin B1 destruction in metaphase. *Nat Cell Biol,* 1**,** 82-7.

Cohen, J. I., F. Wang, J. Mannick & E. Kieff (1989) Epstein-Barr virus nuclear protein 2 is a key determinant of lymphocyte transformation. *Proc Natl Acad Sci U S A,* 86**,** 9558-62.

Cordier, M., A. Calender, M. Billaud, U. Zimber, G. Rousselet, O. Pavlish, J. Banchereau, T. Tursz, G. Bornkamm & G. M. Lenoir (1990) Stable transfection of Epstein-Barr virus (EBV) nuclear antigen 2 in lymphoma cells containing the EBV P3HR1 genome induces expression of B-cell activation molecules CD21 and CD23. *J Virol,* 64**,** 1002-13.

Cox, C. J., K. Dutta, E. T. Petri, W. C. Hwang, Y. Lin, S. M. Pascal & R. Basavappa (2002) The regions of securin and cyclin B proteins recognized by the ubiquitination machinery are natively unfolded. *FEBS Lett,* 527**,** 303-8.

Dalal, S. N., C. M. Schweitzer, J. Gan & J. A. DeCaprio (1999) Cytoplasmic localization of human cdc25C during interphase requires an intact 14-3-3 binding site. *Mol Cell Biol,* 19**,** 4465-79.

Dalbies-Tran, R., E. Stigger-Rosser, T. Dotson & C. E. Sample (2001) Amino acids of Epstein-Barr virus nuclear antigen 3A essential for repression of Jkappa-mediated transcription and their evolutionary conservation. *J Virol,* 75**,** 90-9.

Dambaugh, T., K. Hennessy, L. Chamnankit & E. Kieff (1984) U2 region of Epstein-Barr virus DNA may encode Epstein-Barr nuclear antigen 2. *Proc Natl Acad Sci U S A,* 81**,** 7632-6.

Davenport, M. G. & J. S. Pagano (1999) Expression of EBNA-1 mRNA is regulated by cell cycle during Epstein-Barr virus type I latency. *J Virol,* 73**,** 3154-61.

De Matteo, E., A. V. Baron, P. Chabay, J. Porta, M. Dragosky & M. V. Preciado (2003) Comparison of Epstein-Barr virus presence in Hodgkin lymphoma in pediatric versus adult Argentine patients. *Arch Pathol Lab Med,* 127**,** 1325-9.

Deacon, E. M., G. Pallesen, G. Niedobitek, J. Crocker, L. Brooks, A. B. Rickinson & L. S. Young (1993) Epstein-Barr virus and Hodgkin's disease: transcriptional analysis of virus latency in the malignant cells. *J Exp Med,* 177**,** 339-49.

Decaussin, G., F. Sbih-Lammali, M. de Turenne-Tessier, A. Bouguermouh & T. Ooka (2000) Expression of BARF1 gene encoded by Epstein-Barr virus in nasopharyngeal carcinoma biopsies. *Cancer Res,* 60**,** 5584-8.

Dietzmann, K., E. Kirches, B. von, K. Jachau & C. Mawrin (2001) Increased human polo-like kinase-1 expression in gliomas. *J Neurooncol,* 53**,** 1-11.

Dinarina, A., L. H. Perez, A. Davila, M. Schwab, T. Hunt & A. R. Nebreda (2005) Characterization of a new family of cyclin-dependent kinase activators. *Biochem J,* 386**,** 349-55.

Dittmer, D. P., C. J. Hilscher, M. L. Gulley, E. V. Yang, M. Chen & R. Glaser (2008) Multiple pathways for Epstein-Barr virus episome loss from nasopharyngeal carcinoma. *Int J Cancer,* 123**,** 2105-12.

Donninger, H., T. Bonome, M. Radonovich, C. A. Pise-Masison, J. Brady, J. H. Shih, J. C. Barrett & M. J. Birrer (2004) Whole genome expression profiling of advance stage papillary serous ovarian cancer reveals activated pathways. *Oncogene,* 23**,** 8065-77.

Drescher, D. G., N. A. Ramakrishnan & M. J. Drescher (2009) Surface plasmon resonance (SPR) analysis of binding interactions of proteins in inner-ear sensory epithelia. *Methods Mol Biol,* 493**,** 323-43.

Dunphy, W. G., L. Brizuela, D. Beach & J. Newport (1988) The Xenopus cdc2 protein is a component of MPF, a cytoplasmic regulator of mitosis. *Cell,* 54**,** 423-31.

Elledge, S. J. (1996) Cell cycle checkpoints: preventing an identity crisis. *Science,* 274**,** 1664-72.

Epstein, M. A., B. G. Achong & Y. M. Barr (1964) Virus Particles in Cultured Lymphoblasts from Burkitt's Lymphoma. *Lancet,* 1**,** 702-3.

Fahraeus, R., A. Jansson, A. Ricksten, A. Sjoblom & L. Rymo (1990) Epstein-Barr virus-encoded nuclear antigen 2 activates the viral latent membrane protein promoter by modulating the activity of a negative regulatory element. *Proc Natl Acad Sci U S A,* 87**,** 7390-4.

Ferby, I., M. Blazquez, A. Palmer, R. Eritja & A. R. Nebreda (1999) A novel p34(cdc2)-binding and activating protein that is necessary and sufficient to trigger G(2)/M progression in Xenopus oocytes. *Genes Dev,* 13**,** 2177-89.

Ferrer, M., T. N. Chernikova, M. M. Yakimov, P. N. Golyshin & K. N. Timmis. 2003. Chaperonins govern growth of Escherichia coli at low temperatures. In *Nat Biotechnol*, 1266-7. United States.

Foley, E. A. & T. M. Kapoor (2013) Microtubule attachment and spindle assembly checkpoint signalling at the kinetochore. *Nat Rev Mol Cell Biol,* 14**,** 25-37.

Fosbrink, M., C. Cudrici, F. Niculescu, T. C. Badea, S. David, A. Shamsuddin, M. L. Shin & H. Rus (2005) Overexpression of RGC-32 in colon cancer and other tumors. *Exp Mol Pathol,* 78**,** 116-22.

Frappier, L. (2015) EBNA1. *Curr Top Microbiol Immunol,* 391**,** 3-34.

Fuentes-Panana, E. M., R. Peng, G. Brewer, J. Tan & P. D. Ling (2000) Regulation of the Epstein-Barr virus C promoter by AUF1 and the cyclic AMP/protein kinase A signaling pathway. *J Virol,* 74**,** 8166-75.

Gahn, T. A. & B. Sugden (1995) An EBNA-1-dependent enhancer acts from a distance of 10 kilobase pairs to increase expression of the Epstein-Barr virus LMP gene. *J Virol,* 69**,** 2633-6.

Gascoigne, K. E., K. Takeuchi, A. Suzuki, T. Hori, T. Fukagawa & I. M. Cheeseman (2011) Induced ectopic kinetochore assembly bypasses the requirement for CENP-A nucleosomes. *Cell,* 145**,** 410-22.

Gastwirt, R. F., C. W. McAndrew & D. J. Donoghue (2007) Speedy/RINGO regulation of CDKs in cell cycle, checkpoint activation and apoptosis. *Cell Cycle,* 6**,** 1188-93.

Gautier, J., J. Minshull, M. Lohka, M. Glotzer, T. Hunt & J. L. Maller (1990) Cyclin is a component of maturation-promoting factor from Xenopus. *Cell,* 60**,** 487-94.

Gautier, J., C. Norbury, M. Lohka, P. Nurse & J. Maller (1988) Purified maturation-promoting factor contains the product of a Xenopus homolog of the fission yeast cell cycle control gene cdc2+. *Cell,* 54**,** 433-9.

Ghosh, D. & E. Kieff (1990) cis-acting regulatory elements near the Epstein-Barr virus latent-infection membrane protein transcriptional start site. *J Virol,* 64**,** 1855-8.

Glover, D. M., I. M. Hagan & A. A. Tavares (1998) Polo-like kinases: a team that plays throughout mitosis. *Genes Dev,* 12**,** 3777-87.

Golsteyn, R. M., S. J. Schultz, J. Bartek, A. Ziemiecki, T. Ried & E. A. Nigg (1994) Cell cycle analysis and chromosomal localization of human Plk1, a putative homologue of the mitotic kinases Drosophila polo and Saccharomyces cerevisiae Cdc5. *J Cell Sci,* 107 (Pt 6)**,** 1509-17.

Grasser, F. A., P. G. Murray, E. Kremmer, K. Klein, K. Remberger, W. Feiden, G. Reynolds, G. Niedobitek, L. S. Young & N. Mueller-Lantzsch (1994) Monoclonal antibodies directed against the Epstein-Barr virus-encoded nuclear antigen 1 (EBNA1): immunohistologic detection of EBNA1 in the malignant cells of Hodgkin's disease. *Blood,* 84**,** 3792-8.

Gratama, J. W., M. M. Zutter, J. Minarovits, M. A. Oosterveer, E. D. Thomas, G. Klein & I. Ernberg (1991) Expression of Epstein-Barr virus-encoded growth-transformation-associated proteins in lymphoproliferations of bone-marrow transplant recipients. *Int J Cancer,* 47**,** 188-92.

Graves, P. R., L. Yu, J. K. Schwarz, J. Gales, E. A. Sausville, P. M. O'Connor & H. Piwnica-Worms (2000) The Chk1 protein kinase and the Cdc25C regulatory pathways are targets of the anticancer agent UCN-01. *J Biol Chem,* 275**,** 5600-5.

Gregory, C. D., M. Rowe & A. B. Rickinson (1990) Different Epstein-Barr virus-B cell interactions in phenotypically distinct clones of a Burkitt's lymphoma cell line. *J Gen Virol,* 71 (Pt 7)**,** 1481-95.

Gunnell, A., H. M. Webb, C. D. Wood, M. J. McClellan, B. Wichaidit, B. Kempkes, R. G. Jenner, C. Osborne, P. J. Farrell & M. J. West (2016) RUNX super-enhancer control through the

Notch pathway by Epstein-Barr virus transcription factors regulates B cell growth. *Nucleic Acids Research,* 44**,** 4636-4650.

Hagting, A., M. Jackman, K. Simpson & J. Pines (1999) Translocation of cyclin B1 to the nucleus at prophase requires a phosphorylation-dependent nuclear import signal. *Curr Biol,* 9**,** 680-9.

Hagting, A., C. Karlsson, P. Clute, M. Jackman & J. Pines (1998) MPF localization is controlled by nuclear export. *EMBO J,* 17**,** 4127-38.

Hammerschmidt, W. & B. Sugden (1989) Genetic analysis of immortalizing functions of Epstein-Barr virus in human B lymphocytes. *Nature,* 340**,** 393-7.

Harada, S. & E. Kieff (1997) Epstein-Barr virus nuclear protein LP stimulates EBNA-2 acidic domain-mediated transcriptional activation. *J Virol,* 71**,** 6611-8.

Harrison, S., K. Fisenne & J. Hearing (1994) Sequence requirements of the Epstein-Barr virus latent origin of DNA replication. *J Virol,* 68**,** 1913-25.

Hayles, J., D. Beach, B. Durkacz & P. Nurse (1986) The fission yeast cell cycle control gene cdc2: isolation of a sequence suc1 that suppresses cdc2 mutant function. *Mol Gen Genet,* 202**,** 291-3.

Heald, R., M. McLoughlin & F. McKeon (1993) Human wee1 maintains mitotic timing by protecting the nucleus from cytoplasmically activated Cdc2 kinase. *Cell,* 74**,** 463-74.

Henle, G., W. Henle, P. Clifford, V. Diehl, G. W. Kafuko, B. G. Kirya, G. Klein, R. H. Morrow, G. M. Munube, P. Pike, P. M. Tukei & J. L. Ziegler (1969) Antibodies to Epstein-Barr virus in Burkitt's lymphoma and control groups. *J Natl Cancer Inst,* 43**,** 1147-57.

Henle, G., W. Henle & V. Diehl (1968) Relation of Burkitt's tumor-associated herpes-ytpe virus to infectious mononucleosis. *Proc Natl Acad Sci U S A,* 59**,** 94-101.

Hennessy, K., S. Fennewald & E. Kieff (1985) A third viral nuclear protein in lymphoblasts immortalized by Epstein-Barr virus. *Proc Natl Acad Sci U S A,* 82**,** 5944-8.

Hertle, M. L., C. Popp, S. Petermann, S. Maier, E. Kremmer, R. Lang, J. Mages & B. Kempkes (2009) Differential gene expression patterns of EBV infected EBNA-3A positive and negative human B lymphocytes. *PLoS Pathog,* 5**,** e1000506.

Hickabottom, M., G. A. Parker, P. Freemont, T. Crook & M. J. Allday (2002) Two nonconsensus sites in the Epstein-Barr virus oncoprotein EBNA3A cooperate to bind the co-repressor carboxyl-terminal-binding protein (CtBP). *J Biol Chem,* 277**,** 47197-204.

Hjalgrim, H., J. Askling, P. Sorensen, M. Madsen, N. Rosdahl, H. H. Storm, S. Hamilton-Dutoit, L. S. Eriksen, M. Frisch, A. Ekbom & M. Melbye (2000) Risk of Hodgkin's disease and other cancers after infectious mononucleosis. *J Natl Cancer Inst,* 92**,** 1522-8.

Hochberg, D., J. M. Middeldorp, M. Catalina, J. L. Sullivan, K. Luzuriaga & D. A. Thorley-Lawson (2004) Demonstration of the Burkitt's lymphoma Epstein-Barr virus phenotype in dividing latently infected memory cells in vivo. *Proc Natl Acad Sci U S A,* 101**,** 239-44.

Holmes, R. D. & R. J. Sokol (2002) Epstein-Barr virus and post-transplant lymphoproliferative disease. *Pediatr Transplant,* 6**,** 456-64.

Holowaty, M. N., M. Zeghouf, H. Wu, J. Tellam, V. Athanasopoulos, J. Greenblatt & L. Frappier (2003) Protein profiling with Epstein-Barr nuclear antigen-1 reveals an interaction with the herpesvirus-associated ubiquitin-specific protease HAUSP/USP7. *J Biol Chem,* 278**,** 29987-94.

Hurley, E. A. & D. A. Thorley-Lawson (1988) B cell activation and the establishment of Epstein-Barr virus latency. *J Exp Med,* 168**,** 2059-75.

Iizasa, H., A. Nanbo, J. Nishikawa, M. Jinushi & H. Yoshiyama (2012) Epstein-Barr Virus (EBV)-associated gastric carcinoma. *Viruses,* 4**,** 3420-39.

Imai, S., S. Koizumi, M. Sugiura, M. Tokunaga, Y. Uemura, N. Yamamoto, S. Tanaka, E. Sato & T. Osato (1994) Gastric carcinoma: monoclonal epithelial malignant cells expressing Epstein-Barr virus latent infection protein. *Proc Natl Acad Sci U S A,* 91**,** 9131-5.

Jang, Y. J., S. Ma, Y. Terada & R. L. Erikson (2002) Phosphorylation of threonine 210 and the role of serine 137 in the regulation of mammalian polo-like kinase. *J Biol Chem,* 277**,** 44115-20.

Jha, H. C., J. M. A, A. Saha, S. Banerjee, J. Lu & E. S. Robertson (2014) Epstein-Barr virus essential antigen EBNA3C attenuates H2AX expression. *J Virol,* 88**,** 3776-88.

Jha, H. C., J. Lu, A. Saha, Q. Cai, S. Banerjee, M. A. Prasad & E. S. Robertson (2013) EBNA3C-mediated regulation of aurora kinase B contributes to Epstein-Barr virus-induced B-cell proliferation through modulation of the activities of the retinoblastoma protein and apoptotic caspases. *J Virol,* 87**,** 12121-38.

Jiang, S., B. Willox, H. Zhou, A. M. Holthaus, A. Wang, T. T. Shi, S. Maruo, P. V. Kharchenko, E. C. Johannsen, E. Kieff & B. Zhao (2014) Epstein-Barr virus nuclear antigen 3C binds to BATF/IRF4 or SPI1/IRF4 composite sites and recruits Sin3A to repress CDKN2A. *Proc Natl Acad Sci U S A,* 111**,** 421-6.

Jin, X. W. & S. H. Speck (1992) Identification of critical cis elements involved in mediating Epstein-Barr virus nuclear antigen 2-dependent activity of an enhancer located upstream of the viral BamHI C promoter. *J Virol,* 66**,** 2846-52.

Jo, M. & T. E. Curry, Jr. (2006) Luteinizing hormone-induced RUNX1 regulates the expression of genes in granulosa cells of rat periovulatory follicles. *Mol Endocrinol,* 20**,** 2156-72.

Johannsen, E., C. L. Miller, S. R. Grossman & E. Kieff (1996) EBNA-2 and EBNA-3C extensively and mutually exclusively associate with RBPJkappa in Epstein-Barr virus-transformed B lymphocytes. *J Virol,* 70**,** 4179-83.

Jones, C. H., S. D. Hayward & D. R. Rawlins (1989) Interaction of the lymphocyte-derived Epstein-Barr virus nuclear antigen EBNA-1 with its DNA-binding sites. *J Virol,* 63**,** 101-10.

Juvonen, E., S. M. Aalto, J. Tarkkanen, L. Volin, P. S. Mattila, S. Knuutila, T. Ruutu & K. Hedman (2003) High incidence of PTLD after non-T-cell-depleted allogeneic haematopoietic stem cell transplantation as a consequence of intensive immunosuppressive treatment. *Bone Marrow Transplant,* 32**,** 97-102.

Kaiser, C., G. Laux, D. Eick, N. Jochner, G. W. Bornkamm & B. Kempkes (1999) The proto-oncogene c-myc is a direct target gene of Epstein-Barr virus nuclear antigen 2. *J Virol,* 73**,** 4481-4.

Kang, Y., P. M. Siegel, W. Shu, M. Drobnjak, S. M. Kakonen, C. Cordon-Cardo, T. A. Guise & J. Massague (2003) A multigenic program mediating breast cancer metastasis to bone. *Cancer Cell,* 3**,** 537-49.

Karaiskou, A., L. H. Perez, I. Ferby, R. Ozon, C. Jessus & A. R. Nebreda (2001) Differential regulation of Cdc2 and Cdk2 by RINGO and cyclins. *J Biol Chem,* 276**,** 36028-34.

Kashuba, E., M. Yurchenko, S. P. Yenamandra, B. Snopok, M. Isaguliants, L. Szekely & G. Klein (2008) EBV-encoded EBNA-6 binds and targets MRS18-2 to the nucleus, resulting in the disruption of pRb-E2F1 complexes. *Proc Natl Acad Sci U S A,* 105**,** 5489-94.

Kelly, G. L., A. E. Milner, G. S. Baldwin, A. I. Bell & A. B. Rickinson (2006) Three restricted forms of Epstein-Barr virus latency counteracting apoptosis in c-myc-expressing Burkitt lymphoma cells. *Proc Natl Acad Sci U S A,* 103**,** 14935-40.

Kennedy, G. & B. Sugden (2003) EBNA-1, a bifunctional transcriptional activator. *Mol Cell Biol,* 23**,** 6901-8.

Kim, H. S. & M. S. Lee (2007) STAT1 as a key modulator of cell death. *Cell Signal,* 19**,** 454-65.

Kirby, H., A. Rickinson & A. Bell (2000) The activity of the Epstein-Barr virus BamHI W promoter in B cells is dependent on the binding of CREB/ATF factors. *J Gen Virol,* 81**,** 1057-66.

Kis, L. L., N. Gerasimcik, D. Salamon, E. K. Persson, N. Nagy, G. Klein, E. Severinson & E. Klein (2011) STAT6 signaling pathway activated by the cytokines IL-4 and IL-13 induces expression of the Epstein-Barr virus-encoded protein LMP-1 in absence of EBNA-2: implications for the type II EBV latent gene expression in Hodgkin lymphoma. *Blood,* 117**,** 165-74.

Kis, L. L., D. Salamon, E. K. Persson, N. Nagy, F. A. Scheeren, H. Spits, G. Klein & E. Klein (2010) IL-21 imposes a type II EBV gene expression on type III and type I B cells by the repression of C- and activation of LMP-1-promoter. *Proc Natl Acad Sci U S A,* 107**,** 872-7.

Kis, L. L., M. Takahara, N. Nagy, G. Klein & E. Klein (2006) IL-10 can induce the expression of EBV-encoded latent membrane protein-1 (LMP-1) in the absence of EBNA-2 in B lymphocytes and in Burkitt lymphoma- and NK lymphoma-derived cell lines. *Blood,* 107**,** 2928-35.

Kitay, M. K. & D. T. Rowe (1996) Cell cycle stage-specific phosphorylation of the Epstein-Barr virus immortalization protein EBNA-LP. *J Virol,* 70**,** 7885-93.

Knight, J. S., N. Sharma, D. E. Kalman & E. S. Robertson (2004) A cyclin-binding motif within the amino-terminal homology domain of EBNA3C binds cyclin A and modulates cyclin A-dependent kinase activity in Epstein-Barr virus-infected cells. *J Virol,* 78**,** 12857-67.

Knight, J. S., N. Sharma & E. S. Robertson (2005) Epstein-Barr virus latent antigen 3C can mediate the degradation of the retinoblastoma protein through an SCF cellular ubiquitin ligase. *Proc Natl Acad Sci U S A,* 102**,** 18562-6.

Knowles, D. M. (1999) Immunodeficiency-associated lymphoproliferative disorders. *Mod Pathol,* 12**,** 200-17.

Krabbe, S., J. Hesse & P. Uldall (1981) Primary Epstein-Barr virus infection in early childhood. *Arch Dis Child,* 56**,** 49-52.

Krauer, K. G., A. Burgess, M. Buck, J. Flanagan, T. B. Sculley & B. Gabrielli (2004) The EBNA-3 gene family proteins disrupt the G2/M checkpoint. *Oncogene,* 23**,** 1342-53.

Kumagai, A. & W. G. Dunphy (1991) The cdc25 protein controls tyrosine dephosphorylation of the cdc2 protein in a cell-free system. *Cell,* 64**,** 903-14.

--- (1996) Purification and molecular cloning of Plx1, a Cdc25-regulatory kinase from Xenopus egg extracts. *Science,* 273**,** 1377-80.

Kunwar, S., G. Mohapatra, A. Bollen, K. R. Lamborn, M. Prados & B. G. Feuerstein (2001) Genetic subgroups of anaplastic astrocytomas correlate with patient age and survival. *Cancer Res,* 61**,** 7683-8.

Kuppers, R. (2009) The biology of Hodgkin's lymphoma. *Nat Rev Cancer,* 9**,** 15-27.

Kuppers, R. & M. L. Hansmann (2005) The Hodgkin and Reed/Sternberg cell. *Int J Biochem Cell Biol,* 37**,** 511-7.

Labbe, J. C., J. P. Capony, D. Caput, J. C. Cavadore, J. Derancourt, M. Kaghad, J. M. Lelias, A. Picard & M. Doree (1989) MPF from starfish oocytes at first meiotic metaphase is a heterodimer containing one molecule of cdc2 and one molecule of cyclin B. *EMBO J,* 8**,** 3053-8.

Labbe, J. C., M. G. Lee, P. Nurse, A. Picard & M. Doree (1988) Activation at M-phase of a protein kinase encoded by a starfish homologue of the cell cycle control gene cdc2+. *Nature,* 335**,** 251-4.

Le Roux, A., B. Kerdiles, D. Walls, J. F. Dedieu & M. Perricaudet (1994) The Epstein-Barr virus determined nuclear antigens EBNA-3A, -3B, and -3C repress EBNA-2-mediated transactivation of the viral terminal protein 1 gene promoter. *Virology,* 205**,** 596-602.

Lee, M. A., M. E. Diamond & J. L. Yates (1999) Genetic evidence that EBNA-1 is needed for efficient, stable latent infection by Epstein-Barr virus. *J Virol,* 73**,** 2974-82.

Lee, S., S. Sakakibara, S. Maruo, B. Zhao, M. A. Calderwood, A. M. Holthaus, C. Y. Lai, K. Takada, E. Kieff & E. Johannsen (2009) Epstein-Barr virus nuclear protein 3C domains necessary for lymphoblastoid cell growth: interaction with RBP-Jkappa regulates TCL1. *J Virol,* 83**,** 12368-77.

Lenormand, J. L., R. W. Dellinger, K. E. Knudsen, S. Subramani & D. J. Donoghue (1999) Speedy: a novel cell cycle regulator of the G2/M transition. *EMBO J,* 18**,** 1869-77.

Li, F., Z. Luo, W. Huang, Q. Lu, C. S. Wilcox, P. A. Jose & S. Chen (2007) Response gene to complement 32, a novel regulator for transforming growth factor-beta-induced smooth muscle differentiation of neural crest cells. *J Biol Chem,* 282**,** 10133-7.

Li, R. & S. D. Hayward (2011) The Ying-Yang of the virus-host interaction: control of the DNA damage response. *Future Microbiol,* 6**,** 379-83.

Lin, C. T., C. I. Wong, W. Y. Chan, K. W. Tzung, J. K. Ho, M. M. Hsu & S. M. Chuang (1990) Establishment and characterization of two nasopharyngeal carcinoma cell lines. *Lab Invest,* 62**,** 713-24.

Ling, P. D. & S. D. Hayward (1995) Contribution of conserved amino acids in mediating the interaction between EBNA2 and CBF1/RBPJk. *J Virol,* 69**,** 1944-50.

Liu, D., O. Davydenko & M. A. Lampson (2012) Polo-like kinase-1 regulates kinetochore-microtubule dynamics and spindle checkpoint silencing. *J Cell Biol,* 198**,** 491-9.

Liu, F., J. J. Stanton, Z. Wu & H. Piwnica-Worms (1997) The human Myt1 kinase preferentially phosphorylates Cdc2 on threonine 14 and localizes to the endoplasmic reticulum and Golgi complex. *Mol Cell Biol,* 17**,** 571-83.

Luo, B., Y. Wang, X. F. Wang, H. Liang, L. P. Yan, B. H. Huang & P. Zhao (2005) Expression of Epstein-Barr virus genes in EBV-associated gastric carcinomas. *World J Gastroenterol,* 11**,** 629-33.

Macsween, K. F. & D. H. Crawford (2003) Epstein-Barr virus-recent advances. *Lancet Infect Dis,* 3**,** 131-40.

Macurek, L., A. Lindqvist, D. Lim, M. A. Lampson, R. Klompmaker, R. Freire, C. Clouin, S. S. Taylor, M. B. Yaffe & R. H. Medema (2008) Polo-like kinase-1 is activated by aurora A to promote checkpoint recovery. *Nature,* 455**,** 119-23.

Magrath, I. (1990) The pathogenesis of Burkitt's lymphoma. *Adv Cancer Res,* 55**,** 133-270.

Magrath, I., V. Jain & K. Bhatia (1992) Epstein-Barr virus and Burkitt's lymphoma. *Semin Cancer Biol,* 3**,** 285-95.

Maier, S., G. Staffler, A. Hartmann, J. Hock, K. Henning, K. Grabusic, R. Mailhammer, R. Hoffmann, M. Wilmanns, R. Lang, J. Mages & B. Kempkes (2006) Cellular target genes of Epstein-Barr virus nuclear antigen 2. *J Virol,* 80**,** 9761-71.

Mailand, N., S. Bekker-Jensen, J. Bartek & J. Lukas (2006) Destruction of Claspin by SCFbetaTrCP restrains Chk1 activation and facilitates recovery from genotoxic stress. *Mol Cell,* 23**,** 307-18.

Malik-Soni, N. & L. Frappier (2012) Proteomic profiling of EBNA1-host protein interactions in latent and lytic Epstein-Barr virus infections. *J Virol,* 86**,** 6999-7002.

Maller, J. L. (1991) Mitotic control. *Curr Opin Cell Biol,* 3**,** 269-75.

Malvezzi, F., G. Litos, A. Schleiffer, A. Heuck, K. Mechtler, T. Clausen & S. Westermann (2013) A structural basis for kinetochore recruitment of the Ndc80 complex via two distinct centromere receptors. *Embo j,* 32**,** 409-23.

Mamely, I., M. A. van Vugt, V. A. Smits, J. I. Semple, B. Lemmens, A. Perrakis, R. H. Medema & R. Freire (2006) Polo-like kinase-1 controls proteasome-dependent degradation of Claspin during checkpoint recovery. *Curr Biol,* 16**,** 1950-5.

Mannick, J. B., J. I. Cohen, M. Birkenbach, A. Marchini & E. Kieff (1991) The Epstein-Barr virus nuclear protein encoded by the leader of the EBNA RNAs is important in B-lymphocyte transformation. *J Virol,* 65**,** 6826-37.

Marafioti, T., M. Hummel, I. Anagnostopoulos, H. D. Foss, B. Falini, G. Delsol, P. G. Isaacson, S. Pileri & H. Stein (1997) Origin of nodular lymphocyte-predominant Hodgkin's disease from a clonal expansion of highly mutated germinal-center B cells. *N Engl J Med,* 337**,** 453-8.

Maruo, S., E. Johannsen, D. Illanes, A. Cooper, B. Zhao & E. Kieff (2005) Epstein-Barr virus nuclear protein 3A domains essential for growth of lymphoblasts: transcriptional regulation through RBP-Jkappa/CBF1 is critical. *J Virol,* 79**,** 10171-9.

Maruo, S., Y. Wu, S. Ishikawa, T. Kanda, D. Iwakiri & K. Takada (2006) Epstein-Barr virus nuclear protein EBNA3C is required for cell cycle progression and growth maintenance of lymphoblastoid cells. *Proc Natl Acad Sci U S A,* 103**,** 19500-5.

Maruo, S., Y. Wu, T. Ito, T. Kanda, E. D. Kieff & K. Takada (2009) Epstein-Barr virus nuclear protein EBNA3C residues critical for maintaining lymphoblastoid cell growth. *Proc Natl Acad Sci U S A,* 106**,** 4419-24.

Maruo, S., B. Zhao, E. Johannsen, E. Kieff, J. Zou & K. Takada (2011) Epstein-Barr virus nuclear antigens 3C and 3A maintain lymphoblastoid cell growth by repressing p16INK4A and p14ARF expression. *Proc Natl Acad Sci U S A,* 108**,** 1919-24.

Masui, Y. & C. L. Markert (1971) Cytoplasmic control of nuclear behavior during meiotic maturation of frog oocytes. *J Exp Zool,* 177**,** 129-45.

Matsuoka, S., M. Huang & S. J. Elledge (1998) Linkage of ATM to cell cycle regulation by the Chk2 protein kinase. *Science,* 282**,** 1893-7.

McAinsh, A. D. & P. Meraldi (2011) The CCAN complex: linking centromere specification to control of kinetochore-microtubule dynamics. *Semin Cell Dev Biol,* 22**,** 946-52.

McCann, E. M., G. L. Kelly, A. B. Rickinson & A. I. Bell (2001) Genetic analysis of the Epstein-Barr virus-coded leader protein EBNA-LP as a co-activator of EBNA2 function. *J Gen Virol,* 82**,** 3067-79.

McClellan, M. J., S. Khasnis, C. D. Wood, R. D. Palermo, S. N. Schlick, A. S. Kanhere, R. G. Jenner & M. J. West (2012) Downregulation of integrin receptor-signaling genes by Epstein-Barr virus EBNA 3C via promoter-proximal and -distal binding elements. *J Virol,* 86**,** 5165-78.

McClellan, M. J., C. D. Wood, O. Ojeniyi, T. J. Cooper, A. Kanhere, A. Arvey, H. M. Webb, R. D. Palermo, M. L. Harth-Hertle, B. Kempkes, R. G. Jenner & M. J. West (2013) Modulation of enhancer looping and differential gene targeting by Epstein-Barr virus transcription factors directs cellular reprogramming. *PLoS Pathog,* 9**,** e1003636.

McGowan, C. H. & P. Russell (1993) Human Wee1 kinase inhibits cell division by phosphorylating p34cdc2 exclusively on Tyr15. *EMBO J,* 12**,** 75-85.

--- (1995) Cell cycle regulation of human WEE1. *EMBO J,* 14**,** 2166-75.

Miller, G., J. Robinson, L. Heston & M. Lipman (1974) Differences between laboratory strains of Epstein-Barr virus based on immortalization, abortive infection, and interference. *Proc Natl Acad Sci U S A,* 71**,** 4006-10.

Miller, N. & L. M. Hutt-Fletcher (1992) Epstein-Barr virus enters B cells and epithelial cells by different routes. *J Virol,* 66**,** 3409-14.

Mueller, P. R., T. R. Coleman, A. Kumagai & W. G. Dunphy (1995) Myt1: a membrane-associated inhibitory kinase that phosphorylates Cdc2 on both threonine-14 and tyrosine-15. *Science,* 270**,** 86-90.

Muramatsu, M., K. Kinoshita, S. Fagarasan, S. Yamada, Y. Shinkai & T. Honjo (2000) Class switch recombination and hypermutation require activation-induced cytidine deaminase (AID), a potential RNA editing enzyme. *Cell,* 102**,** 553-63.

Murray, P. G. & L. S. Young (2001) Epstein-Barr virus infection: basis of malignancy and potential for therapy. *Expert Rev Mol Med,* 3**,** 1-20.

Murray, P. G., L. S. Young, M. Rowe & J. Crocker (1992) Immunohistochemical demonstration of the Epstein-Barr virus-encoded latent membrane protein in paraffin sections of Hodgkin's disease. *J Pathol,* 166**,** 1-5.

Nemerow, G. R., R. Wolfert, M. E. McNaughton & N. R. Cooper (1985) Identification and characterization of the Epstein-Barr virus receptor on human B lymphocytes and its relationship to the C3d complement receptor (CR2). *J Virol,* 55**,** 347-51.

Neri, A., F. Barriga, G. Inghirami, D. M. Knowles, J. Neequaye, I. T. Magrath & R. Dalla-Favera (1991) Epstein-Barr virus infection precedes clonal expansion in Burkitt's and acquired immunodeficiency syndrome-associated lymphoma. *Blood,* 77**,** 1092-5.

Niculescu, F., T. Badea & H. Rus (1999) Sublytic C5b-9 induces proliferation of human aortic smooth muscle cells: role of mitogen activated protein kinase and phosphatidylinositol 3-kinase. *Atherosclerosis,* 142**,** 47-56.

Niculescu, F., H. Rus, T. van Biesen & M. L. Shin (1997) Activation of Ras and mitogen-activated protein kinase pathway by terminal complement complexes is G protein dependent. *J Immunol,* 158**,** 4405-12.

Niederman, J. C., R. W. McCollum, G. Henle & W. Henle (1968) Infectious mononucleosis. Clinical manifestations in relation to EB virus antibodies. *Jama,* 203**,** 205-9.

Niederman, J. C., G. Miller, H. A. Pearson, J. S. Pagano & J. M. Dowaliby (1976) Infectious mononucleosis. Epstein-Barr-virus shedding in saliva and the oropharynx. *N Engl J Med,* 294**,** 1355-9.

Niedobitek, G., E. Kremmer, H. Herbst, L. Whitehead, C. W. Dawson, E. Niedobitek, C. von Ostau, N. Rooney, F. A. Grasser & L. S. Young (1997) Immunohistochemical detection of the Epstein-Barr virus-encoded latent membrane protein 2A in Hodgkin's disease and infectious mononucleosis. *Blood,* 90**,** 1664-72.

Nikitin, P. A., C. M. Yan, E. Forte, A. Bocedi, J. P. Tourigny, R. E. White, M. J. Allday, A. Patel, S. S. Dave, W. Kim, K. Hu, J. Guo, D. Tainter, E. Rusyn & M. A. Luftig (2010) An ATM/Chk2-mediated DNA damage-responsive signaling pathway suppresses Epstein-Barr virus transformation of primary human B cells. *Cell Host Microbe,* 8**,** 510-22.

Nishizaki, T., S. Ozaki, K. Harada, H. Ito, H. Arai, T. Beppu & K. Sasaki (1998) Investigation of genetic alterations associated with the grade of astrocytic tumor by comparative genomic hybridization. *Genes Chromosomes Cancer,* 21**,** 340-6.

Noda, C., T. Murata, T. Kanda, H. Yoshiyama, A. Sugimoto, D. Kawashima, S. Saito, H. Isomura & T. Tsurumi (2011) Identification and characterization of CCAAT enhancer-binding protein (C/EBP) as a transcriptional activator for Epstein-Barr virus oncogene latent membrane protein 1. *J Biol Chem,* 286**,** 42524-33.

Nonkwelo, C., J. Skinner, A. Bell, A. Rickinson & J. Sample (1996) Transcription start sites downstream of the Epstein-Barr virus (EBV) Fp promoter in early-passage Burkitt lymphoma cells define a fourth promoter for expression of the EBV EBNA-1 protein. *J Virol,* 70**,** 623-7.

Nurse, P. (1990) Universal control mechanism regulating onset of M-phase. *Nature,* 344**,** 503-8.

O'Connor, L., A. Strasser, L. A. O'Reilly, G. Hausmann, J. M. Adams, S. Cory & D. C. Huang (1998) Bim: a novel member of the Bcl-2 family that promotes apoptosis. *Embo j,* 17**,** 384-95.

Obaya, A. J. & J. M. Sedivy (2002) Regulation of cyclin-Cdk activity in mammalian cells. *Cell Mol Life Sci,* 59**,** 126-42.

Ookata, K., S. Hisanaga, E. Okumura & T. Kishimoto (1993) Association of p34cdc2/cyclin B complex with microtubules in starfish oocytes. *J Cell Sci,* 105 (Pt 4)**,** 873-81.

Pagano, J. S., C. H. Huang, G. Klein, G. de-The, K. Shanmugaratnam & C. S. Yang (1975) Homology of Epstein-Barr virus DNA in nasopharyngeal carcinomas from Kenya, Taiwan, Singapore and Tunisia. *IARC Sci Publ***,** 179-90.

Parker, G. A., R. Touitou & M. J. Allday (2000) Epstein-Barr virus EBNA3C can disrupt multiple cell cycle checkpoints and induce nuclear division divorced from cytokinesis. *Oncogene,* 19**,** 700-9.

Paschos, K., G. A. Parker, E. Watanatanasup, R. E. White & M. J. Allday (2012) BIM promoter directly targeted by EBNA3C in polycomb-mediated repression by EBV. *Nucleic Acids Res,* 40**,** 7233-46.

Paschos, K., P. Smith, E. Anderton, J. M. Middeldorp, R. E. White & M. J. Allday (2009) Epstein-barr virus latency in B cells leads to epigenetic repression and CpG methylation of the tumour suppressor gene Bim. *PLoS Pathog,* 5**,** e1000492.

Patra, D., S. X. Wang, A. Kumagai & W. G. Dunphy (1999) The xenopus Suc1/Cks protein promotes the phosphorylation of G(2)/M regulators. *J Biol Chem,* 274**,** 36839-42.

Peng, R., A. V. Gordadze, E. M. Fuentes Panana, F. Wang, J. Zong, G. S. Hayward, J. Tan & P. D. Ling (2000a) Sequence and functional analysis of EBNA-LP and EBNA2 proteins from nonhuman primate lymphocryptoviruses. *J Virol,* 74**,** 379-89.

Peng, R., J. Tan & P. D. Ling (2000b) Conserved regions in the Epstein-Barr virus leader protein define distinct domains required for nuclear localization and transcriptional cooperation with EBNA2. *J Virol,* 74**,** 9953-63.

Penn, I. (2000) Post-transplant malignancy: the role of immunosuppression. *Drug Saf,* 23**,** 101-13.

Perry, J. & N. Kleckner (2003) The ATRs, ATMs, and TORs are giant HEAT repeat proteins. *Cell,* 112**,** 151-5.

Peschiaroli, A., N. V. Dorrello, D. Guardavaccaro, M. Venere, T. Halazonetis, N. E. Sherman & M. Pagano (2006) SCFbetaTrCP-mediated degradation of Claspin regulates recovery from the DNA replication checkpoint response. *Mol Cell,* 23**,** 319-29.

Petri, E. T., A. Errico, L. Escobedo, T. Hunt & R. Basavappa (2007) The crystal structure of human cyclin B. *Cell Cycle,* 6**,** 1342-9.

Petti, L., C. Sample & E. Kieff (1990) Subnuclear localization and phosphorylation of Epstein-Barr virus latent infection nuclear proteins. *Virology,* 176**,** 563-74.

Pines, J. (1995) Cyclins and cyclin-dependent kinases: a biochemical view. *Biochem J,* 308 (Pt 3)**,** 697-711.

Pines, J. & T. Hunter (1989) Isolation of a human cyclin cDNA: evidence for cyclin mRNA and protein regulation in the cell cycle and for interaction with p34cdc2. *Cell,* 58**,** 833-46.

--- (1991) Human Cyclin-a and Cyclin-B1 Are Differentially Located in the Cell and Undergo Cell-Cycle Dependent Nuclear Transport. *Journal of Cell Biology,* 115**,** 1-17.

Polack, A., K. Hortnagel, A. Pajic, B. Christoph, B. Baier, M. Falk, J. Mautner, C. Geltinger, G. W. Bornkamm & B. Kempkes (1996) c-myc activation renders proliferation of Epstein-Barr virus (EBV)-transformed cells independent of EBV nuclear antigen 2 and latent membrane protein 1. *Proc Natl Acad Sci U S A,* 93**,** 10411-6.

Pope, J. H., M. K. Horne & W. Scott (1968) Transformation of foetal human keukocytes in vitro by filtrates of a human leukaemic cell line containing herpes-like virus. *Int J Cancer,* 3**,** 857-66.

Portal, D., B. Zhao, M. A. Calderwood, T. Sommermann, E. Johannsen & E. Kieff (2011) EBV nuclear antigen EBNALP dismisses transcription repressors NCoR and RBPJ from enhancers and EBNA2 increases NCoR-deficient RBPJ DNA binding. *Proc Natl Acad Sci U S A,* 108**,** 7808-13.

Porter, L. A., R. W. Dellinger, J. A. Tynan, E. A. Barnes, M. Kong, J. L. Lenormand & D. J. Donoghue (2002) Human Speedy: a novel cell cycle regulator that enhances proliferation through activation of Cdk2. *J Cell Biol,* 157**,** 357-66.

Porter, L. A., M. Kong-Beltran & D. J. Donoghue (2003) Spy1 interacts with p27Kip1 to allow G1/S progression. *Mol Biol Cell,* 14**,** 3664-74.

Puglielli, M. T., M. Woisetschlaeger & S. H. Speck (1996) *oriP* is essential for EBNA gene promoter activity in Epstein-Barr virus-immortalized lymphoblastoid cell lines. *J Virol,* 70**,** 5758-68.

Ramiro, A. R., M. Jankovic, E. Callen, S. Difilippantonio, H. T. Chen, K. M. McBride, T. R. Eisenreich, J. Chen, R. A. Dickins, S. W. Lowe, A. Nussenzweig & M. C. Nussenzweig (2006) Role of genomic instability and p53 in AID-induced c-myc-Igh translocations. *Nature,* 440**,** 105-9.

Ramiro, A. R., M. Jankovic, T. Eisenreich, S. Difilippantonio, S. Chen-Kiang, M. Muramatsu, T. Honjo, A. Nussenzweig & M. C. Nussenzweig (2004) AID is required for c-myc/IgH chromosome translocations in vivo. *Cell,* 118**,** 431-8.

Reedman, B. M. & G. Klein (1973) Cellular localization of an Epstein-Barr virus (EBV)-associated complement-fixing antigen in producer and non-producer lymphoblastoid cell lines. *Int J Cancer,* 11**,** 499-520.

Reisman, D., J. Yates & B. Sugden (1985) A putative origin of replication of plasmids derived from Epstein-Barr virus is composed of two cis-acting components. *Mol Cell Biol,* 5**,** 1822-32.

Rickinson, A. B. & D. J. Moss (1997a) Human cytotoxic T lymphocyte responses to Epstein-Barr virus infection. *Annual Review of Immunology,* 15**,** 405-431.

--- (1997b) Human cytotoxic T lymphocyte responses to Epstein-Barr virus infection. *Annu Rev Immunol,* 15**,** 405-31.

Robbiani, D. F., A. Bothmer, E. Callen, B. Reina-San-Martin, Y. Dorsett, S. Difilippantonio, D. J. Bolland, H. T. Chen, A. E. Corcoran, A. Nussenzweig & M. C. Nussenzweig (2008) AID is required for the chromosomal breaks in c-myc that lead to c-myc/IgH translocations. *Cell,* 135**,** 1028-38.

Robertson, E. S., S. Grossman, E. Johannsen, C. Miller, J. Lin, B. Tomkinson & E. Kieff (1995) Epstein-Barr virus nuclear protein 3C modulates transcription through interaction with the sequence-specific DNA-binding protein J kappa. *J Virol,* 69**,** 3108-16.

Robertson, E. S., J. Lin & E. Kieff (1996) The amino-terminal domains of Epstein-Barr virus nuclear proteins 3A, 3B, and 3C interact with RBPJ(kappa). *J Virol,* 70**,** 3068-74.

Rowe, D. T., M. Rowe, G. I. Evan, L. E. Wallace, P. J. Farrell & A. B. Rickinson (1986) Restricted expression of EBV latent genes and T-lymphocyte-detected membrane antigen in Burkitt's lymphoma cells. *Embo j,* 5**,** 2599-607.

Rowe, M., D. T. Rowe, C. D. Gregory, L. S. Young, P. J. Farrell, H. Rupani & A. B. Rickinson (1987) Differences in B cell growth phenotype reflect novel patterns of Epstein-Barr virus latent gene expression in Burkitt's lymphoma cells. *Embo j,* 6**,** 2743-51.

Rowe, M., L. S. Young, K. Cadwallader, L. Petti, E. Kieff & A. B. Rickinson (1989) Distinction between Epstein-Barr virus type A (EBNA 2A) and type B (EBNA 2B) isolates extends to the EBNA 3 family of nuclear proteins. *J Virol,* 63**,** 1031-9.

Ruf, I. K., P. W. Rhyne, H. Yang, C. M. Borza, L. M. Hutt-Fletcher, J. L. Cleveland & J. T. Sample (2001) EBV regulates c-MYC, apoptosis, and tumorigenicity in Burkitt's lymphoma. *Curr Top Microbiol Immunol,* 258**,** 153-60.

Rus, H. G., F. Niculescu & M. L. Shin (1996) Sublytic complement attack induces cell cycle in oligodendrocytes. *J Immunol,* 156**,** 4892-900.

Saha, A., S. Halder, S. K. Upadhyay, J. Lu, P. Kumar, M. Murakami, Q. Cai & E. S. Robertson (2011) Epstein-Barr virus nuclear antigen 3C facilitates G1-S transition by stabilizing and enhancing the function of cyclin D1. *PLoS Pathog,* 7**,** e1001275.

Saha, A. & E. S. Robertson (2013) Impact of EBV essential nuclear protein EBNA-3C on B-cell proliferation and apoptosis. *Future Microbiol,* 8**,** 323-52.

Saigusa, K., I. Imoto, C. Tanikawa, M. Aoyagi, K. Ohno, Y. Nakamura & J. Inazawa (2007) RGC32, a novel p53-inducible gene, is located on centrosomes during mitosis and results in G2/M arrest. *Oncogene,* 26**,** 1110-21.

Sample, J., E. B. Henson & C. Sample (1992) The Epstein-Barr virus nuclear protein 1 promoter active in type I latency is autoregulated. *J Virol,* 66**,** 4654-61.

Sancar, A., L. A. Lindsey-Boltz, K. Unsal-Kacmaz & S. Linn (2004) Molecular mechanisms of mammalian DNA repair and the DNA damage checkpoints. *Annu Rev Biochem,* 73**,** 39-85.

Saridakis, V., Y. Sheng, F. Sarkari, M. N. Holowaty, K. Shire, T. Nguyen, R. G. Zhang, J. Liao, W. Lee, A. M. Edwards, C. H. Arrowsmith & L. Frappier (2005) Structure of the p53 binding domain of HAUSP/USP7 bound to Epstein-Barr nuclear antigen 1 implications for EBV-mediated immortalization. *Mol Cell,* 18**,** 25-36.

Savitsky, K., A. Bar-Shira, S. Gilad, G. Rotman, Y. Ziv, L. Vanagaite, D. A. Tagle, S. Smith, T. Uziel, S. Sfez, M. Ashkenazi, I. Pecker, M. Frydman, R. Harnik, S. R. Patanjali, A. Simmons, G. A. Clines, A. Sartiel, R. A. Gatti, L. Chessa, O. Sanal, M. F. Lavin, N. G. Jaspers, A. M. Taylor, C. F. Arlett, T. Miki, S. M. Weissman, M. Lovett, F. S. Collins & Y. Shiloh (1995) A single ataxia telangiectasia gene with a product similar to PI-3 kinase. *Science,* 268**,** 1749-53.

Sbih-Lammali, F., D. Djennaoui, H. Belaoui, A. Bouguermouh, G. Decaussin & T. Ooka (1996) Transcriptional expression of Epstein-Barr virus genes and proto-oncogenes in north African nasopharyngeal carcinoma. *J Med Virol,* 49**,** 7-14.

Schaefer, B. C., J. L. Strominger & S. H. Speck (1995) Redefining the Epstein-Barr virus-encoded nuclear antigen EBNA-1 gene promoter and transcription initiation site in group I Burkitt lymphoma cell lines. *Proc Natl Acad Sci U S A,* 92**,** 10565-9.

Schleiffer, A., M. Maier, G. Litos, F. Lampert, P. Hornung, K. Mechtler & S. Westermann (2012) CENP-T proteins are conserved centromere receptors of the Ndc80 complex. *Nat Cell Biol,* 14**,** 604-13.

Schlick, S. N., C. D. Wood, A. Gunnell, H. M. Webb, S. Khasnis, A. Schepers & M. J. West (2011) Upregulation of the cell-cycle regulator RGC-32 in Epstein-Barr virus-immortalized cells. *PLoS One,* 6**,** e28638.

Schuck, P. (1997) Use of surface plasmon resonance to probe the equilibrium and dynamic aspects of interactions between biological macromolecules. *Annu Rev Biophys Biomol Struct,* 26**,** 541-66.

Seki, A., J. A. Coppinger, C. Y. Jang, J. R. Yates & G. Fang (2008) Bora and the kinase Aurora a cooperatively activate the kinase Plk1 and control mitotic entry. *Science,* 320**,** 1655-8.

Seki, T., K. Yamashita, H. Nishitani, T. Takagi, P. Russell & T. Nishimoto (1992) Chromosome condensation caused by loss of RCC1 function requires the cdc25C protein that is located in the cytoplasm. *Mol Biol Cell,* 3**,** 1373-88.

Shah, K. M. & L. S. Young (2009) Epstein-Barr virus and carcinogenesis: beyond Burkitt's lymphoma. *Clin Microbiol Infect,* 15**,** 982-8.

Shannon-Lowe, C. D., B. Neuhierl, G. Baldwin, A. B. Rickinson & H. J. Delecluse (2006) Resting B cells as a transfer vehicle for Epstein-Barr virus infection of epithelial cells. *Proc Natl Acad Sci U S A,* 103**,** 7065-70.

Shibata, D. & L. M. Weiss (1992) Epstein-Barr virus-associated gastric adenocarcinoma. *Am J Pathol,* 140**,** 769-74.

Shibata, D., L. M. Weiss, A. M. Hernandez, B. N. Nathwani, L. Bernstein & A. M. Levine (1993) Epstein-Barr virus-associated non-Hodgkin's lymphoma in patients infected with the human immunodeficiency virus. *Blood,* 81**,** 2102-9.

Shiloh, Y. (1997) Ataxia-telangiectasia and the Nijmegen breakage syndrome: related disorders but genes apart. *Annu Rev Genet,* 31**,** 635-62.

Shire, K., D. F. Ceccarelli, T. M. Avolio-Hunter & L. Frappier (1999) EBP2, a human protein that interacts with sequences of the Epstein-Barr virus nuclear antigen 1 important for plasmid maintenance. *J Virol,* 73**,** 2587-95.

Sinclair, A. J., I. Palmero, A. Holder, G. Peters & P. J. Farrell (1995) Expression of cyclin D2 in Epstein-Barr virus-positive Burkitt's lymphoma cell lines is related to methylation status of the gene. *J Virol,* 69**,** 1292-5.

Sinclair, A. J., I. Palmero, G. Peters & P. J. Farrell (1994) EBNA-2 and EBNA-LP cooperate to cause G0 to G1 transition during immortalization of resting human B lymphocytes by Epstein-Barr virus. *Embo j,* 13**,** 3321-8.

Sivachandran, N., F. Sarkari & L. Frappier (2008) Epstein-Barr nuclear antigen 1 contributes to nasopharyngeal carcinoma through disruption of PML nuclear bodies. *PLoS Pathog,* 4**,** e1000170.

Skalska, L., R. E. White, M. Franz, M. Ruhmann & M. J. Allday (2010) Epigenetic repression of p16(INK4A) by latent Epstein-Barr virus requires the interaction of EBNA3A and EBNA3C with CtBP. *PLoS Pathog,* 6**,** e1000951.

Skalska, L., R. E. White, G. A. Parker, E. Turro, A. J. Sinclair, K. Paschos & M. J. Allday (2013) Induction of p16(INK4a) is the major barrier to proliferation when Epstein-Barr virus (EBV) transforms primary B cells into lymphoblastoid cell lines. *PLoS Pathog,* 9**,** e1003187.

Skare, J., C. Edson, J. Farley & J. L. Strominger (1982) The B95-8 isolate of Epstein-Barr virus arose from an isolate with a standard genome. *J Virol,* 44**,** 1088-91.

Smith, L. D. & R. E. Ecker (1971) The interaction of steroids with Rana pipiens Oocytes in the induction of maturation. *Dev Biol,* 25**,** 232-47.

Smits, V. A., R. Klompmaker, L. Arnaud, G. Rijksen, E. A. Nigg & R. H. Medema (2000) Polo-like kinase-1 is a target of the DNA damage checkpoint. *Nat Cell Biol,* 2**,** 672-6.

Solomon, M. J., T. Lee & M. W. Kirschner (1992) Role of phosphorylation in p34cdc2 activation: identification of an activating kinase. *Mol Biol Cell,* 3**,** 13-27.

Spender, L. C., G. H. Cornish, A. Sullivan & P. J. Farrell (2002) Expression of transcription factor AML-2 (RUNX3, CBF(alpha)-3) is induced by Epstein-Barr virus EBNA-2 and correlates with the B-cell activation phenotype. *J Virol,* 76**,** 4919-27.

Stone, S., P. Jiang, P. Dayananth, S. V. Tavtigian, H. Katcher, D. Parry, G. Peters & A. Kamb (1995) Complex structure and regulation of the P16 (MTS1) locus. *Cancer Res,* 55**,** 2988-94.

Sugden, B. & N. Warren (1989) A promoter of Epstein-Barr virus that can function during latent infection can be transactivated by EBNA-1, a viral protein required for viral DNA replication during latent infection. *J Virol,* 63**,** 2644-9.

Sugiura, M., S. Imai, M. Tokunaga, S. Koizumi, M. Uchizawa, K. Okamoto & T. Osato (1996) Transcriptional analysis of Epstein-Barr virus gene expression in EBV-positive gastric carcinoma: unique viral latency in the tumour cells. *Br J Cancer,* 74**,** 625-31.

Sung, N. S., S. Kenney, D. Gutsch & J. S. Pagano (1991) EBNA-2 transactivates a lymphoid-specific enhancer in the BamHI C promoter of Epstein-Barr virus. *J Virol,* 65**,** 2164-9.

Sunkel, C. E. & D. M. Glover (1988) polo, a mitotic mutant of Drosophila displaying abnormal spindle poles. *J Cell Sci,* 89 (Pt 1)**,** 25-38.

Takai, N., R. Hamanaka, J. Yoshimatsu & I. Miyakawa (2005) Polo-like kinases (Plks) and cancer. *Oncogene,* 24**,** 287-91.

Tanaka, K. (2012) Dynamic regulation of kinetochore-microtubule interaction during mitosis. *J Biochem,* 152**,** 415-24.

--- (2013) Regulatory mechanisms of kinetochore-microtubule interaction in mitosis. *Cell Mol Life Sci,* 70**,** 559-79.

Tanaka, T. U., M. J. Stark & K. Tanaka (2005) Kinetochore capture and bi-orientation on the mitotic spindle. *Nat Rev Mol Cell Biol,* 6**,** 929-42.

Tassan, J. P., S. J. Schultz, J. Bartek & E. A. Nigg (1994) Cell cycle analysis of the activity, subcellular localization, and subunit composition of human CAK (CDK-activating kinase). *Journal of Cell Biology,* 127**,** 467-78.

Taylor, A. L., R. Marcus & J. A. Bradley (2005) Post-transplant lymphoproliferative disorders (PTLD) after solid organ transplantation. *Crit Rev Oncol Hematol,* 56**,** 155-67.

Taylor, W. R. & G. R. Stark (2001) Regulation of the G2/M transition by p53. *Oncogene,* 20**,** 1803-15.

Thompson, A. A., H. N. Do, A. Saxon & R. Wall (1999) Widespread B29 (CD79b) gene defects and loss of expression in chronic lymphocytic leukemia. *Leuk Lymphoma,* 32**,** 561-9.

Thorley-Lawson, D. A. (2015) EBV Persistence--Introducing the Virus. *Curr Top Microbiol Immunol,* 390**,** 151-209.

Thorley-Lawson, D. A., E. M. Miyashita & G. Khan (1996) Epstein-Barr virus and the B cell: that's all it takes. *Trends Microbiol,* 4**,** 204-8.

Tomkinson, B. & E. Kieff (1992) Use of second-site homologous recombination to demonstrate that Epstein-Barr virus nuclear protein 3B is not important for lymphocyte infection or growth transformation in vitro. *J Virol,* 66**,** 2893-903.

Tomkinson, B., E. Robertson & E. Kieff (1993) Epstein-Barr virus nuclear proteins EBNA-3A and EBNA-3C are essential for B-lymphocyte growth transformation. *J Virol,* 67**,** 2014-25.

Touitou, R., M. Hickabottom, G. Parker, T. Crook & M. J. Allday (2001) Physical and functional interactions between the corepressor CtBP and the Epstein-Barr virus nuclear antigen EBNA3C. *J Virol,* 75**,** 7749-55.

Tzellos, S., P. B. Correia, C. E. Karstegl, L. Cancian, J. Cano-Flanagan, M. J. McClellan, M. J. West & P. J. Farrell (2014) A single amino acid in EBNA-2 determines superior B lymphoblastoid cell line growth maintenance by Epstein-Barr virus type 1 EBNA-2. *J Virol,* 88**,** 8743-53.

Tzellos, S. & P. J. Farrell (2012) Epstein-barr virus sequence variation-biology and disease. *Pathogens,* 1**,** 156-74.

Valentine, R., C. W. Dawson, C. Hu, K. M. Shah, T. J. Owen, K. L. Date, S. P. Maia, J. Shao, J. R. Arrand, L. S. Young & J. D. O'Neil (2010) Epstein-Barr virus-encoded EBNA1 inhibits the canonical NF-kappaB pathway in carcinoma cells by inhibiting IKK phosphorylation. *Mol Cancer,* 9**,** 1.

Van Scoy, S., I. Watakabe, A. R. Krainer & J. Hearing (2000) Human p32: a coactivator for Epstein-Barr virus nuclear antigen-1-mediated transcriptional activation and possible role in viral latent cycle DNA replication. *Virology,* 275**,** 145-57.

Walls, D. & M. Perricaudet (1991) Novel downstream elements upregulate transcription initiated from an Epstein-Barr virus latent promoter. *Embo j,* 10**,** 143-51.

Waltzer, L., M. Perricaudet, A. Sergeant & E. Manet (1996) Epstein-Barr virus EBNA3A and EBNA3C proteins both repress RBP-J kappa-EBNA2-activated transcription by inhibiting the binding of RBP-J kappa to DNA. *J Virol,* 70**,** 5909-15.

Wang, F., C. D. Gregory, M. Rowe, A. B. Rickinson, D. Wang, M. Birkenbach, H. Kikutani, T. Kishimoto & E. Kieff (1987) Epstein-Barr virus nuclear antigen 2 specifically induces expression of the B-cell activation antigen CD23. *Proc Natl Acad Sci U S A,* 84**,** 3452-6.

Wang, F., S. F. Tsang, M. G. Kurilla, J. I. Cohen & E. Kieff (1990) Epstein-Barr virus nuclear antigen 2 transactivates latent membrane protein LMP1. *J Virol,* 64**,** 3407-16.

Wang, Q., S. W. Tsao, T. Ooka, J. M. Nicholls, H. W. Cheung, S. Fu, Y. C. Wong & X. Wang (2006) Anti-apoptotic role of BARF1 in gastric cancer cells. *Cancer Lett,* 238**,** 90-103.

Wang, Y., J. E. Finan, J. M. Middeldorp & S. D. Hayward (1997) P32/TAP, a cellular protein that interacts with EBNA-1 of Epstein-Barr virus. *Virology,* 236**,** 18-29.

Wang, Y., C. Jacobs, K. E. Hook, H. Duan, R. N. Booher & Y. Sun (2000) Binding of 14-3-3beta to the carboxyl terminus of Wee1 increases Wee1 stability, kinase activity, and G2-M cell population. *Cell Growth Differ,* 11**,** 211-9.

Watanabe, N., M. Broome & T. Hunter (1995) Regulation of the human WEE1Hu CDK tyrosine 15-kinase during the cell cycle. *EMBO J,* 14**,** 1878-91.

Wei, M. X., J. C. Moulin, G. Decaussin, F. Berger & T. Ooka (1994) Expression and tumorigenicity of the Epstein-Barr virus BARF1 gene in human Louckes B-lymphocyte cell line. *Cancer Res,* 54**,** 1843-8.

Weiss, L. M., L. A. Movahed, R. A. Warnke & J. Sklar (1989) Detection of Epstein-Barr viral genomes in Reed-Sternberg cells of Hodgkin's disease. *N Engl J Med,* 320**,** 502-6.

White, R. E., I. J. Groves, E. Turro, J. Yee, E. Kremmer & M. J. Allday (2010) Extensive co-operation between the Epstein-Barr virus EBNA3 proteins in the manipulation of host gene expression and epigenetic chromatin modification. *PLoS One,* 5**,** e13979.

White, R. E., P. C. Ramer, K. N. Naresh, S. Meixlsperger, L. Pinaud, C. Rooney, B. Savoldo, R. Coutinho, C. Bodor, J. Gribben, H. A. Ibrahim, M. Bower, J. P. Nourse, M. K. Gandhi, J. Middeldorp, F. Z. Cader, P. Murray, C. Munz & M. J. Allday (2012) EBNA3B-deficient EBV promotes B cell lymphomagenesis in humanized mice and is found in human tumors. *J Clin Invest,* 122**,** 1487-502.

Woisetschlaeger, M., X. W. Jin, C. N. Yandava, L. A. Furmanski, J. L. Strominger & S. H. Speck (1991) Role for the Epstein-Barr virus nuclear antigen 2 in viral promoter switching during initial stages of infection. *Proc Natl Acad Sci U S A,* 88**,** 3942-6.

Woisetschlaeger, M., C. N. Yandava, L. A. Furmanski, J. L. Strominger & S. H. Speck (1990) Promoter switching in Epstein-Barr virus during the initial stages of infection of B lymphocytes. *Proc Natl Acad Sci U S A,* 87**,** 1725-9.

Wolf, H., J. Werner & H. zur Hausen (1975) EBV DNA in nonlymphoid cells of nasopharyngeal carcinomas and in a malignant lymphoma obtained after inoculation of EBV into cottontop marmosets. *Cold Spring Harb Symp Quant Biol,* 39 Pt 2**,** 791-6.

Wood, V. H., J. D. O'Neil, W. Wei, S. E. Stewart, C. W. Dawson & L. S. Young (2007) Epstein-Barr virus-encoded EBNA1 regulates cellular gene transcription and modulates the STAT1 and TGFbeta signaling pathways. *Oncogene,* 26**,** 4135-47.

Wu, H., P. Kapoor & L. Frappier (2002) Separation of the DNA replication, segregation, and transcriptional activation functions of Epstein-Barr nuclear antigen 1. *J Virol,* 76**,** 2480-90.

Wysokenski, D. A. & J. L. Yates (1989) Multiple EBNA1-binding sites are required to form an EBNA1-dependent enhancer and to activate a minimal replicative origin within *oriP* of Epstein-Barr virus. *J Virol,* 63**,** 2657-66.

Xu, B., S. T. Kim, D. S. Lim & M. B. Kastan (2002) Two molecularly distinct G(2)/M checkpoints are induced by ionizing irradiation. *Mol Cell Biol,* 22**,** 1049-59.

Yalamanchili, R., X. Tong, S. Grossman, E. Johannsen, G. Mosialos & E. Kieff (1994) Genetic and biochemical evidence that EBNA 2 interaction with a 63-kDa cellular GTG-binding protein is essential for B lymphocyte growth transformation by EBV. *Virology,* 204**,** 634-41.

Yang, J., E. S. Bardes, J. D. Moore, J. Brennan, M. A. Powers & S. Kornbluth (1998) Control of cyclin B1 localization through regulated binding of the nuclear export factor CRM1. *Genes Dev,* 12**,** 2131-43.

Yao, Q. Y., A. B. Rickinson & M. A. Epstein (1985) A re-examination of the Epstein-Barr virus carrier state in healthy seropositive individuals. *Int J Cancer,* 35**,** 35-42.

Yates, J. L., S. M. Camiolo & J. M. Bashaw (2000) The minimal replicator of Epstein-Barr virus *oriP*. *J Virol,* 74**,** 4512-22.

Yates, J. L. & N. Guan (1991) Epstein-Barr virus-derived plasmids replicate only once per cell cycle and are not amplified after entry into cells. *J Virol,* 65**,** 483-8.

Yates, J. L., N. Warren & B. Sugden (1985) Stable replication of plasmids derived from Epstein-Barr virus in various mammalian cells. *Nature,* 313**,** 812-5.

Yokoyama, A., M. Tanaka, G. Matsuda, K. Kato, M. Kanamori, H. Kawasaki, H. Hirano, I. Kitabayashi, M. Ohki, K. Hirai & Y. Kawaguchi (2001) Identification of major phosphorylation sites of Epstein-Barr virus nuclear antigen leader protein (EBNA-LP): ability of EBNA-LP to induce latent membrane protein 1 cooperatively with EBNA-2 is regulated by phosphorylation. *J Virol,* 75**,** 5119-28.

Young, L., C. Alfieri, K. Hennessy, H. Evans, C. O'Hara, K. C. Anderson, J. Ritz, R. S. Shapiro, A. Rickinson, E. Kieff & et al. (1989) Expression of Epstein-Barr virus transformation-associated genes in tissues of patients with EBV lymphoproliferative disease. *N Engl J Med,* 321**,** 1080-5.

Young, L. S. & A. B. Rickinson (2004) Epstein-Barr virus: 40 years on. *Nat Rev Cancer,* 4**,** 757-68.

Young, L. S., Q. Y. Yao, C. M. Rooney, T. B. Sculley, D. J. Moss, H. Rupani, G. Laux, G. W. Bornkamm & A. B. Rickinson (1987) New type B isolates of Epstein-Barr virus from Burkitt's lymphoma and from normal individuals in endemic areas. *J Gen Virol,* 68 (Pt 11)**,** 2853-62.

Zech, L., U. Haglund, K. Nilsson & G. Klein (1976) Characteristic chromosomal abnormalities in biopsies and lymphoid-cell lines from patients with Burkitt and non-Burkitt lymphomas. *Int J Cancer,* 17**,** 47-56.

Zhan, F., Y. Huang, S. Colla, J. P. Stewart, I. Hanamura, S. Gupta, J. Epstein, S. Yaccoby, J. Sawyer, B. Burington, E. Anaissie, K. Hollmig, M. Pineda-Roman, G. Tricot, F. van Rhee,

R. Walker, M. Zangari, J. Crowley, B. Barlogie & J. D. Shaughnessy, Jr. (2006) The molecular classification of multiple myeloma. *Blood,* 108**,** 2020-8.

Zhang, Y., Y. Lin, C. Bowles & F. Wang (2004) Direct cell cycle regulation by the fibroblast growth factor receptor (FGFR) kinase through phosphorylation-dependent release of Cks1 from FGFR substrate 2. *J Biol Chem,* 279**,** 55348-54.

Zhao, B., J. C. Mar, S. Maruo, S. Lee, B. E. Gewurz, E. Johannsen, K. Holton, R. Rubio, K. Takada, J. Quackenbush & E. Kieff (2011) Epstein-Barr virus nuclear antigen 3C regulated genes in lymphoblastoid cell lines. *Proc Natl Acad Sci U S A,* 108**,** 337-42.

Zhao, H. & H. Piwnica-Worms (2001) ATR-mediated checkpoint pathways regulate phosphorylation and activation of human Chk1. *Mol Cell Biol,* 21**,** 4129-39.

Zimber, U., H. K. Adldinger, G. M. Lenoir, M. Vuillaume, M. V. Knebel-Doeberitz, G. Laux, C. Desgranges, P. Wittmann, U. K. Freese, U. Schneider & et al. (1986) Geographical prevalence of two types of Epstein-Barr virus. *Virology,* 154**,** 56-66.

zur Hausen, A., A. A. Brink, M. E. Craanen, J. M. Middeldorp, C. J. Meijer & A. J. van den Brule (2000) Unique transcription pattern of Epstein-Barr virus (EBV) in EBV-carrying gastric adenocarcinomas: expression of the transforming BARF1 gene. *Cancer Res,* 60**,** 2745-8.